

**Mechanisms underlying *Leishmania* parasites
survival and dissemination at late stage of infection in
human macrophages**

Rajeev Rai (BSc Hons, MRes)

A thesis submitted in partial fulfillment of the requirements of the
University of Greenwich for the
Degree of Doctor of Philosophy

January 2016

DECLARATION

I certify that this work has not been accepted in substance for any degree, and is not concurrently being submitted for any degree other than that of Doctor of Philosophy being studied at the University of Greenwich. I also declare that this work is the result of my own investigations except where otherwise identified by references and that I have not plagiarized the work of others.

Candidate:

Rajeev Rai

Date: 7/1/2016

Supervisor:

Dr. Giulia Getti

Date: 7/1/2016

AKNOWLEDGEMENTS

I would like to thank my supervisor Dr. Giulia Getti for her continuous help, advice and guidance throughout my research project.

I would also like to thank Dr. Simon Richardson and Dr. Paul Dyer for assisting the use of fluorescence microscope and X-ray machine.

I would also like to thank Andrew Deacon, Medhavi Ranatunga, Kareem Mosa, Sara Medhat, Sam Ingram and Sam Lewis for their support and assistance in the lab.

Finally, I am very grateful to my parents for inspiring me to learn science and motivating me to enter the field of scientific research.

ABSTRACT

Leishmania parasites are the causative agent of a wide range of human diseases known as leishmaniasis. The progression of disease pathogenesis is dependent on the ability of intracellular parasites to disseminate between human macrophages. It is assumed that parasites could exit macrophages following cell lysis. However, there is still a major gap in knowledge in understanding the exact mechanism pertaining to this critical step. This has been partially caused by the lack of reliable experimental models to study this stage of host-parasite interaction. This research aims to elucidate the mechanism behind cell-to-cell spreading of *Leishmania in vitro*.

A link between host cell apoptosis and *Leishmania* propagation was initially established by determining the effect of apoptotic induction on infection over a period of 96 hours. The result showed that 60-90% of cells were inoculated with *L. aethiopica* and *L. mexicana* within 72 and 96 hours infection. Although, the concentration of viable cells was greatly reduced as compared to non-induced samples, a heavily infected cell population was obtained with this approach. Hence, this population of *L. aethiopica* and *L. mexicana* infected cells at 72 hours was used to infect differentiated THP-1 macrophages and validated as a model for infection spreading. Amastigotes spreading was detected within 12 hours of co-culture as confirmed by flow cytometry and live cell imaging techniques. Interestingly, the live imaging revealed inter-cellular extrusion of *L. aethiopica* and *L. mexicana* from infected to a recipient cells without cell lysis. To address whether parasite extrusion is linked to apoptotic induction, this model was used to detect expression of several apoptotic markers. The results showed that *L. aethiopica* (but not *L. mexicana*) dissemination was correlated with host apoptotic induction, as there was a significant increase ($p < 0.05$) in phosphatidyl serine (PS) externalization and active caspase-3 expression. In addition, western blot analysis demonstrated that *L. aethiopica* spread was associated with downregulation of three major apoptotic signaling pathways: AKT, NF- κ B and PKC- δ . Further comparative proteomic analysis of this model supported these findings and showed that during *L. aethiopica* spreading, a number of host physiological processes were subverted. Specifically caspase-3 and caspase-9 activation strengthens the involvement of mitochondria in initiation of apoptosis. Interestingly, chitinase-3-like protein (inducer of IL-13 production) and butyrophilin (inhibitor of IFN- γ and IL-12) were markedly increased confirming the downregulation of inflammatory response. Finally, elevated increase in glutathione reductase and metallothionein-2 proteins, which are involved in scavenging free radicals, suggests that anti-microbial activity is also downregulated during *L. aethiopica* spreading.

In conclusion, by developing and validating for the first time a credible *in vitro* spreading model in human macrophages, this research has clarified the mechanism of *Leishmania* spreading. *L. aethiopica* promotes host cell apoptosis in order to disseminate from cell-to-cell without activating inflammatory and anti-microbial responses. In particular, apoptotic induction takes place via downregulation of AKT and NF- κ B, release of cytochrome C and consequent activation of caspase-3 and PS exhibition, independently from PKC- δ . This model clearly fits with the silent spread of parasites that takes place in the first weeks (to months) of infection in mice model. Interestingly, the fact that *L. mexicana* utilizes a non-apoptotic strategy to spread suggests that alternative mechanisms of parasitic extrusion also exist underlying the necessity of species specific investigations. Understanding the molecular basis of *Leishmania* spreading contributes to filling a current gap in knowledge in the biology of *Leishmania* infection strategy of this very successful parasite. Moreover, it has the potential to open up a novel set of targets for drugs and vaccine development against this increasingly widespread neglected disease.

Table of Contents

Chapter 1 – Introduction.....	1
1.1 <i>Leishmania</i> parasites.....	1
1.2 Life cycle of <i>Leishmania</i>.....	1
1.3 Leishmaniasis.....	7
1.4 Expression of virulence factors in <i>Leishmania</i>.....	12
1.5 Interaction between <i>Leishmania</i> and host immune cells.....	16
1.5.1 T cells.....	16
1.5.2 Natural Killer (NK) cells.....	17
1.5.3 Neutrophils.....	18
1.5.4 Macrophages.....	18
1.6 Molecular interaction between <i>Leishmania</i> and macrophage....	20
1.6.1 Phagocytic uptake of <i>Leishmania</i>	20
1.6.2 Survival strategy for <i>Leishmania</i>	22
1.6.3 Modulation of intracellular signaling pathways during <i>Leishmania</i> infection.....	22
1.6.4 Dissemination of <i>Leishmania</i>	26
1.7 Apoptosis.....	28
1.8 Infection and Apoptosis.....	33
1.9 Aims of the Thesis.....	36
Chapter 2 – Materials and Methods.....	38
2.1 Parasite culture.....	38
2.2 Human cell culture.....	38
2.3 Infection of differentiated THP-1 macrophage with GFP expressing <i>Leishmania</i>.....	39
2.3.1 Preparation of stationary phase metacyclic promastigotes.....	39
2.3.2 Preparation of differentiated THP-1 macrophages.....	39
2.3.3 Parasite to cell ratio.....	40
2.4 Induction of apoptosis.....	40
2.5 Infection of differentiated THP-1 macrophage with <i>Leishmania</i> infected cells.....	40

2.6 Inhibition of caspase-3 activity.....	42
2.7 Detection of apoptosis.....	42
2.7.1 Annexin V / 7AAD assay.....	44
2.7.2 Caspase-3 enzymatic assay.....	44
2.8 Flow cytometry.....	45
2.9 Real time lapse microscopy.....	48
2.10 Western blot.....	50
2.11 Quantitative proteomics by mass spectrometry.....	52
2.11.1 Precipitation and enzymatic digestion of the protein samples.....	52
2.11.2 Peptide labeling and mass spectrometry.....	53
2.12 Statistical Analysis.....	54
Chapter 3 – <i>Leishmania</i> infection and host cell apoptosis.....	55
3.1 Introduction.....	55
3.2 Results and Discussion.....	56
3.2.1 Infection of differentiated THP-1 macrophages with <i>Leishmania</i> promastigotes.....	56
3.2.2 Effect of <i>Leishmania</i> promastigotes infection on the apoptosis of differentiated THP-1 macrophages.....	60
3.2.3 Effect of apoptotic induction on <i>Leishmania</i> infection.....	63
3.2.3a Longer duration of treatment with camptothecin.....	63
3.2.3b Time limited treatment with camptothecin.....	66
3.2.4 Assessment of viable cell concentration during <i>Leishmania</i> infection in the presence of camptothecin.....	71
3.3 Conclusions.....	71
Chapter 4 – The <i>in vitro</i> development of <i>Leishmania</i> dissemination model during late stage of macrophage infection.....	74
4.1 Introduction.....	74
4.2 Results and Discussion.....	76
4.2.1 Optimization of camptothecin treatment in <i>L. mexicana</i> (M5G) infected cells.....	76
4.2.2 Infection of differentiated THP-1 macrophage with L8G and M5G infected cells.	76

4.2.3 Live cell imaging of intracellular L8G and M5G amastigotes spreading.....	81
4.2.4 Effect of <i>Leishmania</i> spreading on the apoptosis of host cells	84
4.2.5 Effect of caspase-3 inhibition on the apoptosis and infection spread.....	90
4.3 Conclusions.....	90
Chapter 5 – Regulation of apoptosis signaling pathways in human macrophage during <i>Leishmania</i> spreading.....	93
5.1 Introduction.....	93
5.2 Results and Discussion.....	96
5.2.1 Effect of L8G infected cells on AKT activation during cell-to-cell infection spread.....	96
5.2.2 Effect of AKT downregulation on the phosphorylation of BAD expression and cytochrome C release.....	98
5.2.3 Effect of L8G infected cells on NF- κ B signaling pathways during cell-to-cell infection spread.....	100
5.2.4 Effect of L8G infected cells on PKC- δ signaling pathways during cell-to-cell infection spread.....	103
5.3 Conclusions.....	105
Chapter 6 – Global protein response during late stage of <i>Leishmania</i> infection in human macrophage.....	107
6.1 Introduction.....	107
6.2 Results and Discussion.....	108
6.2.1 Identification and functional annotation of differentially expressed proteins.....	108
6.2.2 Proteins involved in apoptosis and cell death.....	110
6.2.3 Proteins involved in immune response.....	114
6.2.4 Proteins involved in vesicular trafficking.....	116
6.2.5 Proteins involved in metabolic pathways.....	117
6.2.6 Proteins involved in gene expression.....	118
6.3 Conclusions.....	119
Chapter 7 – Discussion.....	120
7.1 Discussion.....	120

Chapter 8 – Conclusion and future works.....	128
8.1 Conclusions.....	128
8.2 Future works.....	129
Chapter 9 – References.....	131
Chapter 10 – Appendices.....	144

List of Figures

Figure 1.1. Scanning electron microscope of two life stage of <i>Leishmania</i> parasites.....	3
Figure 1.2. Life cycle of <i>Leishmania</i> parasites between the Female sandfly (vector) and mammals (host)	4
Figure 1.3. Developmental profile of various morphological forms of <i>Leishmania</i> inside the sandfly vector.....	6
Figure 1.4. Interaction of <i>Leishmania</i> parasites with the phagocytic pathway of host macrophages.....	8
Figure 1.5. Major clinical pathologies associated with human leishmaniasis.	10
Figure 1.6. Structural organization of <i>Leishmania</i> Lipophosphoglycan (LPG).....	14
Figure 1.7. Trojan horse model for neutrophils.	19
Figure 1.8. Two different types of receptor mediated approach undertaken by macrophage to phagocytize metacyclic promastigote.....	21
Figure 1.9. Schematic representation showing the differences in the molecular interaction of endosomal vesicles with the Wild type (Wt) and LPG defective (mutant) <i>Leishmania</i> promastigote.....	23
Figure 1.10. Upstream and downstream effectors in NF- κ B signaling pathway.	25
Figure 1.11. Schematic diagram representing the disruption of macrophage signaling pathways during <i>Leishmania</i> infection.....	27
Figure 1.12. Evolution of dermal lesions in C57BL/6 mice during <i>Leishmania</i> infection.....	29
Figure 1.13. Mechanism of apoptosis is comprised of extrinsic and intrinsic pathways.....	31
Figure 2.1. Schematic diagram representing the optimization strategy of camptothecin treatment on the percentage of infected cells.....	41
Figure 2.2. Flow cytometry analysis of PE-Annexin V / 7-AAD stained cells.	46
Figure 2.3. Flow cytometry analysis of apoptosis in infected cultures.....	47

Figure 2.4. Flow cytometry analysis of PE-Caspase 3 stained cells.....	49
Figure 3.1. Time course of differentiated THP-1 macrophage infection with <i>Leishmania</i> promastigotes.	58
Figure 3.2. Measurement of viable cell concentration in the presence or absence of infection.	59
Figure 3.3. Effect of <i>Leishmania</i> promastigotes infection on the apoptosis of differentiated THP-1 macrophages.	61
Figure 3.4. Time course of differentiated THP-1 macrophage infection with <i>Leishmania</i> promastigotes.	62
Figure 3.5. Effect of longer exposure to camptothecin treatment on <i>Leishmania</i> infection.....	64
Figure 3.6. Effect of longer exposure to camptothecin treatment on the apoptosis of differentiated THP-1 macrophages infected with <i>Leishmania</i>	65
Figure 3.7. Flow cytometry analysis of Annexin V versus 7-AAD dot plot.	67
Figure 3.8. Flow cytometry analysis of Annexin V versus 7-AAD dot plot after washing protocol.....	68
Figure 3.9. Effect of shorter exposure to camptothecin treatment on <i>Leishmania</i> infection.....	69
Figure 3.10. Effect of shorter exposure to camptothecin treatment on the apoptosis of differentiated THP-1 macrophages infected with <i>Leishmania</i>	70
Figure 3.11. Effect of camptothecin on viable cell concentration in the presence or absence of infection.	72
Figure 4.1. Time course of differentiated THP-1 macrophage infection with <i>L. mexicana</i> (M5G) in the presence and/or absence of apoptotic induction.....	77
Figure 4.2. Infection of THP-1 macrophages with <i>Leishmania</i> infected cells.....	79
Figure 4.3. Measurement of viable cell concentration during infection with <i>Leishmania</i> infected cells.	80
Figure 4.4. Live cell imaging of <i>L. aethiopica</i> (L8G) amastigotes spread from cell-to-cell.	82

Figure 4.5. Live cell imaging of <i>L. mexicana</i> (M5G) amastigotes spread from cell-to-cell.....	83
Figure 4.6. Effect of L8G infection spreading on host cell apoptosis.....	85
Figure 4.7. Effect of L8G infection spreading on the activation of caspase-3 in host cells.	87
Figure 4.8. Effect of M5G infection spreading on host cell apoptosis.....	88
Figure 4.9. Effect of M5G infection spreading on the activation of caspase-3 in host cells.	89
Figure 4.10. Effect of caspase-3 inhibition on the apoptosis and infection spread after infection with L8G infected cells.....	91
Figure 5.1. Schematic diagram representing apoptotic signalling pathways in macrophages.....	95
Figure 5.2. Effect of <i>L. aethiopica</i> (L8G) infected cells on AKT activation during infection spreading.....	97
Figure 5.3. Effect of AKT downregulation on BAD phosphorylation and cytochrome C release.....	99
Figure 5.4. Effect of <i>L. aethiopica</i> (L8G) infected cells on NF- κ B signaling during infection spreading.....	102
Figure 5.5. Effect of <i>L. aethiopica</i> (L8G) infected cells on PKC- δ signaling during infection spreading.	104
Figure 6.1. Pie-diagram showing functional annotation and relative distribution of the total proteins detected in differentiated THP-1 macrophages co-cultured with <i>L. aethiopica</i> infected cells.....	111
Figure 6.2. Functional distribution of differentially expressed proteins during <i>L. aethiopica</i> infected co-culture cells at 10 hours.....	112
Figure 7.1. Schematic diagram representing the complex nature of intracellular signaling pathways associated with apoptosis.....	124

List of Tables

Table 1.1. Classification of <i>Leishmania</i> parasites causing human disease into Old and New World species.....	2
Table 1.2. Classification of human leishmaniasis.....	9
Table 1.3. Summary of the diverse range of virulence factors expressed by <i>Leishmania</i>	13
Table 1.4. Summary of the diverse macrophage signaling pathways altered by <i>Leishmania</i>	24
Table 2.1. List of experiments designed for apoptosis and their time of analysis.	43
Table 2.2. List of antibodies and their appropriate dilution and appropriate blocking buffers used in western blot experiments.	51
Table 6.1. List of differentially expressed proteins during late stage of <i>L. aethiopica</i> infection.	109
Table 7.1. Summary of the involvement of apoptotic signaling pathways concomitant with spreading of <i>L. aethiopica</i> infection.....	125

Abbreviations

APAF-1	Apoptotic Protease Activating Factor-1
APC	Antigen Presenting Cells
CL	Cutaneous Leishmaniasis
CP	Cysteine Peptidase
CR	Complement Receptor
CRD	Carbohydrate Recognition Domain
DAG	Di-Acyl Glycerol
DCL	Diffuse Cutaneous Leishmaniasis
DED	Death Effector Domain
DISC	Death Inducing Signaling Complex
ERK	Extracellular Signal Regulated Kinase
FADD	Fas-associated Death Domain
FCS	Fetal Calf Serum
FnR	Fibronectin Receptor
FSC	Forward Scatter
GFP	Green Fluorescent Protein
GIPL	Glycophosphatidylinositol Lipid
GP63	Glycoprotein 63
GPCR	G Protein Coupled Receptor
GPI	Glycosylphosphatidylinositol
IAP	Inhibitor of Apoptosis
ICS	Interconnecting Segment
iNOS	Inducible Nitric Oxide Synthase
JAK	Janus Kinase
JNK	c-Jun N terminal protein
LAMP	Lysosomal Associated Membrane Protein
LPG	Lipophosphoglycan
LPS	Lipopolysaccharide
LRR	Leucine Rich Repeat
MAC	Membrane Attack Complex
MAPK	Mitogen Activated Protein Kinase
MCL	Muco Cutaneous Leishmaniasis
MIP	Macrophage Inflammatory Protein
MR	Mannose Receptor
mRNA	Messenger RNA
NET	Neutrophil Extracellular Trap
NF	Nuclear Factor
NK	Natural Killer
NO	Nitric Oxide
PARP	Poly ADP Ribose Polymerase

PBS	Phosphate Buffer Saline
PCD	Programmed Cell Death
PE	Phycoerythrin
PH	Pleckstrin Homology
PI3K	Phosphatidylinositol 3 Kinase
PKDL	Post Kala Azar Leishmaniasis
PM	Peritrophic Matrix
PPG	Proteophosphoglycan
PS	Phosphatidyl Serine
PSA-2	Protein Surface Antigen-2
PSG	Promastigote Secretory Gel
PV	Parasitophorous Vacuole
RA	Retinoic Acid
RANTES	Regulated on Activation Normal T cell Expressed and Secreted
RAS	Rat Sarcoma
ROS	Reactive Oxygen Species
SHP-1	Src-homology-2 domain containing Phosphatase
SP	Serine Peptidase
SSC	Side Scatter
STAT	Signal Transducers and Activators of Transcription
TGF	Transforming Growth Factor
Th 1/2	T helper cells 1/2
TLR	Toll Like Receptor
TNF	Tumor Necrosis Factor
VL	Visceral Leishmaniasis
WASP	Wiscott Aldrich Syndrome Protein
WHO	World Health Organization

Chapter 1 – Introduction

1.1. *Leishmania* parasites

Unicellular protozoan parasites belonging to the genus *Leishmania* are the causative agent of a spectrum of human diseases known as leishmaniasis. Ever since the discovery of this parasite in 1903 (Leishman, 1903; Donovan, 1903; Bailey and Bishop, 1959), more than 30 species of *Leishmania* have been reported, out of which 12 species have been known to cause human leishmaniasis (Banuls et al., 2007). Depending on the location site of the disease, these species have been classified into Old World and New World and further sub-divided into *Leishmania* and *Viannia* sub-genus (Table 1.1). Affecting over 350 million people in 88 countries worldwide, the transmission of this parasite occurs through the bite of phlebotomine sandflies (Kedzierski, 2010).

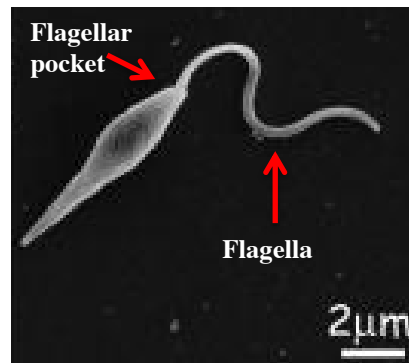
1.2. Life cycle of *Leishmania*

Leishmania undergoes structural and biochemical transformations throughout its life cycle. In sandfly, the parasite develops as flagellated and motile forms called promastigotes whereas a non-motile oval shaped amastigotes are found inside the mammalian host (Figure 1.1). The parasitic life cycle initiates when the sandfly ingests the amastigotes infected macrophages during its blood meal (Figure 1.2). After the first 12 hours post feeding, the increase in pH and reduced temperature triggers the differentiation of amastigotes into a non-infective procyclic promastigotes, which are relatively resistant against sandfly digestive enzymes (Bates, 2007). At this time point, the replicating promastigotes located in the endoperitrophic space are separated from the anterior midgut by a layer of protein and chitin mesh called peritrophic matrix (PM).

Old World (<i>Leishmania</i> sub-genus)	New World (<i>Leishmania</i> sub-genus)	New World (<i>Viannia</i> sub-genus)
<i>L. major</i>	<i>L. mexicana</i>	<i>L. braziliensis</i>
<i>L. tropica</i>	<i>L. amazonensis</i>	<i>L. guyanensis</i>
<i>L. aethiopica</i>	<i>L. pifanoi</i>	<i>L. panamensis</i>
<i>L. donovani</i>		<i>L. peruviana</i>
<i>L. infantum</i>		

Table 1.1. Classification of *Leishmania* parasites causing human disease into Old and New World species. Species are further categorized into two different sub-genus, *Leishmania* and *Viannia*. Adapted from Kaye and Scott, 2011.

A



B

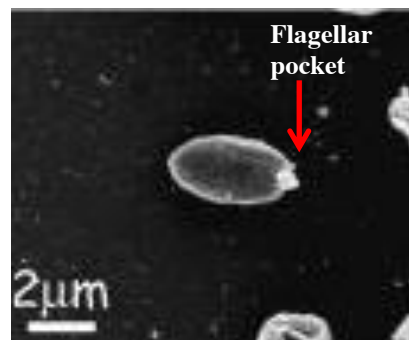


Figure 1.1. Scanning electron microscope images of two life cycle stage of *Leishmania* parasites. (A) Promastigote (motile and flagellated) and (B) Amastigote (oval shaped and non-motile). The flagellar pocket marks the anterior side of the parasites. Adapted from Besteiro et al., 2007.

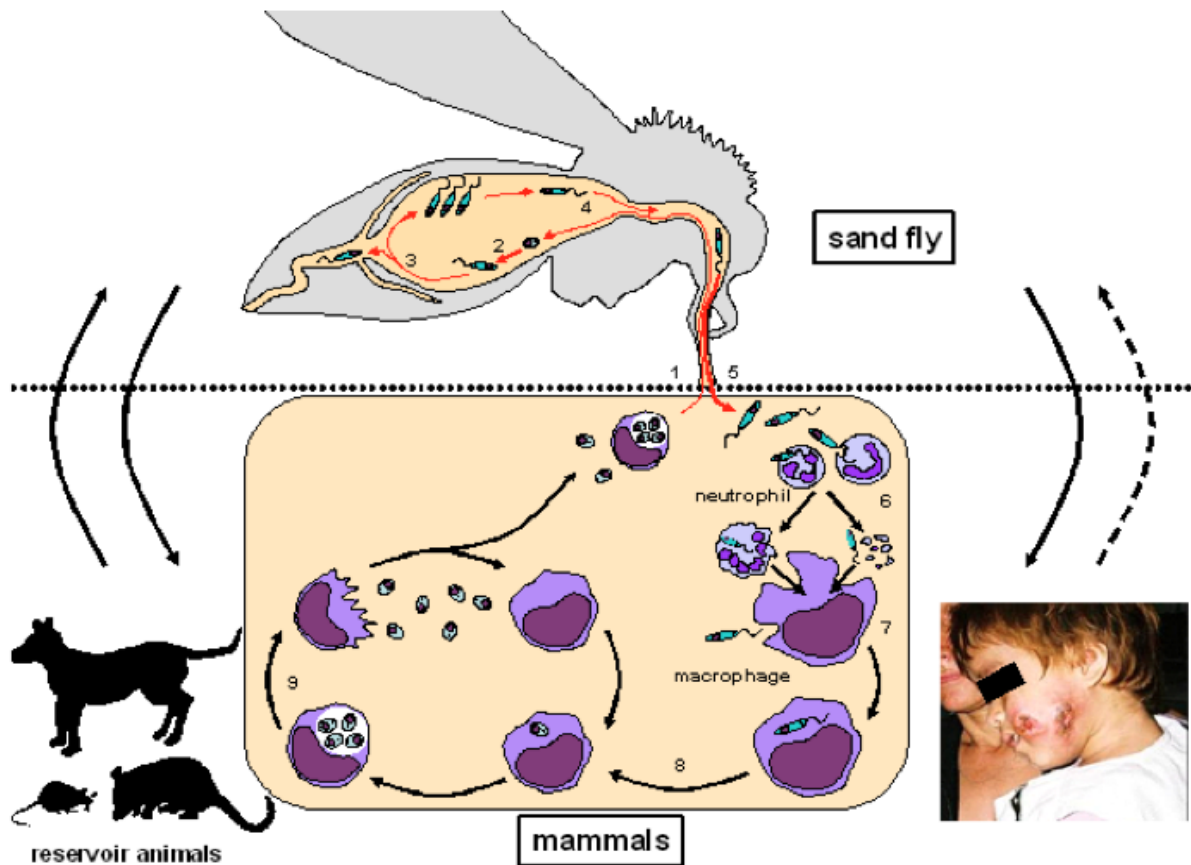


Figure 1.2. Life cycle of *Leishmania* parasites between the Female sandfly (vector) and mammals (host). During blood meal, the healthy sandfly consumes infected blood, containing amastigotes, from the host [1]. Changes in the pH and temperature inside the sandfly's midgut triggers differentiation of amastigotes into flagellated procyclic promastigotes [2]. Following replication and attachment on the peritrophic matrix of midgut, the parasites migrate towards the proboscis, where the procyclic differentiates into non-dividing and highly motile metacyclic promastigotes [3,4]. The infected sandfly then injects another healthy host during its next blood meal [5]. The metacyclic promastigotes is then phagocytized either directly by macrophages (definitive host cells) or indirectly through neutrophils (which then becomes a secondary meal for macrophage) [6]. Following its survival inside the phagolysosome of the macrophage, the promastigote differentiate into a non-motile amastigote [7, 8], which then undergoes replication and re-infection into other neighboring macrophages [9]. The life cycle is complete when infected macrophages are taken up by another healthy sandfly with the blood meal [1]. Adapted from Kato et al., 2010.

Within 2-3 post feeding, replication of procyclic form is reduced and differentiation into nectomonad promastigotes begins (Figure 1.3). This elongated and motile parasitic form secretes chitinase enzymes (PM degradation) and subsequently migrates to the anterior midgut in order to avoid expulsion during blood defecation (Rogers et al., 2008). As the nectomonads reaches the stomodeal valve, the parasite undergoes further differentiation into replicating leptomonads, which secrete promastigote secretory gel (PSG) (Rogers et al., 2002). The significance of PSG, which is composed of filamentous proteophosphoglycans, is not only linked to effective transmission via the sandfly proboscis but is also involved in dampening down the mammalian host immune response during the inoculation phase (Rogers et al., 2009; Rogers, 2012). From day five onwards, some leptomonads differentiates into haptomonads, whose primary role is to form a ball shaped mass in order to impede the blood flow into the midgut. The remaining leptomonads transform into the non-dividing infectious metacyclics promastigotes, which possess long flagella and are highly motile to migrate towards the pharynx and proboscis, ready for inoculation (Bates, 2007).

During blood meal, the infected sandfly transmits metacyclic promastigotes into the skin of the mammalian host, where the parasites become phagocytized either by macrophages or by neutrophils. Neutrophils, which are generally the first cells to be recruited to the site of infection, have an extremely short half-life and undergo spontaneous apoptosis within 24 hours of infiltration from the blood stream. However, during this early infection period, promastigote delays neutrophil apoptosis for further 24 hours (Aga et al., 2002). After this interruption, the promastigote infected neutrophils then become phagocytized by macrophages (Kaye and Scott, 2011), as discussed in more detail later (section 1.5.3).

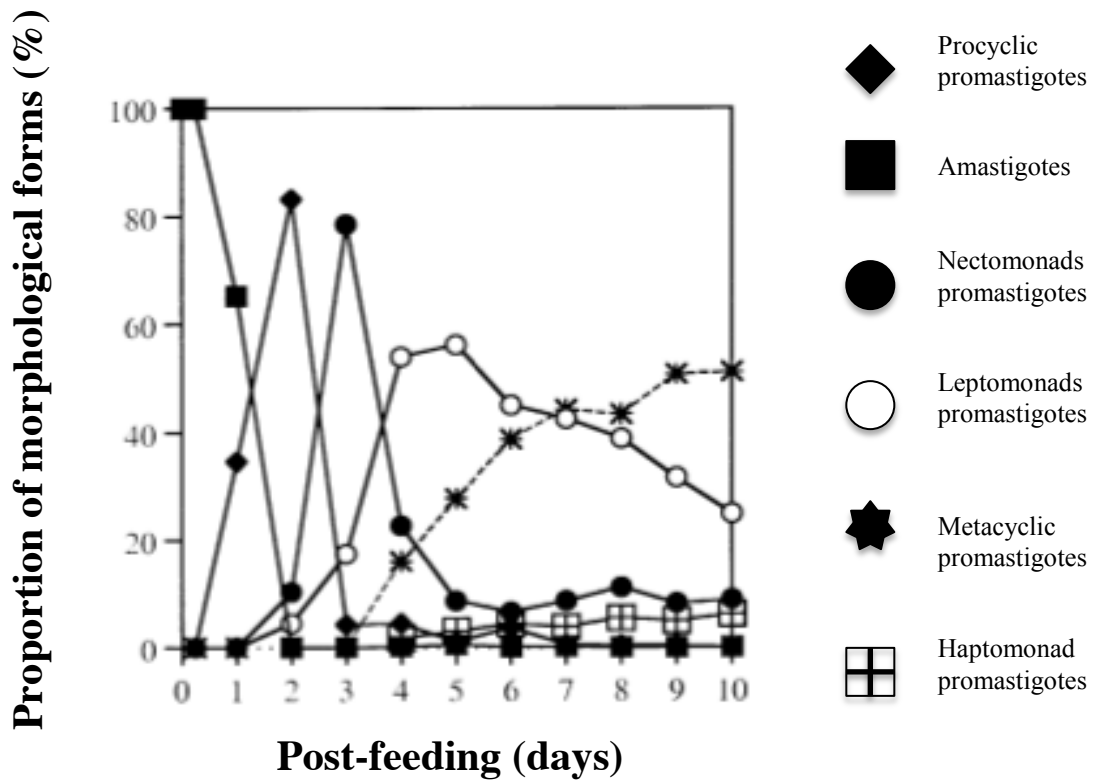


Figure 1.3. Developmental profile of various morphological forms of *Leishmania* inside the sandfly vector. Amastigotes undergoes complete transformation into procyclic within day 2 of post infection. From day 2, nectomonad and leptomonads are observed at low prevalence for the first time. Procyclic then begins to decrease rapidly, which is coincident with an increase in the number of nectomonad and leptomonad promastigotes. From day 5, the proportion of leptomonad slowly drops while the nectomonad already persist at a very low level. Within the same day, two forms begin to make their appearance; haptomonad and metacyclic promastigotes. Although the haptomonad fails to increase in number, the metacyclic gradually increases and becomes the predominant parasite population by day 10, at the expense of leptomonad promastigotes. Adapted from Rogers et al., 2002.

Immediately after phagocytosis, the promastigotes are located inside macrophage derived phagosomes (Figure 1.4). Interestingly, the lipophosphoglycan (LPG) of metacyclic promastigotes delays the fusion between phagosome containing parasites and acidic enzyme containing lysosomes hence preventing the formation of phagolysosomal vesicles (Lodge and Descoteaux, 2005). This sudden delay in phagosome biogenesis, which is referred to as pre-pregnant pause, is thought to allow promastigote sufficient time to differentiate into amastigote (Swanson and Fernandez-Moreira, 2002). After the release from pre-pregnant pause, the acidic environment within the phago-lysosome causes the maturation and replication of amastigotes. During the late stage of infection, replication is followed by virulent exit of intracellular amastigotes to re-infect other phagocytic cells (macrophages or dendritic cells). The mechanism of this spreading is not fully understood. It has been assumed that cell lysis of macrophage results in the release of free amastigotes. The transmission cycle is complete once the infected phagocytes and free amastigotes are consumed by a sandfly during the next blood meal.

1.3. Leishmaniasis

The interaction between amastigotes and macrophages is a key determinant for the clinical manifestation of leishmaniasis. The disease can be categorized into two main forms, cutaneous and visceral leishmaniasis (Table 1.2). Cutaneous leishmaniasis (CL) can further develop into Localized cutaneous leishmaniasis (LCL), Diffuse cutaneous leishmaniasis (DCL) and Mucocutaneous leishmaniasis (MCL). LCL is the most common form of cutaneous disease and results in ulcerative lesions on the site of sandfly bite (Figure 1.5.A). The main species responsible for LCL are *L. aethiopica*, *L. major*, *L. tropica*, *L. mexicana*, *L. amazonensis* and *L. braziliensis*.

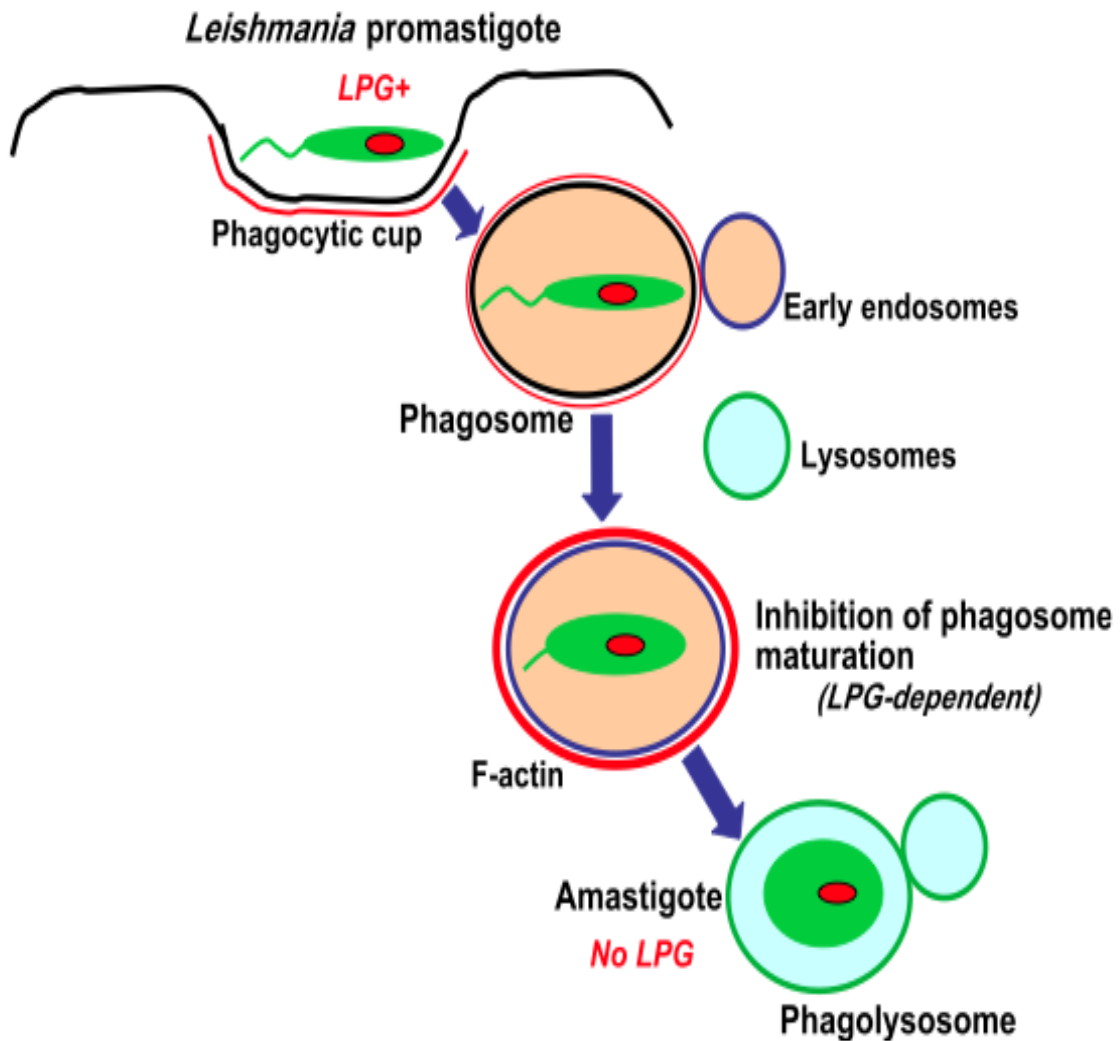


Figure 1.4. Interaction of *Leishmania* parasites with the phagocytic pathway of host macrophages. Following phagocytosis by macrophages, the promastigote is surrounded by the phagosome with additional accumulation of F-actin (red ring). Although the phagosome containing the parasite fuses with the early endosomes, the phagosome does not interact with the lysosomes until the promastigote differentiates into mature form of amastigote. Adapted from Lodge and Descoteaux, 2005.

	Disease	<i>Leishmania</i> species	Geographical distribution
Old world	Cutaneous	<i>L. aethiopica</i>	Ethiopia, Kenya
		<i>L. major</i>	North Africa, Middle east and Central Asia, Sub-saharan Africa and Sahel Belt
		<i>L. tropica</i>	Mediterranean coast
	Visceral	<i>L. donovani</i>	Indian subcontinent and Sudan
New world	Cutaneous	<i>L. mexicana</i>	Central America
		<i>L. amazonensis</i>	South America, North of Amazon
		<i>L. panamensis</i>	Panama and Colombia
		<i>L. guyanensis</i>	Pacific coast of South America
		<i>L. braziliensis</i>	South and Central America
	Visceral	<i>L. infantum</i>	Mediterranean basin, Middle east and Central Asia to Pakistan, China, Central and South America

Table 1.2. Classification of human leishmaniasis. Based upon clinical symptoms and pathology, the disease is mainly categorized into cutaneous (skin lesions) and visceral disease (organ failure and death). *Leishmania* species responsible for cutaneous and visceral leishmaniasis are linked with their geographical location. Adapted from Dawit et al., 2013.

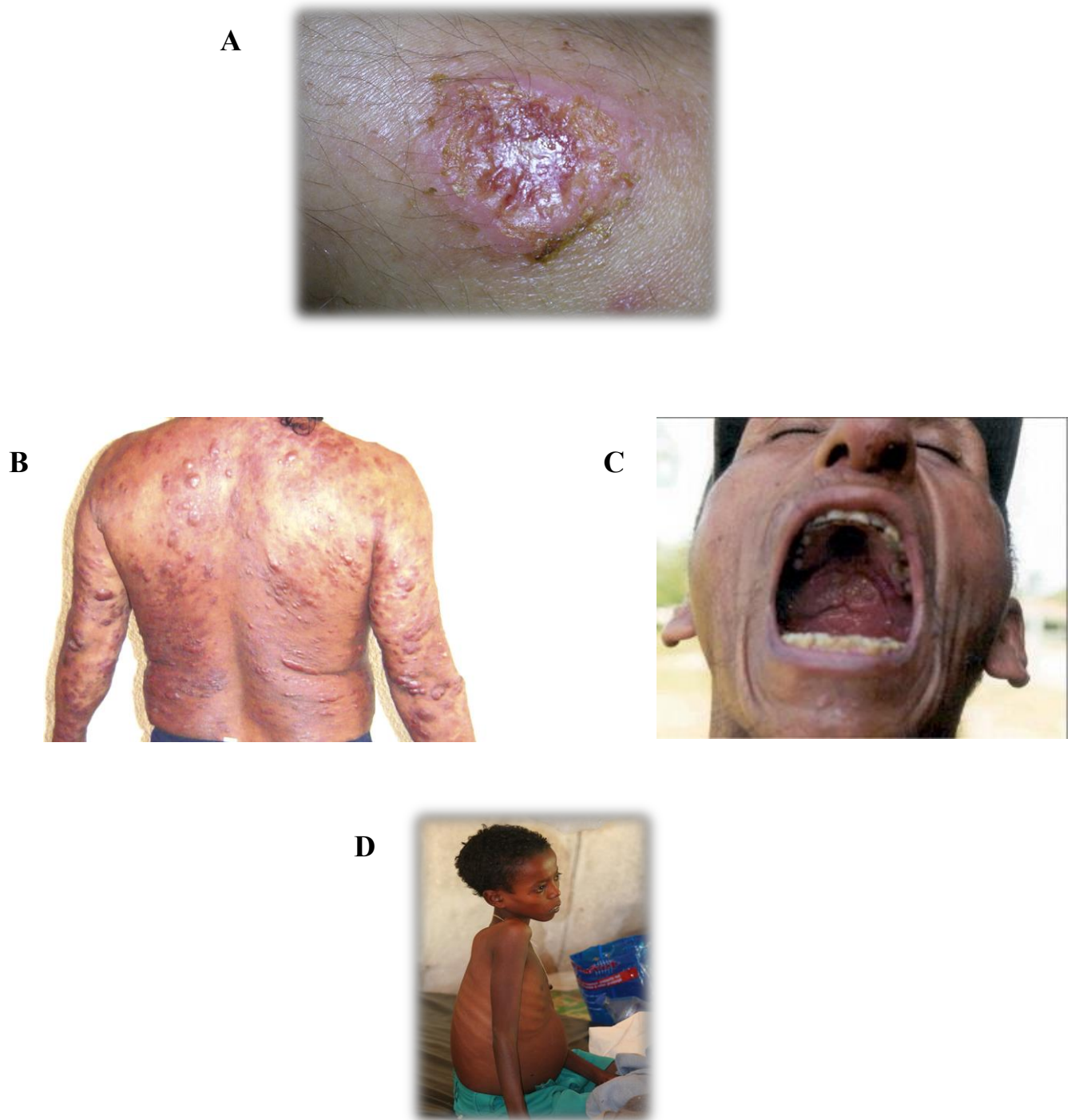


Figure 1.5. Major clinical pathologies associated with human leishmaniasis. (A) Localized cutaneous leishmaniasis. **(B)** Diffuse cutaneous leishmaniasis. **(C)** Muco cutaneous leishmaniasis. **(D)** Visceral leishmaniasis. Pictures for A and D were adapted from WHO, 2012 (www.who.int/leishmaniasis/clinical_forms_leishmaniasis). Pictures for B and D were adapted from Calvopina et al., 2006 and Reithinger et al., 2007, respectively.

DCL is an extensive and chronic form of CL, whereby multiple non-ulcerative nodules are found throughout the body (Figure 1.5.B). This is largely linked to an inefficient cell-mediated immune response against the leishmanial antigen (Desjeux, 1996). It is caused mainly by *L. aethiopica*, *L. mexicana* and *L. amazonensis* and is untreatable. MCL is characterized by the development of sores on the oronasal and pharyngeal mucosal membranes (Figure 1.5.C). This leads to facial mutilation and disfigurement and is mainly caused by *L. guyanensis*, *L. panamensis* and *L. braziliensis* and *L. aethiopica*.

Visceral leishmaniasis (VL), commonly referred to as “Kala azar”, is the most severe form of the disease (Figure 1.5.D). The infected patient is more than likely to die (99% probability), if left untreated (Kumar and Nylen, 2012). Symptoms for VL include fever, extreme weight loss, anaemia, hepatosplenomegaly, pancytopenia and hypergammaglobulinaemia (Assimina et al., 2008). The main species responsible for VL are *L. donovani* (Indian subcontinent and Eastern Africa) and *L. infantum* (Mediterranean region and Latin America). Interestingly treatment of VL infected patients with antimonial drugs can lead to a dermal sequel of this specific disease called Post-Kala-azar Dermal Leishmaniasis (PKDL). PKDL appears to be caused by the host immune response against the latent parasites in the skin, which may have migrated from the VL infected organs (Ganguly et al., 2010). The disease is endemic in the Indian subcontinent and Sudan. Although, *L. donovani* is the major culprit in both regions, there are striking differences in the time intervals between VL cure and the onset of PKDL. The Indian PKDL occurs after 1-7 years (or even 20-30 years) after VL treatment, whereas the Sudanese PKDL arises concomitantly along with VL (Ganguly et al., 2010).

1.4. Expression of virulence factors in *Leishmania*

In order for the disease development, *Leishmania* needs to continually survive and replicate in hostile environments inside the mammalian host. This influences the parasite to express a number of specific virulence factors (Table 1.3). The unicellular membrane of *Leishmania* promastigotes consist of a densely coated glycocalyx that acts as an interface between the parasite and the extracellular environment (Smith and Rangarajan, 1995). Covering the entire surface of parasite, including flagellum, this complex coat is rich in lipophosphoglycan (LPG), proteophosphoglycan (PPG), glycoprotein 63 (GP63) and low molecular weight glycoposphatidylinositol lipids (GIPLs). These molecules are covalently attached towards the surface of the parasite via the glycosylphosphatidylinositol (GPI) lipid (Descoteaux and Turco, 1999).

LPG is the major surface glycoconjugate of promastigote and is expressed at approximately 5×10^6 molecules per cell (Franco et al., 2012). LPG consists of a terminal oligosaccharide chain cap, phosphoglycan polymer (6-Gal[β 1,4]Man[α 1]-PO₄) and glycan core region inserted into the membrane via a GPI lipid anchor (Figure 1.6). During promastigote to amastigote differentiation, LPG expression becomes downregulated by at least three orders of magnitude (Sacks, 1992). Analysis of LPG mutant parasite indicates that this molecule plays a critical role in establishing infection in macrophage through counteracting free radical production and complement mediated lysis, delays phagolysosome fusion and promoting an early non-protective IL-4 host response (Spath et al., 2003; Lodge et al., 2006; Liu et al., 2009; Moradin and Descoteaux, 2012).

Interestingly, the fact that LPG mutant promastigotes are still able to infect and replicate within phagocytes suggests the existence of LPG independent survival mechanism (McNeely and Turco 1990; Spath et al., 2003).

Virulence factor	Parasite stage expression	Functions
LPG	Promastigote (Pro/Met)	Protection against complement mediated lysis (Spath et al., 2003); Impairment in phagosome maturation (Moradin and Descoteaux, 2012); Inhibition of ROS production (Lodge et al., 2006)
GP63	Promastigote (Pro/Met) and Amastigote	Protection against complement mediated lysis (Brittingham et al., 1995); Degradation of anti-microbial peptides (Kulkarni et al., 2006); Initiates receptor mediated phagocytosis (Ueno et al., 2012); Alteration of various intracellular signaling pathways (e.g. PKC, MAPK, JAK-STAT, TLR-IRAK and mTOR) (Isnard et al., 2012)
PPG	Promastigote (Pro/Met)	Induction of arginase-1 expression to promote polyamine synthesis for parasite survival (Rogers, 2012)
CP	Promastigote (Met) and Amastigote	Cleavage of MHC class II gene product to inhibit antigen presentation (De Souza et al., 1995); Inhibition of IL-12 and NO production via NF- κ b and STAT-1 degradation (Cameron et al., 2004; Abu-Dayyeh et al., 2010)
SP	Amastigote	Associated with downregulation of TLR and TNF receptors in macrophages (Swenerton et al., 2011)
PSA-2	Promastigote/Amastigote	Protection against complement mediated lysis (Lincoln et al., 2004)

Table 1.3. Summary of the diverse range of virulence factors expressed by *Leishmania*. LPG, Lipophosphoglycan; GP63, Glycoprotein 63; PPG, Proteophosphoglycan; CP; Cysteine Protease; SP, Serine Protease; PSA-2, Protein Surface Antigen; Pro, Procyclic; Met, Metacyclic; NO, Nitric oxide; ROS, Reactive Oxygen Species.

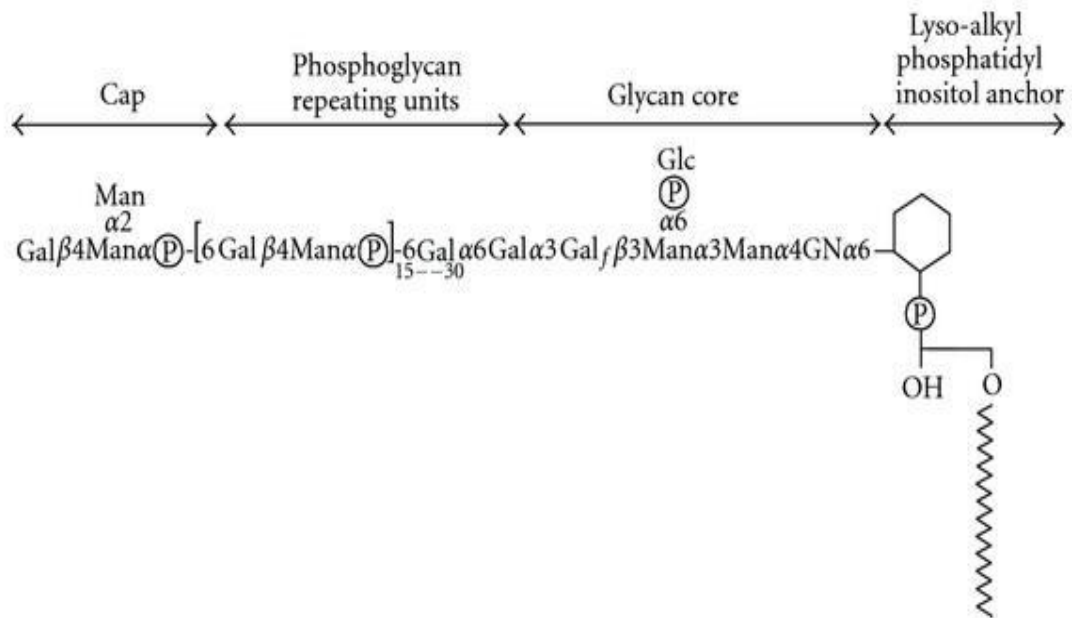


Figure 1.6. Structural organization of *Leishmania* Lipophosphoglycan (LPG). In general, LPG is composed of four domains (terminal cap, phosphoglycan repeating units, glycan core and GPI lipid anchor). In different species of *Leishmania*, the glycan core and lipid anchor remains conserved, whereas the cap structure and number of repeating phosphoglycan units becomes variable. Gal, galactose; Man, mannose; GN, glucosamine; Glc; glucose. Adapted from Franco et al., 2012.

This led to the identification of a zinc containing metalloprotease called GP63. One of the critical functions of GP63 is to prolong the parasite survival inside the phagolysosomes by altering the host macrophage signaling pathways such as JAK/STAT, MAP kinase and NF- κ B pathways (Isnard et al., 2012). Although GP63 is present both in promastigotes and amastigotes (Medina-Acosta et al., 1989), its expression is ten times higher in former than latter. Localized mainly at the parasite surface via the GPI anchor, this protein can also be secreted either through auto-proteolytic N terminal cleavage of GPI or direct release from the parasite vesicular trafficking (Ellis et al., 2002).

Similarly to GP63, another protein family called Cysteine peptidase (CP) is responsible for subverting NF- κ B signaling pathway. This resulted in the inhibition of IL-12 cytokine expression and nitric oxide production (Cameron et al., 2004; Abu-Dayyeh et al., 2010). The CP is grouped into five clans, of which clan CA family members (CPA, CPB and CPC) are the most studied due to their role in establishing host infection (Mottram et al., 2004). Expressed only in amastigotes, CPB has been clearly identified as the main virulence factor as its deletion alone caused reduced infection and fewer lesions in BALB/c mice, compared with wild type, CPA and CPC mutant parasites (Alexander et al., 1998).

Overall, the effect of the above *Leishmania* virulence factors is to disarm the microbicidal activity within macrophages. Interestingly, this effect also influences the generation of cytokines and chemokines from various other immune cells. Hence, it is very important to consider the interaction between parasite and other host immune cells.

1.5. Interaction between *Leishmania* and host immune cells

1.5.1. T cells

The involvement of T cells in regulating host immune response during leishmaniasis has been known since the late 19th century (Heinzel et al., 1989). Nevertheless, there are still contrasting views on the role of different T cells subset during *Leishmania* infection in humans (Alexander and Brombacher, 2012). This is due to large number of cases whereby patients with diverse genetic background are infected with various parasitic species, which can lead to a range of host clinical symptoms. T cells are mainly categorized into two different subsets, CD4⁺ and CD8⁺; with the former further divided into T helper 1 (Th1) and T helper 2 (Th2) cells.

Th1 cells are involved in the resolution and complete elimination of *Leishmania* (Sacks and Noben-Trauth, 2002). During infection, the binding between CD40 ligand of Th1 with CD40 receptor of macrophages causes IL-12 release from infected macrophages. The secreted IL-12 then stimulates the production of IFN- γ (from Th1 cells), which in turn activates macrophage mediated nitric oxide production to initiate parasite killing (Sacks and Noben-Trauth, 2002). These pathways are mainly observed on resistant C57BL/6 mice, where the infection site of *Leishmania* is rapidly healed. However, the parasite exposure in susceptible BALB/c mice leads to a non-healing chronic infection, which is supported by Th2 activation (Sacks and Noben-Trauth, 2002). Th2 cells are characterized as producing IL-4, IL-10 and IL-13 cytokines in response to V β 4V α 8CD4⁺ T cells activation. From the above three secreted cytokines, IL-4 is of particular importance because it downregulates the expression of IL-12 β 2 receptor of Th1 cells during *L. major* infection of BALB/c mice, hence disabling IL-12 mediated Th1 response (Himmelrich et al., 1998).

Similarly, there appears to be a multifaceted role of CD8⁺ T cells during the

course of *Leishmania* infection (Stager and Rafati, 2012). Primed to kill any invading pathogenic microorganisms, CD8⁺ T cells display cytotoxicity towards infected cells via mechanisms involving secretion of toxic granules and TNF/Fas ligand induced apoptosis (Zhang and Bevan, 2011). In the context of *L. major* infection in mice, INF- γ production from CD8⁺ T cells were directly responsible for activating Th1 mediated healing response (Uzonna et al., 2004). However, this phenomenon appeared to be dependent on parasite inoculation as high concentration of *L. major* promastigotes had no impact on CD8⁺ T cell activation, even though the lesion healed via Th1 response (Uzonna et al., 2004). During visceral leishmaniasis in mice, the CD8⁺ T cells induced cytotoxic activity towards infected cells through FasL/Fas mediated apoptosis, followed by INF- γ and TNF- α secretions (Tsagozis et al., 2003). However, the authors also observed secretion of pro-inflammatory chemokines, such as MIP-1 α (Macrophage Inflammatory Protein-1) and RANTES (Regulated on Activation Normal T cell Expressed and Secreted) from CD8⁺ T cells in response to *L. infantum* infection, which severely questions the protective nature of CD8⁺ T cells.

1.5.2. Natural Killer (NK) cells

During *Leishmania* infection, NK cells are activated in response to various cytokines such as IL-12 (from myeloid dendritic cells), IL-2 (from Th1 cells), INF- α/β and IL-18 (from macrophages) (Bogdan, 2012). NK cells are engaged in protective immune response against *Leishmania* parasites. For example, in cutaneous leishmaniasis in mice, NK cells depletion prevented the elimination of *L. amazonensis* (Laurenti et al., 1999; Sanabria et al., 2008). As for visceral disease, it was shown that mice NK cells activated by IL-12/IL-18 released INF- γ and TNF- α , which in turn led to the nitric oxide production in *L. infantum* infected macrophages and subsequent parasite death (Prajeeth et al., 2011).

1.5.3. Neutrophils

Neutrophils are the first immune cells involved in the phagocytosis of *Leishmania* (Peters et al., 2008). In addition to hosting the parasite, neutrophils are thought to act as a Trojan horse for the transfer of *Leishmania* into macrophages (Figure 1.7). The model suggest that promastigotes delay spontaneous apoptosis of infected neutrophils for 2-3 days after which the infiltrating macrophages are able to phagocytize the apoptotic neutrophil harboring promastigotes (Laskay et al., 2003). However, conflicting evidence have been emerging that challenge this model. For example, NET released by human neutrophils was found to be effective in direct killing of *L. amazonensis* promastigotes (Guimaraes-Costa et al., 2009). Similarly, *L. major* was susceptible to neutrophil elastase mediated activation of macrophage in C57BL/6 mice (Ribeiro-Gomez et al., 2007). In summary, the exact role of neutrophils on *Leishmania* infection needs future investigation.

1.5.4. Macrophages

Macrophages are the definitive host cells for *Leishmania* survival and replication. With a distinctive pseudopodia membrane structure, macrophages are involved in the phagocytosis and subsequent killing of foreign microbes (Dale et al., 2008). However, intracellular pathogens such as *Leishmania* have evolved strategies to counteract the microbicidal activity of macrophages. In order to understand how such potent killing ability is inactivated, the precise molecular events that take place in the early, intermediate and late phase of *Leishmania* infection will be discussed in the following section.

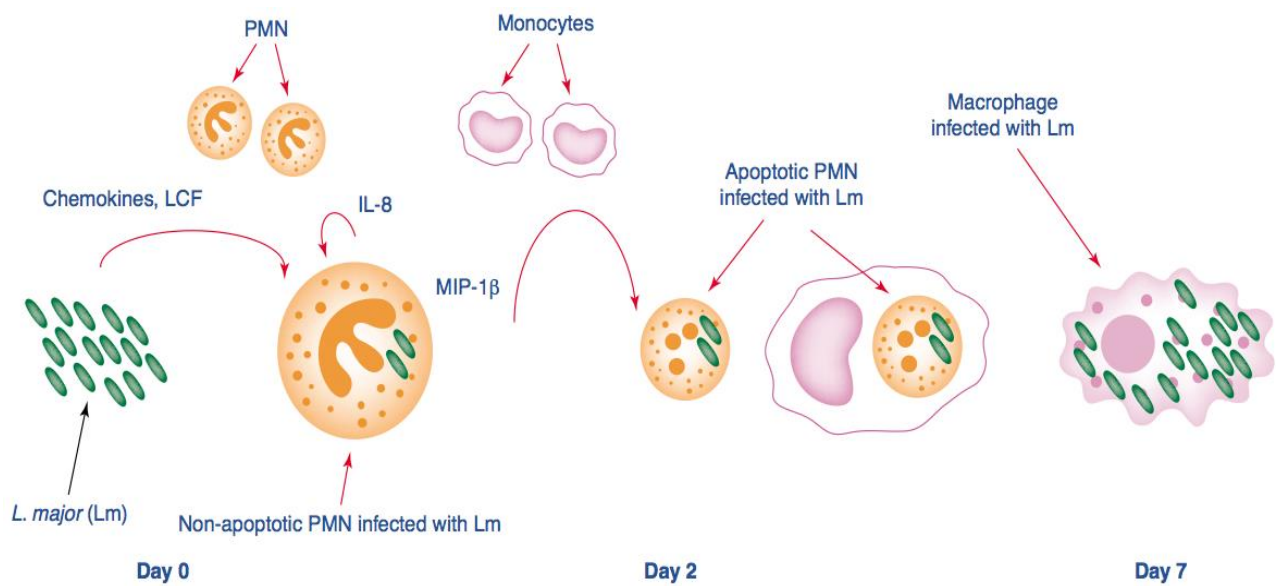


Figure 1.7. Trojan horse model for neutrophils. *Leishmania* promastigotes, which are inoculated by the sandfly, are primarily phagocytized by neutrophil (PMN). The promastigotes delays apoptosis of the infected neutrophils for 2 days, giving monocytes/macrophages enough time to enter the site of infection. After 2 days, the apoptotic neutrophils (containing promastigotes) are phagocytized by macrophages. In this way, promastigotes silently enter and replicate within macrophages without activating its microbicidal activity. Adapted from Laksay et al., 2003.

1.6. Molecular interaction between *Leishmania* and macrophage

1.6.1. Phagocytic uptake of *Leishmania*

The primary survival mechanism for metacyclic promastigote is to be engulfed by macrophages through receptor mediated phagocytosis (Ueno and Wilson, 2012). Receptors that are known to facilitate the phagocytosis of metacyclic promastigote include the complement receptor family (CR3 and CR1) and fibronectin receptor (FnR) (Figure 1.8); all of which will be discussed below.

CR3 is an integrin, which is comprised of complement and lectin binding sites (Quinton-Leslie, 2001). Localized on the surface of macrophage and neutrophil, the function of CR3 ranges from binding to inactivated complement (iC3b) and pathogen ligands to assisting phagocyte migration and actin cytoskeletal rearrangement. The promastigotes GP63 is responsible for binding with CR3 either directly on the lectin domain or indirectly to the complement binding sites via iC3b opsonin (Blackwell et al., 1985; Mosser and Wilson, 1985). The iC3b is generated following CR1 mediated cleavage of C3b opsonin (Sutterwala et al., 1996; Rosenthal et al., 1996).

Similar to CR3, the FnR can either bind directly or indirectly (via fibronectin opsonin) to the GP63 ligand of promastigote (Brittingham et al., 1999). FnR is an integrin comprised of alpha and beta subunits, which is found in immune (e.g. monocytes and macrophages, neutrophils) and non-immune (e.g. fibroblast) cells. Interestingly, GP63 is responsible for the degradation of fibronectin opsonin to generate ICS (Interconnecting Segment) fragment (Kulkarni et al., 2008). This resulted in the binding between GP63 and ICS that prevented the superoxide production while still allowing FnR mediated phagocytosis (Kulkarni et al., 2008).

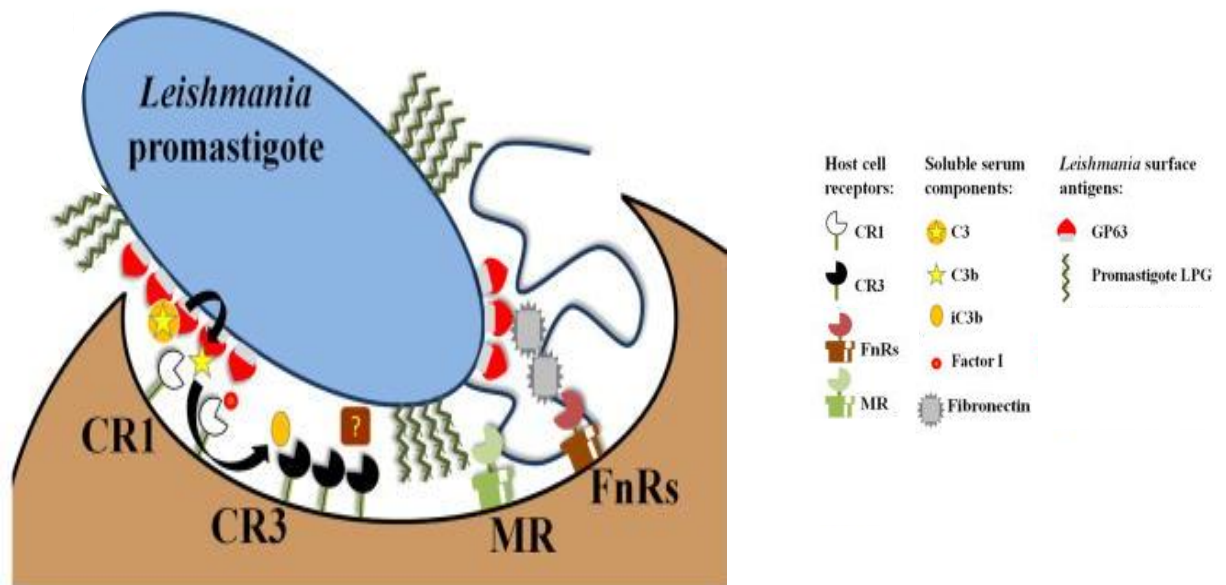


Figure 1.8. Two different types of receptor mediated approach undertaken by macrophage to phagocytose metacyclic promastigote. The GP63 expressed in promastigotes convert C3 opsonins into C3b, the natural ligand for Complement Receptor 1 (CR1). CR1 (with factor I) cleaves C3b into iC3b, which acts as a bridge between GP63 and CR3. CR3 may also mediate direct binding to promastigotes via a yet unknown surface epitope on promastigotes, possibly Protein Surface Antigen (PSA-2). GP63 also binds fibronectin, which then bridges the parasite to Fibronectin Receptor (FnR) for phagocytosis. It should be noted that Mannose Receptor (MR) is only involved in phagocytosis of procyclic promastigotes. Adapted from Ueno and Wilson, 2012.

1.6.2. Survival strategy for *Leishmania*

Following phagocytosis, *Leishmania* promastigote builds a safe niche within the infected macrophages. In order to achieve this, the LPG of promastigote delays the fusion of endosomes and lysosomes (Dermine et al., 2000; Rodriguez et al., 2011). In addition, the promastigote induces the accumulation of various actin polymerisation molecule including F-actin, Arp2/3, WASP and α -actinin around the phagosomes. Similarly, families of Rho GTPase, such as RhoA, cdc42 and Rac-1 have also been retained within the phagosome during phagocytosis (Lodge and Descoteaux, 2008). Although the reason behind the accumulation of these various molecules is unclear, it may block the recruitment of vesicle trafficking proteins required for phagolysosome formation, hence contributing to the survival of parasites (Figure 1.9).

1.6.3. Modulation of intracellular signaling pathways during *Leishmania* infection

Successful inhibition of lysosome fusion represents the earliest survival strategy of *Leishmania*. However, in order to further evade the host immune response, the parasite interferes with many signaling pathways of the macrophages (Table 1.4). The Nuclear Factor (NF)- κ B transcription factor, which is the master regulator of innate immunity, is one of the targets for *Leishmania*. The family of NF- κ B is comprised of five subunit members including: Rel-A (p65), c-Rel, Rel-B, p50 and p52, of which the first three possess higher transactivation domain activity than the latter two. In unstimulated cells, the subunit dimer (mainly p65-p50) is bound to an inhibitor I κ B α . Following stimulation, the degradation of inhibitor releases the dimer, which translocate into the nucleus to induce gene expression of various inflammatory cytokines and chemokines (Figure 1.10).

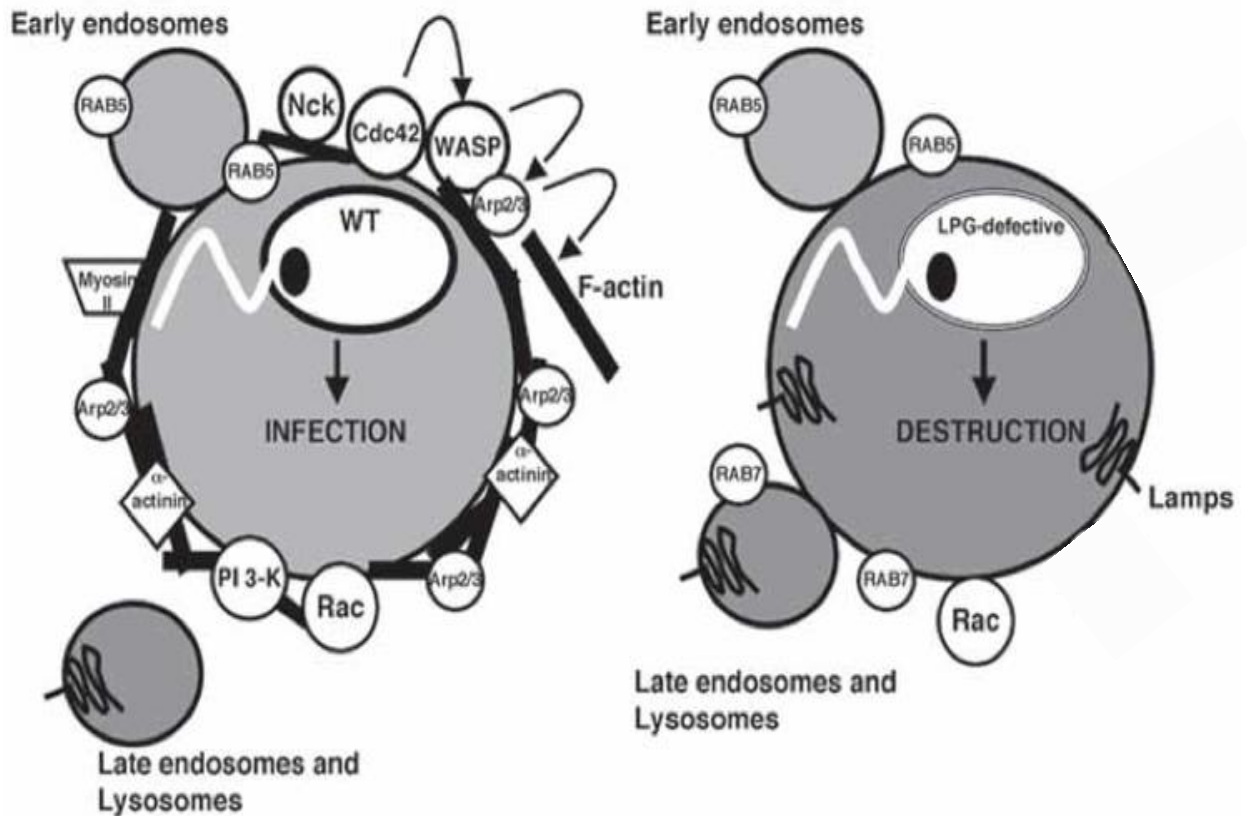


Figure 1.9. Schematic representation showing the differences in the molecular interaction of endosomal vesicles with the Wild type (Wt) and LPG defective (mutant) *Leishmania promastigote*. Within minutes from phagocytosis, both Wt and mutant parasites are localized inside the phagosome and interacts with the early endosomes. However, in contrast to mutant, the Wt induces F-actin accumulation through recruitment of Cdc42, WASP and Arp2/3. It is thought that accumulation of the above molecules around the phagosome may delay the recruitment of LAMP and RAB7 (markers for late endosomes and lysosomes), subsequently delaying the fusion between phagosome and acid hydrolase containing lysosomes. This inhibition of lysosome fusion would allow the virulent promastigote to survive. As for mutant form, there is a rapid recruitment of LAMP and RAB7 associated lysosomes resulting in the destruction of the parasites. Adapted from Lodge and Descoteaux, 2008. WASP, Wiskott-Aldrich Syndrome Protein; LAMP, Lysosome-associated membrane glycoprotein; Nck, Non-catalytic region of tyrosine kinase adaptor protein 1; PI3-K, Phosphoinositide 3- kinase

Signaling pathways	Macrophage function	<i>Leishmania</i> mediated alteration
Protein Kinase C (PKC)	Production of reactive oxygen species (ROS)	Downregulation of PKC expression, which reduces phosphorylation of p67 and p47 subunits of NADPH oxidase (Bhattacharya et al., 2001). This leads to inhibition of ROS production.
JAK/STAT	Production of nitric oxide (NO)	De-phosphorylation of JAK (via phosphatase activation) and/or proteasome mediated STAT degradation causes reduced translocation of transcription factors necessary for NO production (Blanchette et al., 1999; Forget et al., 2005).
ERK1/2 and p38 MAPK	Induction of inflammatory cytokines	Downregulation of p38 MAPK leads to IL-12 inhibition whereas activation of ERK1/2 leads to IL-10 secretion (Mathur et al., 2004; Yang et al., 2007).
NF-κB	Induction of inflammatory cytokine and NO production	Degradation of p65 NF-κB subunit results in IL-10 expression and inhibits IL-12 and NO production (Cameron et al., 2004; Guizane-Tabbane et al., 2004; Calgeri-Silva et al., 2009).

Table 1.4. Summary of the diverse macrophage signaling pathways altered by *Leishmania*. JAK/STAT, Janus Kinase/Signal Transducer and Activation of Transcription; ERK, Extracellular Regulated Kinase; MAPK, Mitogen Activated Protein Kinase; NF-κB, Nuclear Factor kappa B; SHP-1,

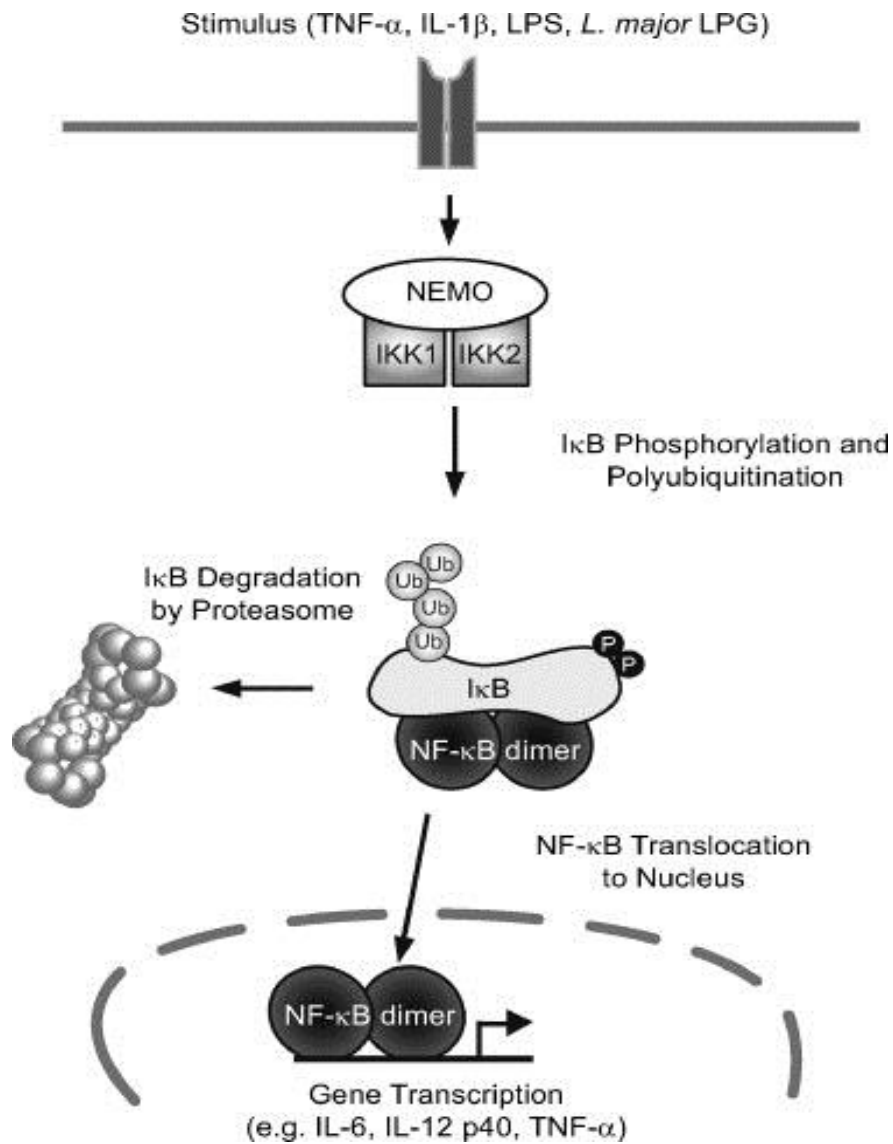


Figure 1.10. Upstream and downstream effectors in NF- κB signaling pathway. Initially, NF- κB dimer is inactivated due to its binding with an inhibitory IκB protein in un-stimulated cells. In the presence of diverse range of stimuli including, TNF-α, IL-1β, LPS and LPG, the activated receptor transduces the signal towards the IKK complex (NEMO, IKK1 and IKK2). The complex phosphorylates two serine residues of IκB, which targets IκB for ubiquitination and subsequent proteosomal degradation. This causes the release of NF- κB dimer, which translocate to the nucleus to induce the transcription of various gene targets. NF- κB, Nuclear Factor-kappa B; TNF, Tumor Necrosis Factor; IL-1, Interleukin-1; LPS, Lipopolysaccharide; LPG, Lipophosphoglycan. Adapted from Reinhard et al., 2012.

Both promastigotes and amastigotes form of *Leishmania* modulate NF- κ B signaling response. For example, *L. amazonensis* promastigotes were shown to activate the p50-p50 dimer (repressor complex) while causing degradation of p65 proteins at the same time of infection, hence resulting in reduced iNOS genes expression required for NO production (Calegari-Silva et al., 2009). Similarly, a study involving wider range of promastigote species including *L. major*, *L. mexicana*, *L. donovani* and *L. braziliensis* found that all parasites cleaved p65 into p35 subunit, which in turn dimerized with p50 (Gregory et al., 2008). This heterodimer induces various chemokines (examples: MIP-1 α , MIP-1 β and MCP-1) that cause recruitment of phagocytes (without activating iNOS genes) and eventual tissue destruction (Gregory et al., 2008). In another study, degradation of p65 was also observed during *L. major* and *L. mexicana* amastigotes infection resulting in the induction of IL-10 (Guizane-Tabbane et al., 2004) and inhibition of LPS induced IL-12 production (Cameron et al., 2004), respectively.

In summary, the above findings have provided substantial evidence of *Leishmania* capability to manipulate the signaling pathways of host macrophages. Both promastigotes and amastigotes survive by downregulating of pro-inflammatory cytokines, NO production and upregulating anti-inflammatory cytokines (Summarized in Figure 1.11).

1.6.4. Dissemination of *Leishmania*

Following the intracellular survival and replication of amastigotes, *Leishmania* parasite must disseminate from infected to neighboring uninfected macrophages. This process of cell-to-cell spreading is a critical step for the development of leishmaniasis pathogenesis.

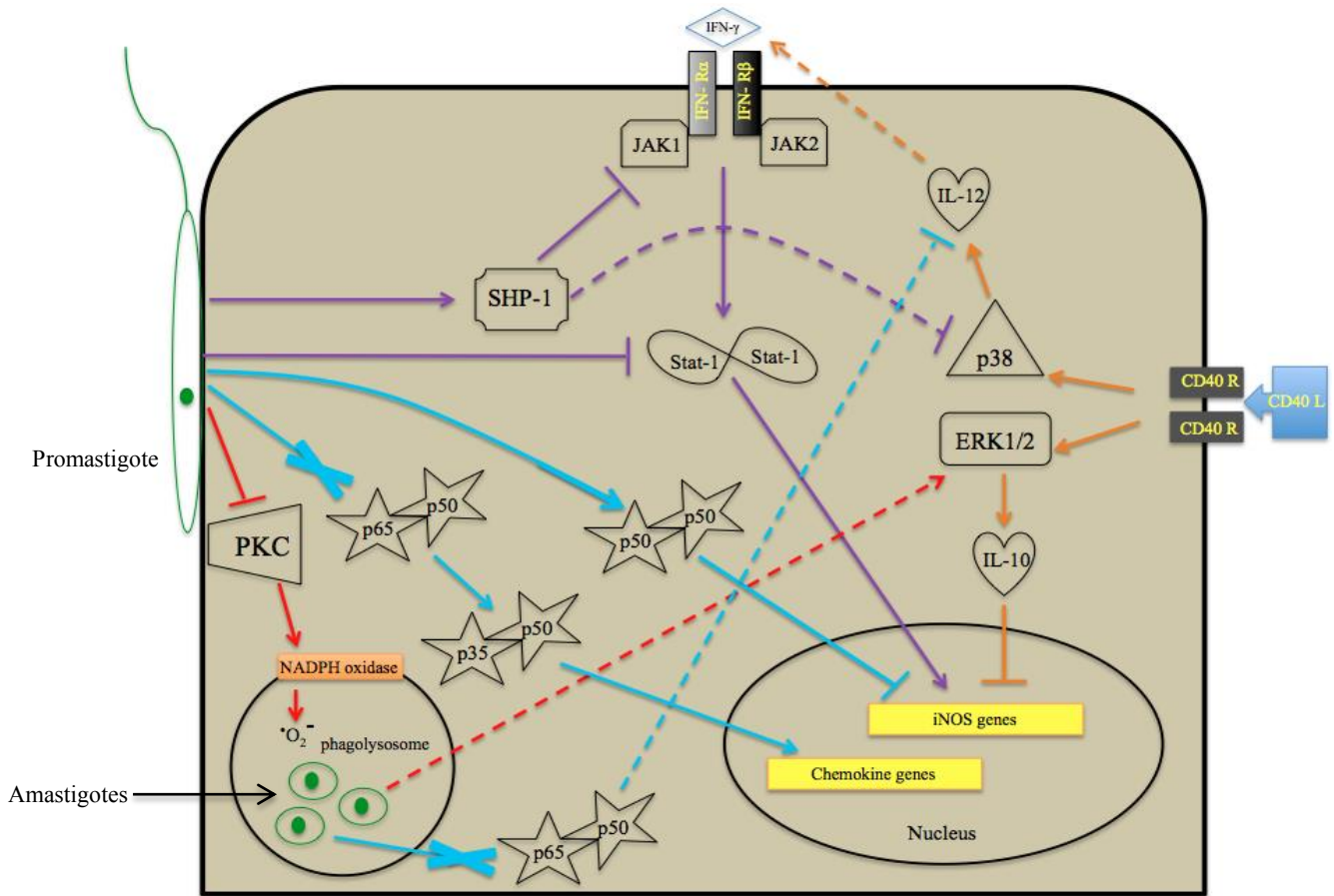


Figure 1.11. Schematic diagram representing the disruption of macrophage signaling pathways during *Leishmania* infection. The promastigotes and amastigotes modulates various signaling molecules associated with inflammatory pathways including PKC (red line), JAK-STAT (purple line), MAPK (orange line) and NF- κ B (blue line). Briefly, the promastigote inhibits PKC, resulting in the defective formation of NADPH oxidase and blocking superoxide radical production, which leads to survival of replicating amastigotes inside phagolysosome. Similarly, the promastigote can directly or indirectly (via SHP-1 activation) prevent IFN- γ stimulated Stat-1 dimer translocation that leads to repression of iNOS genes required for NO production. Moreover, SHP-1 activation is responsible for the de-phosphorylation of p38 (member of MAPK). This inhibits IL-12 production which in turn reduces IFN- γ release from T cells. Interestingly, amastigotes induces ERK1/2 mediated IL-10 production, which suppress iNOS gene expression. Finally, both forms of *Leishmania* degrade p65 subunit of NF- κ B to induce chemokine genes expression and suppress the IL-12 production. Additionally, the promastigote also activate the p50-p50 dimer in order to inhibit iNOS gene expression. Dotted lines represent cross talk between two signaling pathways. PKC, Protein Kinase C; JAK-STAT, Janus Kinase – Signal Transduction of Activated Transcription; MAPK, Mitogen Activated Protein Kinase; NF, Nuclear Factor; SHP-1, Src-homology 2 domain containing Phosphatase -1; IFN, Interferon; IL, Interleukin.

It has been generally assumed that parasitic egress occurs via host cell lysis following amastigote replication. However, a recent study showed that the released *L. amazonensis* amastigotes remained surrounded by host membranes until engulfed by uninfected macrophages (Real et al., 2014). This finding was linked with an *in vivo* study from Belkaid and colleagues (Belkaid et al., 2000). By infecting C57BL/6 mice with low dose of *L. major* promastigotes, the authors detected a sharp increase in parasite number for first four weeks after infection without accompanying any inflammatory lesions (Figure 1.12). This silent phase could be representative of apoptotic mediated parasite spreading. Apoptotic cell death is the removal of damaged or dying cells without eliciting host immune response. Hence, it is possible to speculate that the parasite could hijack the mechanism of apoptosis of infected macrophage and hide inside the apoptotic bodies without alerting the host adaptive immunity.

Therefore the physiological significance of apoptosis (section 1.7) and its current role during pathogenic infection (section 1.8) will be discussed before exploring the relationship between *Leishmania* infection and host cell apoptosis (section 1.9).

1.7. Apoptosis

Apoptosis is an evolutionary conserved process of cell death, which occurs in a controlled manner. Apoptosis allows the elimination of dead cells without causing any damage to the surrounding cells, therefore avoiding inflammation and any consequent immune response (Danial and Korsmeyer, 2003).

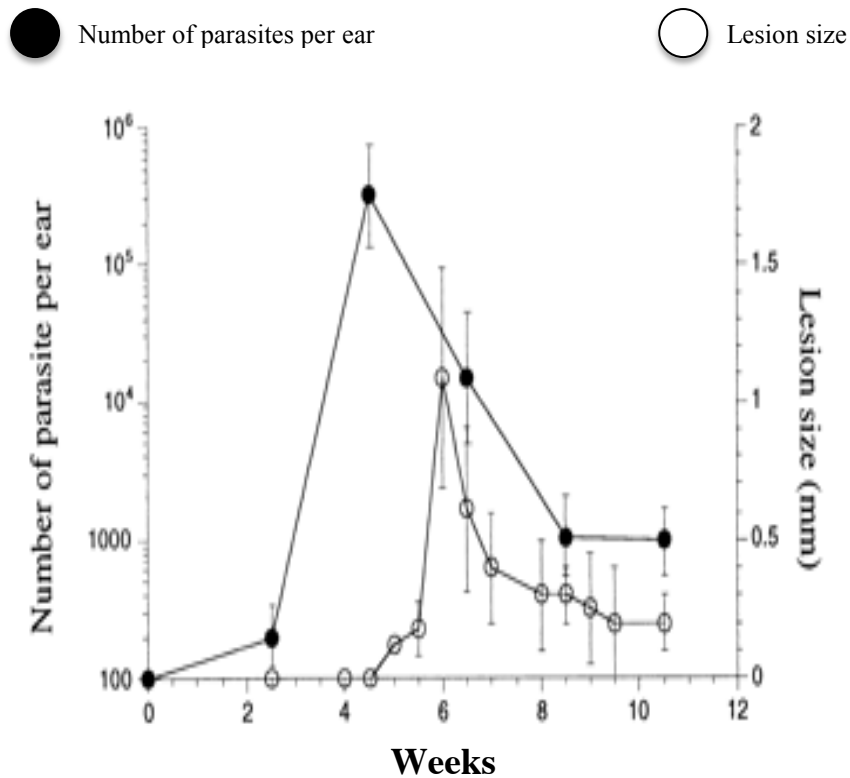


Figure 1.12. Evolution of dermal lesions in C57BL/6 mice during *Leishmania* infection. Intradermal inoculations with *L. major* metacyclic promastigotes (~100) were carried out on both ears of C57BL/6 mice. The numbers of parasites and lesion size were monitored and examined every 2 and once a week, respectively, over a period of 10.5 weeks. From week 2 to 4, a dramatic rise in the parasitic load per ear was observed without accompanied by any lesion development. The first appearance of lesion (1±0.5mm) was detected at week 6 and was coincident with a dramatic reduction (~95%) in parasite number from week 4 to 9. The lesion development was resolved before week 12. Adapted from Belkaid et al., 2000.

The characteristic features of apoptotic cells include plasma membrane blebbing, changes in the distribution of membrane lipids and enzymatic fragmentation of chromosomal DNA (Green, 2005). The significance of apoptosis has been well characterized in the development of mammalian homeostasis from removal of tissue cells between the developing finger digit of the fetus to removal of self-reactive T and B-lymphocytes (Jacobson et al., 1997).

There are two main signaling pathways, which participate in the induction of apoptosis. These are extrinsic and intrinsic pathways (Figure 1.13). The extrinsic pathway involves the activation of death receptors whereas the intrinsic pathway is activated intracellularly in response to cellular stress such as UV radiation and DNA damage. Although the source of activation is distinct, both pathways utilize specialized mediators of cysteine proteases called caspases, which are synthesized as inactive pro-caspase (Siegel, 2006). There are two groups of caspases involved in apoptosis; initiator and executioner caspases (Kumar, 2007). As their name suggest, the initiator caspases (e.g. caspase 2, 8, 9, 10 in humans) are the first caspase to be generated from the proteolytic cascade, whose role is to cleave and activate other pro-caspase, i.e. executioner caspases. The executioner caspases (e.g. caspase 3, 6 and 7 in humans) then cleave varieties of target proteins associated with the structure and integrity of cell membrane and DNA (Kumar, 2007). The engagement of caspases during extrinsic and intrinsic pathways will be discussed below.

The extrinsic pathway is initiated following the activation of death receptors. Homo-trimer in nature, this type of receptors is a member of large TNF receptor super family, which includes Fas and TNF receptor itself (Aggarwal, 2003).

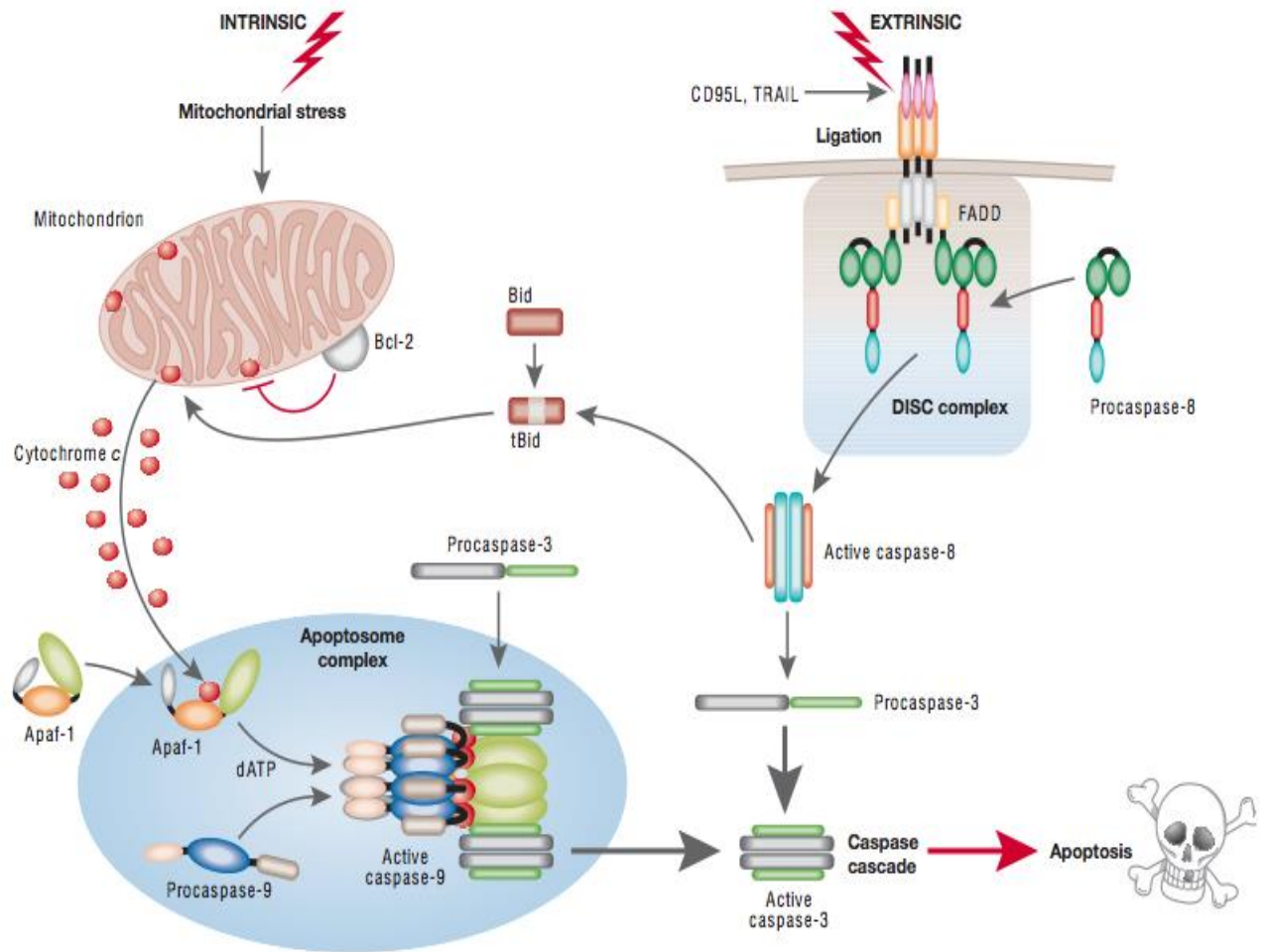


Figure 1.13. Mechanism of apoptosis is comprised of extrinsic and intrinsic pathways. Extrinsic and intrinsic pathways are activated by death receptors and stress-inducing stimuli, respectively. Briefly, triggering of death receptors, i.e. TNF and TRAIL receptors, initially causes rapid activation of the initiator caspase-8 following the DISC formation. Similarly, in the intrinsic pathway, stress induced apoptosis results in perturbation of mitochondria, releasing cytochrome c from the inner mitochondrial membrane space. The cytochrome c, which is regulated by anti-apoptotic Bcl-2 and pro-apoptotic Bax family members, binds to Apaf-1 resulting in the formation of Apaf1-caspase 9 apoptosome complex and activation of caspase-9. The activated initiator caspases 8 and 9 then activate effector caspases 3, 6 and 7, which are responsible for the cleavage of cellular substrates resulting in the classical biochemical and morphological changes associated with apoptotic phenotype. Adapted from Macfarlane and Williams, 2004.

For example, in Fas mediated apoptosis, trimers of Fas ligand binds to Fas receptor and results in clustering of death domain (MacFarlane and Williams, 2004). This allows the death domain to recruit a specific type of adaptor protein called FADD (Fas-associated via death domain), which comprises of death domain and death effector domain (DED). The death receptor and FADD bind via the death domain, leaving DED to recruit the initiator pro-caspase-8 (Figure 1.13). The resulting formation of complex between death receptor, adaptor protein and caspase is called Death Inducing Signaling Complex (DISC). Within the DISC, the initiator pro-caspase-8 molecules are brought into close proximity, resulting in self-activation. Once activated, the initiator caspase 8 is released from the DISC and leads to downstream activation of executioner pro-caspases (Macfarlane and Williams, 2004).

In contrast, the activation of the intrinsic pathway depends upon the release of mitochondrial protein known as cytochrome C (Jiang and Wang, 2004). During cellular stress, cytochrome C is released from the inter-membrane space of mitochondria to the cytoplasm and binds to an adaptor protein called Apaf-1 (apoptotic protease activating factor-1). Each Apaf-1 (bound with cytochrome C) then oligomerizes with the remaining six Apaf-1 proteins to form a wheel like heptamer called an apoptosome (Figure 1.13). The Apaf-1 in the apoptosome then recruits initiator pro-caspase-9, which are activated by close proximity in the apoptosome. The activated caspase-9 then cleaves and further activates the downstream executioner caspases (Kumar, 2007).

Similar to various biological processes, the intrinsic pathway of apoptosis is tightly regulated to ensure that a cell death occurs only when there is an apoptotic stimulus. There are two major regulators of intracellular proteins, which include: Bcl-2 family and IAP (Inhibitors of Apoptosis). The Bcl-2 family comprise of pro-apoptotic (e.g. Bax, Bak, Bad, Bid, Bim) and anti-apoptotic (e.g. bcl-2 and bcl-xl)

members. In addition, the pro-apoptotic group is further divided into two classes; BH123 (e.g. Bax and Bak) and BH-3 only proteins (e.g. Bad, Bim, Bid, Puma and Noxa). The inactive forms of BH123, which are membrane bound, aggregates and oligomerize to form a pore in the presence of an apoptotic stimulus, resulting in cytochrome C release (Danial, 2007). In the absence of an apoptotic stimulus, the anti-apoptotic bcl-2 proteins, which are located in the cytosol, directly inhibit the BH123 proteins (Danials, 2007). It has been proposed that an apoptotic stimulus activates the BH3-only protein and directly inhibits the anti-apoptotic bcl-2 protein by binding via the BH3 domain. Since the inhibition effect of bcl-2 protein is removed, the BH123 protein becomes activated, thereby releasing cytochrome C and inducing apoptosis (Shamas-Din et al., 2011). Finally, IAP is a group of cytosolic protein that provides further regulation in the intrinsic pathway. The mechanism of inhibition by IAP is either through direct binding or marking caspases with ubiquitin for proteasome degradation (Wei et al., 2008). However, in the presence of an apoptotic stimulus, anti-IAP (e.g. Smac/Diablo and Omi) is also released from mitochondria via the oligomeric pore of BH123 protein (Wei et al., 2008). These anti-IAP proteins bind and block the inhibitory activity of IAP, triggering caspase activation and apoptosis.

1.8. Infection and Apoptosis

The innate immune effector cells such as macrophages kill foreign microbes through phagocytosis and helps to prime the development of adaptive immunity, leading to the prevention of excessive tissue damage. In failure to eliminate infecting pathogens, macrophages will be programmed to undergo apoptosis as a last resort to resolve the infection. However, intracellular pathogens have evolved strategies to regulate host apoptosis (Thi et al., 2012). Depending upon the source and stage of infection, intracellular pathogens can either block apoptosis to protect its intracellular

niche or induce apoptosis to disseminate its progeny and evade the immune system (Swanson and Fernandez-Moreira, 2002; Thi et al., 2012). The following section will include findings that have been reported for bacterial, viral and protozoan infection and eventually discuss the current insight of how *Leishmania* species subvert apoptosis.

Pathogenic bacterial species, including *Legionella*, *Helicobacter* and *Chlamydia* are known to inhibit apoptosis to facilitate intracellular replication, whereas, *Yersinia* is known to only promote host cell apoptosis (Ashida et al., 2011). Interestingly, *Mycobacterium tuberculosis* exerts two distinctive strategies during macrophage infection to control cell death; the pathogen postpones cell death during early infection (Miller et al., 2010) but induces cell death in the later stage of infection to promote bacterial egress (Aguilo et al., 2013).

Similarly the balance between survival and apoptosis is also found in viral infected cells. Adenovirus, which is responsible for upper tract respiratory infection in humans, utilizes its transcription factor E1b 19k protein (homologue of bcl-2 protein) to suppress FasL and TNF induced apoptosis by inhibiting the activation of caspase-3 and processing of caspase substrate called PARP (O'Brien, 1998). However, the virus also encodes pro-apoptotic death proteins, such as E311.6 K and E4orf4 during the later stage of infection, whose probable role is to promote efficient cell lysis and release from the infected cell (Tollefson et al., 1996; Shtrichman et al., 1999).

Depending on the genus, infection with protozoa also elicits either apoptotic induction or inhibition of the host. *Trypanosoma brucei*, which causes African sleeping sickness disease, has been recently reported to induce B cell apoptosis so as to deplete the antibody response of the host (Bockstal et al., 2011). In addition, malaria causing Plasmodium species of *P. yeolli* prevented Fas mediated apoptosis of hepatocytes via Bcl-2 activation, which resulted in higher parasitic load and survival

rate (Kaushansky et al., 2013).

As for *Leishmania*, Moore and Mathlaskewski in 1994 were the first to report on the interaction between infection and apoptosis, where the authors found that *L. donovani* prevented the BALB/c mice macrophage from undergoing apoptosis in the absence of stimulating factors (Moore and Mathalaskewski, 1994). Since apoptotic detection from the above report was solely based upon DNA fragmentation, Akarid and colleagues demonstrated that the prevention of apoptosis by *L. major* was due to blockage in cytochrome C release and subsequent caspase-3 activation (Akarid et al., 2004). Further studies have now shown that various *Leishmania* species including *L. infantum*, *L. major*, *L. amazonensis*, *L. pifanoi* suppress the host cell apoptosis induced with various apoptotic inducers through intracellular mechanism such as PKC cleavage, NF- κ B, PI-3 kinase and Bcl-xL (Lisi et al., 2005; Ruhland et al., 2007; Donovan et al., 2009). Thus, from above findings it is clear the *Leishmania* parasites can interfere with the apoptotic process to protect its intracellular niche to allow survival and replication. In contrast, few studies have reported apoptotic induction during late stage of *Leishmania* infection (Getti et al., 2008; DaMata et al., 2015). However, these findings have not provided any evidence of an association between host cell apoptosis and *Leishmania* spreading.

Therefore, an urgent need is required to study the relation between *Leishmania* infection and apoptotic induction in order to consider the disease pathogenesis of leishmaniasis.

1.9. Aims of the Thesis

Although advances have been made in clarifying the infection mechanism behind human leishmaniasis, there is a major lack of understanding surrounding the late interaction between *Leishmania* and its mammalian host cells. One of such area in the field of *Leishmania* biology is the virulent strategy of amastigotes to disseminate from infected to uninfected healthy macrophages during late stage of infection in human cells. This is an exciting research area for parasitology and immunology because this process represents the basis for the development of disease pathogenesis. Although a number of studies have demonstrated a crucial link between *Leishmania* infection and host apoptosis, there is only one study that has provided evidence supporting a link between apoptosis and parasitic spreading (Real et al., 2014). However the infection model from this earlier study is based on macrophages derived from mice, which are not an ideal model for human *Leishmania* infection (Loria-Cervera and Andrada-Narvaez, 2014).

It is therefore an utmost importance to generate an *in vitro* infection model comprising of human macrophages to allow studies of late infection stages. To date, studies based on human cells are limited to early stages of infection. Such model will then form the basis for elucidating the mechanism behind cell-to-cell spreading of *Leishmania* parasites.

Hence, the five major aims of this project are:

1. To establish whether there is a link between *Leishmania* infection and human macrophages apoptosis *in vitro* using a current infection model.
2. To develop and validate *in vitro* infection model representative of the late stage of human macrophages infection to study the dissemination of *Leishmania*.

3. To use the above model to clarify whether there is a link between parasites spreading and host cell apoptosis. This will be carried out by determining the effect of spreading on two major markers of apoptosis: Phosphatidyl serine (PS) externalization and caspase-3 activation.
4. To define the mechanism by which *Leishmania* modulates human macrophage apoptotic pathways. Three major signaling pathways associated with apoptosis including AKT, PKC and NF- κ B will be investigated.
5. To quantify and evaluate the global cellular response of human macrophages during *Leishmania* spreading. Through isotopic labeling coupled with tandem mass spectrometry (MS/MS) approach, comparative analysis will be performed to determine quantitative changes in protein between uninfected and infected cells.

Chapter 2 – Materials and Methods

2.1. Parasite culture

The promastigotes of four *Leishmania* species, *L. aethiopica* (MHOM/ET/72/L100), *L. major* (MHOM/SU/73/5ASKH), *L. mexicana* (MNYC/BZ/62/M379) and *L. tropica* (MHOM/SU/58/OD) were obtained from the London School of Hygiene and Tropical Medicine (LSHTM). A green fluorescent protein (GFP) reporter gene construct (pRib1.2 α Neo α GFP) was transfected by Patel and colleagues in the above four species, which resulted in the constitutive expression of GFP throughout their life cycle, hence allowing flow cytometry and fluorescence microscopic analysis (Patel et al., 2014). For simplicity, the transgenic GFP expressing *Leishmania* clones were named as: L8G (*L. aethiopica*), S1G (*L. major*), M5G (*L. mexicana*) and O5G (*L. tropica*). The promastigotes were grown in Schneider's Drosophila Medium (Fisher Scientific, UK) supplemented with 23% Foetal Calf Serum (FCS) (Fisher Scientific) and 1 \times Penicillin-Streptomycin-Glutamine (Fisher Scientific) at neutral pH. The parasites were sub-cultured once a week at a concentration of 1 \times 10⁶ per ml, supplemented with 700 μ g/ml of G418 (Sigma, UK), and were incubated at 24°C cooling incubator.

2.2. Human cell culture

Human THP-1 monocyte (ATCC) was sub-cultured, every 3 days, at a concentration of 2.5 \times 10⁵ per ml in complete RPMI 1640 medium (Fisher Scientific) and incubated at 37°C in a humidified CO₂ (5%) incubator. The medium was made complete following supplementation with 10% FCS and 1 \times Penicillin-Streptomycin-Glutamine. This lineage of human cell line was chosen to study infection as THP-1

cells are known to support the intracellular replication and growth of *Leishmania* parasites (Ogunkolade et al., 1990).

2.3. Infection of differentiated THP-1 macrophage with GFP expressing *Leishmania*

Differentiated THP-1 macrophages were infected with metacyclic promastigotes derived from all four species of *Leishmania* as described below.

2.3.1. Preparation of stationary phase metacyclic promastigotes

Initially, stationary phase promastigotes were obtained by culturing the parasites at 5×10^5 per ml, 96 hours prior to infection. The metacyclic promastigotes were isolated by peanut agglutination as previously described (Parbhu-Patel et al., 2013). Briefly, stationary phase parasite cultures were centrifuged at 1000 g for 10 minutes. Following agglutination with 50 µg/ml peanut lectin (Vector, UK) for 18 minutes, the parasites were further centrifuged at 500 g for 5 minutes. The resulting supernatant containing the metacyclic promastigotes was collected and subsequent concentration determined by microscopic counting. Metacyclic S1G parasites were not purified through the above technique due to low concentration after agglutination.

2.3.2. Preparation of differentiated THP-1 macrophages

THP-1 monocytes at a concentration of 2.5×10^5 per ml were treated with 1 µM of retinoic acid (RA) (Sigma) for 72 hours to induce differentiation of monocytes into non-replicating and non-adherent macrophages-like cells. Before infection with metacyclic promastigotes, the differentiated THP-1 macrophages were washed twice with $1 \times$ PBS (Sigma) to remove excess RA. After the final wash, the cells were re-suspended in complete RPMI 1640 medium and counted via Trypan blue staining

(Sigma). Cell viability greater than 80% was the threshold level to be used for subsequent infection experiments.

2.3.3. Parasite to cell ratio

Parasite concentration of 5×10^6 per ml was used to infect 5×10^5 per ml of differentiated THP-1 macrophage at a ratio of 10:1 (parasite to cell ratio). The infected cells were then incubated at 37°C in a humidified CO₂ (5%) incubator. The percentage of infection was determined via flow cytometry (section 2.7).

2.4. Induction of apoptosis

Following infection with all four species of promastigotes, the induction of apoptosis was carried out by treatment with 3 μM of camptothecin (Sigma). To determine the effect of camptothecin treatment on the percentage of infected cells, the length of treatment was optimized (Figure 2.1). The first optimization involved the addition of camptothecin at 0 hour after infection and continuously detecting the percentage of infection via flow cytometry at 24, 48, 72 and 96 hours (Figure 2.1.A). The second optimization involved camptothecin addition at 0 hour before washing away excess camptothecin from the culture medium with 1× PBS at 24 hours after infection and subsequently detecting the percentage of infection via flow cytometry at 24, 48, 72 and 96 hours (Figure 2.1.B). In the above experiments, both uninfected and infected cultures without camptothecin treatment were used as an appropriate control.

2.5. Infection of differentiated THP-1 macrophage with *Leishmania* infected cells

L. aethiopica (L8G) and *L. mexicana* (M5G) infected cells induced with 3 μM of camptothecin were seeded on 24 well plates.

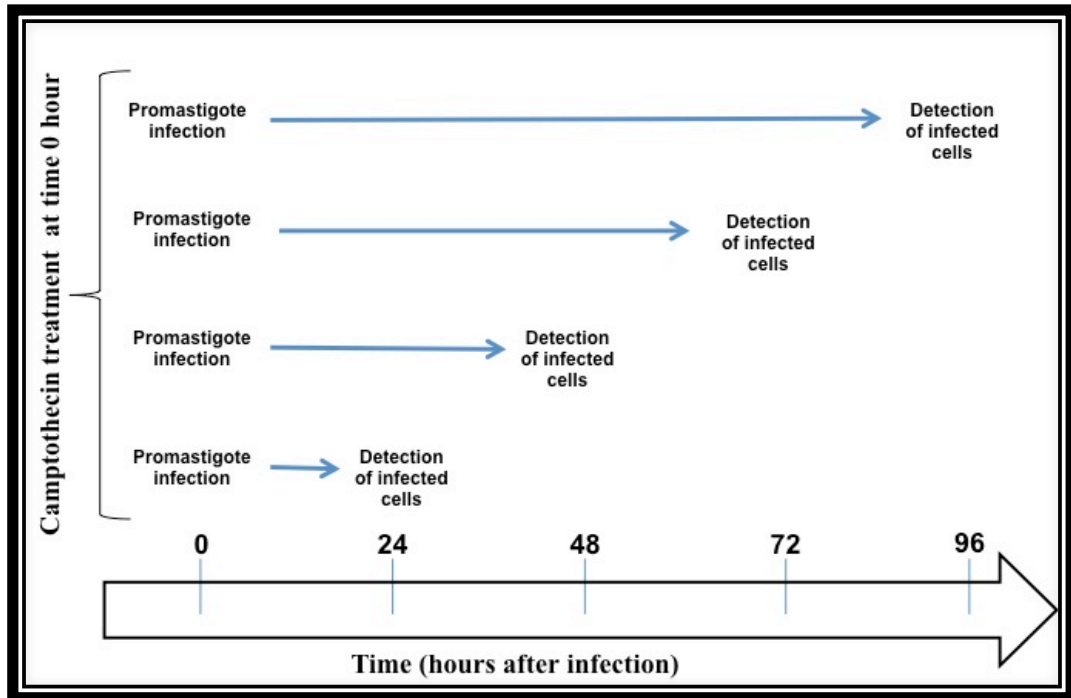
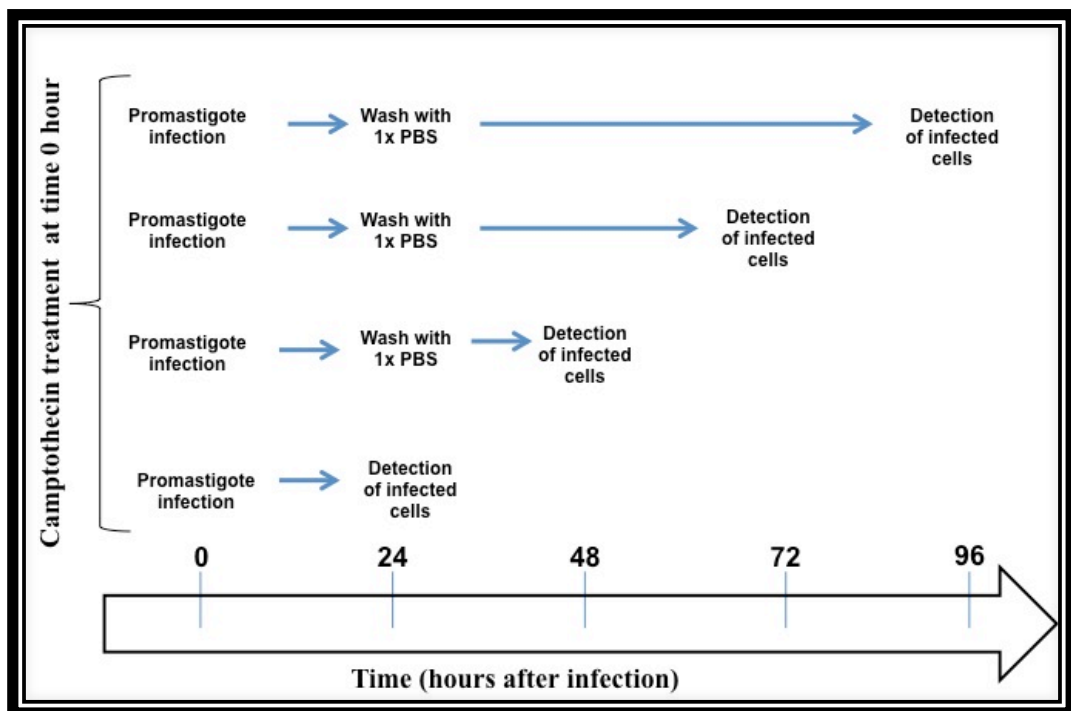
A**B**

Figure 2.1. Schematic diagram representing the optimization strategy of camptothecin treatment on the percentage of infected cells. (A) Following promastigote infection, camptothecin was treated at 0 hour and the percentage of infected cells was detected from 24 to 96 hours. **(B)** Following promastigote infection, camptothecin was treated at 0 hour before washing excess drug at 24 hours after infection. The percentage of infected cells was detected from 24 to 96 hours.

Excess camptothecin from M5G and L8G infected culture were washed away with 1× PBS at 5 and 24 hours after infection respectively. After 72 hours of incubation at 37°C in a humidified CO₂ (5%) incubator, viable cell concentration from both infected culture was determined via Trypan blue staining. The infected cells were then centrifuged at 500 g for 10 minutes to remove the supernatant, before the addition of a freshly prepared batch of differentiated THP-1 macrophages. Three different infection ratios were tested including 10:1, 5:1 and 1:1 (infected cell per uninfected cell ratio). The percentage of infection was determined at 0, 12, 24 and 48 hours after co-culture via flow cytometry. In addition, live imaging of parasite transmission carried out through real time lapse microscopy (Section 2.8).

2.6. Inhibition of caspase-3 activity

L8G infected cells from 72 hours were pre-treated with 25 µM and 100 µM of Z-DEVD-FMK (BD Biosciences, UK) for 4 hours and incubated at 37°C in a humidified CO₂ (5%) incubator. After washing with 1× PBS, the infected cells were co-cultured with freshly prepared batch of differentiated THP-1 macrophages at 1:1 ratio (infected cell per uninfected cell ratio). The percentage of infection and caspase-3 expression were determined at 3 and 12 hours after co-culture. Untreated L8G infected cells were taken as a positive control.

2.7. Detection of apoptosis

Apoptosis assays were carried at different times after infection according to specific experiments (Table 2.1).

Type of experiments	Time of apoptotic assay
Promastigote infection of differentiated THP- macrophages	24, 48, 72 and 96 hours after infection
Camptothecin treatment of differentiated THP-1 macrophages infected with promastigote	24, 48, 72 and 96 hours after infection
Infection of differentiated THP-1 macrophages with infected cells (1 to 1 infection ratio)	0, 24 and 48 hours post infection

Table 2.1. List of experiments designed for apoptosis and their time of analysis.

2.7.1. Annexin V / 7AAD assay

PE Annexin V apoptosis kit I (BD Biosciences) was used to determine the externalization of phosphatidyl serine (PS) and membrane permeability of the cell. Annexin V protein binds to PS, which is externalized during early stages of apoptosis, whereas 7AAD intercalates with the cellular DNA if the membrane is damaged during late stage of apoptosis (necrosis). The kit was used according to manufacturer protocol. Briefly, the harvested cells were centrifuged at 500 g for 10 minutes and washed twice with ice-cold 1× PBS.

After re-suspension in 1× binding buffer at a cell concentration of 1×10^6 per ml, 100 µl of cells were then stained with 5 µl of PE Annexin V and 5 µl of 7AAD and incubated for 15 minutes in the dark at room temperature. Finally, 400 µl of 1× binding buffer was added to the stained cells and the percentage of Annexin V positive / 7AAD negative (early apoptosis) and Annexin V positive / 7AAD positive (late apoptosis or necrosis) cells were analysed through flow cytometry within 1 hour of staining.

2.7.2. Caspase-3 enzymatic assay

The PE Caspase-3 detection kit (BD Biosciences) was used to measure the activation level of caspase-3 enzyme of the cell. The kit was used according to the manufacturer protocol. Briefly, the harvested cells were centrifuged at 500 g for 10 minutes before washing twice with ice-cold 1× PBS. The cells were incubated at 0-4°C for 20 minutes with 1× Perm and Fix buffer at a cell concentration of 2×10^6 per ml. After incubation, the cells were washed twice with 1× washing buffer before staining with PE anti-caspase-3 antibody (20 µl per 1×10^6 cells). Following 30 minutes incubation in dark, the stained cells were washed with 500 µl of 1× washing

buffer. After final re-suspension in 400 μ l of $1\times$ washing buffer, the percentage of caspase-3 positive cells were analysed through flow cytometry within 1 hour of staining.

2.8. Flow cytometry

The C6 flow cytometry (BD Accuri, UK) which is comprised of blue (excitation λ : 488 nm) and red (excitation λ : 640 nm) lasers, was used to detect the percentage of infected cells and apoptotic cells. In this flow cytometer, the FL-1, FL-2 and FL-3 optical filters detected emissions from blue lasers, whereas FL-4 filters detected emission from red lasers. The blue laser was used to excite different types of fluorochromes, specific to GFP (FL1), PE Annexin V and PE Caspase-3 (FL-2) and 7AAD (FL-3).

To measure the percentage of infection along with Annexin V and 7AAD stained cells, the cell populations were initially gated according to Forward scatter (FSC) and Side scatter (SSC) parameters (Figure 2.2.A), which defines cell size and cell granularity, respectively. After exclusion of doublet cells (Figure 2.2.B), two separate plots were designed. Figure 2.2.C.i shows a histogram plot of GFP versus count to determine the percentage of infection whereas Figure 2.2.C.ii represents a dot plot of Annexin V versus 7AAD to determine apoptosis. In this thesis, this plot will be referred as total population apoptosis. Each quadrant represents the percentage of live cells (Annexin V negative / 7AAD negative), early apoptotic cells (Annexin V positive / 7AAD negative), late apoptotic/necrotic cells (Annexin V positive / 7AAD positive) and dead cells (Annexin V negative / 7AAD positive). Furthermore, within infected cultures, the percentage of apoptosis from total population was sub-divided into infected only and uninfected only population (Figure 2.3).

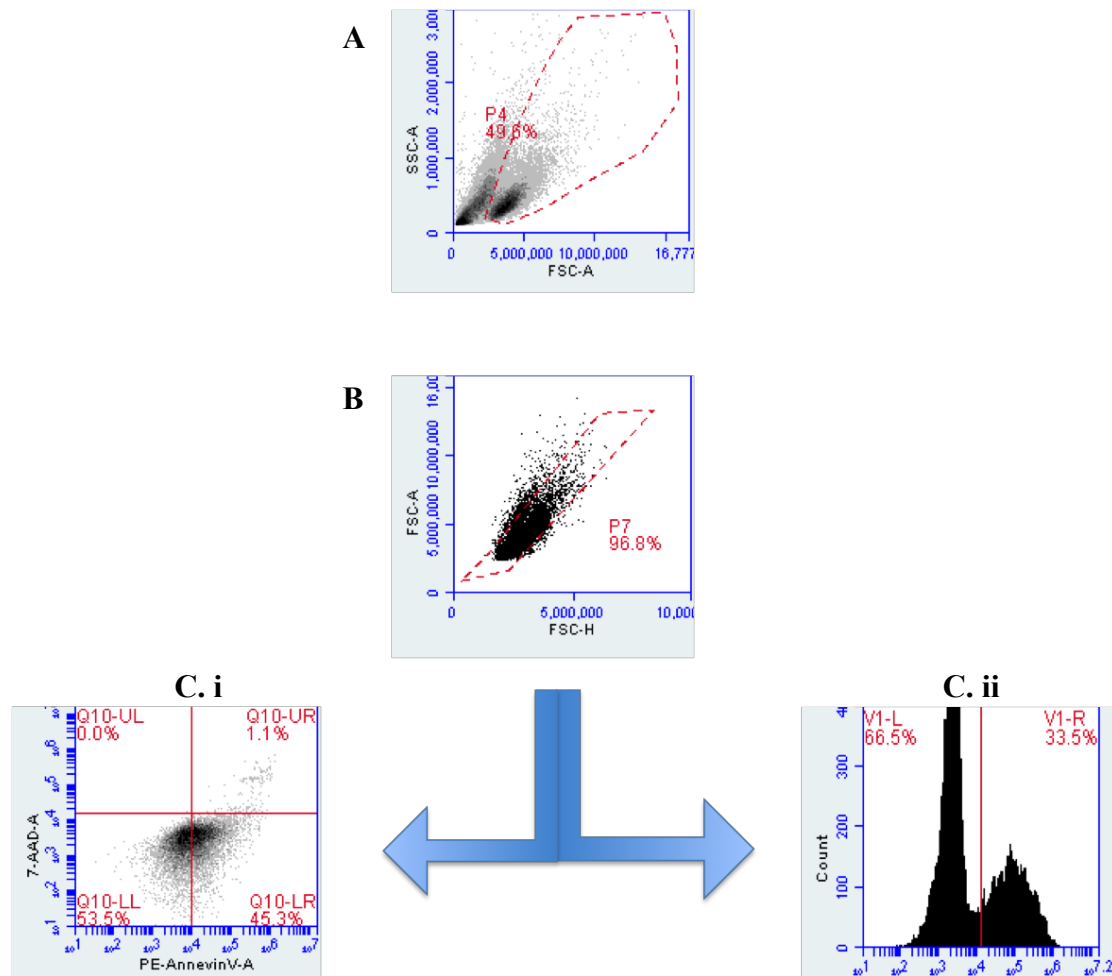


Figure 2.2. Flow cytometry analysis of PE-Annexin V / 7-AAD stained cells. (A) The total population of differentiated THP-1 macrophages (double stained with PE-Annexin V and 7AAD) were initially gated as P4, according to FSC-A and SSC-A parameters. (B) The doublet cells were excluded. (C) Following exclusion, two plots were created. (C.i) A dot plot comprising of PE-Annexin V (X-axis) versus 7-AAD (Y-axis) was created to isolate live (Q9-LL), early apoptotic (Q9-LR), late apoptotic (Q9-UR) and dead (Q9-UL) cells. (C.ii) A histogram plot comprising of GFP (X-axis) versus Count (Y-axis) was created to detect the percentage of infected cells in V1-R region from uninfected cells in V1-L region.

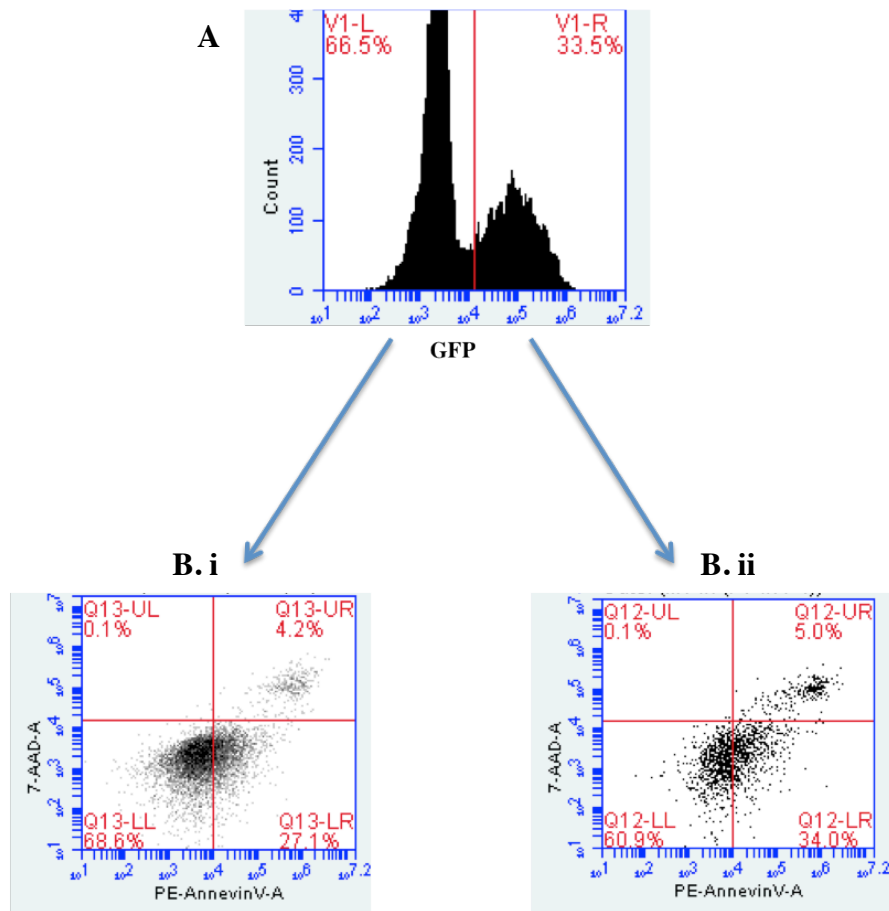


Figure 2.3. Flow cytometry analysis of apoptosis in infected cultures. (A) Representative histogram plot of infection based on GFP expression. (B.i) A dot plot comprising of PE-Annexin V (X-axis) versus 7AAD (Y-axis) was created from V1-L region. This apoptotic plot is called uninfected only population. (B.ii) Similarly, a dot plot comprising of PE-Annexin V (X-axis) versus 7AAD (Y-axis) was created from V1-R region. This apoptotic plot is called infected only population.

Similarly for caspase-3 activity, the stained cell populations were gated according to FSC and SSC (Figure 2.4.A) from which the doublet cells were excluded (Figure 2.4.B). Then, a histogram plot of caspase-3 versus count was created to measure the percentage of active caspase-3 cells (Figure 2.4.C). It should be noted that limits for the quadrants were always based upon positive and negative control.

2.9. Real time lapse microscopy

A fresh population of differentiated THP-1 macrophages at a concentration of 1×10^5 per ml was labelled with $0.5 \times$ CellMaskTM orange plasma membrane stain (Fisher Scientific) for 15 minutes at 37°C. After washing three times with $1 \times$ PBS the cells were re-suspended in RPMI medium and seeded in a 6 well culture plate containing 1×10^5 of either L8G or M5G infected cells (from 72 hour incubation). Immediately, the RPMI complete medium was removed from this co-culture and was replaced by RP buffer solution (1 mM Magnesium acetate (Sigma), 1 mM Calcium chloride (Sigma), 5 mM glucose (Sigma), 5 mM glutamate (Sigma), 10% FCS, $1 \times$ PBS). The 6 well culture plate was then mounted on 37°C hot plate connected to a fluorescent Eclipse Ti-S inverted microscope (Nikon, UK). Using an in built digital DS-Fi camera (Nikon), live images were acquired every 5 minutes with bright field and TRITC filters for a maximum period of 12 hours under 20 \times objectives. After acquisition, images were processed by NIS advanced version 4.2 software (Nikon), which allowed for the construction of multidimensional time-lapse videos.

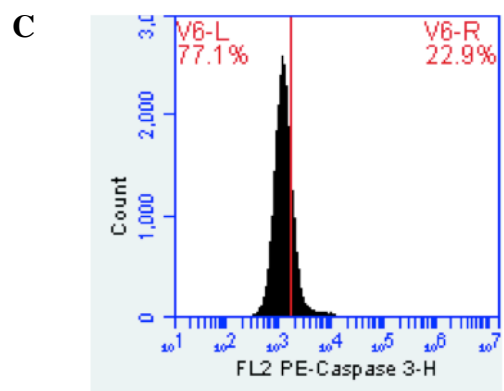
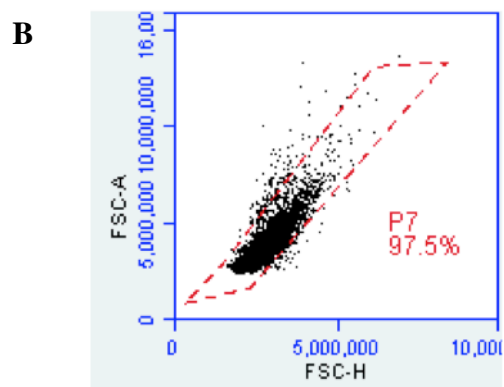
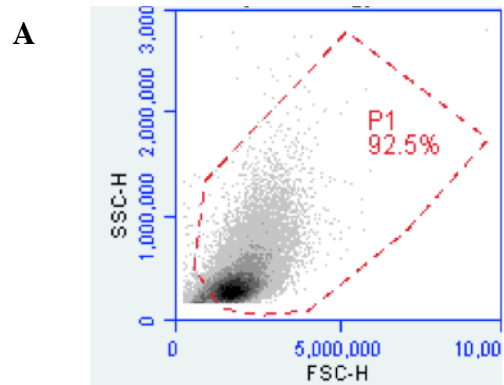


Figure 2.4. Flow cytometry analysis of PE-Caspase 3 stained cells. (A) The total population of differentiated THP-1 macrophages, which are stained with anti PE-Caspase 3 antibody is initially gated as P1, according to FSC-A and SSC-A parameters. (B) The doublet cells are excluded. (C) Following exclusion, a histogram plot comprising of PE-Caspase 3 (X-axis) versus Count (Y-axis) was created to detect the percentage of cells with activated caspase 3.

2.10. Western blot

Western blots were carried out to analyse the involvement of proteins associated with apoptotic pathways during L8G infection spreading specifically, AKT, PKC- δ and NF- κ B. The lists of antibodies (Santa Cruz, UK) used in this experiment are listed in Table 2.2. Briefly, from each incubation time point, 1×10^6 cells were harvested by centrifugation at 500 g for 10 minutes. After removing the supernatant, the cell pellet was res-suspended in ice cold $1 \times$ PBS and centrifuged at 1000 g for 5 minutes. Then, 100 μ l of $1 \times$ RIPA buffer (Abcam, UK), which was supplemented with $1 \times$ protease cocktail inhibitor (Fisher Scientific), was added to the pellet. After re-suspension, the samples were lysed on ice for 15 minutes with gentle shaking. The whole cell proteins were then collected from the supernatant through centrifugation at 10,000 g for 10 minutes at 4°C. For extracting cytosolic protein, the pellet was re-suspended in cell extraction buffer (Fisher Scientific) supplemented with $1 \times$ protease cocktail inhibitor.

The sample was lysed on ice for 30 minutes before collecting the supernatant through centrifugation at 10,000 g for 10 minutes at 4°C. The resulting protein concentration from a sample was determined through BCA absorbance assay kit (Fisher Scientific) according to the manufacturer protocol. To separate the proteins according to their sizes, 20 μ g of proteins were run on a 10% Tris glycine SDS gels (Fisher Scientific) for 50 minutes under a constant 185 volts. The proteins were then transferred successfully onto a nitrocellulose membrane (BioRad, UK) before overnight blocking at 4°C with 5% non-fat dry milk TBS tween or 5% BSA TBS tween solution (BioRad).

List of antibodies	Dilution Factor	Blocking buffer
Anti-phospho (Thr 308) AKT	1 in 500	5% BSA in TBS tween
Anti-phospho (Ser 473) AKT	1 in 500	5% BSA in TBS tween
Anti-total AKT	1 in 1000	5% Milk in TBS tween
Anti-total PKC- δ	1 in 1000	5% Milk in TBS tween
Anti-total p65	1 in 1000	5% Milk in TBS tween
Anti-phospho (Ser 32/36) I κ B α	1 in 500	5% BSA in TBS tween
Anti-total I κ B α	1 in 500	5% Milk in TBS tween
Anti-Cytochrome C	1 in 500	5% Milk in TBS tween
Anti- phospho (Ser 136) BAD	1 in 250	5% BSA in TBS tween
Anti-total BAD	1 in 500	5% Milk in TBS tween
Anti- β actin	1 in 1000	5% Milk in TBS tween

Table 2.2. List of antibodies and their appropriate dilution and appropriate blocking buffers used in western blot experiments.

The membrane was then incubated with primary antibody at room temperature under gentle agitation for 1 hour. After three washes in TBS tween solution, the membrane was incubated with horse radish peroxidase conjugated secondary antibody for 1 hour at room temperature under gentle agitation. The membrane was further washed three times in TBS tween solution before applying an ECL reagent (Fisher Scientific) to detect the protein of interest under X ray film (Fisher Scientific). To re-probe for another protein, the membrane was washed two times in TBS solution before incubating with 1× stripping buffer (Fisher Scientific) for 40 minutes at room temperature. After further two washes in TBS solution, the membrane was ready for another round of blocking and subsequent antibody incubation.

2.11. Quantitative proteomics by mass spectrometry

The differentially expressed proteins during L8G infection spreading were analysed by Tandem Mass TagTM (TMT) 6-plex based liquid chromatography – tandem mass spectrometry (LC-MS/MS). The initial protein extraction was performed as described in section 2.9. The experimental procedures including isotopic protein labelling and mass spectrometry were performed by University of Bristol, UK using the TMT Mass Tagging Kits and Reagent (Fisher Scientific). For this thesis, only two samples (i.e. uninfected and L8G infected co-culture after 10 hours of co-culture) were chosen for labelling. The remaining four samples were designed for other researchers. According to the manufacturer protocol, the brief procedures are described below.

2.11.1. Precipitation and enzymatic digestion of the protein samples

Approximately, 100 µg of proteins from uninfected (control) and L8G infected co-culture samples at 10 hours after co-culture were transferred into a new micro-

centrifuge tube and its final volume was adjusted to 100 μ l with 100 mM TEAB (Tri Ethyl Ammonium Bicarbonate) and 200 mM of TCEP (Tris 2-Carboxy Ethyl Phosphine). After incubating at 55°C for 1 hour, the samples were treated with 5 μ l of 375 mM iodoacetamide and further incubated for 30 minutes in dark room temperature. Following overnight freezing (-20°C) in the presence of 600 μ l of acetone, the samples were centrifuged at 8000 g for 10 minutes at 4°C. After careful removal of supernatant, the protein pellets were re-suspended with 100 μ l of 100 mM TEAB. The protein digestion was completed by overnight incubation of the sample with 2.5 μ l of trypsin at 37°C.

2.11.2. Peptide labelling and mass spectrometry

The peptides from the digested proteins were incubated with appropriate TMT label reagent (-129 and -130) for 1 hour at room temperature. The reaction was quenched following further incubation with 8 μ l of 5% hydroxylamine for 15 minutes. These labelled samples were then combined together with the remaining four samples. The resulting mixture was then separated using liquid chromatography. Mass spectrometry of the column eluate was done using Velos ProsTM ion trap mass spectrometer (Fisher Scientific). The peptide MS/MS data were analysed for protein identification and quantification using Proteome DiscovererTM 1.1 (Fisher Scientific). A false positive discovery rate (FDR) threshold of 5% was employed to ensure that there is at least 95% confidence that every peptide present was a genuine peptide from the database. By comparing the peak intensity of test sample with control, the relative fold change (RFC) was calculated. This allowed the identification of differentially expressed proteins with RFC > 1.5 and RFC < 0.5 considered as upregulated and downregulated, respectively.

2.12. Statistical Analysis

Data shown are representative of at least three independent experiments performed in triplicates wherever necessary. Data represents mean values with statistical error mean (SEM). Statistical analysis was performed using student *t* test provided by Graph pad prism and P values less than 0.05 ($p < 0.05$) were considered significant differences between two independent samples.

Chapter 3 – *Leishmania* infection and host cell apoptosis

3.1. Introduction

Macrophages are the definitive host cell for the invasion by *Leishmania* parasites. The survival of *Leishmania* is due to the ability of the parasite to disable various host macrophages function such as cytokine production, reactive oxygen species and nitric oxide generation (Martinez and Gordon, 2014). Another virulent strategy utilized by *Leishmania* is to prevent the induction of macrophage apoptosis during early stage of infection (Akarid et al., 2004; Lisi et al., 2005; Ruhland et al., 2007). It has been suggested that this would allow sufficient time for the parasite to replicate before spreading its progeny towards neighbouring macrophages. However, the exact mechanism of parasite dissemination is far from clear.

Natural transmission studies in mice have shown that early phase of infection propagation occurs silently for weeks to months, without immunological and pathological changes (Belkaid et al., 2000; Nylon and Eidsmo, 2012). Since apoptosis is the removal of damaged cells by macrophages without eliciting an inflammatory response, this led to speculate that *Leishmania* could utilize this form of host cell death in order to spread. Indeed, this unique process would offer selective advantage to the parasites, which could potentially exit the host cell within apoptotic bodies and subsequently evade the host immune defence system. Similar strategies of cell-to-cell spreading through host cell apoptosis have been reported in a number of infectious pathogens including *Mycobacterium tuberculosis* (Aguilo et al., 2013) and Adenovirus (Mi et al., 2001). Interestingly, *L. amazonensis* has been the only

protozoa that have recently been shown to spread from cell-to-cell via mechanism resembling apoptosis (Real et al., 2014).

In this chapter, the link between *Leishmania* infection progression and apoptosis of host macrophages *in vitro* was investigated. This relationship was determined via two routes. Firstly, the effect of four GFP expressing *Leishmania* promastigotes (*L. aethiopica*, *L. major*, *L. mexicana* and *L. tropica*) infection on the apoptosis of differentiated THP-1 macrophages from 24 to 96 hours was analysed. Secondly, the effect of apoptotic induction on the parasitic infection was evaluated. Flow cytometry was used to detect the percentage of GFP expressing *Leishmania* infected cells as well as percentage of apoptotic marker (i.e. Phosphatidyl Serine [PS] externalisation) during infection. In addition, for the very first time, the apoptosis level (PS externalization) within an infected sample was analysed separately into infected only and uninfected only population.

3.2. Results and Discussion

3.2.1. Infection of differentiated THP-1 macrophages with *Leishmania* promastigotes

In order to test the effect of *Leishmania* infection on apoptosis, the infectivity level and survival period of four promastigotes species in differentiated THP-1 macrophages were initially determined. Flow cytometry analysis was used to monitor the course of infection by measuring the percentage of macrophages containing GFP positive parasites at early (24 and 48 hours) and late (72 and 96 hours) incubation time point.

After 24 hours incubation, between 30 to 60% of cells were successfully infected by all four promastigote species (Figure 3.1). The percentage of infection was highest for L8G ($57.1\pm 0.8\%$), M5G ($56.8\pm 9.1\%$) and O5G ($57.1\pm 4.5\%$), whereas the lowest infection was observed for S1G, which only infected $31\pm 2.2\%$ of cells. The infection rate seemed to stabilize after two days (48 hours) of continuous incubation for all species. From 48 to 96 hours, a significant decrease ($p < 0.05$) in the percentage of cells infected with L8G, M5G and O5G were observed before maintaining low infectivity level. To query this dramatic reduction, trypan blue assay was performed which showed a two-fold increase in the concentration of viable cells from 48 to 96 hours in both uninfected and infected cells (Figure 3.2). This suggests that the inhibitory effect of retinoic acid on THP-1 replication terminated at 48 hours after which the monocytes underwent cellular replication.

Interestingly, the percentage of S1G infected cells remained low throughout the time period. This is likely due to loss of infectivity associated with high number of sub-culturing carried out on S1G (Segovia et al., 1992). In contrast, M5G and O5G were recently obtained and L8G has been reverted to axenic amastigote several times (personal communication), hence these species showed higher infective capacity (Getti et al., 2008).

In summary, all species (except S1G) displayed maximum infective level within the first 48 hours. However, the spreading of parasite was not detected partially due to intense replication of uninfected THP-1 cells. In terms of parasite survival, the infection remained existent till 96 hours, although significantly lower than 48 hours, indicating the survival of parasites within cell.

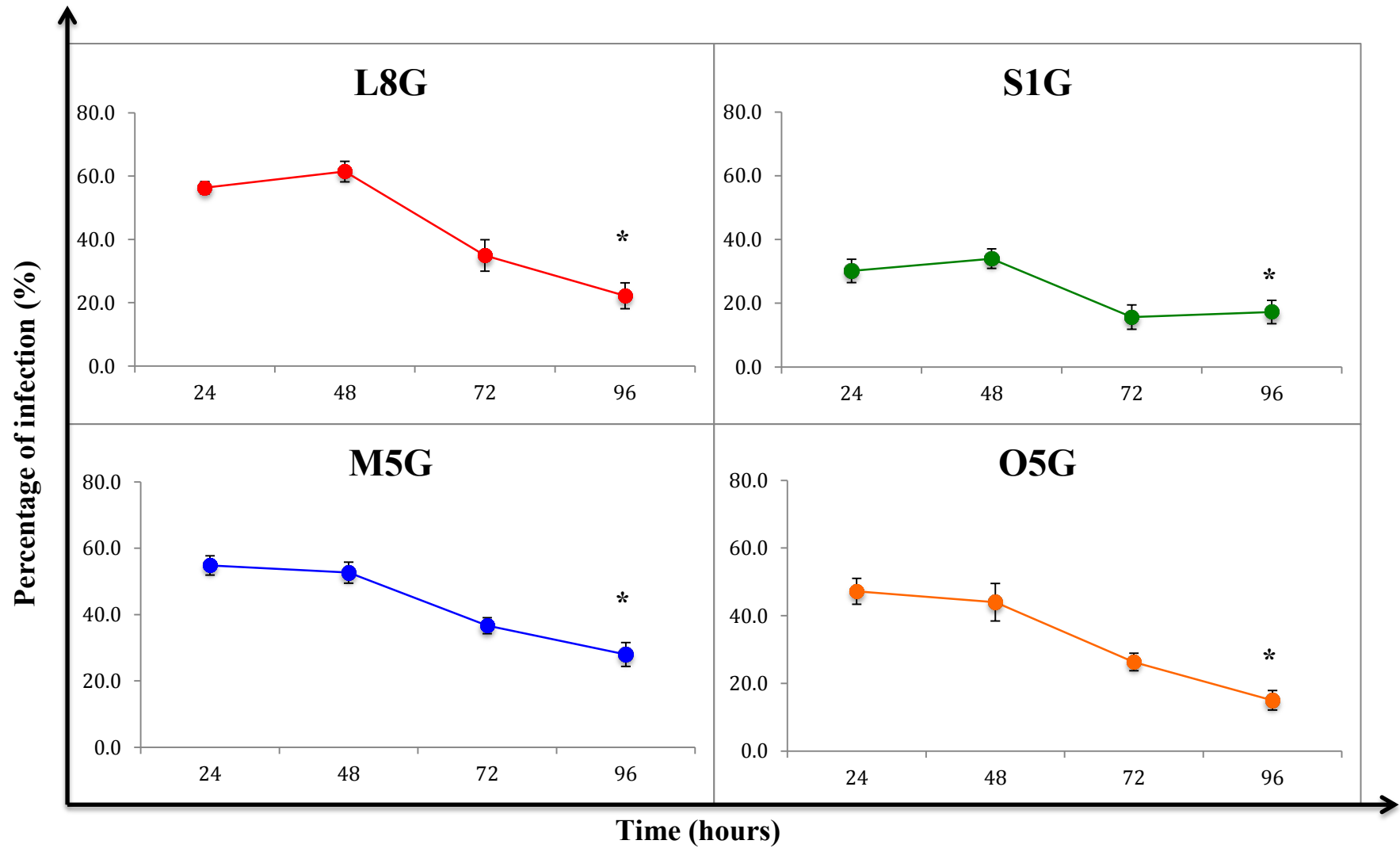


Figure 3.1. Time course of differentiated THP-1 macrophage infection with *Leishmania* promastigotes. Differentiated THP-1 macrophages were infected with four GFP expressing promastigotes species, *L. aethiopica* (L8G), *L. major* (S1G) and *L. mexicana* (M5G) and *L. tropica* (O5G) at 10:1 ratio (parasites to cell ratio). The percentage of infection was determined through flow cytometry at 24, 48, 72 and 96 hours. The data represents mean percentage (mean \pm SEM) from three independent experiments. * = $p < 0.05$

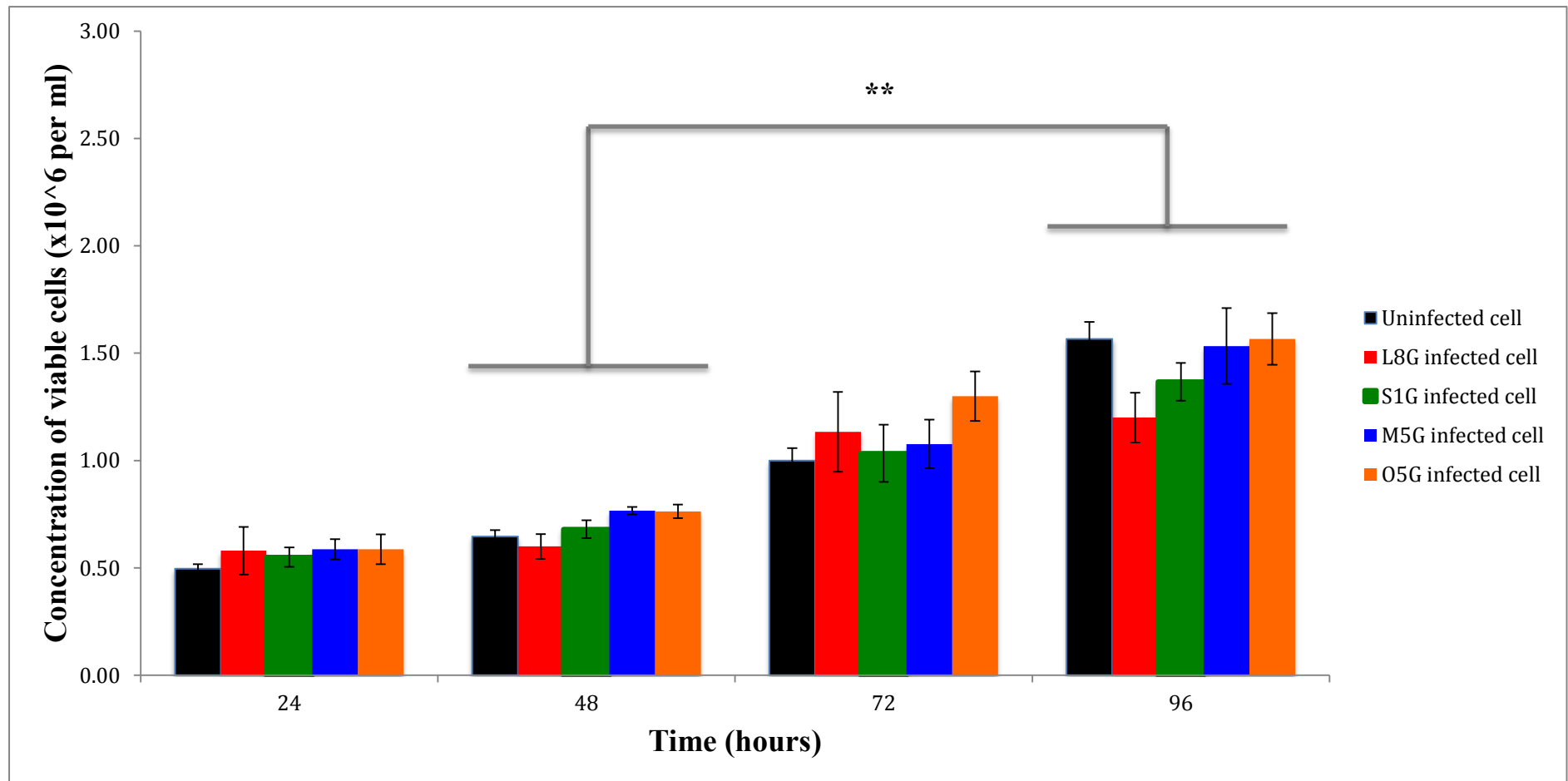


Figure 3.2. Measurement of viable cell concentration in the presence or absence of infection. Uninfected or infected cell by L8G, S1G, M5G and O5G were stained with trypan blue solution at 24, 48, 72 and 96 hours. The data represents mean concentration of viable cells (mean±SEM) from three independent experiments. ** = p<0.01.

3.2.2. Effect of *Leishmania* promastigotes infection on the apoptosis of differentiated THP-1 macrophages

Since the above results showed that parasites persisted till 96 hours, the next aim was to test the impact of host cell apoptosis during *Leishmania* promastigotes infection. Through Annexin V / 7-AAD assay, flow cytometry analysis of apoptosis in *Leishmania* infected cells was performed. In this experiment, cells undergoing early apoptosis (Annexin V positive / 7-AAD negative) and late apoptosis (Annexin V negative / 7-AAD negative) were termed apoptotic and necrotic, respectively. Due to the constitutive GFP expression of the parasites, comparison between the percentage of apoptosis (Figure 3.3) and infection (Figure 3.4) was analysed together. Furthermore, the apoptosis in the infected culture (total population) were divided into infected only and uninfected only populations.

As illustrated in figure 3.3, $29 \pm 2.3\%$ of the uninfected control cells (black line) underwent apoptosis at 24 hours. In the infected only population, approximately 60% of L8G, M5G and O5G infected cells (Figure 3.4) showed significantly higher percentage ($p < 0.05$) of apoptosis at 24 hours compared to the control (Figure 3.3 A[ii], C[ii] and D[ii]). As for S1G, the induction of apoptosis in the infected only cells was observed from 48 hours after infection (Figure 3.3 B[ii]). Interestingly, this increased level of apoptosis for all four species was maintained till 96 hours, despite the fact that infection rate decreased dramatically from 48 hours (Figure 3.4). This finding is in agreement with studies whereby infection with promastigotes of *L. aethiopica*, *L. tropica*, *L. major* and *L. amazonensis* induced apoptotic cell death in human and mice macrophages (Getti et al., 2008; Filardi et al., 2014; DaMata et al., 2015).

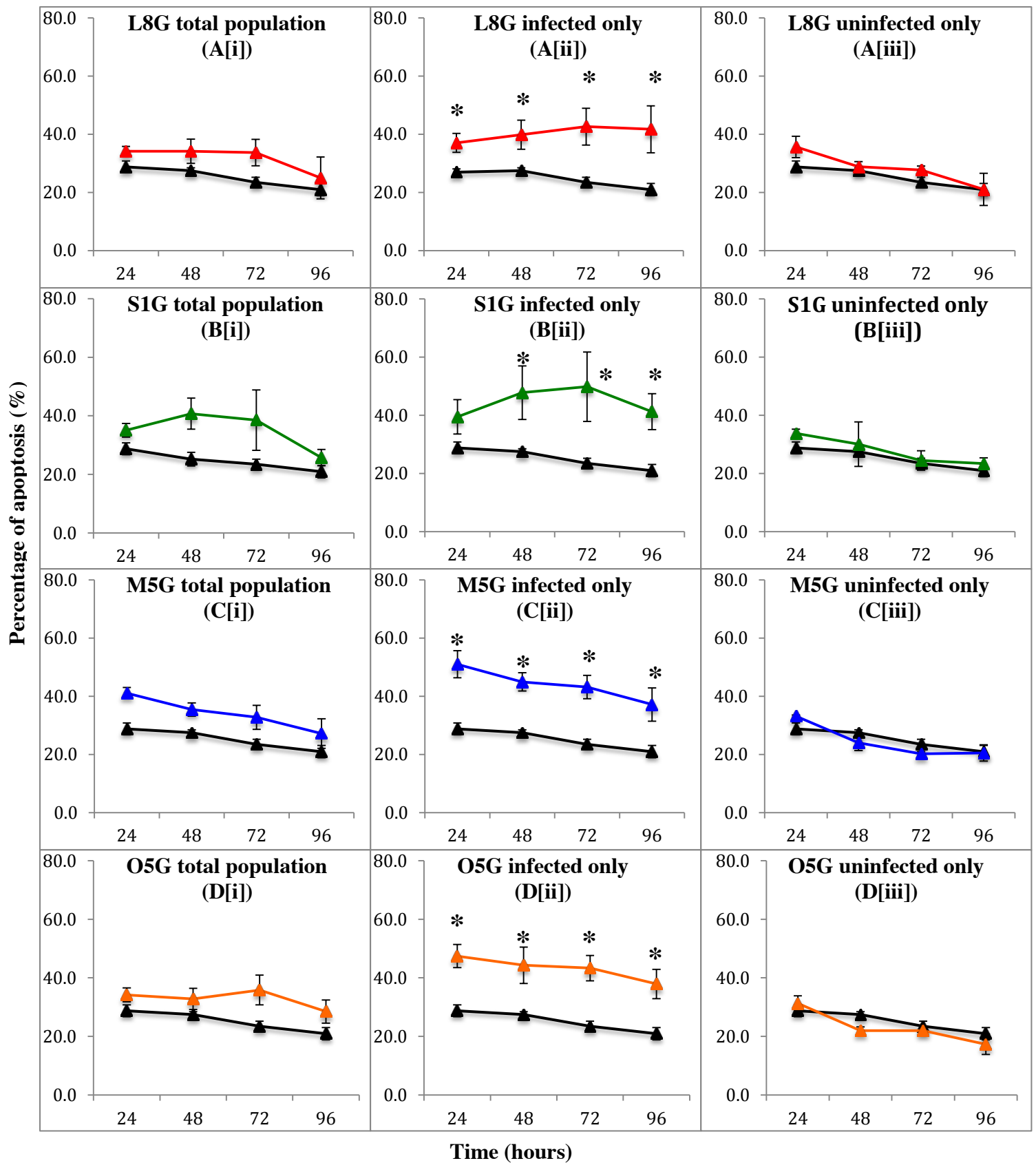


Figure 3.3. Effect of *Leishmania* promastigotes infection on the apoptosis of differentiated THP-1 macrophages. Following infection (10 parasites per 1 cell ratio), the percentage of apoptosis in L8G (A[i]), S1G (B[i]), M5G (C[i]) and O5G (D[i]) infected cells were detected at 24, 48, 72 and 96 hours. This data was divided into infected only [ii] and uninfected only [iii] populations. In the graph, the black line refers to uninfected cell (control). The data represents mean percentage (mean \pm SEM) from three independent experiments. * = $p < 0.05$.

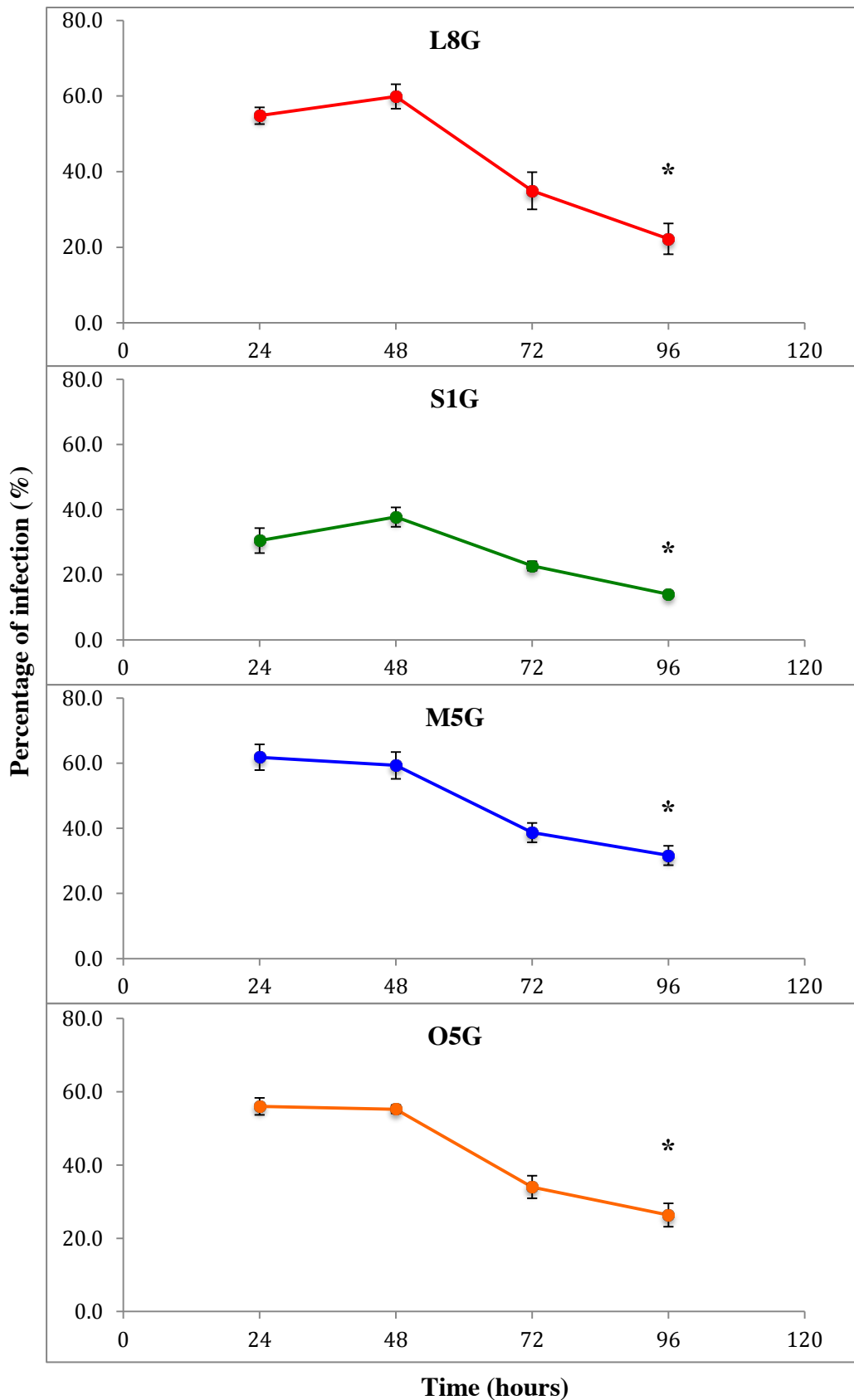


Figure 3.4. Time course of differentiated THP-1 macrophage infection with *Leishmania* promastigotes. In addition to the assessment of apoptosis during infection in Figure 3.3, information regarding the percentage of cells infected with L8G, S1G, M5G and O5G were also extracted and determined at 24, 48, 72 and 96 hours through flow cytometry. The data represents mean percentage (mean \pm SEM) from three independent experiments. * = $p < 0.05$.

Overall, the above results suggest that *Leishmania* induces spontaneous host apoptosis within infected only cells. Although this experiment showed a correlation between infection and apoptosis, whether such induction in cell death leads to parasitic spreading could not be extrapolated.

3.2.3. Effect of apoptotic induction on *Leishmania* infection

As the above result was unable to clarify the link between infection propagation and host cell apoptosis, the next step was to determine the effect of apoptotic induction on parasite infection. By treating infected cells with camptothecin (an intrinsic apoptosis inducing drug), the infection outcome and apoptosis were analysed. In order to achieve this, an optimisation was needed to determine the effect of the camptothecin treatment on the percentage of infection over a period of 96 hours.

3.2.3a. Longer duration of treatment with camptothecin

Infected and uninfected cells were treated with (or without) 3 μ M camptothecin at the start of infection (0 hour) and subsequent infection and apoptosis were detected by flow cytometry every 24 hours (Chapter 2, Figure 2.1.A). Interestingly after 48 hours, there was a significant increase ($p < 0.05$) in the percentage of L8G infected cells, which reached a maximum of 65.1 \pm 4% by 96 hours (Figure 3.5). For S1G, a gradual non-significant elevation in infection rate was observed. In contrast, camptothecin appeared to have an adverse effect on O5G infected cells, as the percentage of infection was lower than non-induced O5G infected cells at 48, 72 and 96 hours (Figure 3.5). Despite the increase in L8G infection, no significant increase in the percentage of apoptosis was detected in infected only population (Figure 3.6 A[ii]).

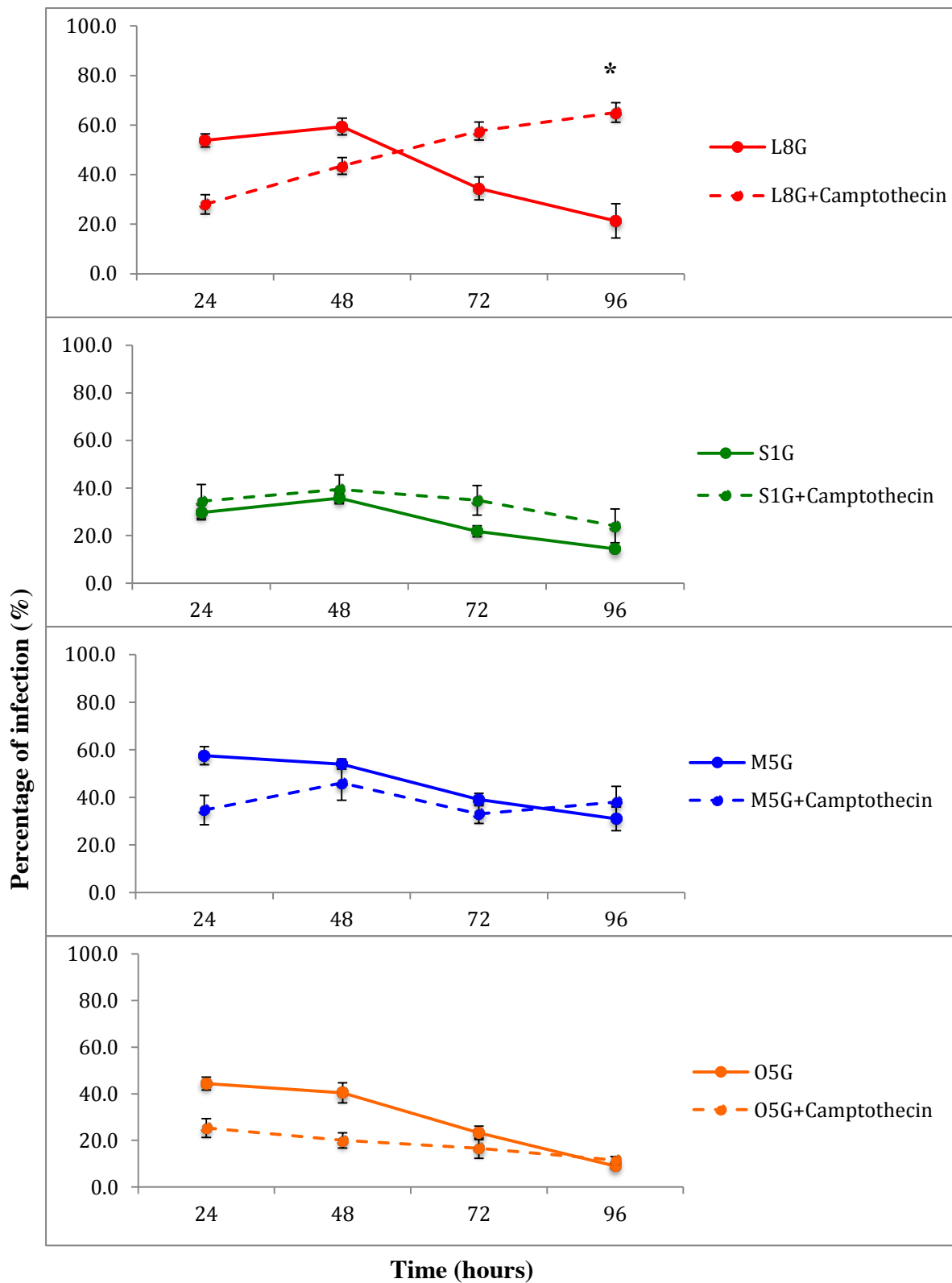


Figure 3.5. Effect of longer exposure to camptothecin treatment on *Leishmania* infection. Following infection (10 parasites per 1 cell ratio) with L8G, S1G, M5G and O5G, the infected cells were treated with or without camptothecin. The percentage of infection was determined at 24, 48, 72 and 96 hours through flow cytometry. The data represents mean percentage (mean \pm SEM) from three independent experiments. * = $p < 0.05$.

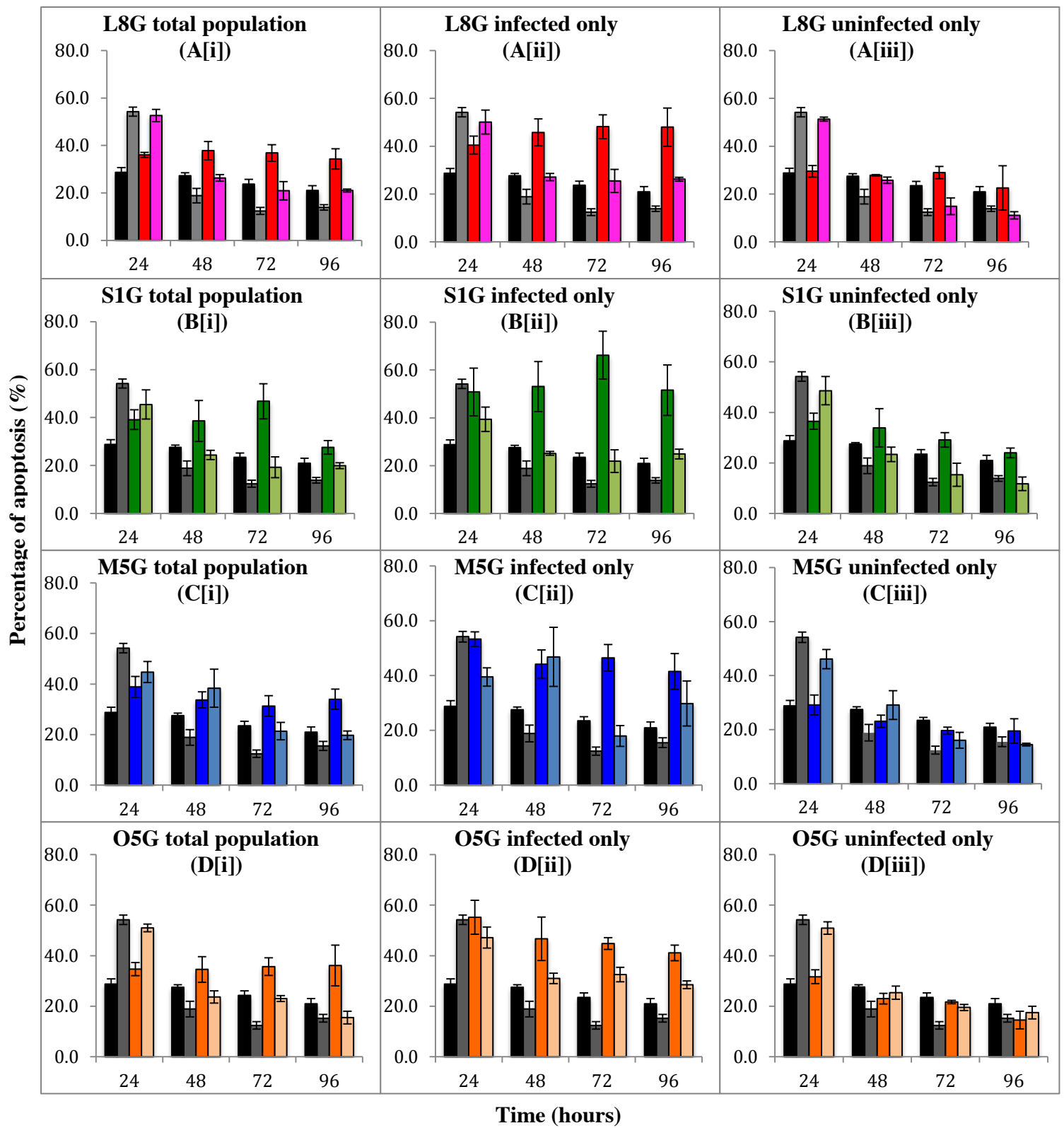


Figure 3.6. Effect of longer exposure to camptothecin treatment on the apoptosis of differentiated THP-1 macrophages infected with *Leishmania*. Following infection (10 parasites per 1 cell ratio) with L8G, S1G, M5G and O5G, the infected cells were treated with or without camptothecin. The percentage of apoptosis in total population was detected at 24, 48, 72 and 96 hours [i]. The data was divided into infected only [ii] and uninfected only [iii] populations. The data represents mean percentage (mean \pm SEM) from three independent experiments.

This finding suggested two possibilities. 1) There is no correlation between apoptotic induction and infection. 2) The longer duration of camptothecin treatment led to necrosis. Examination of Annexin V/ 7-AAD dot plot supported the latter notion, as significant proportions of cells were undergoing necrosis in the uninfected and L8G infected culture post 24 hours (Figure 3.7). This clearly indicates that L8G infection rise was not due to parasite spreading, but instead caused by the death of uninfected bystander cells. Hence this optimization approach was not suitable to further investigate infection spreading.

3.2.3b. Time limited treatment with camptothecin

In order to minimise camptothecin induced necrosis, the exposure time of apoptotic inducer in both infected and uninfected cultures was decreased. Excess camptothecin was removed from the culture media after 24 hours of infection. The subsequent percentage of apoptosis and infection were determined at 24, 48, 72 and 96 hours through flow cytometry (Chapter 2, Figure 2.1.B). This method clearly reduced the percentage of necrotic cells post 24 hours, as indicated from Annexin V/ 7-AAD dot plot (Figure 3.8).

Similar to the previous experiment, the camptothecin induction showed a significant increase in the percentage of cells infected with L8G from 48 hours, reaching a maximum of $73.1 \pm 6.3\%$ at 96 hours (Figure 3.9). However, such effects were not detected for S1G, M5G and O5G infected cell (Figure 3.9). Interestingly, in the presence of camptothecin, the percentage of apoptosis in L8G infected only population also markedly increased from 48 to 96 hours (Figure 3.10 A[ii]). This finding suggests a link between apoptotic induction and potential spreading of L8G parasites.

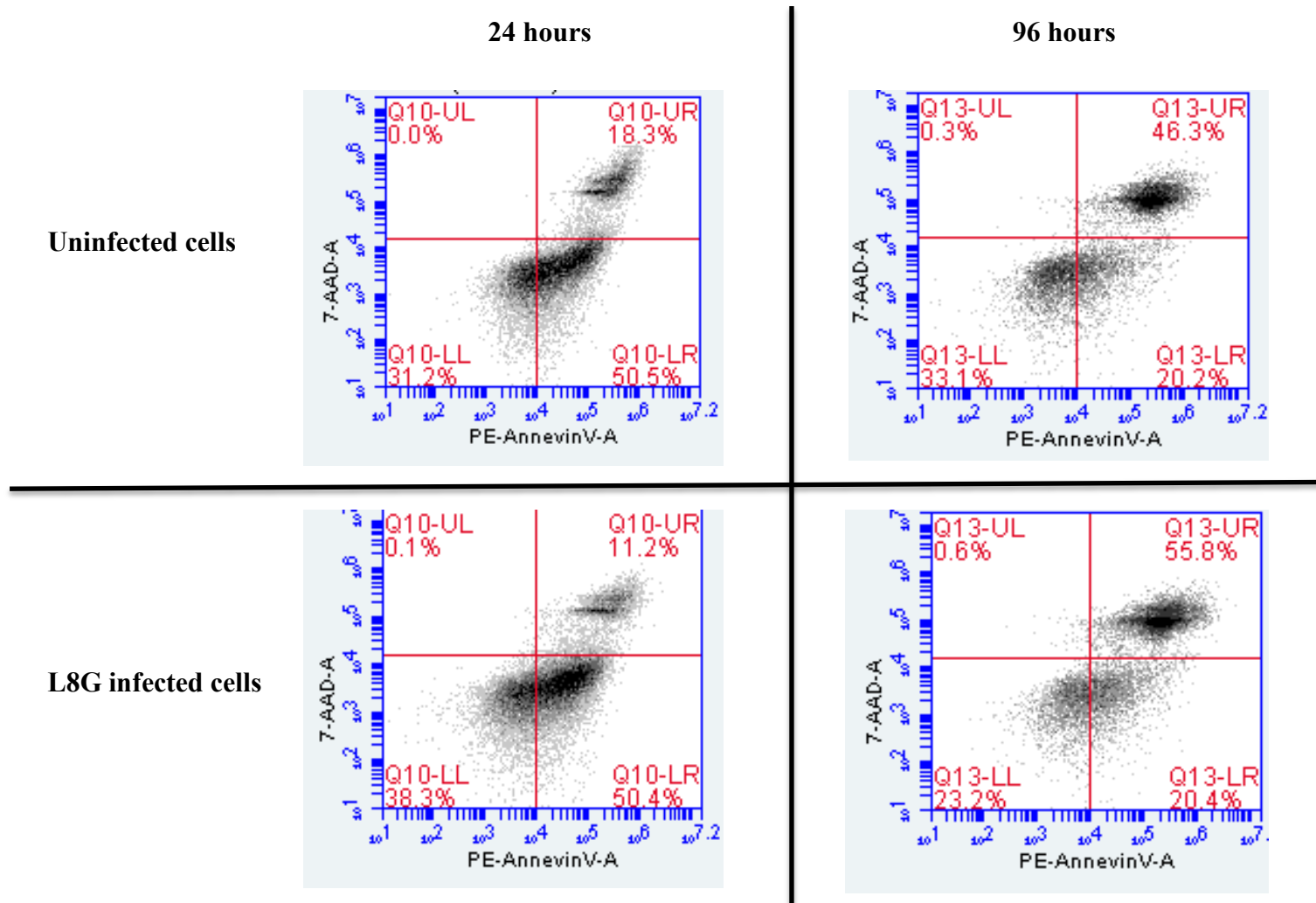


Figure 3.7. Flow cytometry analysis of Annexin V versus 7-AAD dot plot. Infected (e.g. L8G) and uninfected cells were treated with camptothecin and analysed for apoptosis from 24 to 96 hours. Without the removal of camptothecin, uninfected and L8G infected cells at 96 hours incubation showed an extreme level of necrosis (Q13-UR), compared with 24 hours. Moreover, this characteristic was also maintained at 48 and 72 hours from infection as well in all four species examined.

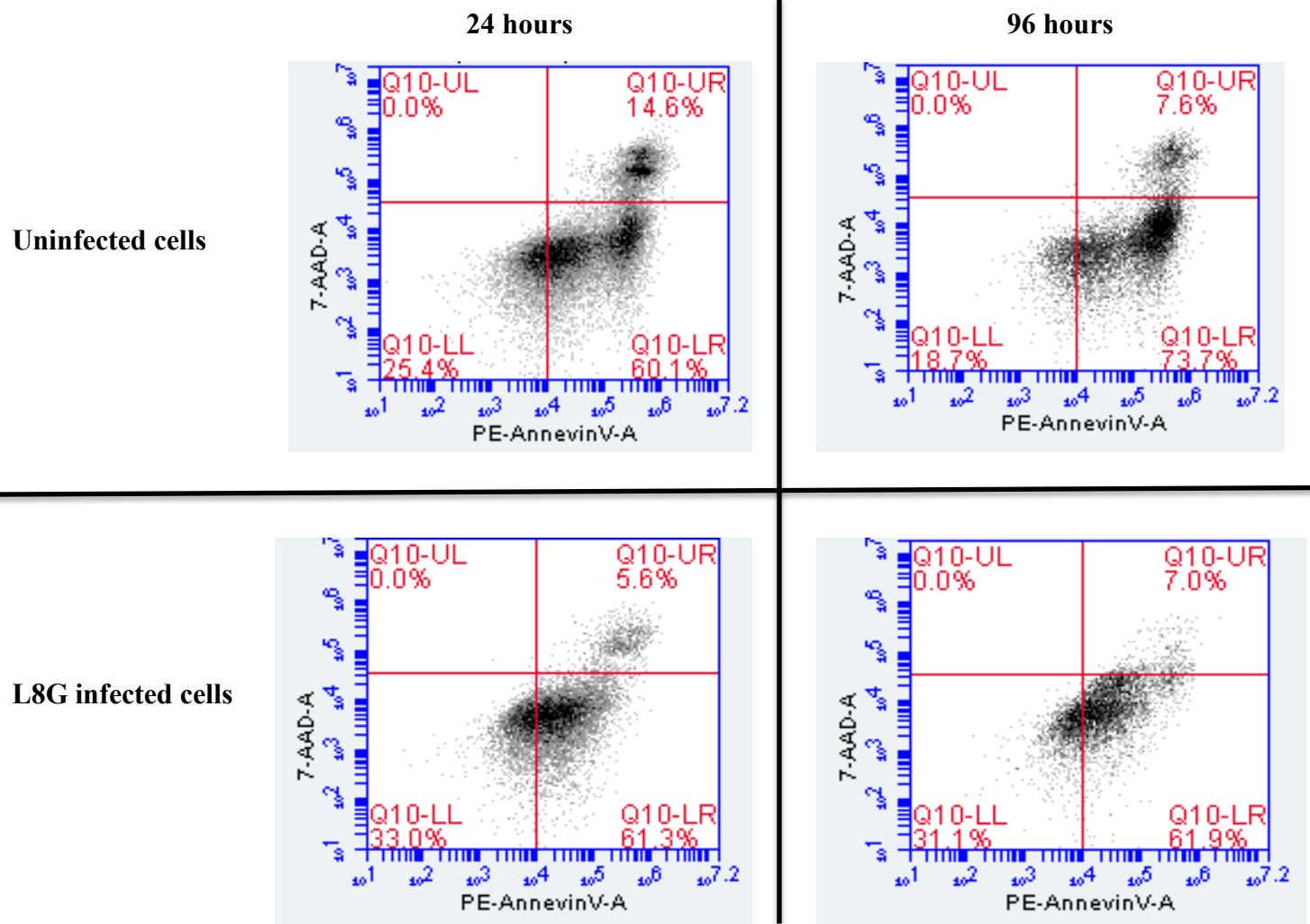


Figure 3.8. Flow cytometry analysis of Annexin V versus 7-AAD dot plot after washing protocol. Infected (e.g. L8G) and uninfected cells were treated with camptothecin and washed after 24 hours before analysing for apoptosis from 24 to 96 hours. By removing excess camptothecin (after 24 hours incubation), uninfected and L8G infected cells at 96 hours incubation showed comparable levels of necrosis in relative to 24 hours. Moreover, this characteristic was maintained at 24 and 72 hours from infection as well in all four species examined.

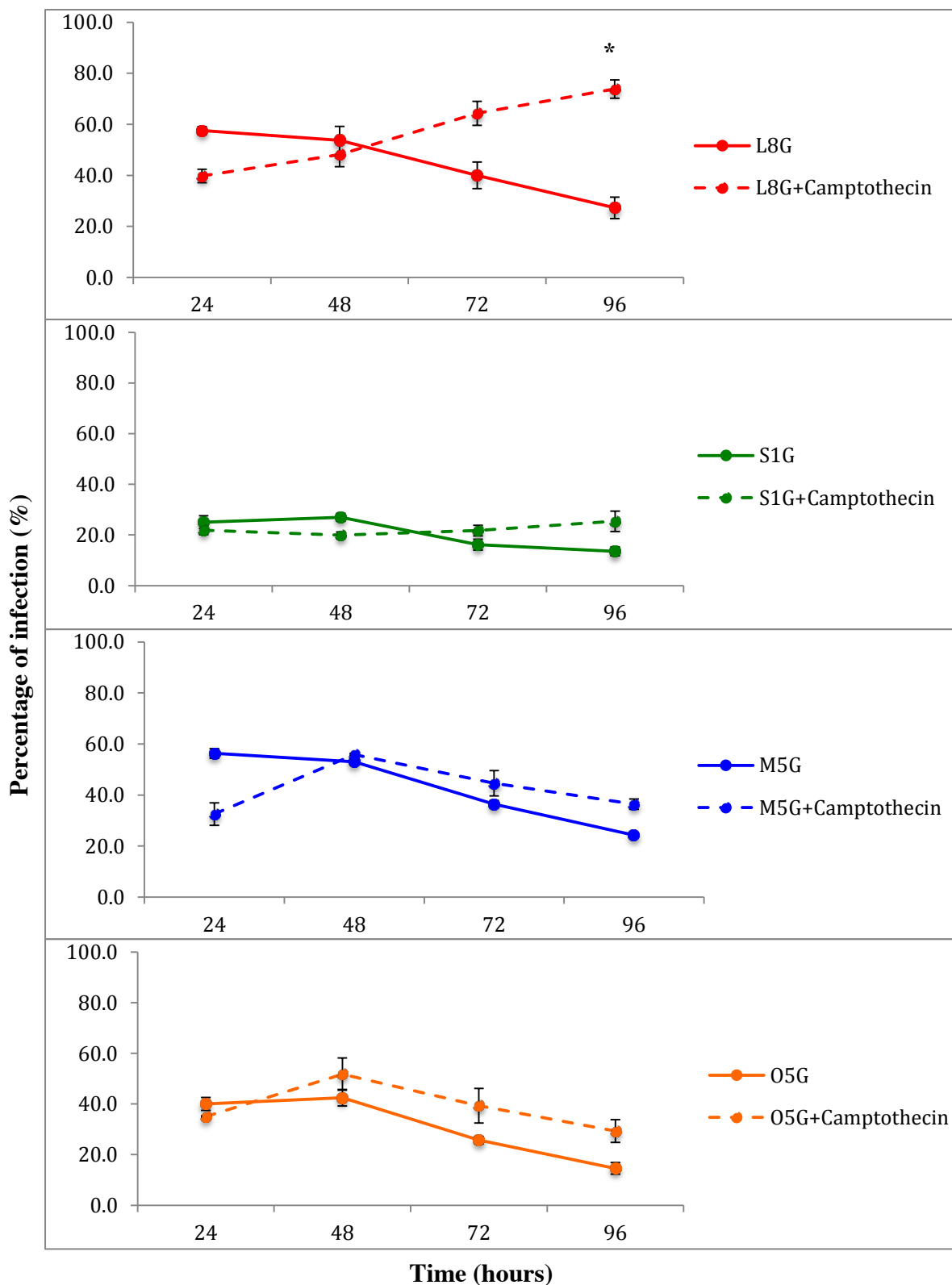


Figure 3.9. Effect of shorter exposure to camptothecin treatment on *Leishmania* infection. Following infection (10 parasites per 1 cell ratio) with L8G, S1G, M5G and O5G, the infected cells were treated with or without camptothecin. After 24 hours of infection, excess drug was washed away. The percentage of infection was then determined at 24, 48, 72 and 96 hours through flow cytometry. The data represents mean percentage (mean \pm SEM) from three independent experiments. * = $p < 0.05$.

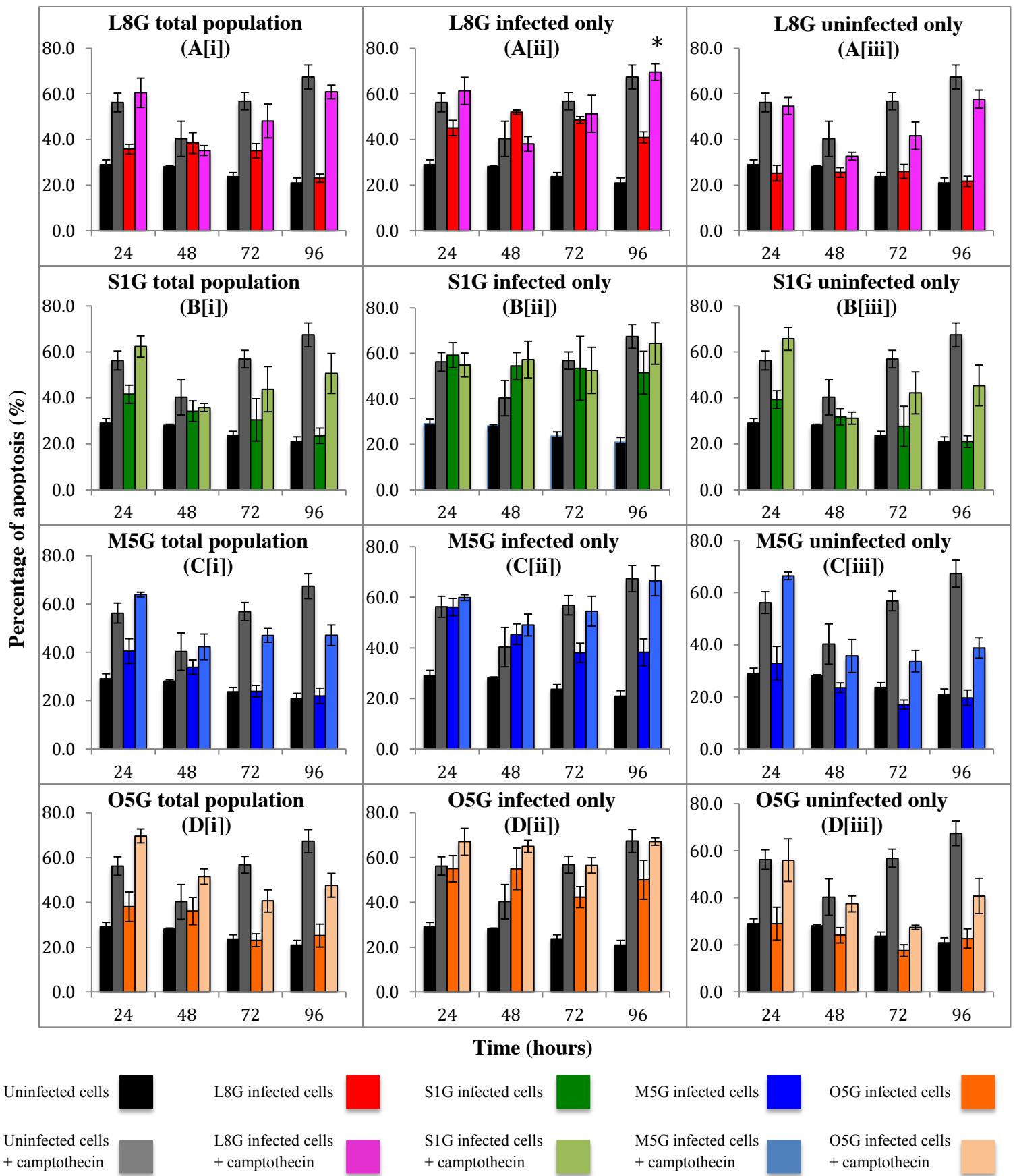


Figure 3.10. Effect of shorter exposure to camptothecin treatment on the apoptosis of differentiated THP-1 macrophages infected with *Leishmania*. Following infection (10 parasites per 1 cell ratio) with L8G, S1G, M5G and O5G, the infected cells were treated with or without camptothecin. After 24 hours of infection, excess drug was washed away. The percentage of apoptosis in total population was detected at 24, 48, 72 and 96 hours [i]. The data was divided into infected only [ii] and uninfected only [iii] populations. The data represents mean percentage (mean \pm SEM) from three independent experiments. * = $p < 0.05$

3.2.4. Assessment of viable cell concentration during *Leishmania* infection in the presence of camptothecin

According to the above data, camptothecin treatment caused a significant rise in L8G infection, which was correlated with an increase in host cell apoptosis. To confirm whether this increase could be due to parasite spreading or loss of viable cells, trypan blue assay was performed. The result showed no significant difference in the concentration of viable cells in L8G infected cells from 24 to 96 hours in the presence of camptothecin (Figure 3.11). This indicates that parasite dissemination must be occurring within this time frame.

However, when the above result is compared against non-treated samples, there is a marked reduction in the concentration of viable cells in L8G infected culture throughout the time point (Figure 3.11). This suggests that the recipient cells within the infected culture may not be healthy and do not represent an effective model to study cell-to-cell spread.

3.3. Conclusions

In conclusion, this chapter demonstrated a clear link between *Leishmania* infection spreading and host cell apoptosis. This was confirmed through two experimental approaches. Firstly, promastigotes infection with *L. aethiopica*, *L. major*, *L. mexicana* and *L. tropica* caused an induction of apoptosis in differentiated THP-1 macrophages till 96 hours. However, as a result of uninfected THP-1 cells replication, there was a significant decrease in the percentage of infection in all four species.

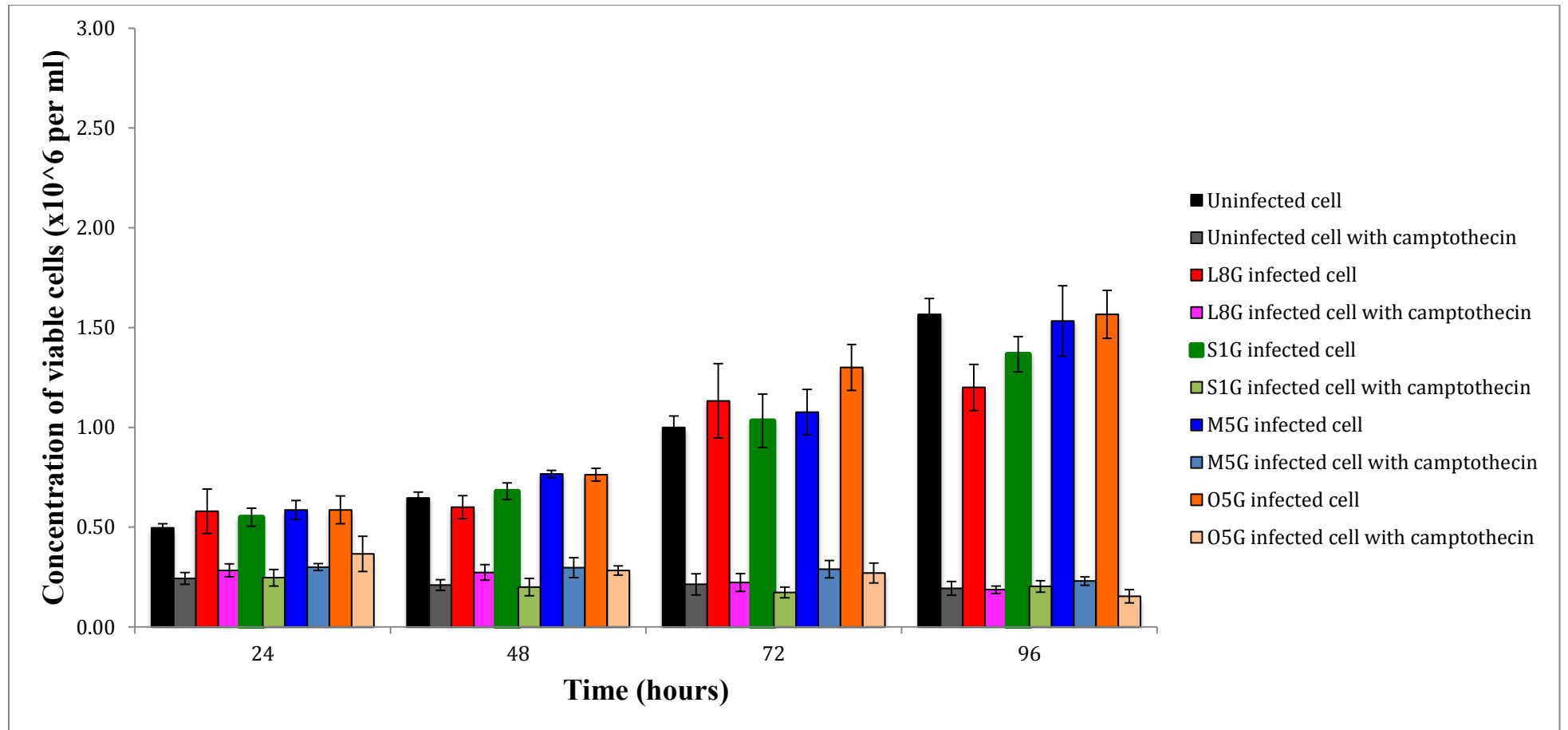


Figure 3.11. Effect of camptothecin on viable cell concentration in the presence or absence of infection. Uninfected or infected cells (L8G, S1G, M5G and O5G) treated with or without camptothecin were stained with trypan blue solution at 24, 48, 72 and 96 hours. The data represents mean concentration of viable cells (mean±SEM) from three independent experiments.

This made it difficult to detect infection and parasite dissemination from 48 hours onwards. This led to a second approach whereby infected cells were treated with apoptotic inducer to determine whether apoptotic induction had an effect on the outcome of infection. By optimizing the length of camptothecin treatment, a time dependent increase in the percentage of *L. aethiopica* infected cells was detected from 48 to 96 hours. As this effect was correlated with increased percentage of apoptosis, a positive link between infection spreading and apoptotic cell death was suggested. However, since the trypan blue assay revealed a marked reduction in the concentration of viable cells when compared to non-treated samples, this raised major doubts on whether the recipient cells are physiologically healthy to represent a cell-to-cell spreading model. Therefore, a novel *in vitro* *Leishmania* infection model needs to be optimized if infection spreading is to be carried out for further investigation.

Chapter 4 – The *in vitro* development of *Leishmania* dissemination model during late stage of macrophage infection

4.1. Introduction

The dissemination of infectious progeny from cell-to-cell is of vital importance for disease establishment by intracellular human pathogens. Various *in vitro* models have been successfully used to study cell-to-cell spreading for a number of human pathogens such as, *Listeria monocytogenes* (Czuczman et al., 2014), *Shigella flexneri* (Fukumatsu et al., 2012), *Legionella pneumophila* (Chen et al., 2004), Human Immunodeficiency Virus (HIV) (Sattentau, 2010) and *Cryptococcus neoformans* fungus (Ma et al., 2007). Although these studies highlighted the diverse mechanism of pathogen spreading, whether such process is also reflected in natural infection transmission requires the use of *in vivo* animal models.

However, animal models designed to address infection spreading have various limitations, which are: 1) The approach is labor intensive and time consuming as it requires large number of animals to be sacrificed to obtain convincing data; 2) Dissection of animal at each set of time point means it would be impossible to monitor the progress of infection for an individual animal over time; 3) The approach is dependent on researcher's knowledge of the infected organs, as dissemination to unexpected anatomical sites or even to particular sub-compartments of the organ being examined may easily be missed. Due to these constraints, *in vitro* model represent a more suitable experimental system to investigate the spreading of human pathogens, including *Leishmania* parasites.

Unfortunately, *in vitro* studies associated with *Leishmania* spreading are very scarce due to experimental difficulty to model late stage of parasite-host interaction. Nevertheless, through live video microscopy, a recent study was able to show the transfer of amastigotes from 20 days *L. amazonensis* infected mice BMDM to RAW mice macrophages within 24 hours of cell-to-cell infection (Real et al., 2014). However, since mice are not the natural host for *Leishmania*, it is difficult to extrapolate the above findings from mice to human macrophage. Interestingly, another study successfully demonstrated *L. infantum chagasi* spreading in human U937 macrophages within 72 hours of infection (Hsiao et al., 2011). However, such phenomena were not observed in primary human monocyte derived macrophages (MDM), thereby underlying the importance of selecting a suitable cell line for *Leishmania* infection.

The present chapter, which is an extension of the work from chapter 3, is aimed at developing a novel *in vitro* model to study the dissemination of two *Leishmania* species, *L. aethiopica* and *L. mexicana*. By employing a cell associated infection strategy, the late stages of *L. aethiopica* and *L. mexicana* infected population were used as a donor cells to re-infect freshly differentiated THP-1 macrophages. Such co-culture system was optimized to identify the time frame behind amastigote spreading, which was confirmed via flow cytometry and real time lapse microscopy analysis. Moreover, to gain an understanding of the possible mechanism behind parasite spreading, two apoptotic markers including phosphatidyl serine (PS) externalization and caspase-3 activation within this time frame was assessed.

4.2. Results and Discussion

4.2.1. Optimization of camptothecin treatment in *L. mexicana* (M5G) infected cells

In order to optimize spreading, population of highly infected cells need to be isolated. As previously reported (Chapter 3, section 3.2.3), the largest proportion of *L. aethiopica* (L8G) infected cells was found at 72 and 96 hours from infection, following 24 hours camptothecin treatment. However, such effects were not detected during M5G infection. Based on a well-known notion that species-specific difference occurs in *Leishmania* parasites (Ilg, 2000), M5G infected cells were treated with camptothecin for only 5 hours from infection.

At 24 hours, there was no significant difference in the percentage of M5G infection between camptothecin treated and non-treated samples (Figure 4.1). Interestingly, the percentage of M5G infected cells increased significantly ($p < 0.05$) from 24 hours, reaching a maximum of 90% by 72 hours in the presence of camptothecin. As expected, M5G infection in the absence of camptothecin stabilized at 48 hours, before dramatic reduction occurred at 72 and 96 hours. However, in camptothecin treated samples, the percentage of M5G infected cells remained high and plateaued till 96 hours. Hence, by reducing the exposure time of apoptotic induction, M5G was clearly able to maintain higher percentage of infected cells during the late stage of infection, similarly to what had been described for L8G in chapter 3.

4.2.2. Infection of differentiated THP-1 macrophage with L8G and M5G infected cells

Since the effect of camptothecin led to an increase in the percentage of L8G and M5G infected cells, this population was isolated and used to infect a freshly prepared culture of differentiated THP-1 macrophages.

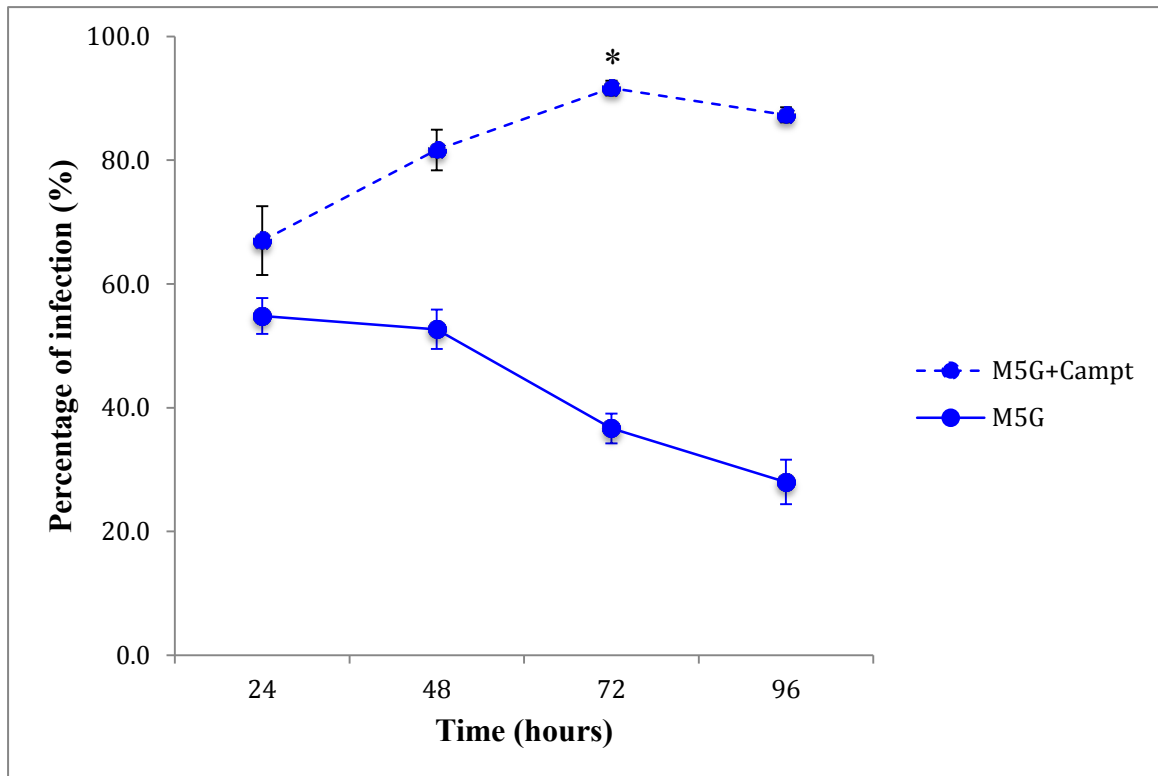


Figure 4.1. Time course of differentiated THP-1 macrophage infection with *L. mexicana* (M5G) in the presence and/or absence of apoptotic induction. Differentiated THP-1 macrophages were infected M5G promastigotes at 10:1 ratio (parasite to cell ratio) and treated with (or without) camptothecin to induce apoptosis. Excess camptothecin was washed away from culture medium at 5 hours after infection. The percentage of infection was determined through flow cytometry at 24, 48, 72 and 96 hours. The data represents mean percentage (mean \pm SEM) from three independent experiments. * = $p < 0.05$

To initiate cell-to-cell infection, L8G and M5G infected cells from 72 hours were used as the donor population. Different infection ratios were tested (1:1, 5:1 and 10:1 [infected per healthy cell ratio]) and the course of infection was detected at 0, 12, 24 and 48 hours after co-culture through flow cytometry. At 0 hour after co-culture between infected and uninfected cells, a dilution effect on the percentage of infection for both L8G and M5G was detected (Figure 4.2.A and 4.2.C). Since a higher proportion of uninfected cells were incorporated with GFP positive infected cells at 1:1 infection ratio, this specific ratio generated a more pronounced decrease in infection than 5:1 and 10:1 ratio at 0 hour after co-culture. Strikingly, after 12 hours of co-culture, the percentage of L8G infected cells significantly increased ($p < 0.05$) from 35 ± 2.6 to $60 \pm 2.1\%$ for 1:1, 54 ± 2.4 to $69 \pm 2.9\%$ for 5:1 and 58 ± 4.1 to $74 \pm 0.8\%$ for 10:1 infection ratios (Figure 4.2.B). Such significant increase in infection was also observed during co-culture with M5G infected cells; 51 ± 2.3 to $76 \pm 5.5\%$ for 1:1, 71 ± 3.5 to $88 \pm 0.6\%$ for 5:1 and 80 ± 2.1 to $90 \pm 2.3\%$ for 10:1 infection ratios (Figure 4.2.D).

The significance of the above findings is strengthened by the viability count, which showed no significant differences in the concentration of viable cells between 0 and 12 hours post infection (Figure 4.3). This strongly suggested that the infection increase from 0 to 12 hours time frame was due to spreading of L8G and M5G amastigotes from the 72 hours donor infected cells to healthy cells and not caused by the reduction of uninfected viable cells. However, there were no further increase in the percentage of L8G and M5G infected cells from 12 to 24 hours after co-culture (Figure 4.2.B and 4.2.D). This suggests that the transferred amastigotes in its new macrophage niche were unable to replicate within this time frame to continue next round of cell-to-cell spreading.

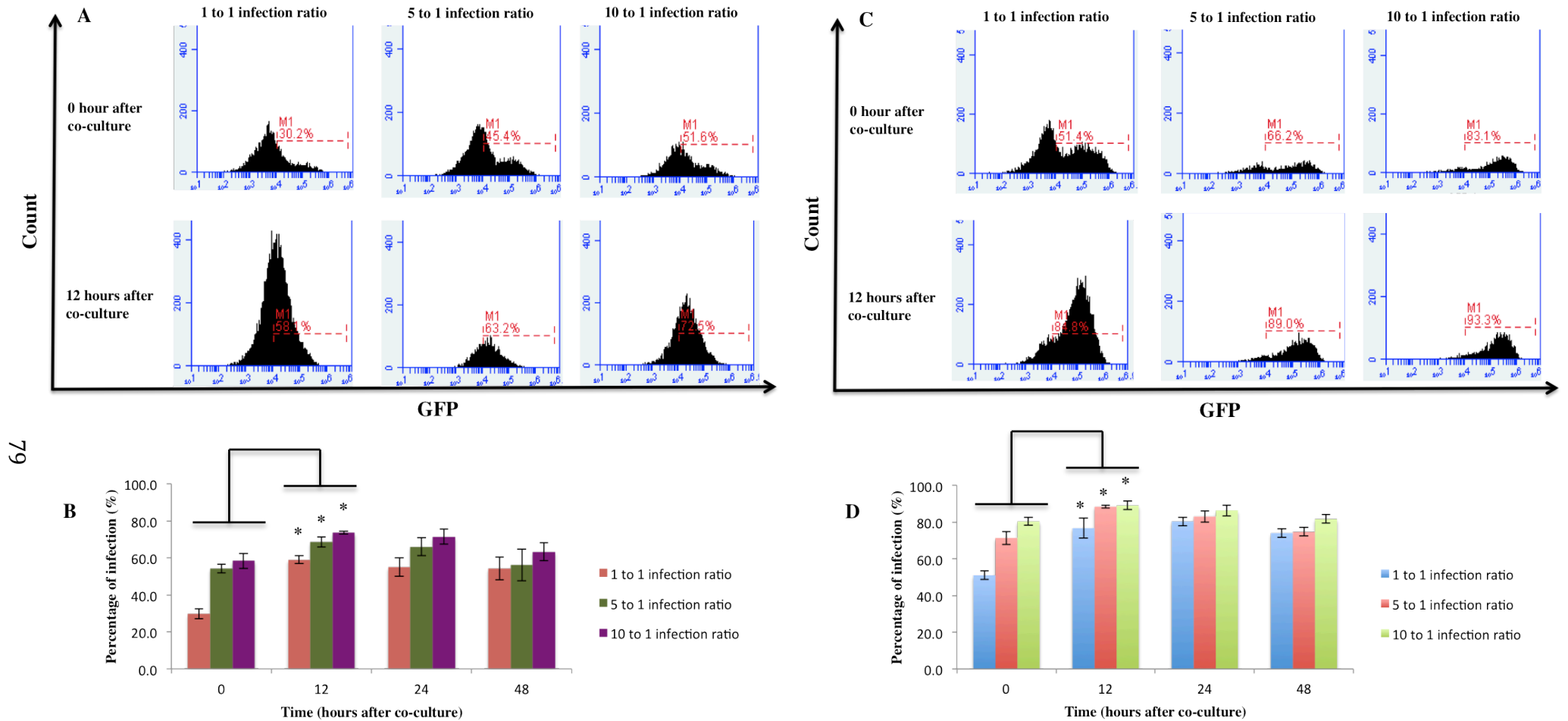


Figure 4.2. Infection of THP-1 macrophages with *Leishmania* infected cells. After 72 hours of infection, L8G and/or M5G infected cells were co-cultured with a fresh population of differentiated THP-1 macrophage at different infection ratios, 1:1, 5:1 and 10:1 (infected to uninfected cell ratio). **(A)** Flow cytometry histogram plot representative of L8G infected cells M1 at 0 and 12 hours after co-culture. **(B)** A bar graph representative of the percentage of L8G infection (mean \pm SEM) at 0, 12, 24 and 48 hours after co-culture. **(C)** Flow cytometry histogram plot representative of M5G infected cells M1 at 0 and 12 hours after co-culture. **(D)** A bar graph representative of the percentage of M5G infection (mean \pm SEM) at 0, 12, 24 and 48 hours after co-culture. * = $p < 0.05$

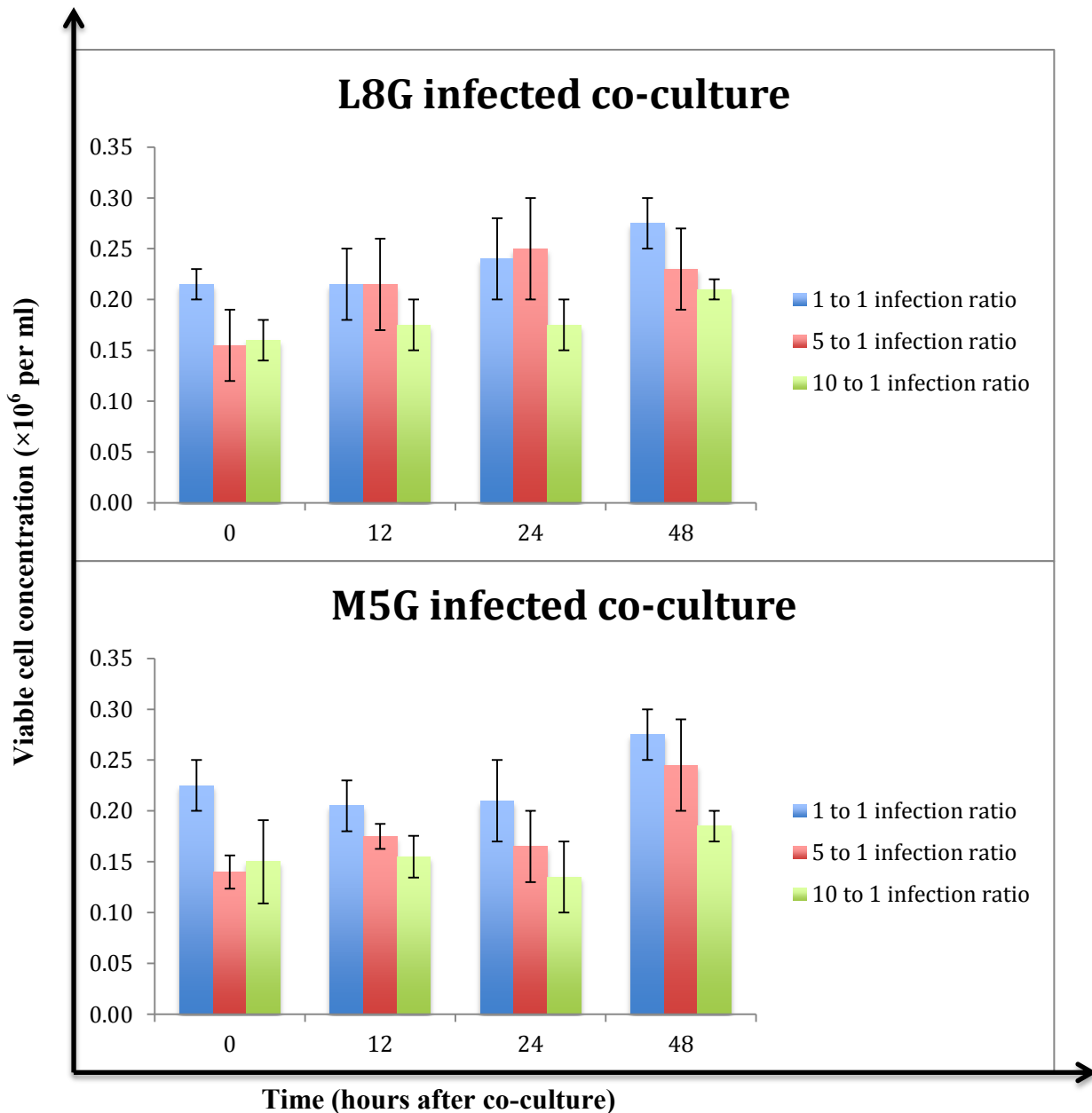


Figure 4.3. Measurement of viable cell concentration during infection with *Leishmania* infected cells. L8G infected and M5G infected co-culture cells at different infection ratios were stained with trypan blue solution at 0, 12, 24 and 48 hours after co-culture. The data represents mean concentration of viable cells (mean \pm SEM) from three independent experiments.

Overall, the above results provided a quantitative evidence for L8G and M5G amastigotes spreading from 0 to 12 hours after co-culture. This *in vitro* spreading model provides an initial platform to address the cellular mechanism behind the 12 hours spreading time period.

4.2.3. Live cell imaging of intracellular L8G and M5G amastigotes spreading

During cell-to-cell infection spreading, intracellular pathogens within the donor cells can trigger either a lytic or a non-lytic release (Sattentau, 2010). To verify whether such process might occur during L8G and M5G release, real time lapse microscopy was performed using the newly developed *in vitro* spreading model comprising of 1:1 infection ratio. An advantage of 1:1 infection ratio over 5:1 and 10:1 was to ensure that there would be sufficient numbers of recipient host cells to harbor the released amastigotes.

Initially, differentiated THP-1 macrophages (pre-stained with membrane dye) were co-cultured with L8G and/or M5G infected cells and live cell imaged over 12 hours. Figure 4.4 shows time lapse events from 8 hours, in which L8G amastigotes (pointed with red arrow) begins to migrate towards the peripheral membrane of the donor cells, before completely transferring into the already infected recipient stained cells within 20 minutes of recording. This phenomenon was also visualized in M5G infected co-culture after 6 hours whereby an amastigote (pointed with red arrow) appeared to be extruded into the recipient stained cells (Figure 4.5). Since the donor cell membrane (in both scenarios) was not damaged during amastigote transfer, this suggests that *Leishmania* spread via non-lytic mode. It is not clear whether recipient macrophages selectively engulf L8G and M5G via recognition of parasite or host associated markers present in the donor cell.

L. aethiopica spreading

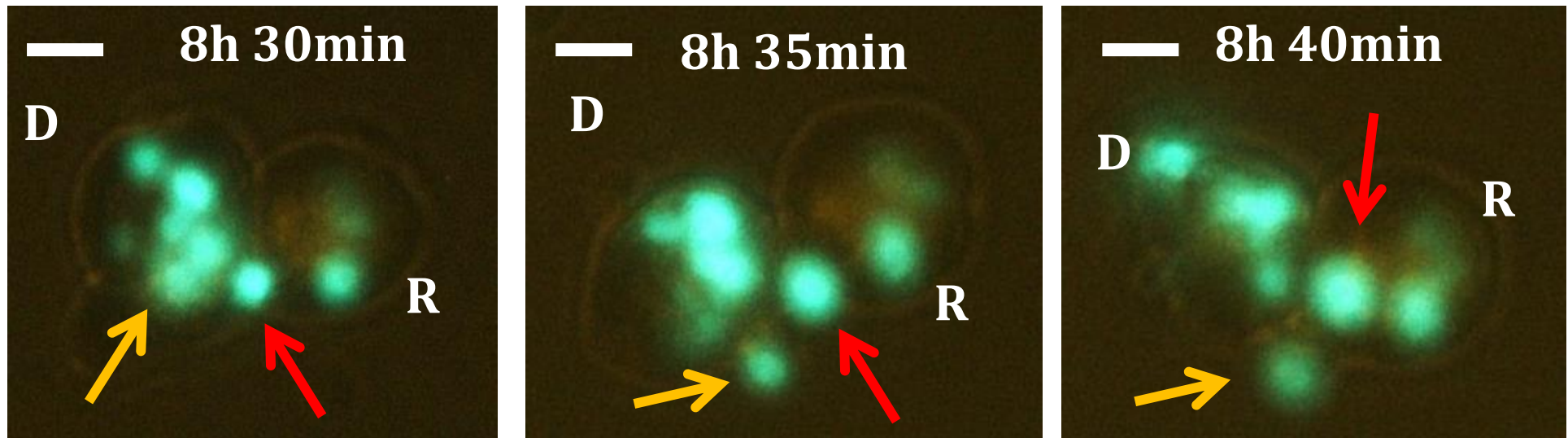


Figure 4.4. Live cell imaging of *L. aethiopica* (L8G) amastigotes spread from cell-to-cell. The differentiated THP-1 macrophage, which is the recipient uninfected cells (labeled as R), was pre-stained with CellMaskTM orange plasma membrane dye. The recipient cells were then co-cultured with L8G infected cells, which is the donor cells (labeled as D) as described in Chapter 2, section 2.8. The time of acquisition is represented by hours (h) and minutes (min). Image acquisition started at 8 hours after co-culture. Bar = 25 μ m.

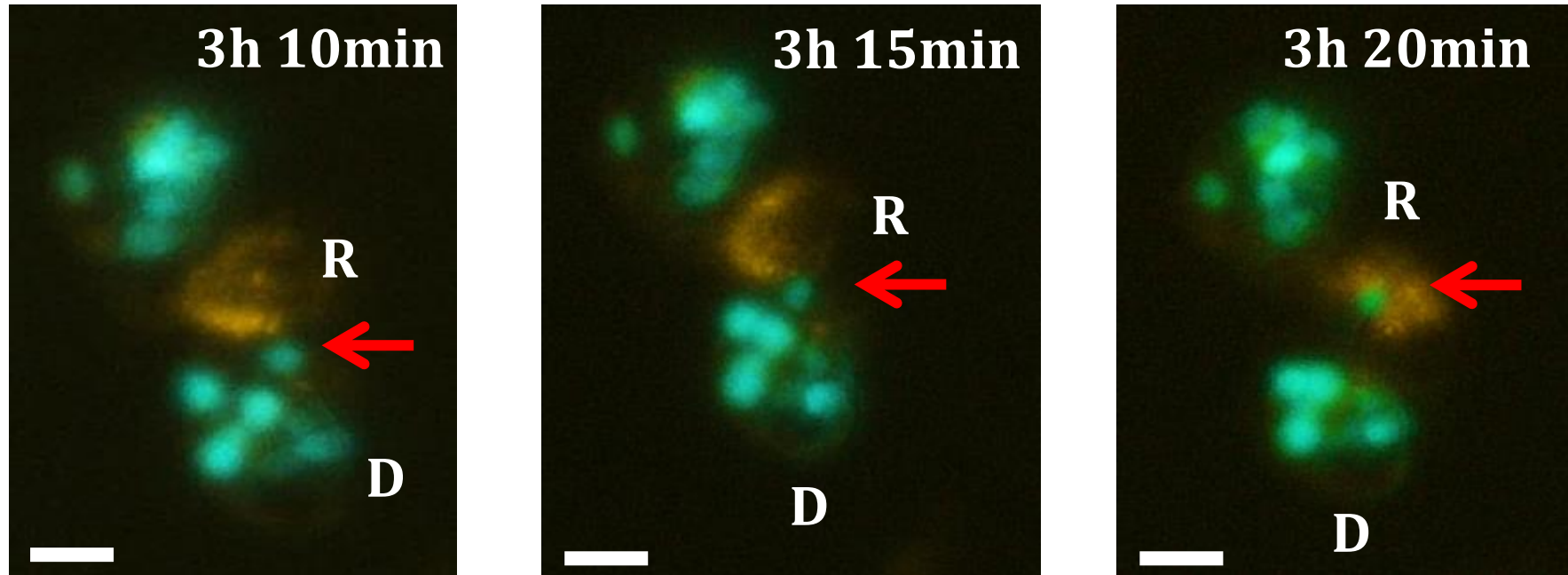
L. mexicana spreading

Figure 4.5. Live cell imaging of *L. mexicana* (M5G) amastigotes spread from cell-to-cell. The differentiated THP-1 macrophage, which is the recipient uninfected cells (labeled as R), was pre-stained with CellMask™ orange plasma membrane dye. The recipient cells were then co-cultured with M5G infected cells, which is the donor cells (labeled as D) as described in Chapter 2, section 2.8. The time of acquisition is represented by hours (h) and minutes (min). Image acquisition started at 3 hours after co-culture. Bar = 25 μ m.

In summary, the real time lapse microscopy revealed the non-lytic release of amastigotes from cell-to-cell and provided confirmation of a strong link with quantitative flow cytometry data on infection spreading. This has now opened up an avenue to further investigate the role of host cells in facilitating the spreading of *Leishmania* amastigotes.

4.2.4. Effect of *Leishmania* spreading on the apoptosis of host cells

A recent study revealed the non-lytic exit of *L. amazonensis* amastigotes from mice macrophage was correlated with apoptotic features such as zeiotic and blebbed membranes (Real et al., 2014). Therefore, in order to determine whether apoptosis could also be involved in the spreading of *L. aethiopica* and *L. mexicana*, the presence of host apoptotic markers, i.e. Phosphatidyl serine (PS) externalization and Caspase-3 activation, were tested using the newly developed model.

Initial assessment of PS externalization showed a time dependent increase in the percentage of apoptosis from 1 to 12 hours after co-culture with L8G infected cells (Figure 4.6.A). This effect appeared to be mediated solely by the intracellular L8G amastigotes since the uninfected cells co-culture displayed no significant changes in apoptosis within 12 hours. Interestingly, direct analysis of the L8G infected only population showed that the percentage of apoptosis was significantly higher ($p < 0.05$) at 12 hours ($55 \pm 3.5\%$) than at 1 hour ($38 \pm 4.1\%$) (Figure 4.6.B). This clearly indicated a positive correlation between apoptotic induction and infection spreading. In contrast, there were no significant differences in the percentage of necrosis from 1 to 12 hours in L8G infected only population (Appendix I). This together with the fact that the necrosis in the uninfected only population was comparable with the control suggested that L8G infection spreading was independent with necrotic cell death (Appendix I).

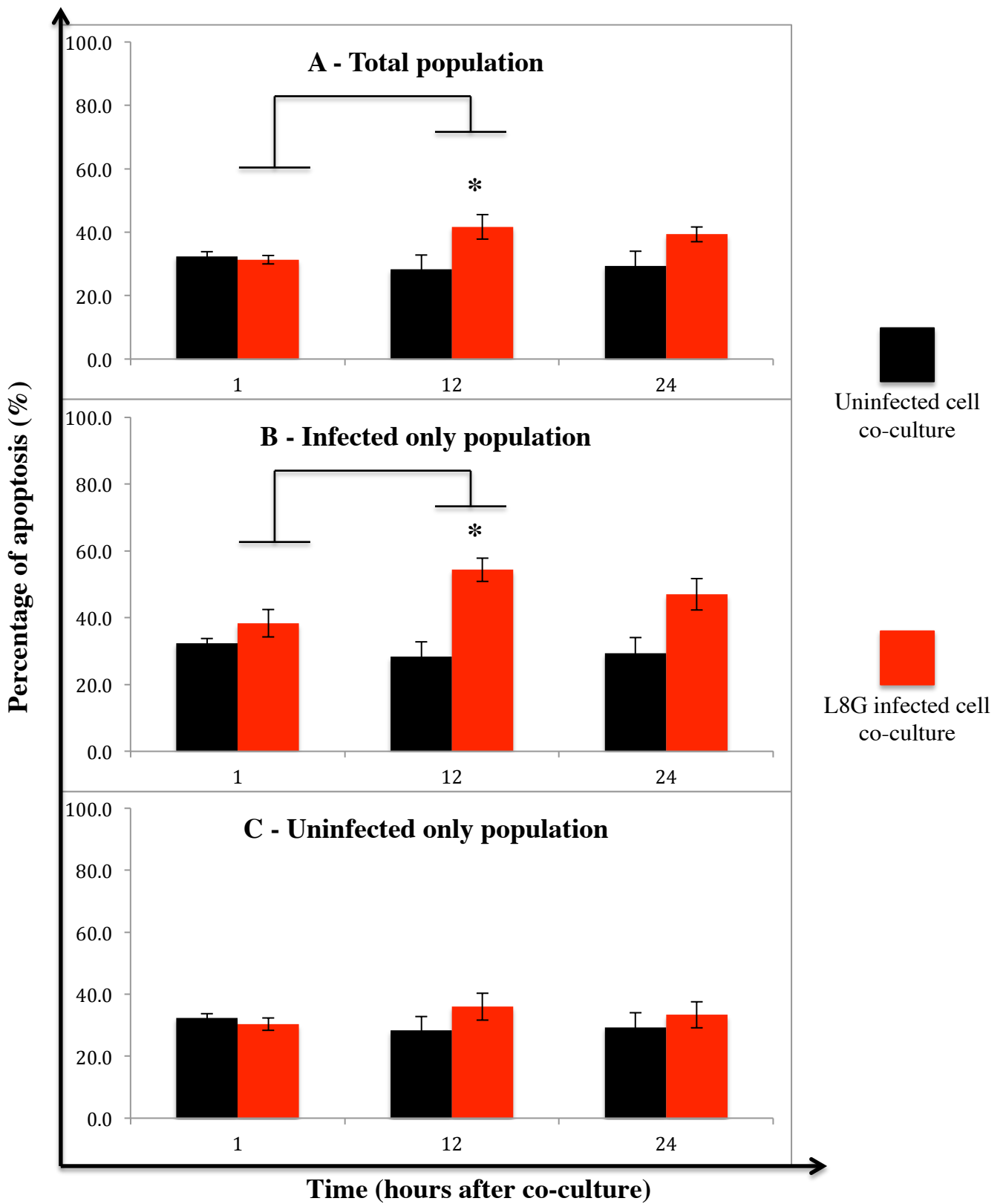


Figure 4.6. Effect of L8G infection spreading on host cell apoptosis. After infection of differentiated THP-1 macrophages with L8G infected cells, the co-culture were analyzed for the percentage of apoptosis (Annexin V+/7AAD-) through flow cytometry at 1, 12 and 24 hours after co-culture. Apoptosis from the total population (A) were divided into infected only (B) and uninfected only (C) populations. Uninfected cells co-cultured with differentiated THP-1 macrophages were taken as a positive control. The data represents mean percentage (mean \pm SEM) from three independent experiments. * = $p < 0.05$

Next, the expression of active caspase-3 was detected at 1, 3 and 6 and 12 hours after co-culture with L8G infected cells. The percentage of active caspase-3 at 1 hour was comparable to uninfected controls (Figure 4.7). Interestingly, from 3 to 12 hours, the active caspase-3 expression remained significantly higher ($p < 0.05$). This data along with PS externalization supports the notion that apoptotic induction is actively occurring during L8G spreading.

These findings were in stark contrast to M5G, as the parasitic spread was not associated with any markers of apoptosis. Firstly, there was no significant increase in the percentage of PS externalized cells from 1 to 12 hours after co-culture (Figure 4.8). Secondly, the percentage of active caspase-3 was comparable with the uninfected control at throughout the spreading time period (Figure 4.9). These suggest the involvement of non-apoptotic mechanism of infection spreading induced by M5G amastigotes.

Dissemination of human pathogens via non-apoptotic has been noted previously. The bacteria *Chlamydia* exit host cells after a non-lytic, actin-dependent extrusion from the host cell. In this process, the bacteria are extruded in a double-membrane vesicle generated from the bacterial intracellular vacuole and cytoplasmic membranes (Hybiske and Stephens, 2007). During *in vitro* cell-to-cell transmission, *M. marinum* is ejected from host cells through an F-actin-rich structure denominated ejectosome (Hagedorn et al., 2009); the bacteria also remain associated with membrane remnants in the process. The fungus *Cryptococcus neoformans* escape from host cells by an active, pathogen-driven extrusion process, apparently without damaging the host (Ma et al., 2007). Whether such mechanism exist during *L. mexicana* spread requires further investigation.

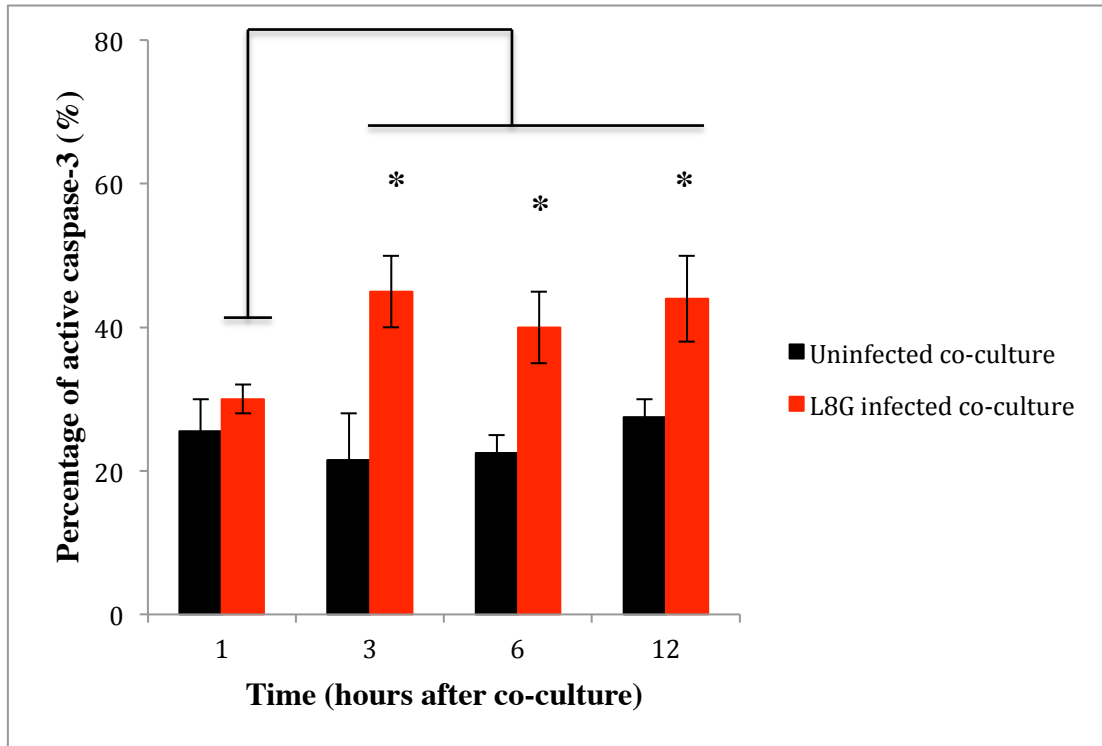


Figure 4.7. Effect of L8G infection spreading on the activation of caspase-3 in host cells.

After re-infection of differentiated THP-1 macrophages with L8G infected cells, the co-culture were analyzed for the percentage of activated caspase-3 through flow cytometry at 1,3, 6 and 12 hours after co-culture. Uninfected cells co-cultured with differentiated THP-1 macrophages were taken as a positive control. The data represents mean percentage (mean \pm SEM) from three independent experiments. * = $p < 0.05$

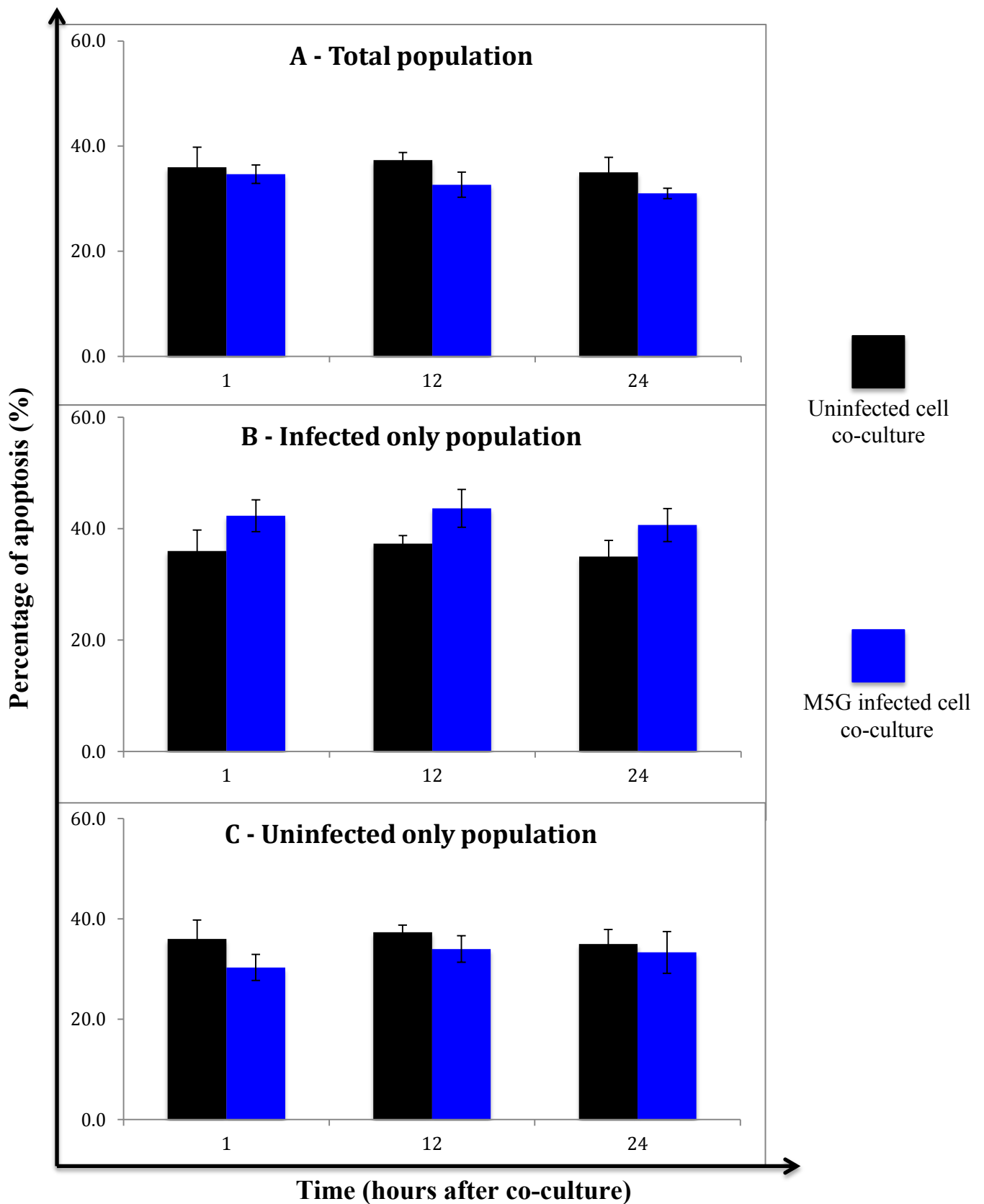


Figure 4.8. Effect of M5G infection spreading on host cell apoptosis. After infection of differentiated THP-1 macrophages with M5G infected cells, the co-culture were analyzed for the percentage of apoptosis (Annexin V+/7AAD-) through flow cytometry at 1, 12 and 24 hours after co-culture. Apoptosis from the total population (**A**) were divided into infected only (**B**) and uninfected only (**C**) populations. Uninfected cells co-cultured with differentiated THP-1 macrophages were taken as a positive control. The data represents mean percentage (mean \pm SEM) from three independent experiments.

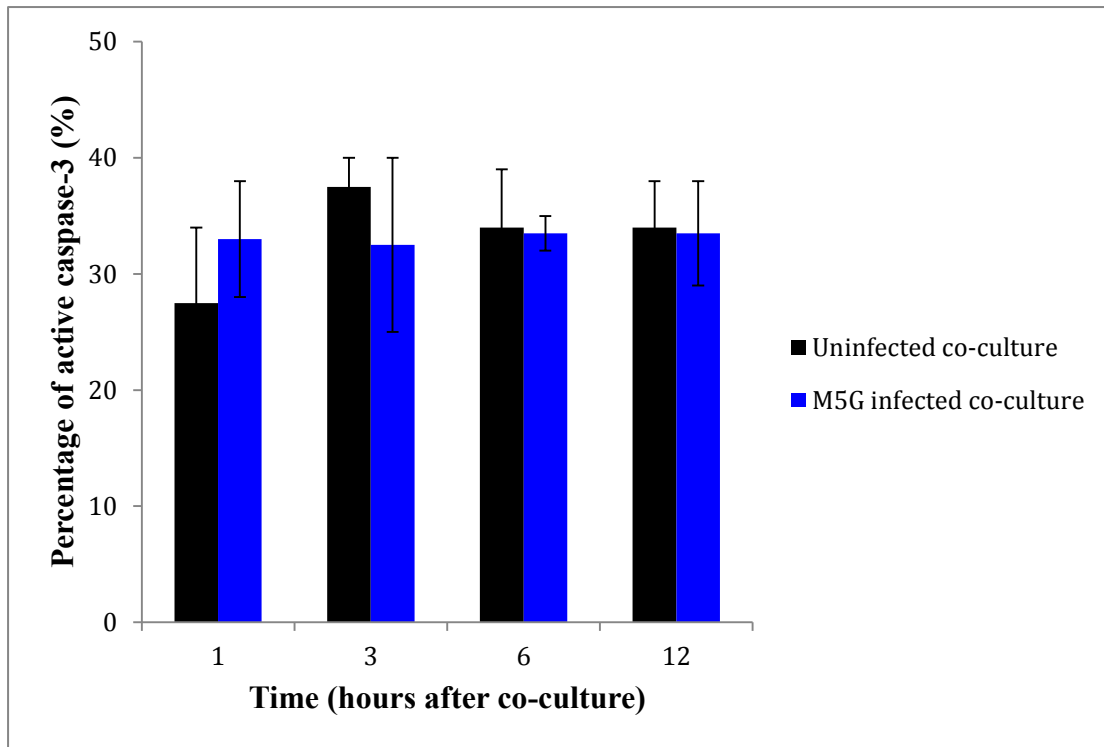


Figure 4.9. Effect of M5G infection spreading on the activation of caspase-3 in host cells.

After re-infection of differentiated THP-1 macrophages with M5G infected cells, the co-culture were analyzed for the percentage of activated caspase-3 through flow cytometry at 1,3, 6 and 12 hours after co-culture. Uninfected cells co-cultured with differentiated THP-1 macrophages were taken as a positive control. The data represents mean percentage (mean \pm SEM) from three independent experiments.

4.2.5. Effect of caspase-3 inhibition on the apoptosis and infection spread

Since the data suggested a clear link between L8G spreading and apoptosis, the next step was to test whether apoptotic induction is critically involved in infection spreading. The infected donor cells were treated with various concentration of Caspase-3 inhibitor (Z-DEVD-FMK) before infecting differentiated THP-1 macrophages. The co-culture was analyzed for infection rate and active caspase-3 expression at 3 and 12 hours. Infected co-culture without Z-DEVD-FMK treatment was taken as a positive control in this experiment.

The result showed that 25 μ M of inhibitor was unable to reduce the percentage of active caspase-3 compared to non-treated samples (Figure 4.10.A). However, the pre-treatment with 100 μ M significantly ($p < 0.05$) reduced the percentage of active caspase-3 at 3 and 12 hours, compared to the non-treated infected co-culture (Figure 4.10.A). Interestingly, this effect of caspase-3 inhibition led to a marked decrease in the percentage of infection at 12 hours in comparison with positive control (Figure 4.10.B). Since the percentage of infection increase observed from 3 to 12 hours was not significant indicates that this inhibitory effect completely blocked, rather than delayed, the spreading of infection.

Together the above findings demonstrate that the L8G amastigotes induces apoptosis via caspase-3 dependent pathway in order to initiate the process of cell-to-cell spreading of infection.

4.3. Conclusions

In conclusion, for the first time, the development of a credible *in vitro* model representing the dissemination of *Leishmania* parasites during late stage of human macrophage infection was reported.

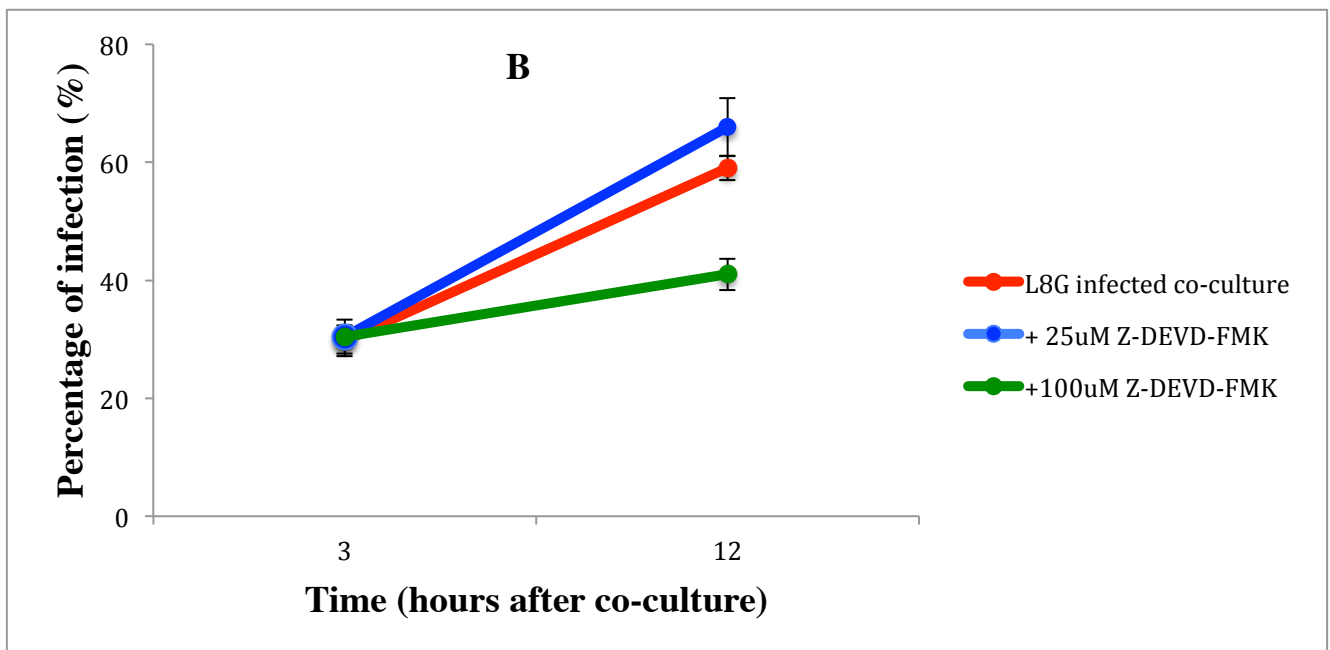
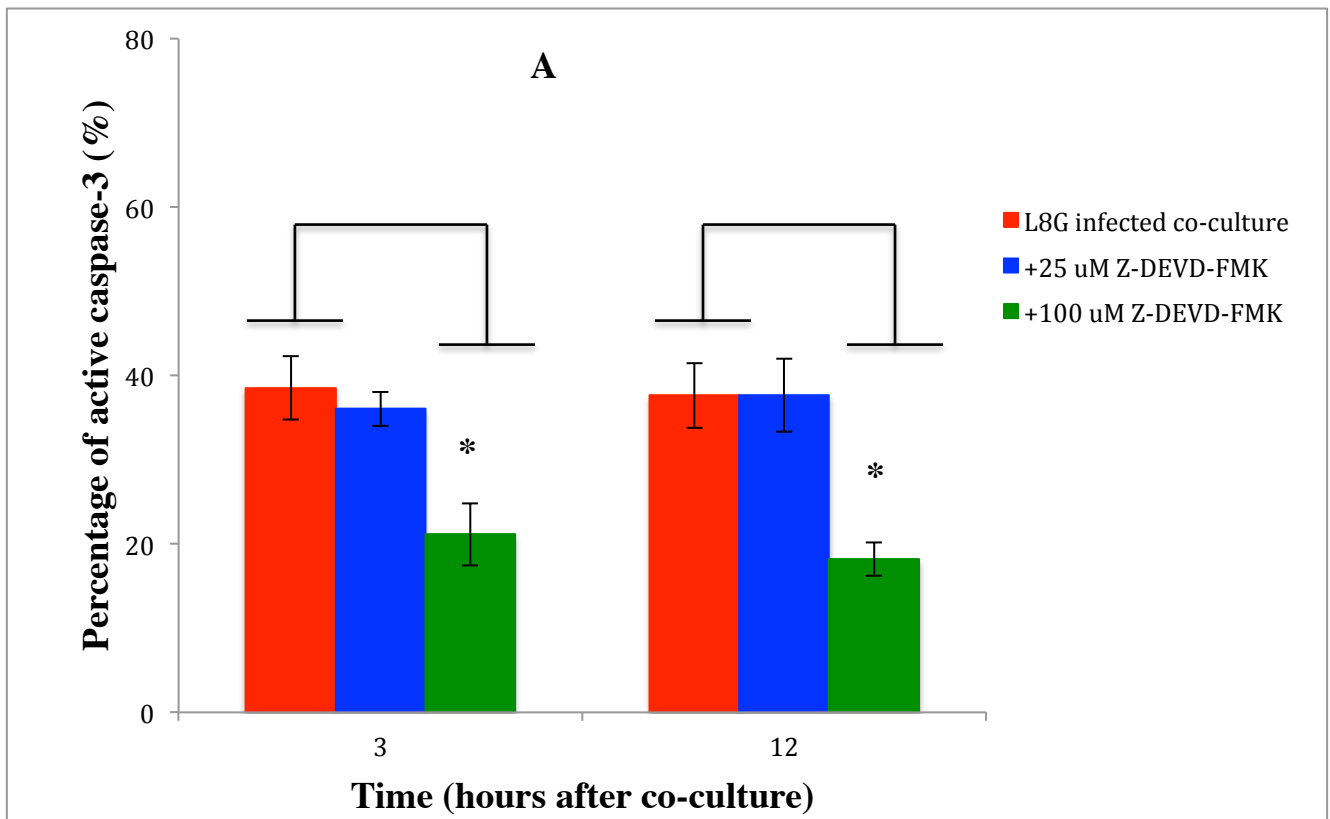


Figure 4.10. Effect of caspase-3 inhibition on the apoptosis and infection spread after infection with L8G infected cells. After L8G infected cell treatment with and/or without Z-DEVD-FMK for 4 hours, it was co-cultured with differentiated THP-1 macrophages. The co-culture was analyzed for the percentage of activated caspase-3 (A) and infection (B) through flow cytometry at 3 and 12 after co-culture. The data represents mean percentage (mean \pm SEM) from three independent experiments. * = $p < 0.05$

Initially, this model involved the co-culture of *L. aethiopica* and *L. mexicana* infected cells (apoptotic induced) with a healthy population of differentiated THP-1 macrophages. This experimental infection with infected cells led to an overall increase in the percentage of infection within 12 hours, demonstrating a potential cell-to-cell spreading of *L. aethiopica* and *L. mexicana* amastigotes. This was confirmed using real time lapse microscopy, which revealed extrusion and subsequent transfer of amastigotes from infected to a healthy macrophage in a non-lytic mode.

Interestingly, this form of cell-to-cell spreading of *L. aethiopica*, but not *L. mexicana*, appeared to be correlated with apoptotic induction as there was a significant increase in the PS externalization and active caspase-3 expression. Furthermore, the inhibition of apoptosis via caspase-3 inhibitor completely prevented an increase in the percentage of infection. This highlighted the critical involvement of *L. aethiopica* mediated apoptosis in driving parasitic spreading from the infected cells and maintain its virulent life cycle in a new macrophage niche.

Chapter 5 – Regulation of apoptosis signaling pathways in human macrophage during *Leishmania* spreading

5.1. Introduction

The promastigotes and amastigotes form of *Leishmania* have a remarkable ability to modulate the host macrophage signaling pathways, which includes; inhibition of lysosomal fusion, disruption of various inflammatory cytokine and chemokine production, downregulation of MHC class II expression and prevention of cell death (Cecilio et al., 2014). These virulent functions prolong the longevity of the parasites within the infected cells by providing sufficient time for promastigote to successfully differentiate into amastigote within the host phagolysosome niche. However, following amastigote replication, the ultimate objective for these intracellular parasites is to successfully disseminate and colonize its progeny into neighboring macrophages. The previous chapter revealed that *L. aethiopica* (L8G) amastigotes spreading from cell-to-cell was associated with host apoptosis induction *in vitro*. Unfortunately, the mechanistic insight into the cell signaling pathways for this type of cell-to-cell dissemination remains poorly understood.

Studies focused on early stage of infection with *Leishmania* promastigotes have shown that various host apoptosis signaling pathways are involved for parasite survival. For example, AKT signaling was found to play an important role in resisting induction of mice macrophage apoptosis during infection with *L. major*, *L. amazonensis* and *L. pifanoi* promastigotes (Ruhland et al., 2007). Similarly, the pro-apoptotic signaling pathway of PKC- δ was severely impaired by *L. infantum*, which resulted in inhibition of human U937 macrophage induced apoptosis (Lisi et al., 2005). Finally, engagement of NF- κ B signaling pathways was responsible for the

survival of infected J774A.1 mice macrophage within 1 hour of *L. donovani* infection (Singh et al., 2004). These reports suggest that *Leishmania* employ a diverse set of mechanistic pathways to block apoptotic induction during the early stages of infection. Since many pathogenic microorganism, including *Mycobacteria* (Aguilo et al., 2014), *Chlamydia* (Byrne and Ojcius, 2004) and retroviruses (Sattentau et al., 2010) are known to subvert the host apoptotic signaling pathways depending on the stage of infection, it is of great interest to further investigate whether the regulation of these signaling pathways fluctuates at later stages of infection that might account for *Leishmania* spreading.

Therefore, this chapter aims to evaluate how the three signaling pathways associated with apoptosis, AKT, NF- κ B and PKC- δ , are modulated by *L. aethiopica* (L8G) amastigotes during spreading (Figure 5.1). The *in vitro* spreading model developed in Chapter 4 was utilized firstly to investigate the protein expression of activated and total AKT through western blot. Further analysis of the downstream pathways of AKT signaling, including BAD phosphorylation and cytochrome C release, were determined. The involvement of NF- κ B was also investigated by analyzing the presence of upstream I κ B phosphorylated protein and downstream p65 total protein through western blot. Finally, the role of PKC- δ protein was assessed. This was implemented by detecting the accumulation of pro-apoptotic cleaved fragment of the protein during *L. aethiopica* (L8G) amastigotes spreading.

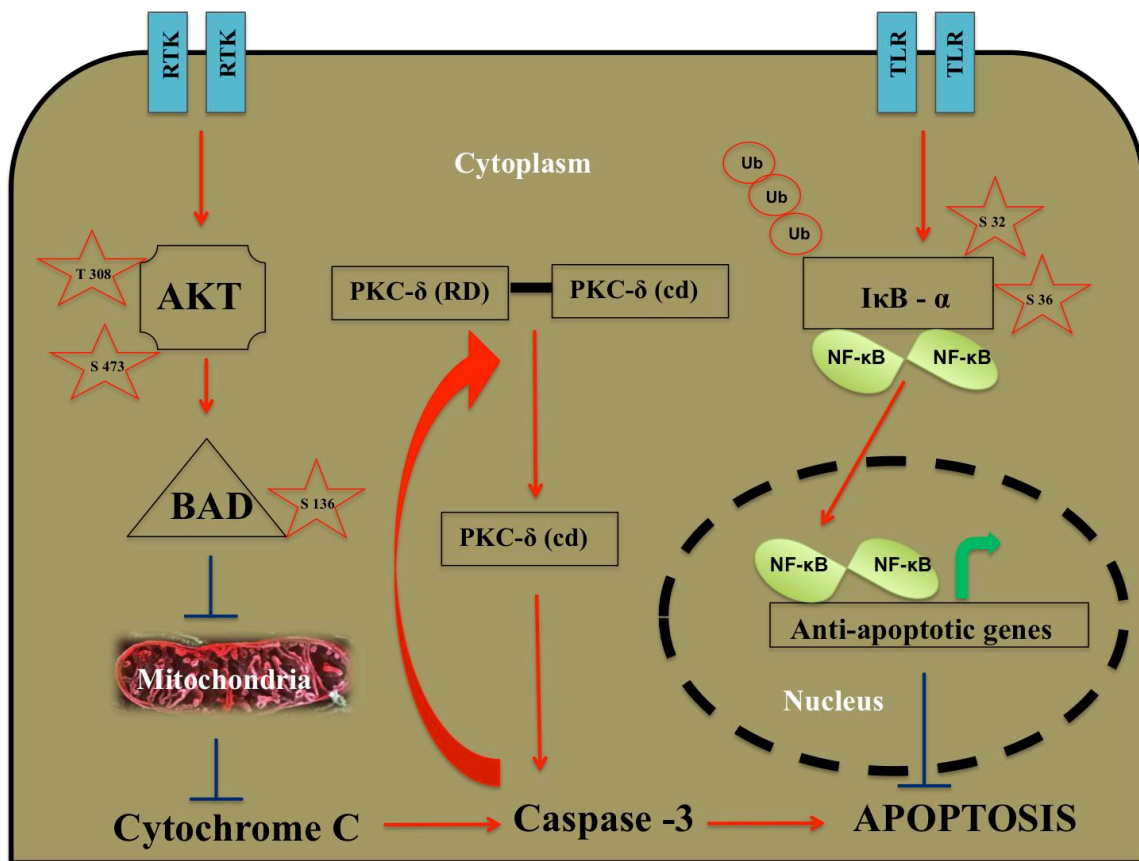


Figure 5.1. Schematic diagram representing apoptotic signalling pathways in macrophages. Upon Receptor Tyrosine Kinase (RTK) stimulation, AKT is phosphorylated at Threonine 308 (T 308) and Serine 473 (S 473). Fully activated AKT then phosphorylates BAD protein at Serine 136 (S 136), which inhibits the permeability of mitochondrial membrane. As cytochrome C is not released from mitochondria to cytoplasm, caspase-3 is not activated which otherwise leads to induction of apoptosis. One of the key targets of active caspase-3 is PKC- δ protein, which is composed of regulatory domain (RD) and catalytic domain (cd). Caspase-3 cleaves the hinge region (indicated by solid bar) of the full length PKC- δ . The released cd initiates the activation of caspase-3 in a positive feedback mechanism. Similarly, Toll Like Receptor (TLR) stimulation induces the phosphorylation at Serine 32 (S 32) and Serine 36 (S 36) of I κ B. This is followed by ubiquitination and subsequent proteosomal degradation of I κ B. This causes the release of NF- κ B dimers, which translocate to the nucleus to induce the transcription of anti-apoptotic genes.

5.2. Results and Discussions

5.2.1. Effect of L8G infected cells on AKT activation during infection spreading

The activation of AKT follows phosphorylation at Threonine (Thr) 308 and Serine (Ser) 473 residues (Garcia-Echeverria and Sellers, 2008). Hence, to determine activation of AKT during infection spreading, L8G infected co-culture was isolated at 1, 6, 12 and 24 hours and were immunoblotted against antibodies specific to Thr 308 and Ser 473 phosphorylation sites. The results were compared to the positive control of co-cultured uninfected cells.

After 1 hour of co-culture, there was a decrease in the band intensity at both Thr 308 and Ser 473 residues of AKT in L8G infected cells when compared to uninfected control (Figure 5.2.A and 5.2.B). The densitometry analysis further showed that this reduction in the expression of phosphorylated AKT at both residues was significant ($p < 0.05$) not only at 1 hour, but also at 6, 12 and 24 hours after co-culture (Figure 5.2.A and 5.2.B). To verify whether this effect is solely caused by de-phosphorylation or low expression of the total protein, the membrane blot were stripped and re-probed with total AKT antibody. Surprisingly, from 6 hours onwards, there was approximately a two fold reduction of the total protein in infected co-culture when compared to control, suggesting lower AKT expression (Figure 5.2.C). Since the band intensity of β actin protein remained constant throughout the time period (Figure 5.2.D), this confirmed that the above effects were not due to unequal loading of the protein during SDS gel electrophoresis. Finally, to discount the fact that the L8G infected cells before co-culture was biased towards AKT reduction, the infected and uninfected cells from 72 hours were separately probed with all three antibodies. The result confirmed no significant differences in band intensity for phosphorylated and total protein between infected and uninfected cells (Appendix II).

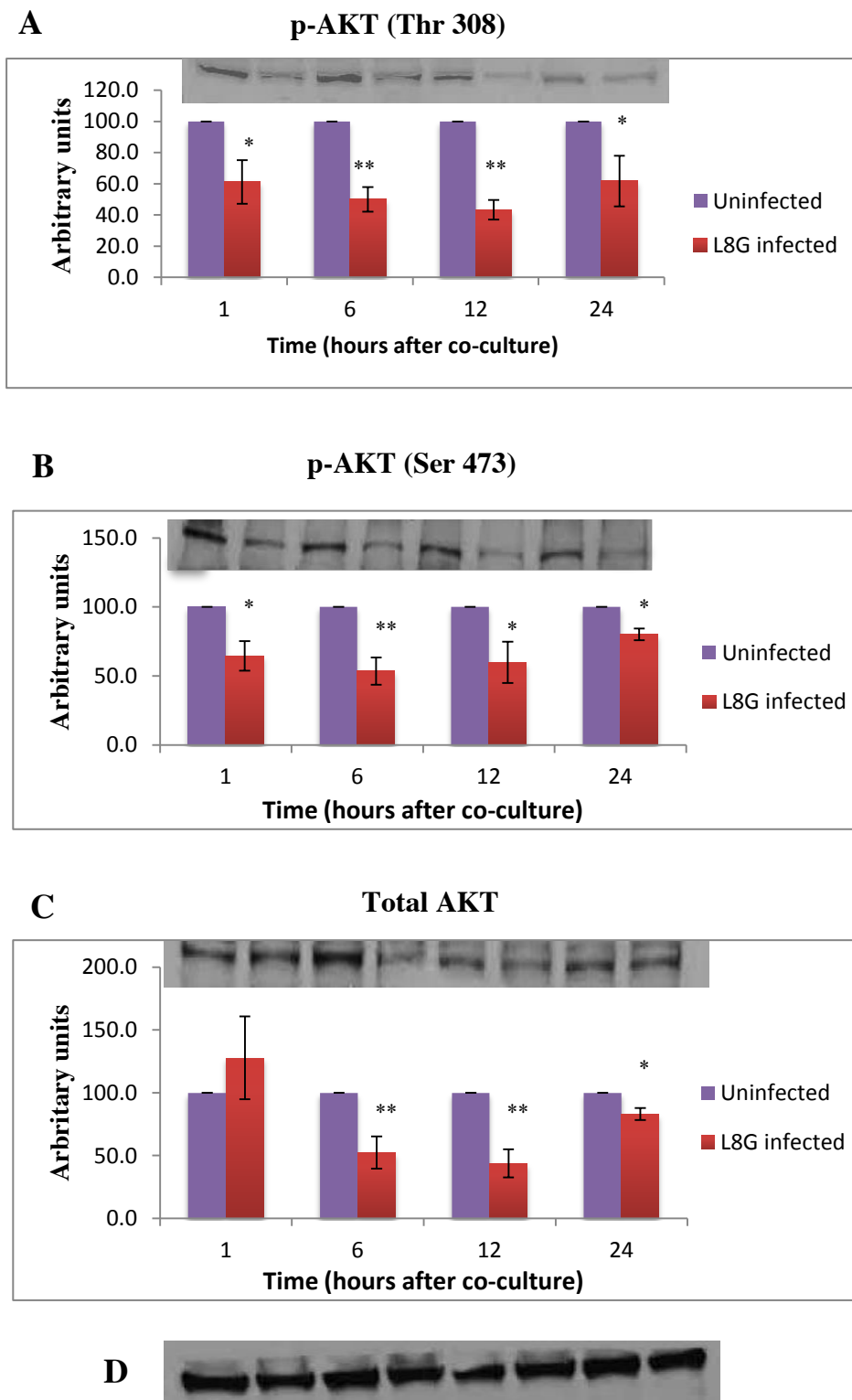


Figure 5.2. Effect of *L. aethiopicus* (L8G) infected cells on AKT activation during infection spreading.

Following infection of differentiated THP-1 macrophages with L8G infected cells, whole cell lysates were collected at 1, 6, 12 and 24 hours after co-culture. Equal amounts (30 μ g) were resolved by SDS-PAGE and analysed through western blotting. (A) Representative blot of p-AKT (Thr 308) and its corresponding densitometry analysis. (B) Representative blot of p-AKT (Ser 473) and its corresponding densitometry analysis. (C) Representative blot of total AKT and its corresponding densitometry analysis. (D) Representative blot of β -actin. Co-culture between differentiated THP-1 macrophages and uninfected cells were taken as a positive control. * = $p < 0.05$ and ** = $p < 0.01$

This confirms that the above effects in AKT reduction were solely caused by L8G infected cells following co-culture experiment. Overall, the above results suggest a temporal double strategy of *L. aethiopica* amastigotes mediated AKT reduction. As *Leishmania* species induces the activation of host serine/threonine phosphatase (PSP) during infection (Kar et al., 2010), this could lead to AKT de-phosphorylation in both Thr 308 and Ser 473 residues within 1 hours of co-culture. Alternatively the secretion of parasite virulent factors such as cysteine/serine protease and GP63 could initiate total AKT degradation from 6 hours onwards, therefore disrupting AKT survival signaling pathways.

5.2.2. Effect of AKT downregulation on the phosphorylation of BAD expression and cytochrome C release

One of the downstream events that occur following AKT activation is the phosphorylation of BAD (Figure 5.1). The resulting phosphorylation at Ser 136 residues initiates binding of BAD with 14-3-3 molecular chaperone protein, thereby attenuating the downstream pro-apoptotic function of BAD (Datta et al., 1997). To confirm whether inactivated AKT during infection spreading has any consequential effect on the status of BAD phosphorylation, cell lysates from L8G infected co-culture were assessed for the expression of phosphorylated BAD at Ser 136 through western blot. The result showed a marked reduction in BAD phosphorylation in infected co-culture from 1 to 24 hours when compared to uninfected control (Figure 5.3.A). However, the expression of total BAD protein was very similar across the time period (Figure 5.3.A). These observations support the notion that BAD de-phosphorylation is dependent on L8G mediated AKT inactivation during *in vitro* spreading.

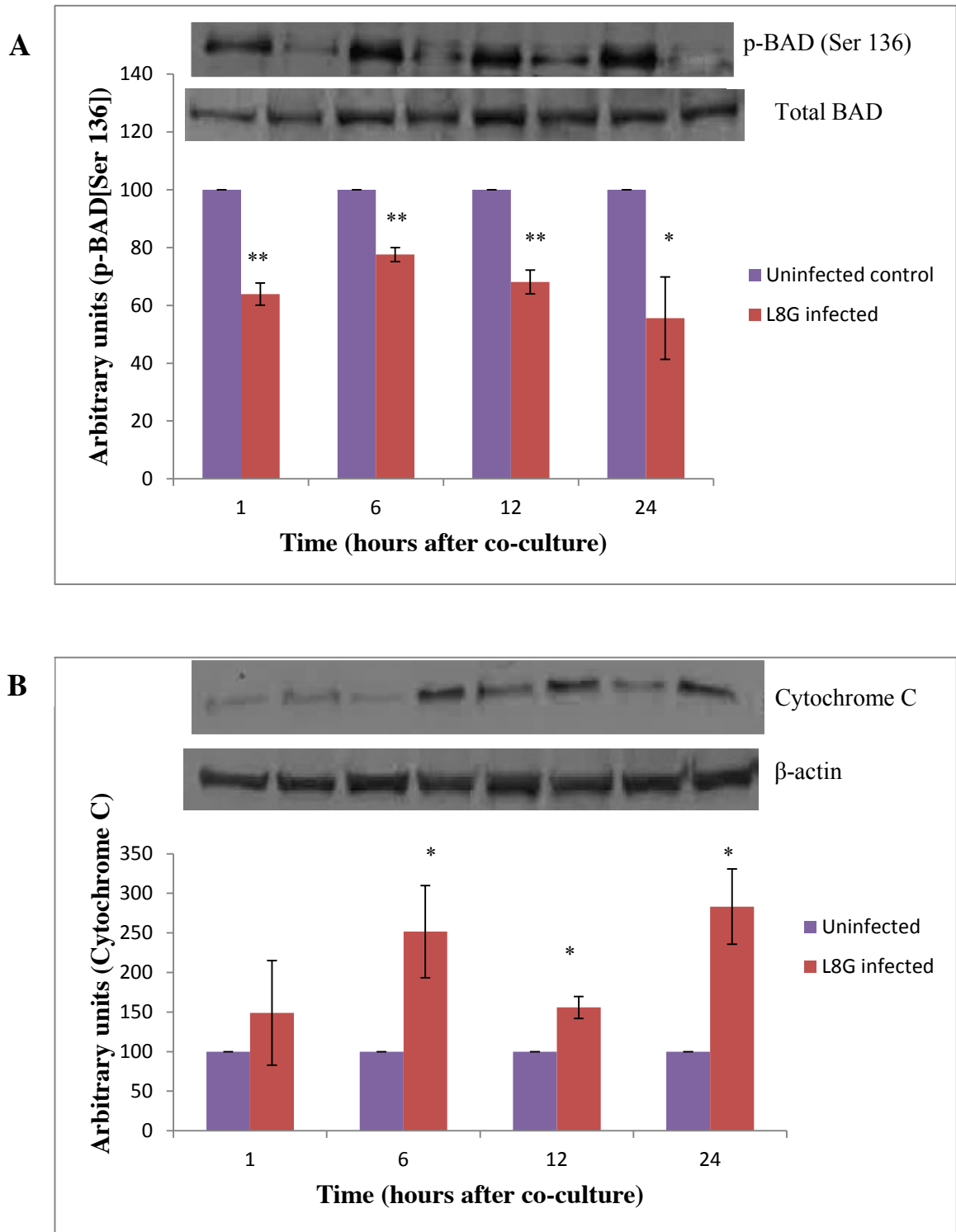


Figure 5.3. Effect of AKT downregulation on BAD phosphorylation and cytochrome C release. Following infection of differentiated THP-1 macrophages with L8G infected cells, whole cell and/or cytosolic lysates were collected at 1, 6, 12 and 24 hours after co-culture. Equal amounts (30 μ g) of proteins were resolved by SDS-PAGE and analysed through western blotting. **(A)** Representative blot of p-Bad (Ser 136) from whole cell lysate and its corresponding densitometry analysis, with β -actin as loading control. **(B)** Representative blot of cytochrome C from cytosolic lysate and its corresponding densitometry analysis with β -actin as loading control. Co-culture between differentiated THP-1 macrophages and uninfected cells were taken as a positive control. * = $p < 0.05$ and ** = $p < 0.01$

The major pro-apoptotic function of de-phosphorylated BAD is induction of mitochondrial membrane permeability via the activation of BAX protein mediated oligomeric pores formation (Danials, 2007). This increase in permeability causes cytochrome C release which, subsequently binds with Apaf-1 protein to induce the activation of caspase-3 enzyme (Jiang and Wong, 2004). To test whether the de-phosphorylated BAD protein affects mitochondrial permeability, the presence of cytochrome C in the cytosolic extract from L8G infected co-culture was detected by western blot. Within 1 hour, there was no significant difference in cytosolic accumulation of cytochrome C between infected and uninfected co-culture (Figure 5.3.B). Interestingly, release of cytochrome C into cytosol increased by approximately two-fold from 6 hours onwards in the infected co-culture, which was maintained till 24 hours time point (Figure 5.3.B). This indicates that the effect of active BAD on cytochrome C release appears to be associated only after 6 hours of co-culture with L8G infected cells. This time delay, independent of AKT inactivation, could be explained by the lag phase associated with BAX oligomeric pores, which involves a slow and stepwise conformational change (Valentijn et al., 2003). Nevertheless, since elevated levels of active caspase-3 was found between 6 and 12 hours after cell-to-cell infection (Chapter 4), this suggest a positive correlation between active BAD mediated cytochrome C release and caspase-3 activation during L8G infection spreading.

5.2.3. Effect of L8G infected cells on NF- κ B signaling during infection spreading

The importance of NF- κ B regulation in stimulating immune response against intracellular pathogen including *Leishmania* has been well documented (Reinhard et al., 2012). As discussed in Chapter 1 (section 1.6.3), various stimuli including LPS,

TNF- α and IL-1 results in phosphorylation (Serine 32 and 36 residues), polyubiquitination and subsequent degradation of the inhibitory I κ -B α . This releases the NF- κ B dimers, mainly p65-p50, which then migrates into the nucleus to induce transcription of inflammatory genes including, IL-6, IL-12 and NOS (Figure 5.1). Although anti-apoptotic gene upregulation is one of the vital function of NF- κ B activation (Barket and Gilmore, 1999), its importance during *Leishmania* infection, particularly late stage has not been studied. Therefore, the next goal was to examine whether NF- κ B signaling could be modulated during infection spreading.

Initially, the phosphorylation of I κ -B α (Ser 32/36) was assessed through western blot. From 1 to 24 hours, a significant ($p < 0.01$) decrease in phosphorylation was detected within infected co-culture compared to uninfected control (Figure 5.4.A). Surprisingly, this effect was correlated to a lower expression of total I κ -B α (Figure 5.4.B). Furthermore, when the infected cell lysates were probed with p65 antibody, a marked reduction of total p65 protein was detected from 1 to 24 hours, as compared to control (Figure 5.4.C). The above result correlates with one study, where the authors found cysteine peptidase of *L. mexicana* amastigotes was responsible for complete degradation of I κ -B α and p65 subunit, resulting in an inhibition of IL-12 production during mice macrophage infection (Cameron et al., 2004).

This interesting finding implies that during L8G infection spreading, NF- κ B signaling is negatively regulated due to degradation of I κ -B α and p65 subunit, which diminishes the expression of anti-apoptotic genes in the nucleus.

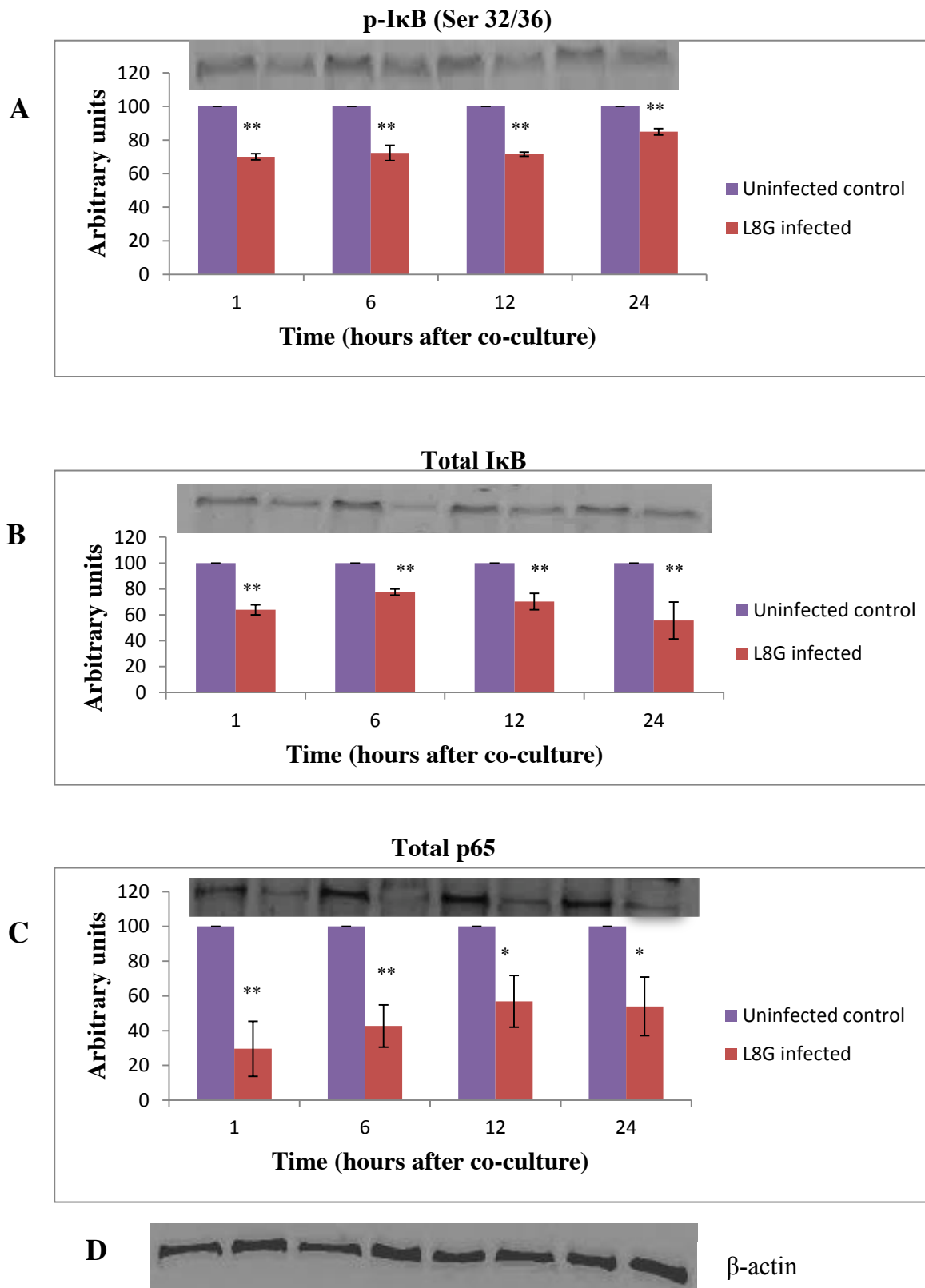


Figure 5.4. Effect of *L. aethiopia* (L8G) infected cells on NF-κB signaling during infection spreading. Following infection of differentiated THP-1 macrophages with L8G infected cells, whole cell lysates were collected at 1, 6, 12 and 24 hours after co-culture. Equal amounts (30 μg) of proteins were resolved by SDS-PAGE and analysed through western blotting. **(A)** Representative blot of p-IκB (Ser 32/36) and its corresponding densitometry analysis. **(B)** Representative blot of total IκB and its corresponding densitometry analysis. **(C)** Representative blot of p65 and its corresponding densitometry analysis. **(D)** Representative blot of β-actin. Co-culture between differentiated THP-1 macrophages and uninfected cells were taken as a positive control. * = $p < 0.05$ and ** = $p < 0.01$

5.2.4. Effect of L8G infected cells on PKC- δ signaling during infection spreading

Leishmania is known to severely alter the macrophage Protein kinase C (PKC) signaling pathways, which results in the disruption of reactive oxygen species production (Bhattacharya et al., 2001).

Although PKC subtypes are known to have either pro or anti-apoptotic function, only PKC- δ has been studied so far in the field of *Leishmania* infection and host cell death (Figure 5.1). Lisi and colleagues showed that early stage *L. infantum* infection prevents actinomycin D induced host apoptosis via PKC- δ inactivation (Lisi et al., 2005). This inactivation was due to the ability of LPG molecule to inhibit PKC- δ cleavage, which was further associated with reduced expression of activated caspase-3. As Chapter 4 revealed caspase-3 involvement in cell-to-cell infection, an investigation was carried out to assess whether there is a link between the activation of caspase-3 and PKC- δ (i.e. PKC- δ cleavage) during L8G infection spreading.

After isolating cell lysates at 1, 6, 12 and 24 hours, the infected co-culture was probed with PKC- δ antibodies before analyzing PKC- δ protein expression through western blot. A band of approximately 78 kDa representative of total PKC- δ protein was detected in uninfected control from 1 to 24 hour (Figure 5.5). However, throughout the time period, the PKC- δ intensity was significantly reduced ($p < 0.01$) in infected co-culture (Figure 5.5). Interestingly, this effect was not due to accumulation of PKC- δ cleaved fragment (CF) as there was no protein band present at 45 kDa (expected size of CF). This observation clearly shows that caspase-3 activation during infection spreading is not linked to PKC- δ activation. Instead, parasite mediated downregulation of PKC- δ appeared to be one of the causal factors behind apoptotic mediated infection spreading.

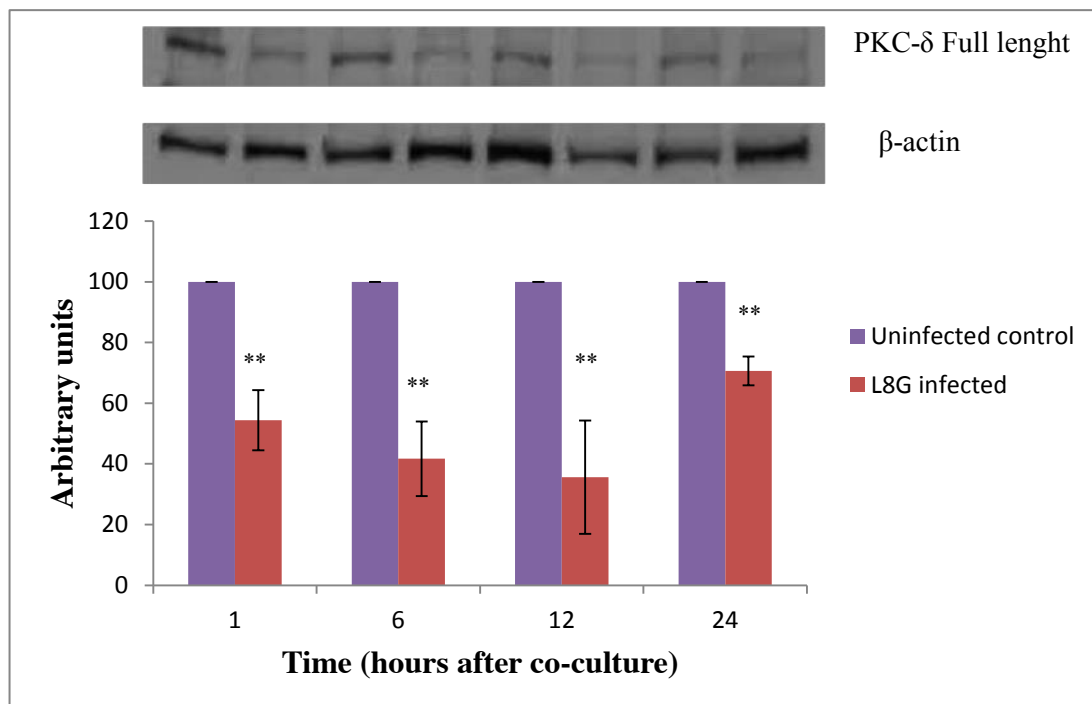


Figure 5.5. Effect of *L. aethiopic* (L8G) infected cells on PKC- δ signaling during infection spreading. Following re-infection of differentiated THP-1 macrophages with L8G infected cells, whole cell lysates were collected at 1, 6, 12 and 24 hours after co-culture. Equal amounts (30 μ g) of proteins were resolved by SDS-PAGE and analysed by western blotting. Representative blot of PKC- δ and β -actin protein expression is shown. The graph represents densitometry analysis of PKC- δ . Co-culture between differentiated THP-1 macrophages and uninfected cells were taken as a positive control. ** = $p < 0.01$

This surprising finding correlates to an *in vivo* study from Guler and colleagues, whereby PKC- δ knockout (-/-) mice exhibited rapid increase in the dissemination of *L. major* parasites from footpad to liver, as compared to wild type control (Guler et al., 2011). Although the above study did not extend the work in defining the apoptotic state of infected cells, it provides an initial platform to further investigate whether there is a link between PKC- δ downregulation and apoptotic induction during L8G infection spreading.

5.3. Conclusions

Experimental results from this chapter have clearly demonstrated the overall impact in host apoptotic signaling pathways during *L. aethiopica* dissemination. By employing an *in vitro* spreading model, significant levels of modulation were observed in three major signaling pathways, AKT, NF- κ B and PKC- δ .

In the earliest stage of infection spread, there was a dramatic reduction in phosphorylation of AKT within *L. aethiopica* infected co-culture cells. Although this caused a decrease in phosphorylated BAD, there was no any effect on cytochrome C release from mitochondria. However, from 6 hours onwards, western blot analysis revealed an increase level of cytochrome C in cytosol when compared to uninfected co-culture cells. This strongly indicates the involvement of intrinsic mitochondrial apoptosis during *L. aethiopica* amastigote spreading. Similarly, the NF- κ B signaling was downregulated during spreading as the infected co-culture cells illustrated a reduced expression of I κ -B α and p65 subunit. This defect in NF- κ B might have a consequential effect on the downstream expression of a number of critical anti-apoptotic genes. Finally, PKC- δ protein was also downregulated instantaneously within 1 hours of infected cell co-culture. Interestingly, this negative effect was

consistent throughout the spreading of L8G infection with no clear evidence of PKC- δ CF accumulation. This rules out any possibility of a link between caspase-3 and PKC- δ activation during spreading of *L. aethiopica*.

In conclusion, a temporal based downregulation of apoptotic signaling pathways during *L. aethiopica* spreading in human macrophages have been revealed in this chapter. Engineering a genetic overexpression of AKT, NF- κ B and PKC- δ proteins will be the next research goal to address whether these signaling pathways are critical during the *Leishmania* infection propagation.

Chapter 6 – Global protein response during late stage of *Leishmania* infection in human macrophage

6.1. Introduction

Parasitic mediated subversion of the macrophage signaling pathways is vital for intracellular survival of *Leishmania* species. Through DNA microarray analysis, efforts to understand such changes have been achieved by studying the modulation of global host gene expression during infection (Buates and Mattelawski, 2001; Chausabel et al., 2003; Rodriguez et al., 2004; Zhang et al., 2010). These studies have revealed the down-regulation of pro-inflammatory genes as a contributing factor behind anti-microbial suppression towards *Leishmania*. However, genomic studies and its associated techniques suffer from one critical limitation, as the final gene product does not necessarily correlate to the total levels of protein due to post-translational modification (Cox and Mann, 2007).

Since proteins are the effectors of biological and cellular functions, investigations have been shifted towards utilizing proteomic approaches to study the effect of *Leishmania* infection on host protein expression. Menezes and colleagues used a liquid chromatography tandem mass spectrometry technique to compare the expression of proteins involved in host cell metabolism during *L. major* and *L. amazonensis* infection in mouse macrophages (Menezes et al., 2013). Through the same approach, GP63 of *L. major* and *L. mexicana* was found to be responsible for degradation of mice macrophage nuclear proteins such as nucleoporins and nucleocytoskeleton (Isnard et al., 2015). Similarly, a study focusing on *L. donovani* infection of human THP-1 macrophage comprehensively identified differential expression of proteins ranging from cell death to immune response and metabolism

(Singh et al., 2015). Although the above studies highlighted modulation in global host signaling pathways by *Leishmania* during early phase of infection, no analysis has been carried out to address whether these critical change take place at later stages of infection.

Therefore, this chapter is aimed to fill the gap in knowledge in global proteomic expression of human macrophage during cell-to-cell *Leishmania* spreading. Using an isotopic labeling coupled with tandem mass spectrometry (MS/MS) approach, comparative analysis was performed to determine quantitative changes in specific sets of protein between uninfected and *L. aethiopica* infected cells.

6.2. Results and Discussion

6.2.1. Identification and functional annotation of differentially expressed protein

Quantitative analysis of protein expressions of *L. aethiopica* infected co-culture at 10 hours were compared with uninfected control and the relative fold change (RFC) was determined. Three independent biological experimental repeats (Set A, B and C) were performed to increase the significance and reliability of the total proteins identified. A total number of 6969, 7070, 5928 proteins were identified at Set A, B and C, respectively (Appendix III). Using RFC as a key indicator, any proteins that showed either upregulation (RFC > 1.5) or downregulation (RFC < 0.5) were classified as differentially expressed protein. Within 10 hours of co-culture, a total of 19 host proteins were differentially modulated during *L. aethiopica* spreading (Table 6.1). These proteins were categorized into 5 major functional groups using Gene Ontology (GO) annotations. These include: apoptosis and cell death; immune response, vesicles trafficking; metabolic pathways; gene expression.

Functional groups	Number	Accession ID	Name	Relative fold change
Apoptosis and cell death	1	H0Y6Y2	Caspase-9 p35	2.0
	2	P42574	Caspase-3 p17	1.8
	3	Q56A86	AKT	0.39
	4	Q01105	SET	0.15
	5	D3DT21	Selenoprotein K	0.30
	6	O95470	Sphingosine-1-phosphate lyase	2.6
Immune response	7	P36222	Chitinase-3-like protein	1.73
	8	B2R577	Protein S-100	0.23
	9	A0A024QZZ1	Butyrophillin	1.87
	10	H0YC68	Glutathione reductase	3.4
	11	P02795	Metallothionein-2	4.0
Vesicular trafficking	12	B8ZZT4	VAMP8	0.3
	13	Q9H1H9	Kinesin-3	4.0
Metabolism	14	P50336	Protoporphyrinogen oxidase	2.5
	15	P48047	ATP synthase subunit	3.8
	16	P31930	Cytochrome bc-1	2.5
Gene expression	17	E9PI38	p65 NF- κ B	0.23
	18	Q1RMZ3	NCoA6	0.1
	19	Q9Y2W1	TRAP	0.43

Table 6.1. List of differentially expressed proteins during late stage of *L. aethiopica* infection. The identified proteins were categorized into 5 major functional groups including apoptotic cell death, immune response, vesicular trafficking, metabolism and gene expression.

The pie diagram shows the percentage distribution of functionally annotated proteins at 10 hours of cell-to-cell infection with *L. aethiopica* (Figure 6.1). The number of proteins that showed either increase and/or decrease in expression is shown in Figure 6.2. The following section will discuss on key proteins modulated from each category during infection spreading of *L. aethiopica*.

6.2.2. Proteins involved in apoptosis and cell death

Among five proteins identified as differentially expressed in apoptosis and cell death category, three proteins showed increased expression whereas the remaining two showed reduced expression under infected co-culture cells (Table 6.1). Initially, there was a two fold increase in expression of Caspase-9 p35. This pro-apoptotic protein, which is a cleaved form of pro-caspase-9, is involved in the downstream activation of caspase-3 (Chapter 1, Figure 1.13). During intrinsic apoptosis, cytochrome C binds to Apaf-1 (apoptotic protease activating factor -1) to form a wheel like heptamer called an apoptosome (Kumar, 2007). The Apaf-1 in the apoptosome then recruits initiator caspase-9 p35, which in turn causes the cleavage of pro-caspase-3 into active caspase-3 and subsequent induction of apoptosis (Twiddy and Cain, 2007). Active caspase-3, which is also known to cleave pro-caspase-9, was upregulated by 1.8 fold suggested a positive amplification of caspase-3 mediated apoptosis during *L. aethiopica* spreading. This result is consistent with the findings in Chapter 4, where caspase-3 was strongly expressed throughout spreading time frame. In addition, the fact that AKT protein expression (RFC = 0.39) was also downregulated confirms the notion that AKT mediated mitochondrial apoptotic response is occurring during late stage of infection.

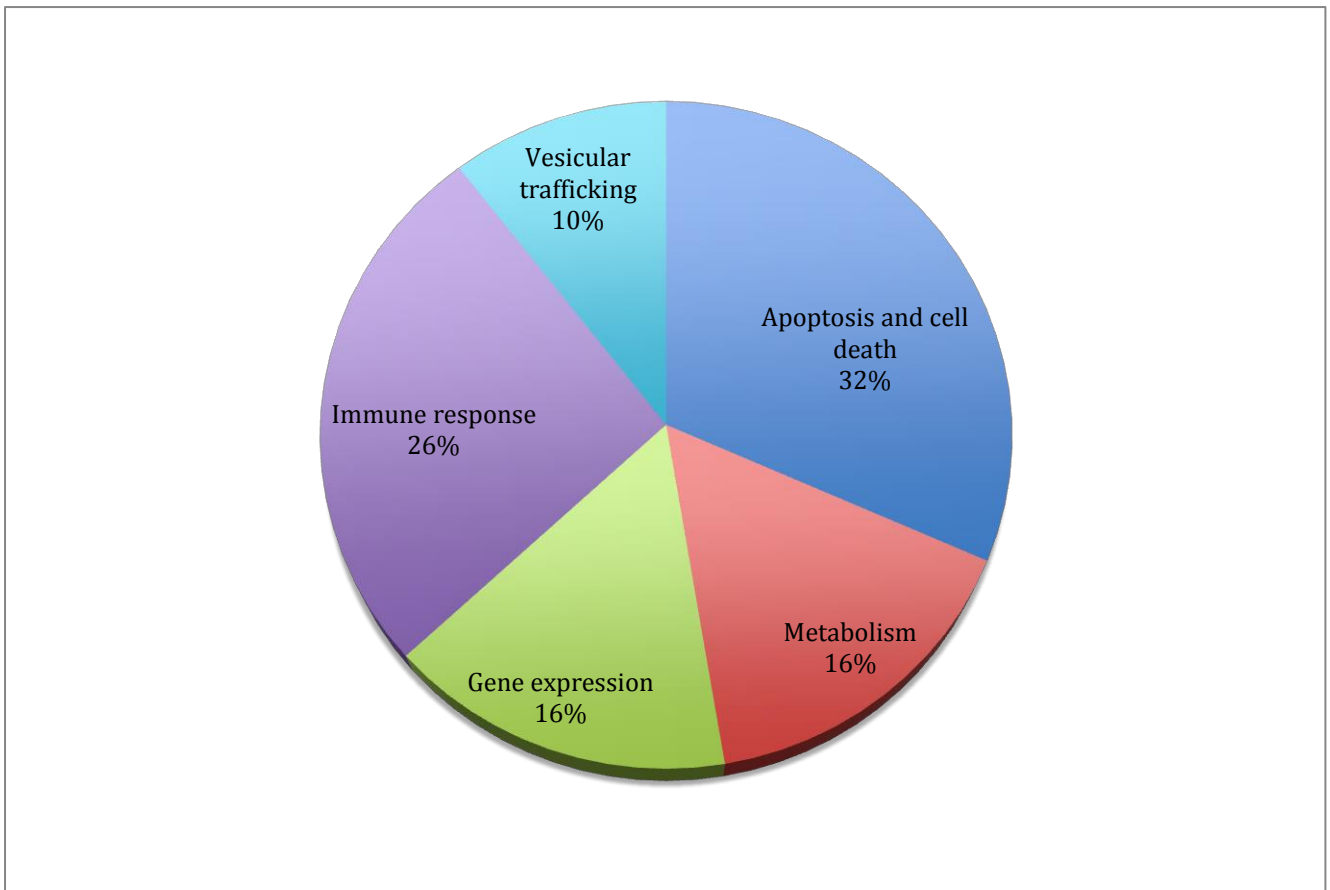


Figure 6.1. Pie-diagram showing functional annotation and relative distribution of the total proteins detected in differentiated THP-1 macrophages co-cultured with *L. aethiopica* infected cells. 5 major functional classes were identified depending on their cellular function using GO annotation.

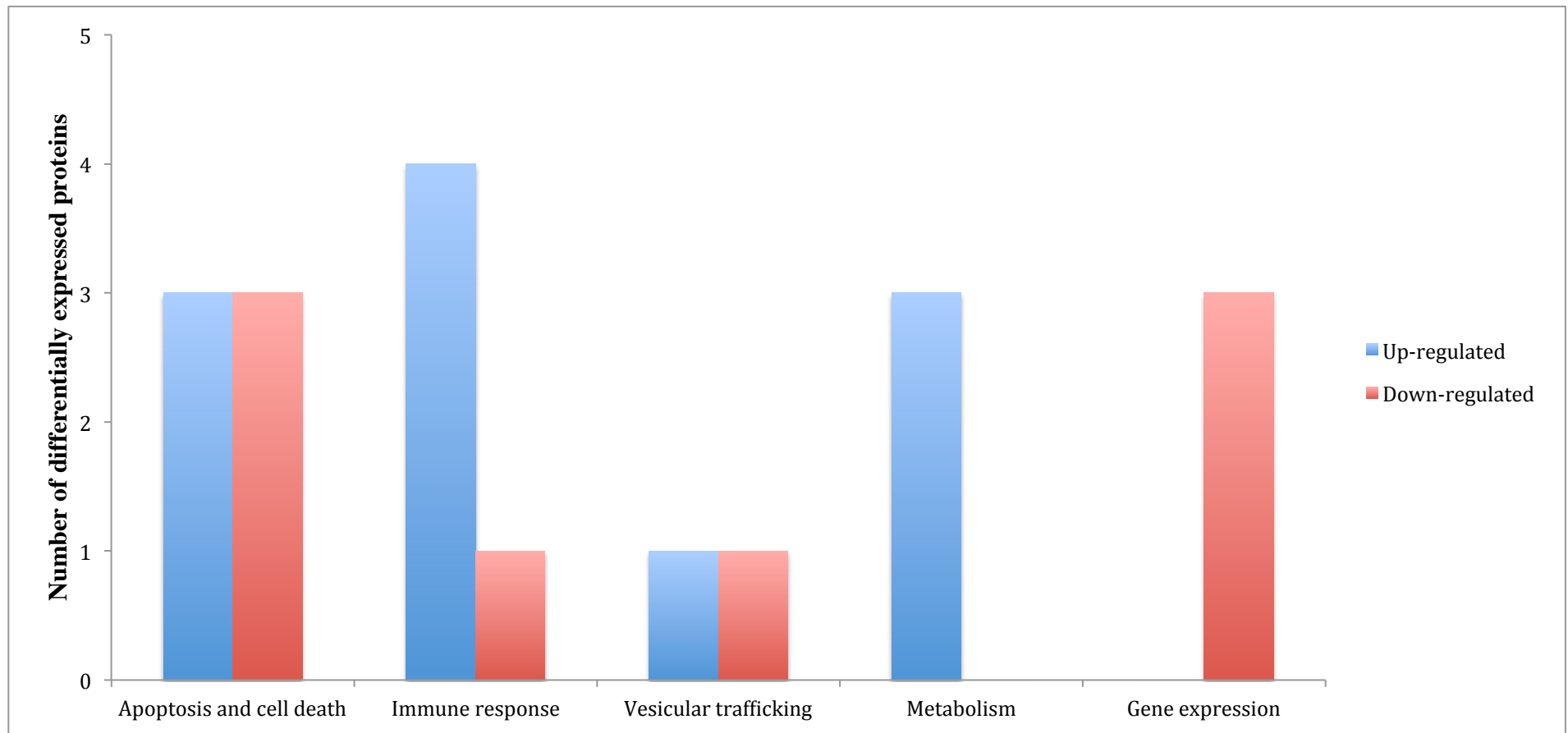


Figure 6.2. Functional distribution of differentially expressed proteins during *L. aethiopica* infected co-culture cells at 10 hours. Using relative fold change (RFC), proteins were assigned either up-regulated (RFC > 1.5) or down-regulated (RFC < 0.5).

Surprisingly, there was a marked decrease (RFC = 0.15) in the expression of SET protein. This 39 kDa phospho-protein is localized in the nucleus and plays an essential role in the inhibition of Granzyme A activated DNAase (GAAD). During T cell mediated macrophage apoptosis, granzyme A, which is a serine protease, cleaves SET protein along with other complex such as HMG2 and Ape1 protein to release GAAD, which then directly causes DNA degradation independent of caspase activity (Chakravarti and Hong, 2003). Since granzyme A activation was not observed in the proteomic data, this suggest that *L. aethiopica* might secrete serine protease, homolog of granzyme A, to degrade SET. Whether this causes caspase independent apoptosis is questionable since HMG2 and Ape1 expression were not reduced at 10 hours after co-culture. However, this does not necessarily rule out the possibility of caspase independent apoptosis during the early time periods of spreading. Similarly, another protein that showed reduced expression was Selenoprotein K (RFC = 0.3). The protein is part of a family of endoplasmic reticulum (ER) membrane protein, which regulates the calcium ion influx (Verma et al., 2011). Disruption in calcium ion regulation leads to ER stress, which is one of the causal factors behind cellular apoptosis (Szegezdi et al., 2006). This could imply that *L. aethiopica* might selectively target Selenoprotein K to impair the ER physiological function and induce apoptosis in the infected cells.

Finally, there was also an enrichment (RFC = 2.6) of Sphingosine-1-phosphate lyase (SPL). The enzyme is responsible for the irreversible cleavage of Sphingosine-1-phosphate (S1P) molecule into fatty acids and phosphoethanolamine (Van Brocklyn and Williams, 2012). The involvement of S1P in apoptosis comes from the fact that this molecule is a well-known inhibitor apoptosis (Van Brocklyn and Williams, 2012). This suggests that *L. aethiopica* upregulation of SPL might be involved in reducing the pool of anti-apoptotic S1P molecule and enhancing apoptotic induction during parasite spreading.

During early stage of infection, *Leishmania* species confers protection to macrophage in the presence of apoptotic induction allowing sufficient time for parasite replication within phagolysosomes (Akarid et al., 2004; Ruhland et al., 2007). In addition, the above proteomic data has revealed that a pro-apoptotic response could be occurring to facilitate *L. aethiopica* infection dissemination, which supports the results from Chapter 4/5 and Real and colleagues (Real et al., 2014).

6.2.3. Proteins involved in immune response

One of the ways through which *Leishmania* averts the immune response is by altering cytokine production in infected cells. The proteomic screen identified five differentially expressed proteins involved in immune response during cell-to-cell infection (Table 6.1). Firstly, Chitinase-3-like (CH3L) protein was upregulated by 1.73 fold. CH3L is a 40 kDa human homolog protein of chitinase found in plants and insects that lacks the enzymatic activity towards chitin (Eurich et al., 2009). Importantly, CH3L is linked with the formation of alternatively activated macrophage and causes the secretion of IL-13 during several inflammatory diseases such as Gaucher disease and asthma (Eurich et al., 2009). Increased expression indicates that a protective Th2 response could be induced during infection spreading of *L. aethiopica*. Interestingly, such event appears to be correlated with a significant down-regulation of pro-inflammatory response.

This was evident from reduced expression of Protein S-100 (RFC = 0.23) and higher expression of Butyrophilin (RFC = 1.87). The calcium binding Protein S-100, which belongs to a group of damage associated molecular pattern protein (DAMP), is released by phagocytes during inflammation and induces the expression of pro-inflammatory cytokines such as TNF- α and IFN- γ (Foell et al., 2007). Similarly, Butyrophilin protein belonging to a family of B7 co-stimulatory molecule is known to

play an inhibitory role in T cell activation (Abeler-Dorner et al., 2012). Indeed, various independent studies have confirmed the ability of this protein to suppress CD3 induced secretion of IL-2 and IFN- γ from both mouse and human Th1 CD4⁺ and CD8⁺ T cells (Smith et al., 2010; Cubillos-Ruiz et al., 2010). By taking these into account, the above result suggests that *L. aethiopica* might reciprocally regulate Protein S-100 and Butyrophilin, respectively, in order to reduce the adaptive pro-inflammatory responses during infection spreading.

The reactive oxygen species (ROS) such as superoxide/hydroxyl radicals along with reactive nitric species (RNS) represent an anti-microbial function of macrophages. However, *Leishmania* is capable of preventing both ROS and RNS production by inactivating NADPH oxidase and JAK/STAT proteins, respectively (Lodge et al., 2006; Matte and Descoteaux, 2010). Although, the proteomic data did not show any reduction of NADPH oxidase and JAK/STAT, it detected a strong elevation in Glutathione reductase (RFC = 3.4) and Metallothionein-2 (RFC = 4). Glutathione reductase is an enzyme responsible for catalyzing the formation of reduced glutathione (GSH), which is considered as intracellular free radical scavengers. Various *in vitro* and *in vivo* studies have demonstrated the role of glutathione reductase and GSH in protecting *Leishmania* during macrophage infection in the presence of ROS and RNS treatment (Romao et al., 1999; Romao et al., 2006; Cruz et al., 2008). Similarly, free radical anti-oxidant properties have also been ascribed to Metallothionein-2, which is a 7 kDa metal binding protein (Viarengo et al., 2000). Two independent genomic studies have shown the induction of metallothionein-2 gene expression during *in vitro* infection with *L. major*, *L. donovani* and *L. panamensis* (Gregory et al., 2008; Gomez et al., 2014). In particular, Gomez and colleagues showed that metallothionein-2 expression was heavily linked with survival of *L. panamensis* within infected human macrophages in the presence of NO inducing drug

(Gomez et al., 2014). Cumulatively, the high protein expression of glutathione reductase and Metallothionein-2 in the proteomic data suggests that during cell-to-cell spreading, the released *L. aethiopica* might induce the expression of the two proteins in the recipient cell in order to prevent from ROS and NO exposure.

Overall, the above results shows that *L. aethiopica* spreading is associated with downregulation of inflammatory response and anti-microbial activity in order to favor the parasite survival during re-infection of uninfected macrophages.

6.2.4. Proteins involved in vesicular trafficking

Phagosome biogenesis involves a transition of early phagosome into phago-lysosomes with a stepwise fusion of endosomal and lysosomal vesicles (Hass, 2007). The formation of phago-lysosome is an important step for the killing of intracellular pathogens. However *Leishmania* have evolved mechanisms to delay phagosome maturation process, thus avoiding an encounter with the macrophage microbicidal machinery. The parasite is able to achieve this task by interfering with the vesicle docking proteins such as syntaxin, WASP and SNAP-25 (Lodge and Descoteaux, 2008).

In accordance, the proteomic results showed a reduced expression of VAMP8 [Vesicle Associated Membrane Protein] (RFC = 0.3) in *L. aethiopica* infected co-culture (Table 6.1). The 25 kDa protein belongs to a family of SNARE complex which is essential for the fusion of lysosome containing hydrolase enzymes into phagosomes (Behrendorff et al., 2011). This is consistent with a recent finding whereby GP63 of *L. donovani* was responsible for the cleavage of VAMP8, which led the prevention of NADPH oxidase assembly and led to parasite survival (Matheoud et al., 2013). Strikingly, there was a four fold elevation in kinesin-3 expression (Table 6.1). Composed of two heavy and two light chains, kinesin-3 protein engages in the plus end

directed transport of vesicular cargoes (Hirokawa et al., 2009). This might suggest that during parasitic exit from the donor cells, there could be an increase activity of kinesin-3 mediated transport of vacuole containing *L. aethiopica* amastigotes towards the peripheral region of the cell. Although this unique process has not been documented in protozoan species, it has already been reported for the transfer of vesicles containing *Salmonella typhimurium* from juxtannuclear position to the HeLa cell periphery (Szeto et al., 2009). The authors noted that bacterial type 3 secretion system effectors, PipB2 and SifA were responsible for the recruitment and subsequent activation of kinesin-1 (similar to kinesin-3) in order to promote the movement of *S. typhimurium* along the micro-tubule for its dissemination (Szeto et al., 2009). Whether such virulent mechanism is exhibited by *Leishmania* is not known.

6.2.5. Proteins involved in metabolic pathways

Leishmania amastigotes successfully reside and replicate within the host phagolysosomes. Although these vacuoles provide a safe niche, there is a limiting source of nutrients such as, purines, vitamins, heme and amino acid within the phagolysosome lumen (Naderer et al., 2008). Therefore scavenging these essential nutrients becomes a top priority for parasites to supplement energy in order to survive during the late stage of infection. The proteomic data showed a 2.5 fold increase in the expression of Protoporphyrinogen oxidase during infected co-culture cells (Table 6.1). This enzyme is responsible for catalyzing the oxidation of protoporphyrinogen to protoporphyrin, which is a precursor for heme group. Since heme is important component for mitochondrial electron transport, this indicates the active involvement of mitochondrial machinery of oxidative phosphorylation during *L. aethiopica* spread. This is further strengthened by the fact that there were also subsequent increase in expression of ATP synthase subunit (RFC = 3.8) and cytochrome bc-1 complex (RFC

= 2.5) (Table 6.1). This was consistent with the finding from a study, which reported upregulation of various host mitochondrial proteins within 24 hours of *L. donovani* infection (Singh et al., 2015). However, this study reported expression of other host enzymes involved in glycolysis and citric acid cycle metabolic pathways. This discrepancy could be due to species specific differences or could be linked to different stage of infection studied.

6.2.6. Proteins involved in gene expression

Infection with *Leishmania* is well known to inhibit the host expression of a wide range of genes involved in cytokine, chemokine and NO production (Buates and Mattelawski, 2001). This occurs as a direct consequence of parasite mediated suppression of transcription factors such as STAT, NF- κ B and AP-1 (Forget et al., 2005; Cameron et al., 2004; Conteras et al., 2010). Consistent with the western blot result in chapter 4, the proteomic data showed a reduce expression of p65 NF- κ B (RFC = 0.23) domain (Table 6.1). Although the expression of inhibitory p50 domain was not affected, the possibility of p50/p50 dimer formation could not be ruled out. Whether this inhibitory dimer activation leads to *Leishmania* induced Th2 cytokine (TGF-beta and IL-10) production and reduced iNOS gene expression would require further investigation (Calegari-Silva et al., 2009). Remarkably, the proteomic data showed a severe reduction in NCoA6 [Nuclear Receptor Co-activator 6] (RFC = 0.1) and TRAP [Thyroid Receptor Associated Protein] (RFC = 0.43) proteins in the presence of *L. aethiopica* infected co-culture (Table 6.1). These two proteins represent a multi-functional co-activator for transcription factors including STAT, NF- κ B and AP-1 (Mahajan and Samuels, 2008). Since this has not been reported during *Leishmania*, this might indicate one of the novel strategies employed by *L. aethiopica* where the parasite

could target the co-activator protein in order to additively lower the effect of transcription factor induced gene expression.

6.3. Conclusions

In conclusion, for the first time, this chapter has evaluated changes in global proteome expression profiles of human macrophages during the late stage of *Leishmania* infection. Using an isotopic labeling proteomic approach, the result showed modulation of diverse range of host proteins ranging from apoptotic cell death and immune response to metabolism and vesicular trafficking during the virulent periods of *L. aethiopica* spreading. Close examination of 19 differentially expressed proteins revealed two major changes at late stage of infection. Firstly, the apoptotic induction was actively involved during parasitic spread, which is consistent with chapter 4 and 5 of this thesis. Secondly, a significant downregulation of pro-inflammatory and anti-microbial activity and upregulation of anti-inflammatory response was involved; both of which are well known strategy utilized by *Leishmania* to promote its survival in macrophage. As very little is known on *L. aethiopica* specific regulation, future work involves validating these differentially expressed proteins through western blot and comparing these data with similar proteomic experiments conducted in different *Leishmania* species over a larger sets of time periods. This will provide a broader picture of global differences in host cell proteome that might be targeted by species specific parasites for their spreading during the establishment of cutaneous and visceral leishmaniasis.

Chapter 7 – Discussion

7.1. Discussion

Cell-to-cell spreading of intracellular amastigotes not only represents an important survival strategy for *Leishmania* parasites but is also forms the basis for pathogenic development of human leishmaniasis. This is emphasized by the fact that majority of promastigotes inoculated by the sandfly are killed by the host complement system (Dominguez et al., 2003). Hence, a selective pressure is exerted on surviving intracellular amastigotes to replicate and disseminate its progeny for disease development. Studies conducted on *Leishmania* infection of mice macrophages have provided indication that parasitic egress could occur via apoptotic cell death and not through host cell lysis as previously assumed (Rittig et al., 1998; Real et al., 2014). Despite this assumption, there is a major gap in knowledge pertaining the mechanism of *Leishmania* spreading in human cells. This has been largely caused by the lack of reliable experimental model to study the late stage of parasite-host interaction.

To preliminary assess the correlation between *Leishmania* infection spread and apoptosis, two experimental approaches were carried out (Chapter 3). These include: (i) determining the effect of *Leishmania* infection on cell apoptosis; (ii) determining the effect of apoptotic induction on parasites infection. Differentiated THP-1 macrophages were chosen as a host cell line for infection as it has been reported to support growth and replication of *Leishmania* (Ogunkolade et al., 1990). *In vitro* studies on *Leishmania* infection have used different cell line lineage to model parasite-host interaction such as U937, PMA treated THP-1 and RAW 26.4 macrophages (Lisi et al., 2005; Ruhland et al., 2007; Getti et al., 2008). The selection of THP-1 in our model stems from the fact that it is non-adherent in nature, which makes them ideal for flow cytometry studies. The use of adherent cell lines requires

detachment through harsh trypsin treatment that might damage cell membrane causing subsequent parasite release, leading to inconsistent data. The result showed significant increase in apoptotic induction during infection with four species of promastigotes including *L. aethiopica*, *L. major*, *L. mexicana* and *L. tropica*. This was consistent with recent experiments involving mice peritoneal macrophage infection with *L. major* (Filardy et al., 2014) and *L. amazonensis* (DaMata et al., 2015) as well as U937 infection with *L. aethiopica*, *L. major*, *L. tropica* (Getti et al., 2008). This suggests that apoptotic response was not due to specific choice of system but rather due to the interaction between parasite and host. However, an intense level of THP-1 replication after 48 hours of infection made it impossible to further study infection as replicating uninfected cells effectively masked infection spreading. The link between infection spread and apoptosis was further confirmed by testing the effect of apoptotic induction on *Leishmania* infection. Such effect was particularly evident for *L. aethiopica* and *L. mexicana* infection. However, this model cannot be considered as an effective system to study cell-to-cell spreading since the treatment with camptothecin affected uninfected bystander cells in both *L. aethiopica* and *L. mexicana* infected samples.

Interestingly, camptothecin treatment generated a population of heavily infected cells at 72 and 96 hours after infection. Therefore, it was possible to use *L. aethiopica* and *L. mexicana* infected cells from 72 hours to set up co-cultures with uninfected differentiated THP-1 macrophages for analysing parasite spreading (Chapter 4). This form of cell-to-cell infection has been successfully utilized in studies of other infectious agents such as HIV-1 (Gropelli et al., 2015), *Mycobacterium* (Hagedorn et al., 2009) and *L. amazonensis* (Real et al., 2014), but never in *Leishmania* infection of human cells. Results from flow cytometry and trypan blue assay confirmed that increase in percentage of infection from 1 to 12 hours was due to intracellular

amastigote dissemination and not caused by a decrease in viable cell number. Moreover, real time lapse microscopy clearly showed that both species of *Leishmania* exit the host cell via non-lytic mode. This is in line with a previous report by Real and colleagues, where the authors observed that *L. amazonensis* amastigotes were surrounded by host membrane during its egress from mice macrophages (Real et al., 2014). Collectively, the above findings support the *in vivo* model of *Leishmania* infection in mice, where an increase in parasite number was detected from 2 to 4 weeks post infection without inflammatory response (Belkaid et al., 2000). The existence feature of this silent phase together with the evidence of non-lytic amastigote release suggested the involvement of apoptosis. This was confirmed during *L. aethiopica* infection as high expression of Phosphatidyl serine (PS) externalization and caspase-3 activation were detected concomitantly with cell-to-cell spreading. This data suggest that apoptosis could be an infectious mechanism that allows *L. aethiopica* to colonize new cells and ensure a safe replication niche. The role of apoptotic induction in facilitating microbial propagation has also been documented for other intracellular pathogens. The secreted ESAT-6 virulent protein of *M. tuberculosis* was responsible for successful replication and dissemination between mice alveolar macrophages (Aguilo et al., 2013). Similarly, TNF- α secreted during adenovirus infection caused the replicated virions inside the metastatic tumours to spread via apoptotic bodies (Mi et al., 2001).

Remarkably, a non-apoptotic response was associated with *L. mexicana* transmission. Several apoptotic independent mechanisms can be proposed for *L. mexicana* spread when other pathogenic exit strategies are considered. For example, *Chlamydia* exit host cells after a non-lytic, actin-dependent extrusion from the host cell. In this process, the bacteria are extruded in a double-membrane vesicle generated from the bacterial intracellular vacuole and cytoplasmic membranes (Hybiske and

Stephens, 2007). Similarly, during *in vitro* cell-to-cell transmission, *M. marinum* are ejected from host cells through an F-actin-rich structure denominated ejectosome (Hagedorn et al., 2009); the bacteria also remain associated with membrane remnants in the process. Finally, HIV-1 has also developed non-lytic strategies to egress from host cells either through virological synapses (Jolly and Sattentau, 2005).

As *L. aethiopica* spread was linked to apoptosis, further analysis was carried out to identify which of the apoptotic signalling pathways are involved and regulated by intracellular amastigotes (Chapter 5). Induction of apoptosis involves a very complex and sophisticated signalling pathway that is tightly regulated at multiple points (Figure 7.1). Current literature reports *Leishmania* promastigotes regulation of host apoptotic induction via three major signalling pathways: AKT, NF- κ B and PKC- δ during the initial stage of infection (Akarid et al., 2004; Ruhland et al., 2007; Singh et al., 2004; Lisi et al., 2005). However, such studies are limited to early stages of promastigotes infection and provide no information on the effect of amastigotes on host apoptosis. This research showed for the first time how *L. aethiopica* amastigotes disrupts the pro-survival pathways of human macrophages in order to promote apoptosis (Table 7.1).

Firstly, a significant reduction in AKT was detected, which led to BAD activation and cytochrome C release from mitochondria. This decrease could be due to the action of parasite mediated host proteasome activation as a recent study showed that *Legionella pneumophilla* stimulated the ubiquitination and subsequent degradation of AKT through proteasome activity in mice macrophages (Ivanov and Roy, 2013). Further analysis showed that p65 subunit, which is the main transactivation domain of NF- κ B responsible for mediating anti-apoptotic gene expression, was also significantly reduced throughout the spreading time period.

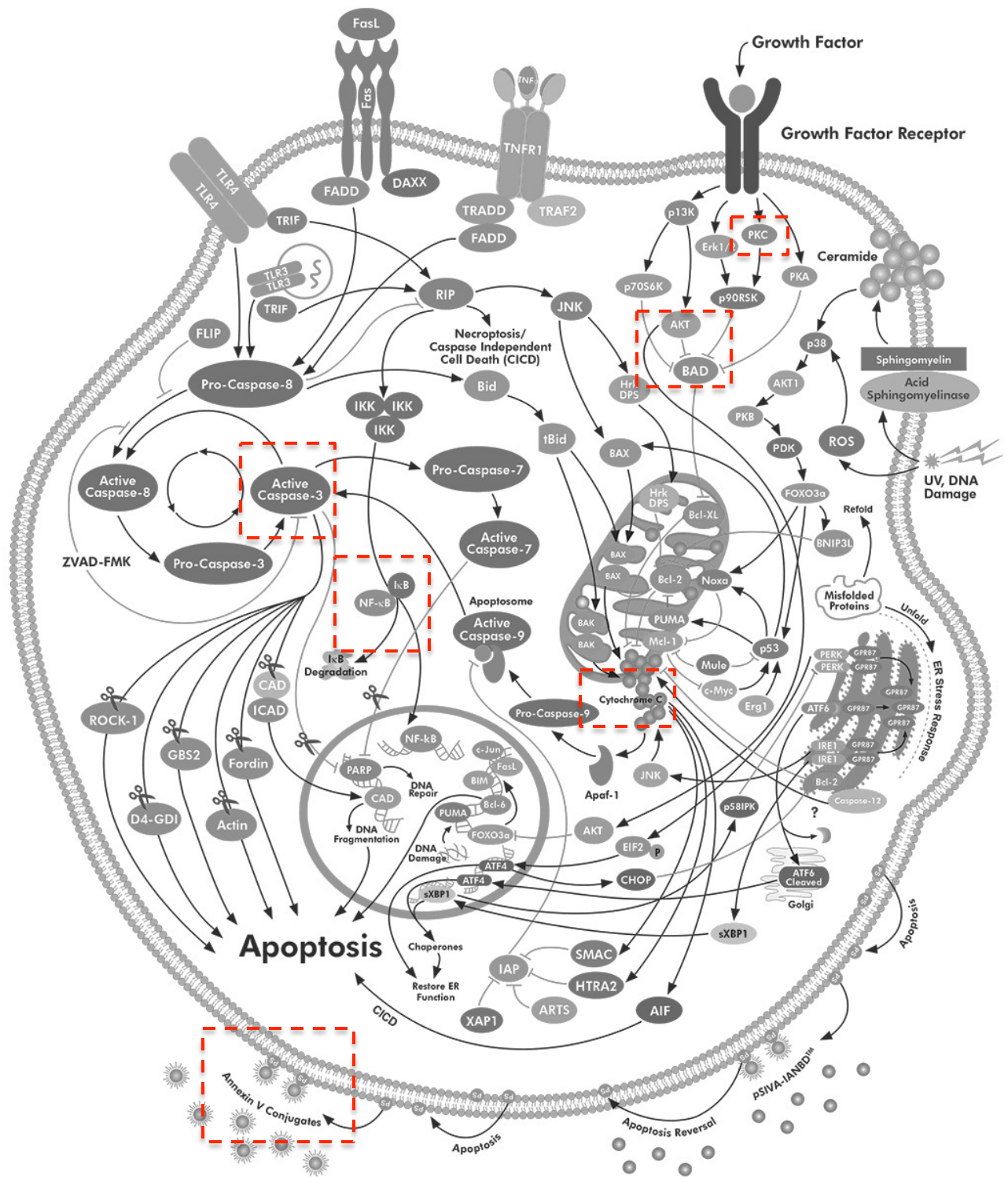


Figure 7.1. Schematic diagram representing the complex nature of intracellular signaling pathways associated with apoptosis. Induction of apoptosis stems from various stimuli that is tightly regulated at multiple points. In the above diagram, dotted red box refers to the specific molecule investigated in this research. Adapted from Novus Biological (www.novusbio.com).

Time (hours after co- culture)	Apoptotic assays		Western blot								
	PS externalization	Active caspase-3	p-AKT	Total AKT	p-BAD	Total BAD	Cytochrome C release	p-IκBα	Total IκBα	p65 NF-κB	PKCδ
1	+/-	+/-	-	+/-	-	+/-	+/-	-	-	-	-
6	n/a	+	-	-	-	+/-	+	-	-	-	-
12	+	+	-	-	-	+/-	+	-	-	-	-
24	+	n/a	-	-	-	+/-	+	-	-	-	-

Table 7.1. Summary of the involvement of apoptotic signaling pathways concomitant with spreading of *L. aethiopica* infection. +/-, similar expression with uninfected control; +, increase in protein expression; -, decrease in protein expression; n/a, data not recorded; PS, Phosphatidyl serine; p-, phosphorylated

Such mechanism of NF- κ B downregulation has been previously reported as, cysteine peptidase from *L. mexicana* amastigotes was accountable for the degradation of p65 in infected mice macrophages (Cameron et al., 2004). Similar effects were also observed in poliovirus infection where the viral protease C degraded p65 in HeLa cell (Neznanov et al., 2005). However, it is interesting to note that other human pathogens have evolved diverse strategies to counteract NF- κ B signalling mediated apoptosis. *Yersinia* secretes YopJ effector to suppress the phosphorylation and degradation of I κ B inhibitor, which prevents the release and nuclear migration of p65 causing apoptotic induction of epithelial cells (Schesser et al., 1998). Whereas, type 3 secretion protein VP1686 of *Vibrio* interacted with p65 in order to block the DNA binding activity of NF- κ B that resulted in apoptosis of RAW macrophage (Bhattacharjee et al., 2006).

Interestingly, the pro-apoptotic protein PKC- δ was not associated with spreading, as there was no presence of catalytic fragment (CF) at the expected 42 kDa region of the western blot. During apoptosis, the catalytic fragment (CF) of PKC- δ is generated following caspase-3 mediated cleavage of full-length protein. The formation of CF is responsible for the activation of pro-apoptotic Bax, cytochrome C release, inhibition of DNA repairing enzyme DNAPk, destruction of nuclear lamin and activating caspase-3 activation (Reyland, 2007). This indicates that *L. aethiopica* does not utilize PKC- δ cleavage as one of the contributing factor for initiating apoptosis.

The mechanism by which *L. aethiopica* selectively targeted the above three pathways suggest that this parasitic species could exploit other apoptotic signalling pathways, which have not been explored yet. It was therefore interesting to determine whether intracellular amastigotes could subvert physiological processes in host cells during parasite transmission. To address this question, a proteomic study was conducted to identify differentially expressed proteins of macrophages involved in

apoptosis, immune response, vesicular trafficking, metabolism and gene expression during *L. aethiopica* spreading (Chapter 6). This was achieved via the use of tandem mass tag (TMT) labelling coupled with tandem mass spectrometry technique. One of the main advantages of this approach over traditional non-labelling methods is its ability to combine and analyse several samples (i.e. uninfected versus *L. aethiopica* infected co-cultures with 3 biological replicates) within one experiment. This eliminates the need to compare multiple mass spectrometry data sets, thereby reducing run-to-run variation and overall analytical time (Rauniyar and Yates, 2014). The proteomic data supported the finding from chapter 4 and 5 where caspase-3 upregulation and AKT/p65 NF- κ B protein downregulation was observed. Furthermore, the activation of caspase-9 and caspase-3 strengthened the involvement of mitochondrial mediated apoptosis.

Finally, identified proteins from immune response and gene expression showed that *L. aethiopica* induces the generation of an anti-inflammatory responses. This is evident from the fact that Chitinase-3-like protein (induces IL-13 production) and butyrophilin (reduces INF- γ and IL-12 response) were strongly upregulated. In particular, elevated increase in the protein expression of glutathione reductase and metallothionein-2, which are very important for scavenging free radicals, suggest that the anti-microbial activity during spreading is disarmed by *L. aethiopica* amastigotes for effective cell-to-cell spreading.

Chapter 8 – Conclusion and future works

8.1. Conclusion

In conclusion, this research has provided for the first time a clear understanding of the mechanism of *Leishmania* spreading between human macrophages, an issue extensively neglected in the study of these parasites. Preliminary experiments showed that apoptotic induction increased the percentage of *L. aethiopica* and *L. mexicana* infected cells during late stage of infection. Although this led to the establishment of a link between host apoptosis and *Leishmania* infection spreading (Aim 1), the viable cell concentration was significantly lower than non-induced cells. Nevertheless, such approach led to the accumulation of heavily infected cells. This provided a platform to develop a novel *in vitro* model to illustrate cell-to-cell spreading of *L. aethiopica* and *L. mexicana* in human macrophage (Aim 2). Through flow cytometry, parasite spreading was detected within 12 hours of co-culture. Interestingly, the live imaging revealed inter-cellular extrusion of *L. aethiopica* and *L. mexicana* from infected to a recipient cells without cell lysis. Interestingly, *L. aethiopica* (but not *L. mexicana*) dissemination was correlated with host apoptotic induction, as there was a significant increase in the phosphatidyl serine (PS) externalization and active caspase-3 expression (Aim 3). In addition, western blot analysis demonstrated that *L. aethiopica* spread was associated with modulation of three major apoptotic signaling pathways: AKT, NF- κ B and PKC- δ (Aim 4). Specifically, the parasite was able to initiate apoptosis by reducing the expression of pro-survival AKT and p65 NF- κ B proteins as well as by inducing cytochrome C release. These selective alterations by *L. aethiopica* prompted a global proteomic study to evaluate the expression of differentially regulated proteins of human macrophages during spreading. Through liquid

chromatography coupled with tandem mass spectrometry, 19 differentially expressed proteins were identified that were either involved in apoptosis, immune response, metabolism, vesicular trafficking and gene transcription (Aim 5). Further examination of these proteins collectively showed that *L. aethiopica* is involved in disarming various inflammatory and anti-microbial responses of human macrophages in order to spread effectively from cell-to-cell.

Infection with *L. aethiopica* is responsible for all forms of cutaneous leishmaniasis (CL) including muco and diffuse CL. Despite such clinical variation, very little is known about the biology and pathogenesis of *L. aethiopica* at the molecular level compared to other *Leishmania* species. This study has greatly contributed to understanding how *L. aethiopica* amastigotes manipulates the host signalling pathways in order to disseminate effectively and promote survival of its infectious progeny in a new macrophage niche, both of which are essential criteria for disease pathogenesis.

8.2. Future works

There are several research questions that can be investigated in future which will aim to further enhance our knowledge into the mechanism of *Leishmania* infection spreading.

1. Critical importance of AKT and NF- κ B signalling pathways

Although the western blot data highlighted that *L. aethiopica* spreading correlated with AKT and NF- κ B inactivation, whether any of these deficient proteins is the underlying factor behind apoptotic induced dissemination is not known. To address this question, transient overexpression of AKT and p65 NF- κ B in the infected cells

will have to be performed. This will indicate whether or not both proteins are the major targets of *L. aethiopica* amastigotes in order to spread from infected to uninfected cells.

2. Involvement of virulence factors in *Leishmania* spreading

If the above host proteins are instrumental for apoptosis, it will be interesting to find whether such effects are influenced by the virulence factors of *L. aethiopica*. To test this proposal, amastigotes mutant for various virulent proteins such as GP63 and Serine/Cysteine peptidase have to be designed. Then, using the spreading model, experiments will be performed to address two key questions. Is there a difference in the protein level of AKT and p65 NF- κ B between wild type and mutant parasites? If the mutant parasite is unable to degrade both proteins, does it have an effect on the percentage of infection and host apoptosis? These would provide a link between virulence factors, host apoptotic response and infection outcome.

3. Elucidate the mechanism for *L. mexicana* spread

This research clearly showed that *L. Mexicana* dissemination mechanism involves extrusion of parasites without cell lysis. But the mechanism behind such behaviour is unclear. Intracellular pathogens such as *Chlamydia*, *Shigella* and *Listeria* have evolved mechanism to recruit the host actin cytoskeleton in order to protrude across the uninfected cells (Ireton, 2013). To determine whether similar process is also utilized by *L. mexicana*, two critical experiments needs to be carried out. First, the infected donor cells can be stained with F-actin before co-culturing with uninfected cells and live cell imaged. This will indicate whether F-actin is concentrated around the region of exiting amastigotes. Secondly, inhibitors designed to block actin polymerization and nucleation can be used to completely prove that molecular networks of cytoskeleton are involved in facilitating *L. mexicana* spreading.

Chapter 9 – References

- Abeler-Dorner, L., Swamy, M., Williams, G., Hayday, A.C and Bas A. (2012). Butrophillins: an emerging family of immune regulators. *Trends Immunol*, 33, 34-41.
- Abu-Dayyeh, I., Hassani, K., Westra, E.R., Mottram, J.C and Olivier, M. (2010). Comparative study of the ability of *Leishmania mexicana* promastigotes and amastigotes to alter macrophage signaling and functions. *Infection and Immunity*, 78, 2438-2445.
- Aga, E., Katschinski, D.M., van Zandbergen, G., Laufs, H., Hansen, B., Muller, K., Solbach, W and Laskay, T. (2002). Inhibition of the spontaneous apoptosis of neutrophil granulocytes by the intracellular parasite *Leishmania major*. *The Journal of Immunology*, 169, 898-905.
- Aguilo, N., Marinova, D., Martin, C and Pardo, J. (2013). ESX-1 induced apoptosis during mycobacterial infection: to be or not be, that is the question. *Frontiers in Cellular and Infection Microbiology*, 3, doi: 10.3389/fcimb.2013.00088.
- Akarid, K., Arnoult, D., Micic-Polianski, J., Sif, J., Estaquier, J and Claude Ameisen, J. (2004). *Leishmania major* mediated prevention of programmed cell death induction in infected macrophages is associated with the repression of mitochondrial release of cytochrome c. *Journal of Leukocyte Biology*, 76, 95-103.
- Alexander, J and Brombacher, F. (2012). T helper1/T helper 2 cells and resistance/susceptibility to *Leishmania* infection: is this paradigm still relevant? *Frontiers in Immunology*, 3, doi: 10.3389/fimmu.2012.00080.
- Alexander, J., Coombs, G.H and Mottram, J.C. (1998). *Leishmania Mexicana* cysteine proteinase deficient mutants have attenuated virulence for mice and potentiate a T helper 1 response. *The Journal of Immunology*, 161, 6794 – 6801.
- Ashida, H., Mimuro, H., Ogawa, M., Kobayashi, T., Sanada, T., Kim, M and Sasakawa, C. (2011). Cell death and infection: a double-edged sword for host and pathogen survival. *The Journal of Cell Biology*, 195, 931-942.
- Assimina, Z., Charilaos, K and Fotoula, B. (2008). Leishmaniasis: an overlooked public health concern. *Health Science Journal*, 2, 196-205.
- Bailey, H and Bishop, W.J. (1959). Leishman-donovan bodies and donovaniasis. *Brit. J. vener. Dis.* 35, 8-9.
- Banuls, A.L., Hide, M and Prugnolle, F. (2007). *Leishmania* and the leishmaniasis: a parasite genetic update and advances in taxonomy, epidemiology and pathogenicity in humans. *Advances in Parasitology*, 64, 1-109.
- Barkett, M and Gimore, T.D. (1999). Control of apoptosis by Rel/NF-kappa B transcription factors. *Oncogene*, 18, 6910-6924.

- Bates, P.A. (2007). Transmission of *Leishmania* metacyclic promastigotes by phlebotomine sand flies. *International Journal for Parasitology*, 37, 1097-1106.
- Behrendorff, N., Dolai, S., Hong, W., Gaisano, H.Y and Thorn, P. (2011). VAMP8 is a SNARE selectively required for sequential granule-to-granule fusion. *J Biol Chem*, 286, 29627-29634.
- Belkaid, Y., Mendez, S., Lira, R., Kadambi, N., Milon, G and Sacks, D. (2000). A natural model of *Leishmania* major infection reveals a prolonged silent phase of parasite amplification in the skin before the onset of lesion formation and immunity. *The Journal of Immunology*, 165, 969-977.
- Besteiro, S., Williams, R.A.M., Coombs, G.H and Mottram, J.C. (2007). Protein turnover and differentiation in *Leishmania*. *International Journal for Parasitology*, 37, 1063-1075.
- Bhattacharjee R.N., Park, K.S., Kumagai, Y., Okada, K., Yamamoto, M., Uematsu, S., Matsui, K., Kumar, H., Kawai, T., Honda, T., Takeuchi, O and Akira, S. (2006). VP1686, a vibrio type III secretion protein, induces toll like receptor independent apoptosis in macrophage through NF-kappa B inhibition. *J Biol Chem*, 281, 36897-36904.
- Bhattacharyya, S., Ghosh, S., Sen, P., Roy, S and Majumdar, S. (2001). Selective impairment of protein kinase C isoforms in murine macrophage by *Leishmania donovani*. *Molecular and Cellular Biochemistry*, 216, 47-57.
- Blackwell, J.M., Ezekowitz, R.A., Roberts, M.B., Channon, J.Y., Sim, R.B and Gordon, S. (1985). Macrophage complement and lectin like receptors bind *Leishmania* in the absence of serum. *Journal of Experimental Medicine*, 162, 324-331.
- Blanchette, J., Racette, N., Faure, R., Siminovitch, K.A and Olivier, M. (1999). *Leishmania* induced increase in activation of macrophage SHP-1 tyrosine phosphatase are associated with impaired IFN-gamma triggered JAK2 activation. *European Journal of Immunology*, 29, 3737-3744
- Bockstal, V., Guirnalda, P., Caljon, G., Goenka, R., Telfer, J.C., Frenkel, D., Radwanska, M., Magez, S and Black, S.J. (2011). *T. brucei* infection reduces B lymphopoiesis in bone marrow and truncates compensatory splenic lymphopoiesis through transitional B cell apoptosis. *PLOS*, 7, e1002089.
- Bogdan, C. (2012). Natural killer cells in experimental and human leishmaniasis. *Frontiers in Cellular and Infection Microbiology*, 2, doi: 10.3389/fcimb.2012.00069.
- Brittingham, A., Chen, G., McGwire, B., Chang, K.P and Mosser, D.M. (1999). Interaction of *Leishmania* gp63 with cellular receptors for fibronectin. *Infection and Immunity*, 67, 4477-4484.
- Brittingham, A., Morrison, C.J., McMaster, W.R., McGwire, B.S., Chang, K.P., Mosser D.M. (1995). Role of the *Leishmania* surface protease gp63 in complement fixation, cell adhesion and resistance to complement mediated lysis. *The Journal of Immunology*, 155, 3102-3111.

- Buates, S and Mattelawski, G. (2001). General suppression of macrophage gene expression during *Leishmania* infection. *Journal of Immunology*, 166, 3416-3422.
- Byrne, G.I and Ojcius, D.M. (2004). *Chlamydia* and apoptosis: life and death decisions of an intracellular pathogen. *Nature Reviews Microbiology*, 2, 802-808.
- Calgeri-Silva, T.C., Pereira, R.M.S., De-Melo, L.D.B., Saraiva, E.M., Soares, D.C., Bellio, M and Lopes, U.G. (2009). NF- κ B mediated repression of iNOS expression in *Leishmania amazonensis* macrophage infection. *Immunology Letters*, 127, 19-25.
- Calvopina, M., Gomez, E.A., Sindermann, H., Cooper, P and Hashiguchi, Y. (2006). Relapse of new world diffuse cutaneous leishmaniasis caused by *L. Mexicana* after mitefosine treatment. *Am. J. Trop. Med. Hug*, 75, 1074-1077.
- Cameron, P., McGachy, A., Anderson, M., Paul, A., Coombs, G.H., Mottram, J.C., Alexander, J and Plevin, R. (2004). Inhibition of Lipopolysaccharide induced macrophage IL-12 production by *Leishmania mexicana* amastigotes: the role of cysteine peptidases and the NF- κ B signaling pathway. *The Journal of Immunology*, 173, 3297-3304.
- Cecilio, P., Perez-Cabezas, B., Santarem, N., Maciel, J., Rodrigues, V and Cordeiro da Silva, A. (2014). Deception and manipulation: the arms of leishmania, a successful parasite. *Front Immunol*, 5, doi: 10.3389/fimmu.2014.00480.
- Chakravarti, D and Hong, R. (2003). SET-ting the stage for life and death. *Cell*, 12, 589-591.
- Chen, J., de Felipe, K.S., Clarke, M., Lu, H., Anderson, R., Segal, G and Shuman, H.A. (2004). *Legionella* effectors that promote nonlytic release from protozoa. *Science*, 303, 1358-1361.
- Conteras, I., Gomez, M.A., Nguyen, O., Shio, M.T., McMaster R.W and Olivier, M. (2010). *Leishmania* induced inactivation of the macrophage transcription factor AP-1 is mediated by the parasite metalloprotease GP63. *PLOS*, 6, e1001148.
- Cox, J and Mann, M. (2007). Is Proteomics the New Genomics? *Cell*, 130, 395-398.
- Cruz, K.K., Fonseca, S.G., Monteiro, M.C., Silva, O.S., Andrade, V.M., Cunha, F.Q and Romao, P.R. (2008). The influence of glutathione modulators on the course of *Leishmania major* infection in susceptible and resistant mice. *Parasite immunology*, 30, 171-174.
- Cubillos-Ruiz, J.R., Martinez, D., Scarlett, U.K., Rutkowski, M.R., Nesbeth, Y.C., Camposeco-Jacobs, A.L and Conejo-Garcia, J.R. (2010). CD277 is a negative co-stimulatory molecule universally expressed by ovarian cancer micro environmental cells. *Oncotarget*, 1, 329-338.
- Czuczman, M.A., Fattouh, R., van Rijn, J., Canadien, V., Osborne, S., Muise, A.M., Kuchroo, V.J., Higgins, D.E and Brumell, J. (2014). *Listeria monocytogenes* exploits efferocytosis to promote cell-to-cell spread. *Nature*, 509, 230-234.
- Dale, D.C., Boxer, L and Conrad Liles, W. (2008). The phagocytes: neutrophils and monocytes. *Blood*, 112, 935-945.

- DaMata, J.P., Mendes, B.P., Maciel-Lima, K., Silva Menezes, C.A., Dutra, W.O., Pires Sousa, L and Horta, M.F. (2015). Distinct macrophage fates after *in vitro* infection with different species of *Leishmania*: induction of apoptosis by *Leishmania amazonensis* but not by *Leishmania guyanensis*. *PLOS*, 10, e0141196.
- Danial, N.N and Korsmeyer, S.J. (2004). Cell death: critical control points. *Cell*, 116, 205-219.
- Danial, N.N. (2007). BCL-2 family proteins: critical checkpoints of apoptotic cell death. *Clinical Cancer Research*, 13, 7254- 7263.
- Dawit, G., Girma, Z and Simenew, K. (2013). A review of biology, epidemiology and public health significance of leishmaniasis. *Journal of Bacteriology and Parasitology*, 4, 1-7.
- De Souza, S., Lang, T., Prina, E., Hellio, R and Antoine, J.C. (1995). Intracellular *Leishmania amazonensis* amastigotes internalize and degrade MHC class II molecules of their host cells. *Journal of Cell Science*, 108, 3219-3231.
- Dermine, J.F., Scianimanico, S., Prive, C., Descoteaux, A and Desjardins, M. (2000). *Leishmania* promastigotes require lipophosphoglycan to actively modulate the fusion properties of phagosomes at an early step of phagocytosis. *Cellular Microbiology*, 2, 115-126.
- Desjeux, P. (1996). Leishmaniasis. *Clinics in Dermatology*, 14, 417-423.
- Donovan, C. (1903). On the possibility of the occurrence of trypanosomiasis in India. *Brit. Med. J*, 2, 79.
- Donovan, M.J., Macluba, B.Z., Mahan, C.E and McDowell, M.A. (2009). *Leishmania* infection inhibits cycloheximide induced macrophage apoptosis in a strain dependent manner. *Exp Parasitol*, 123, 58-64.
- Ellis, M., Sharma, D.K., Hilley, J.D., Coombs, G.H., Mottram, J.C. (2002). Processing and trafficking of *Leishmania Mexicana* gp63. Analysis using gp18 mutants deficient in glycosylphosphatidylinositol protein anchoring. *The Journal of Biological Chemistry*, 277, 27968-27974.
- Eurich, K., Segawa, M., Toei-Shimizu, S and Mizoguchi, E. (2009). Potential role of chitinase 3 like 1 in inflammation associated carcinogenic changes in epithelial cells. *World J Gastroenterol*, 15, 5249-5259.
- Filardy, A., Costa-da-Silva, A.C., Koeller, C. M., Guimaraes-Pinto, K., Ribeiro-Gomes, F., Lopes, M.F., Heise, N., Freire-de-Lima, C.G., Nunes, M.P and DosReis, D. A. (2014). Infection with *Leishmania major* induces a cellular stress response in macrophages. *PLOS*, 9, e85715.
- Foell, D., Wittkowski, H., Vogli, T and Roth, J. (2007). S100 proteins expressed in phagocytes: a novel group of damage associated molecular pattern molecules. *J Leukoc Biol*, 81, 28-37.

- Forget, G., Gregory, D.J and Olivier, M. (2005). Proteasome mediated degradation of STAT-1 alpha following infection of macrophages with *Leishmania donovani*. *Journal of Biological Chemistry*, 280, 30542-30549.
- Franco, L.H., Beverley, S.M and Zamboni, D.S. (2012). Innate immune activation and subversion of mammalian functions by *Leishmania* lipophosphoglycan. *Journal of Parasitology Research*, doi: 10.1155/2012/165126.
- Fukumatsu, M., Ogawa, M., Arakawa, S., Suzuki, M., Nakayama, K., Shimizu, S., Kim, M., Mimuro, H and Sasakawa, C. (2012). *Shigella* targets epithelial tricellular junctions and uses a non-canonical clathrin dependent endocytic pathway to spread between cells. *Cell Host and Microbe*, 11, 325-356.
- Ganguly, S., Das, N.K., Barbhuiya, J.N and Chatterjee, M. (2010). Post-kala-azar dermal leishmaniasis – an overview. *International Journal of Dermatology*, 49, 921-931.
- Garcia-Echerverria, C and Sellers, W.R. (2008). Drug discovery approaches targeting the PI3/AKT pathway in cancer. *Oncogene*, 18, 5511-5526.
- Getti, G., Cheke, R.A and Humber, D.P. (2008). Induction of apoptosis in host cells: a survival mechanism for *Leishmania* parasites? *Parasitology*, 135, 1391-1399.
- Gomez, M.A., Navas, A., Marquez, R., Rojas, L.J., Vargas, D.A., Bianco, V.M., Koren, R., Zilberstein, D and Saravia, N.G. (2014). *Leishmania panamensis* infection and antimonial drugs modulate expression of macrophage drug transporters and metabolizing enzymes: impact on intracellular parasite survival. *J Antimicrob Chemother*, 69, 139-149.
- Gregory, D.J., Godbout, M., Contreras, I., Forget, G and Olivier, M. (2008). A novel form of NF- κ B is induced by *Leishmania* infection: involvement in macrophage gene expression. *European Journal of Immunology*, 38, 1071-1081.
- Gregory, D.J., Sladek, R., Olivier, M and Matlashewski, G. (2008). Comparison of the effects of *Leishmania major* or *Leishmania donovani* infection on macrophage gene expression. *Infect and Immun*, 76, 1186-1192.
- Groppelli, E., Starling, S and Jolly, C. (2015). Contact-induced mitochondrial polarization supports HIV-1 virological synapse formation. *Journal of Virology*, 89, 14-24.
- Guimaraes-Costa, A.B., Nascimento, M.T.C., Froment, G.S., Soares, R.P., Morgado, F.N., Conceicao-Silva, F and Saraiva, E. (2009). *Leishmania amazonensis* promastigotes induce and are killed by neutrophil extracellular traps. *PNAS*, 106, 6748-6753.
- Guizani-Tabbane, L., Ben-Aissa, K., Belghith, M., Sassi, A and Dellagi, K. (2004). *Leishmania major* amastigotes induce p50/c-Rel NF-kappa B transcription factor in human macrophages: involvement in cytokine synthesis. *Infect. Immun*, 72, 2582-2589.
- Guler, R., Asfar, M., Arendse, B., Parihar, S.P., Revaz-Breton, M., Leitges, M., Schwegmann, A and Brombacher, F. (2011). PKC delta regulates IL-12 p40/o70 production by macrophages and dendritic cells, driving a type 1 healer phenotype in cutaneous leishmaniasis. *European Journal of Immunology*, 41, 706-715.

- Hagedorn, M., Rohde, K.H., Russell, D.G and Soldati, T. (2009). Infection by tubercular mycobacteria is spread by nonlytic ejection from their amoeba hosts. *Science*, 323, 1729-1733.
- Hass, A. (2007). The phagosome: compartment with a license to kill. *Traffic*, 8, 311-330.
- Himmelrich, H., Parra-Lopez, C., Tacchini-Cottier, F., Louis, J.A and Launois, P. (1998). The IL-4 rapidly produced in BALB/c mice after infection with *Leishmania major* downregulates IL-12 receptor beta 2 chain expression on CD4+ T cells resulting in a state of unresponsiveness to IL-12. *The Journal of Immunology*, 161, 6156 – 6163.
- Hirokawa, N., Noda, Y., Tanaka, Y and Niwa, S. (2009). Kinesin superfamily motor proteins and intracellular transport. *Nature Review Molecular Cell Biology*, 10, 682-696.
- Hsiao, C.H.C., Ueno, N., Shao, J.Q., Schroeder, K.R., Moore, K.C., Donelson, J.E and Wilson, M.E. (2011). The effects of macrophage source on the mechanism of phagocytosis and intracellular survival of *Leishmania*. *Microbes and Infection*, 13, 1033-1044.
- Hybiske, K and Stephens, R.S. (2007). Mechanisms of host cell exit by the intracellular bacterium *Chlamydia*. *PNAS*, 104, 11430-11435.
- Ilg, T. (2000). Lipophosphoglycan is not required for infection of macrophages or mice by *Leishmania mexicana*. *The EMBO Journal*, 19, 1953-1962.
- Ireton, K. (2013). Molecular mechanism of cell-cell spread of intracellular bacterial pathogens. *Open Biol*, 3, 130079.
- Isnard, A., Christian, J.G., Kodiha, M., Stochaj, U., McMaster, R and Olivier, M. (2015). Impact of *Leishmania* infection on host macrophage nuclear physiology and nucleopore complex integrity. *PLOS*, 11, e1004776.
- Isnard, A., Shio, M.T and Olivier, M. (2012). Impact of *Leishmania* metalloprotease GP63 on macrophage signaling. *Frontiers in Cellular and Infection Microbiology*, 2, doi: 10.3389/fcimb.2012.00072.
- Ivanov, S.S and Roy, C.R. (2013). Pathogen signatures activate a ubiquitination pathway that modulates the function of the metabolic checkpoint kinase mTOR. *Nature Immunology*, 14, 1219-1228.
- Jiang, X and Wang, X. (2004). Cytochrome C mediated apoptosis. *Ann. Rev. Biochem*, 73, 87-106.
- Jolly, C and Sattentau, Q.J. (2005). HIV1 virological synapse formation in T cells requires lipid raft integrity. *Journal of Virology*, 79, 12088-12094.
- Kar, S., Ukil, A., Sharma, G and Das, P.K. (2010). MAPK-directed phosphatase preferentially regulate pro- and anti-inflammatory cytokines in experimental visceral leishmaniasis: involvement of distinct protein kinase C isoforms. *J Leukoc Biol*, 88, 9-20.

- Kato, H., Gomez, E.A., Caceres, A.G., Uezato, H., Mimori, T and Hashiguchi, Y. (2010). Molecular epidemiology for vector research on leishmaniasis. *International Journal of Environmental Research and Public Health*, 7, 814-826.
- Kaushansky, A., Metzger, P.G., Douglass, A.N., Mikolajczak, S.A., Lakshmanana, V., Kain, H.S and Kappe, S.H.I. (2013). Malaria parasite liver stages render host hepatocytes susceptible to mitochondria initiated apoptosis. *Cell Death and Disease*, 4, e762.
- Kaye, P and Scott, P. (2011). Leishmaniasis: complexity at the host-pathogen interface. *Nature Reviews Microbiology*, 9, 604-615.
- Kulkarni, M., Jones, E.A., McMaster, W., McGwire, B. (2008). Fibronectin binding and proteolytic degradation by *Leishmania* and effects on macrophage activation. *Infection and Immunity*, 76, 1738-1747.
- Kulkarni, M.M., McMaster W.R., Kamysz, E., Kamysz, W., Engman, D.M., McGwire, B.S. (2006). The major surface metalloprotease of the parasitic protozoan *Leishmania* protects against anti-microbial peptide induced apoptotic killing. *Mol Microbiol*, 62, 1484-1497.
- Kumar, R and Nysten, S. (2012). Immunobiology of visceral leishmaniasis. *Frontiers in Immunology*, 3, doi: 10.3389/fimmu.2012.00251.
- Kumar, S. (2007). Caspase function in programmed cell death. *Cell Death and Differentiation*, 14, 32-43.
- Laskay, T., van Zandbergen, G and Solbach, W. (2003). Neutrophil granulocytes – Trojan horses for *Leishmania major* and other intracellular microbes? *Trends in Microbiology*, 11, 210-214.
- Laurenti, M.D., Gidlund, M., Ura, D.M., Sinhorini, I.L., Corbett, C.E and Goto, H. (1999). The role of NK cells in the early period of infection in murine cutaneous leishmaniasis. *Braz. J. Med. Biol. Res*, 32, 323-325.
- Leishman, W.B. (1903). On the possibility of the occurrence of trypanosomiasis in India. *Brit. Med. J*, 1, 1252-1254.
- Lincoln, L.M., Ozaki, M., Donelson, J.E and Beetham, J.K. (2004). Genetic complementation of *Leishmania* deficient in PSA (GP46) restores their resistance to lysis by complement. *Molecular and Biochemical Parasitology*, 137, 185-189.
- Lisi, S., Sisto, M., Acquafredda, A., Spinelli, R., Schiavone, M.A., Mitolo, V., Brandonisio, O and Panaro, M.A. (2005). Infection with *Leishmania infantum* inhibits actinomycin D induced apoptosis of human monocytic cell line U-937. *J. Eukaryot. Microbiol*, 52, 211-217.
- Liu, D., Kebaier, C., Pakpour, N., Capul, A., Beverley, S.M., Scott, P., Uzonna, J. (2009). *Leishmania major* phosphoglycans influence the host early immune response by modulating dendritic cell function. *Infect. Immun*, 77, 3272-3283.
- Lodge, R and Descoteaux, A. (2005). Modulation of phagolysosome biogenesis by the lipophosphoglycan of *Leishmania*. *Clinical Immunology*, 114, 256-265.

- Lodge, R and Descoteaux, A. (2008). *Leishmania* invasion and phagosome biogenesis. *Landes Bioscience*, 174-181.
- Lodge, R., Diallo, T and Descoteaux, A. (2006). *Leishmania donovani* lipophosphoglycan blocks NADPH oxidase assembly at the phagosome membrane. *Cellular Microbiology*, 8, 1922-1931.
- Loria-Cervera, E.N and Andrade-Narvaez, F.J. (2014). Animal models for the study of leishmaniasis immunology. *Revista do Instituto de Medicina Tropical de Sao Paulo*, 56, 1-11.
- Ma, H., Croudace, J.E., Lammas, D.A and May, R.C. (2007). Direct cell-to-cell spread of a pathogenic yeast. *BMC Immunology*, 8, doi: 10.1186/1471-2172-8-15.
- MacFarlane, M and Williams, A.C. (2004). Apoptosis and disease: a life or death decision. *EMBO reports*, 5, 674-678.
- Mahajan, M.A and Samuels, H. (2008). Nuclear receptor coactivator/coregulator NCoA6 (NRC) is a pleiotropic coregulator involved in transcription, cell survival, growth and development. *Nucl Recept Signal*, 6, e002.
- Matheoud, D., Moradin, N., Bellemare-Pelletier, A., Shio, M.T., Hong, W.J., Olivier, M., Gagnon, E., Desjardins, M and Descoteaux, A. (2013). *Leishmania* evades host immunity by inhibiting antigen cross-presentation through direct cleavage of the SNARE VAMP8. *Cell Host Microbe*, 14, 15-25.
- Mathur, R.K., Awasthi, A., Wadhone, P., Ramanamurthy, B and Saha, B. (2004). Reciprocal CD40 signals through p38MAPK and ERK-1/2 induce counteracting immune response. *Nature Medicine*, 10, 540-544.
- Matte, C and Descoteaux, A. (2010). *Leishmania donovani* amastigotes impair gamma interferon induced STAT1 alpha nuclear translocation by blocking the interaction between STAT1 alpha and Importin-alpha 5. *Infection and Immunity*, 78, 3736-3743.
- McNeely, T.B., and Turco, S.J. (1990) Requirement of lipophosphoglycan for intracellular survival of *Leishmania donovani* within human monocytes. *The Journal of Immunology*, 144, 2745– 2750.
- Medina-Acosta, E., Karess, R.E., Schwarz, H and Russel, D.G. (1989). The promastigote surface protease (gp63) of *Leishmania* is expressed but differentially processed and localized in the amastigote stage. *Mol Biochem Parasitol*, 37, 263-273.
- Menezes, J.P.B., Almeida, T.F., Petersen, A.L.O.A., Guedes, C.E.S., Mota, M.S.V., Lima, J.G.B., Palma, L.C., Buck, G.A., Kreiger, M.A., Probst, C.M and Veras, P.S.T. (2013). Proteomic analysis reveals differentially expressed proteins in macrophages infected with *Leishmania amazonensis* or *Leishmania major*. *Microbes and Infection*, 15, 579-591.
- Mi, J., Li, Z., Ni, S., Steinwaerder, D and Liber, A. (2001). Induced apoptosis supports spread of adenovirus vectors in tumours. *Human Gene Therapy*, 12, 1343-1352.

- Miller, J.L., Velmurugan, K., Cowan, M.J and Briken, V. (2010). The type I NADH dehydrogenase of *Mycobacterium tuberculosis* counters phagosomal NOX2 activity to inhibit TNF alpha mediated host cell apoptosis. *PLOS*, 6, e1000864.
- Moore, K.J and Matlashewski, G. (1994). Intracellular infection by *Leishmania donovani* inhibits macrophage apoptosis. *The Journal of Immunology*, 15, 2930-2937.
- Moradin, N and Descoteaux, A. (2012). *Leishmania* promastigotes: building a safe niche within macrophages. *Frontiers in Cellular and Infection Microbiology*, 2, doi: 10.3389/fcimb.2012.00121.
- Mosser, D.M and Edelson, P.J. (1985). The mouse macrophage receptor for C3bi is a major mechanism in the phagocytosis of *Leishmania* promastigotes. *The Journal of Immunology*, 135, 2785-2789.
- Mottram, J.C., Coombs, G.H and Alexander, J. (2004). Cysteine peptidases as virulence factors of *Leishmania*. *Curr Opin Microbiol*, 7, 375-381.
- Naderer, T and McConville, M.J. (2007). The *Leishmania*-macrophage interaction: a metabolic perspective. *Cellular Microbiology*, 10, 301-308.
- Neznanov, N., Chumakov, K.M., Neznaova, L., Almasan, A., Bhanerjee, A.K and Gudkov, A.V. (2005). Proteolytic cleavage of the p65-RelA subunit of NF-kappa B during poliovirus infection. *J Biol Chem*, 280, 153-158.
- O'Brien, V. (1998). Viruses and apoptosis. *Journal of General Virology*, 79, 1883-1845.
- Ogunkolade, B.W., Colomb-Valet I., Monjour, L., Rhodes-Feuillette, A., Abita, J.P and Froemel, D. (1990). Interactions between the human monocytic leukaemia THP-1 cell line and Old and New World species of *Leishmania*. *Acta Tropica*, 47, 171-176.
- Patel, A.P., Deacon, A and Getti, G. (2014). Development and validation of four *Leishmania* species constitutively expressing GFP protein. A model for drug discovery and disease pathogenesis studies. *Parasitology*, 141, 501-510.
- Peters, N.C., Egen, J.G., Secundino, N., Debrabant, A., Kimblin, N., Kamhawi, S., Lawyer, P., Fay, M., Germain, R.N and Sacks, D.L. (2008). *In vivo* imaging reveals an essential role for neutrophils in Leishmaniasis transmitted by sand flies. *Science*, 321, 970-974.
- Prajeeth, C.K., Haeberlein, S., Sebald, H., Schleicher, U and Bogdan, C. (2011). *Leishmania* infected macrophages are targets of NK cell derived cytokines but not of NK cell cytotoxicity. *Infection and Immunity*, 79, 2699-2708.
- Quinton-Leslie, R.G. (2001). Complement receptors. *Encyclopedia of Life Sciences*, 1-9.
- Rauniyar, N and Yates, J.R. (2014). Isobaric labeling based relative quantification in shotgun proteomics. *J Proteome Res*, 13, 5293-52309.
- Real, F., Florentina, P.T.V., Reis, L.C., Ramos-Sanchez, E.M., Veras, P.S.T., Goto, H and Mortara, R.A. (2014). Cell-to-cell transfer of *Leishmania amazonensis* amastigotes is

mediated by immunomodulatory LAMP-rich parasitophorous extrusions. *Cellular Microbiology*, 16, 1549-1564.

Reinhard, K., Huber, M., Lohoff, M and Visekruna, A. (2012). The role of NF- κ B activation during protection against *Leishmania* infection. *International Journal of Medical Microbiology*, 302, 230-235.

Reithinger, R., Dujardin, J.C., Louzir, H., Pirmez, C., Alexander, B and Brooker, S. (2007). Cutaneous leishmaniasis. *Lancet Infect Dis*, 7, 581-596.

Reyland, M.E. (2007). Protein kinase C and apoptosis. *Apoptosis, cell signaling and human diseases: molecular mechanism*, 2, 31-55.

Ribeiro-Gomes, F.L., Moniz-de-Souza, M.C., Alexnadre-Moreira, M.S., Dias, W.B., Lopes, M.F., Nunes, M.P., Lungarella, G and DosReis, G.A. (2007). Neutrophils activate macrophages for intracellular killing of *Leishmania major* through recruitment of TLR4 by neutrophil elastase. *The Journal of Immunology*, 179, 3938-3994.

Rittig, M.G., Schroppel, K., Seack, K.H., Sander, U., N' Diaye, E.N., Maridonneau-Parini, I., Solbach, W and Bogdan, C. (1998). Coiling phagocytosis of trypanosomatids and fungal cells. *Infect and Immun*, 66, 4331-4339.

Rodriguez, N.E., Chang, H.K and Wilson, M.E. (2004). Novel program of macrophage gene expression induced by phagocytosis of *Leishmania chagasi*. *Infect Immun*, 72, 2111-2122.

Rodriguez, N.E., Gaur Dixit, U., Allen, L.A and Wilson, M.E. (2011). Stage specific pathways of *Leishmania infantum chagasi* entry and phagosome maturation in macrophages. *PLOS*, 6, e19000.

Rogers, M.E. (2012). The role of *Leishmania* proteophosphoglycans in sand fly transmission and infection of the mammalian host. *Frontiers in Microbiology*, 3, doi: 10.3389/fmicb.2012.00223.

Rogers, M.E., Chance, M.L and Bates, P.A. (2002). The role of promastigote secretory gel in the origin and transmission of the infective stage of *Leishmania mexicana* by the sandfly *Lutzomyia longipalpis*. *Parasitology*, 124, 495-507.

Rogers, M.E., Hajmova, M., Joshi, M.B., Sadlova, J., Dwyer, D.M., Volf, P and Bates, P.A. (2008). *Leishmania chitinase* facilitates colonization of sandfly vectors and enhances transmission to mice. *Cellular Microbiology*, 10, 1363-1372.

Rogers, M.E., Kropf, P., Choi, B.S., Dillon, R., Podinovskala, M., Bates, P.A and Muller, I. (2009). Proteophosphoglycans regurgitated by *Leishmania* infected sand flies target the L-Arginine metabolism of host macrophages to promote parasite survival. *PLOS*, 5, e1000555.

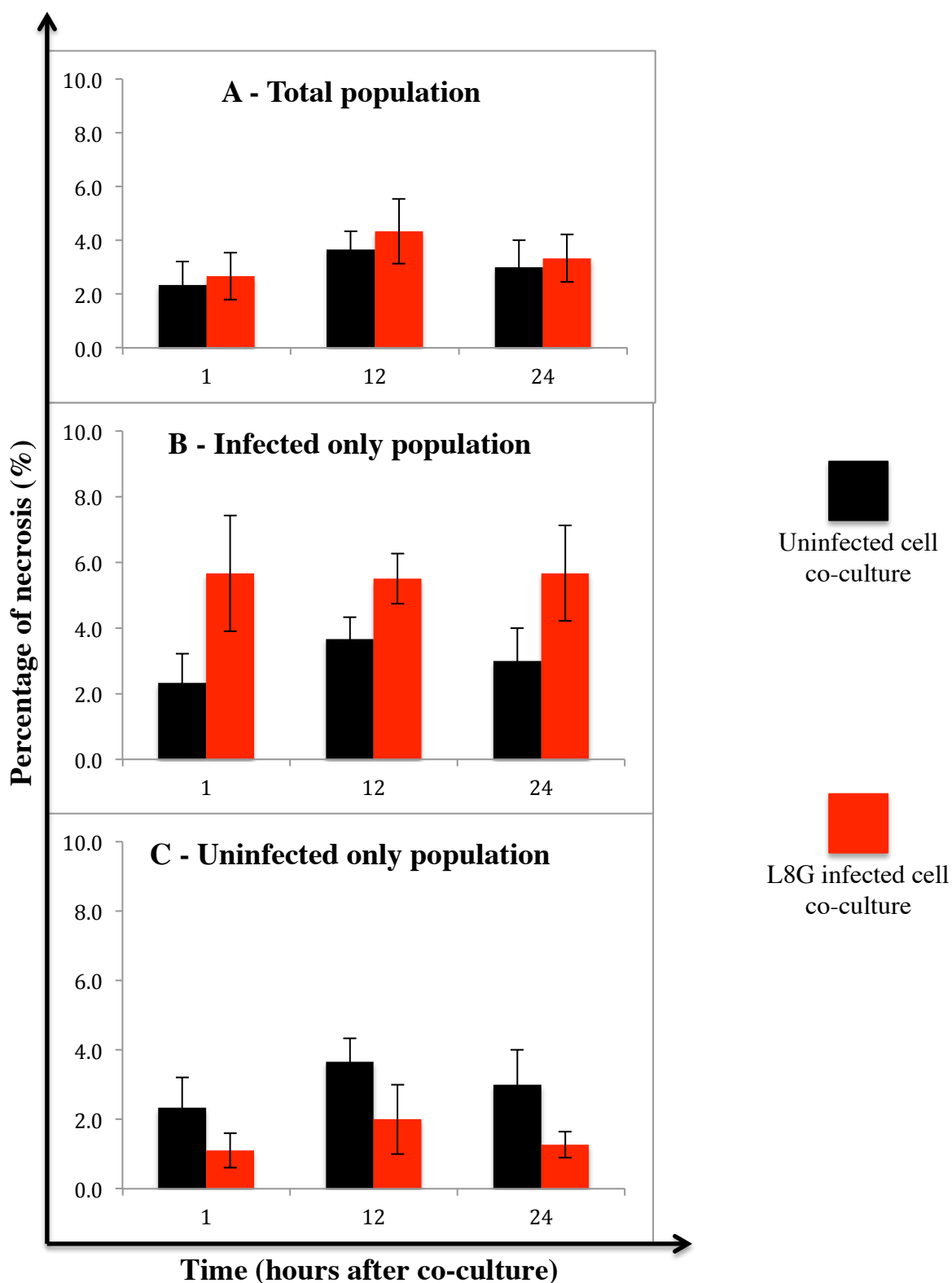
Romao, P.R., Fonseca, S.C., Hothersall, J.S., Noronhna-Dutra, A.A., Ferreira, S.H and Cunha, F.Q. (1999). Glutathione protects macrophages and *Leishmania major* against nitric oxide mediated cytotoxicity. *Parasitology*, 118, 559-566.

- Romao, P.R., Tovar, J., Fonseca, S.C., Moraes, R.H., Cruz, A.K., Horthersall, J.S., Noronhna-Dutra, A.A., Ferrerira, S.H and Cunha, F.Q. (2006). Glutathione and the redox control system trypanothione/trypanothione reductase are involved in the protection of *Leishmania* species against nitrosothiol-induced cytotoxicity. *Braz J Med Biol Res*, 39, 355-363.
- Rosenthal, L.A., Sutterwala, F.S., Kehrl, M and Mosser, D.M. (1996). *Leishmania major* human macrophage interactions: cooperation between Mac-1 and complement receptor type 1 in promastigote adhesion. *Infection and Immunity*, 64, 2206-2215.
- Ruhland, A., Leal, N and Kima, P.E. (2007). *Leishmania* promastigotes activate PI3K/AKT signaling to confer host cell resistance to apoptosis. *Cellular Microbiology*, 9, 84-96.
- Ryan, R., O'Sullivan, M and Keane, J. (2011). *Mycobacterium tuberculosis* infection induces non-apoptotic cell death of human dendritic cells. *BMC Microbiology*, 11, 237-250.
- Sacks, D and Noben-Trauth, N. (2002). The immunology of susceptibility and resistance to *Leishmania major* in mice. *Nature Reviews Immunology*, 2, 845-858.
- Sacks, D.L. (1992). The structure and function of surface lipophosphoglycans on different developmental stages of *Leishmania* promastigotes. *Infect Agents Dis*, 1, 200-206.
- Sanabria, M.X., Vargas-Inchaustegui, D.A., Xin, L and Soong, L. (2008). Role of NK cells in modulating dendritic cell responses to *Leishmania amazonensis* infection. *Infect. Immun*, 76, 5100-5109.
- Sattentau, Q.J. (2010). Cell-to-cell spread of retroviruses. *Viruses*, 2, 1306-1321.
- Schesser, K., Spiik, A.K., Dukuzumuremyi, J.M., Neurath, M.F., Pettersson, S and Wolf-Watz, H. (1998). The yopJ locus is required for Yersinia-mediated inhibition of NF-kappa B activation and cytokine expression: YopJ contains a eukaryotic SH2 like domain that is essential for its repressive activity. *Mol Microbiol*, 28, 1067-1079.
- Segovia, M., Artero, J.M., Mellado, E., Chance, M.L. (1992). Effects of long term *in vitro* cultivation on the virulence of cloned lines of *Leishmania major* promastigotes. *Ann Trop Med Parasitol*, 86, 347-354.
- Shamas-Din, A., Brahmabhatt, H., Leber, B and Andrews, D.W. (2011). BH3-only proteins: orchestrators of apoptosis. *Biochemica et Biophysica Acta*, 1813, 508-520.
- Shtreichman, R., Sharf, R., Barr, H., Dobner, T and Kleinberger, T. (1999). Induction of apoptosis by adenovirus E4orf4 protein is specific to transformed cells and requires an interaction with protein phosphatase 2A. *PNAS*, 96, 10080-10085.
- Singh, A.K., Pandey, R.K., Siqueira,-Neto, J.L., Kwon, Y.J., Freitas-Junior, L.H., Shaha, C and Madhubala, R. (2015). Proteomic based approach to gain insight into reprogramming of THP-1 cells exposed to *Leishmania donovani* over an early temporal window. *Infect Immun*, 83, 1853-1868.
- Singh, V.K., Balaraman, S., Tewary, P and Madhubala, R. (2004). *Leishmania donovani* activates nuclear transcription factor-kappa B in macrophages through reactive oxygen intermediates. *Biochem Biophys Res Commun*, 322, 1086-1095.

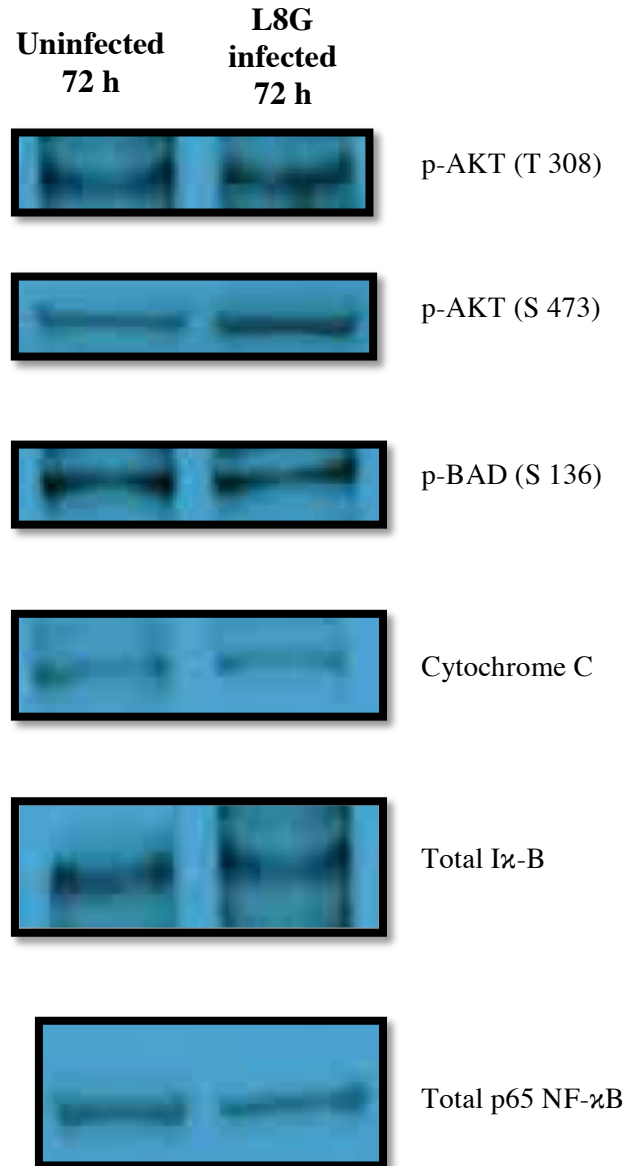
- Smith, D.F and Rangarajan, D. (1995). Cell surface components of *Leishmania*: identification of a novel parasite lectin? *Glycobiology*, 5, 161-166.
- Smith, I.A., Knezevic, B.R., Ammann, J.U., Rhodes, D.A., Aw, D., Palmer, D.B., Mather, I.H and Trowsdale, J. (2010). BTN1A1, the mammary gland butyrophillin, and BTN2A2 are both inhibitors of T cell activation. *Journal of Immunology*, 184, 3514-3525.
- Spath, G.F., Garraway, L.A., Turco, S.J and Beverley, S.M. (2003). The role of lipophosphoglycan (LPG) in the establishment of *Leishmania major* infections in mammalian hosts. *PNAS*, 100, 9536-9541.
- Stager, S and Rafati, S. (2012). CD8+ T cells in *Leishmania* infections: friends or foes? *Frontiers in Immunology*, doi: 10.3389/fimmu.2012.00005.
- Sutterwala, F.S., Rosenthal, L.A and Mosser, D.M. (1996). Cooperation between CR1 and CR3 in the binding of complement opsonized particles. *Journal of Leukocyte Biology*, 59, 883-890.
- Swanson, M.S and Fernandez-Moreira. (2002). A microbial strategy to multiply in macrophages: The pregnant pause. *Traffic*, 3, 170-177.
- Swenerton, R.K., Zhang, S., Sajid, M., Medzihardsky, K.F., Craik, C.S., Kelly, B.L and McKerrow, J.H. (2011). The oligopeptidase B of *Leishmania* regulates parasite enolase and immune evasion. *The Journal of Biological Chemistry*, 286, 429-440.
- Szegezdi, E., Logue, S.E., Gorman, A.M and Samali, A. (2006). Mediators of endoplasmic reticulum stress induced apoptosis. *EMBO Rep*, 7, 880-885.
- Szeto, J., Namolovan, A., Osborne, S.E., Coombes, B.K and Brumell, J.H. (2009). Salmonella containing vacuoles display centrifugal movement associated with cell-to-cell transfer in epithelial cells. *Infect and Immun*, 77, 996-1007.
- Thi, E.P., Lambertz, U and Reiner, N.E. (2012). Sleeping with the enemy: how intracellular pathogens cope with a macrophage lifestyle. *PLOS*, 8, e10002551.
- Tollefson, A.E., Scaria, A., Herminston, T.W., Ryerse, J.S., Wold, L.J and Wold, W.S.M. (1996). The adenovirus death protein (E3-11.6K) is required at very late stages of infection for cell lysis and release of adenovirus from infected cells. *J. Virol*, 70, 2296-2306.
- Tsagozis, P., Karagouni, E and Dotsika, E. (2003). CD8+ T cells with parasite specific cytotoxic activity and a Tc1 profile of cytokine and chemokine secretion develop in experimental visceral leishmaniasis. *Parasite Immunology*, 25, 569-579.
- Twiddy, D and Cain, K. (2007). Caspase-9 cleavage, do you need it? *Biochem J*, 405, e1-2.
- Ueno, N and Wilson, M.E. (2012). Receptor mediated phagocytosis of *Leishmania*: implication for intracellular survival. *Trends in Parasitology*, 28, 335-344.

- Uzonna, J.E., Joyce, K.L and Scott, P. (2004). Low dose *Leishmania major* promotes a transient T helper cell type 2 response that is downregulated by interferon gamma producing CD8+ T cells. *The Journal of Experimental Medicine*, 199, 1559-1566.
- Valentijn, A.J., Metcalfe, A.D., Kott, J., Streuli, C.H and Gilmore, A.P. (2003). Spatial and temporal changes in Bax subcellular localization during anoikis. *J Cell Biol*, 162, 599-612.
- Van Brocklyn and Williams, J.B. (2012). The control of the balance between ceramide and sphingosine 1 phosphate by sphingosine kinase: oxidative stress and the seesaw of cell survival and death. *Comp Biochem Physiol B Biochem Mol Biol*, 163, 26-36.
- Verma, S., Hoffmann, F.W., Kumar, M., Huang, Z., Roe, K., Nguyen-Wu, E., Hashimoto, A.S and Hoffmann, P.R. (2011). Selenoprotein K knockout mice exhibit deficient calcium flux in immune cells and impaired immune responses. *Journal of Immunology*, 186, 2127-2137.
- Viarengo, A., Burlando, B., Ceratto, N and Panfoli, I. (2000). Antioxidant role of metallothioneins: a comparative overview. *Cell Mol Biol*, 46, 407-417.
- Wei, Y., Fan, T and Yu, M. (2008). Inhibitor of apoptosis proteins and apoptosis. *Acta Biochim Biophys Sin*, 40, 278-288.
- World Health Organization (WHO). Clinical forms of the leishmaniasis. www.who.int/leishmaniasis/clinical_forms_leishmaniasis. Accessed on 2012.
- Yang, Z., Mosser, D.M and Zhang, X. (2007). Activation of the MAPK, ERK, following *Leishmania amazonensis* infection of macrophages. *The Journal of Immunology*, 178, 1077-1085.
- Zhang, N and Bevan, M.J. (2011). CD8+ T Cells: Foot soldiers of the immune system. *Immunity*, 35, 161-168.
- Zhang, S., Kim, C.C., Batra, S., McKerrow, J.H and Loke, P. (2010). Delineation of diverse macrophage activation programs in response to intracellular parasites and cytokines. *PLOS*, 4, e648.

Chapter 9 – Appendices



Appendix I – Effect of L8G infection spreading on host cell necrosis. After infection of differentiated THP-1 macrophages with L8G infected cells, the co-culture were analyzed for the percentage of necrosis (Annexin V+/7AAD+) through flow cytometry at 1, 12 and 24 hours after co-culture. Necrosis from the total population (A) were divided into infected only (B) and uninfected only (C) populations. Uninfected cells co-cultured with differentiated THP-1 macrophages were taken as a positive control. The data represents mean percentage (mean \pm SEM) from three independent experiments.



Appendix II – Representative western blot of six different proteins in uninfected and L8G infected cells at 72 hours prior to co-culture. Whole cell and/or cytosolic lysates were collected at 72 hours from uninfected and L8G infected cells. Equal amounts (30 μ g) were resolved by SDS-PAGE. The presence of p-AKT (Ser and Thr), total AKT, p-BAD (Ser), cytochrome C, total I κ -B and total p65 were analyzed by western blot.

**Appendix III – Representative example of protein expression from Set A
following tandem mass spectrometry**

Accession	Description	Coverage	# Proteins	# Unique Peptides	# Peptides	# PSMs	E0/129	E0/129 Count	E0/129 Variability [%]	Score	AAAs	MW [kDa]
BZ28F1	cDNA FL35362, highly similar to Actin, alpha skeletal muscle OS-Homo sapiens PE-2 Sv1+1 [BZ28F1_HUMAN]	31.53	59	1	16	1077	1,000	17	0.000	2707.879	342	38.554
B4W52	Heat shock protein 90 beta class B member OS-Homo sapiens HSP90B1 PE-1 Sv1+1 [B4W52_HUMAN]	51.8	54	23	41	117	1,000	329	7.117	2541.622	724	73.212
BT090	cDNA FL15523, highly similar to Actin, cytoplasmic 1 OS-Homo sapiens PE-2 Sv1+1 [B4W52_HUMAN]	55.19	54	1	14	1078	1,000	17	0.000	2708.053	347	38.608
P1142	Heat shock cognate 71 kDa protein OS-Homo sapiens HSC70 PE-1 Sv1+1 [HSP70_HUMAN]	55.19	54	1	14	1078	1,000	17	0.000	2708.053	347	38.608
B2R0V9	Adenyl cyclase-associated protein OS-Homo sapiens PAC1 PE-1 Sv1+1 [B2R0V9_HUMAN]	55.11	27	13	39	787	1,000	243	9.332	2098.080	466	70.854
B5573	Myosin I class IIb heavy chain OS-Homo sapiens MYO1B PE-1 Sv1+1 [B5573_HUMAN]	56.42	19	26	28	770	1,000	687	11.145	1978.859	476	51.583
ETVE58	Actin, cytoplasmic 1 (Fragment) OS-Homo sapiens GN-AC1B PE-1 Sv1+3 [ETVE58_HUMAN]	51.83	16	1	9	574	1,000	1	0.000	1740.229	184	19.964
K7E3A8	Actin, cytoplasmic 2 (Fragment) OS-Homo sapiens GN-AC1G PE-1 Sv1+1 [K7E3A8_HUMAN]	55.85	16	1	9	574	1,000	1	0.000	1740.229	184	19.964
QY490	Talin-1 OS-Homo sapiens GN-TLN1 PE-1 Sv1+3 [TLN1_HUMAN]	43.72	9	89	109	641	1,000	524	8.653	1738.700	2541	268.599
VHVZ7	Epididymus luminal protein 176 OS-Homo sapiens GN-ELL176 PE-1 Sv1+1 [VHVZ7_HUMAN]	54.71	33	20	12	490	1,000	111	0.000	1389.859	223	23.020
P11021	Alpha-2-macroglobulin OS-Homo sapiens GN-A2M PE-1 Sv1+1 [P11021_HUMAN]	52.31	26	22	27	417	1,000	69	8.249	2911.641	474	71.319
P11021	78 kDa glucose-regulated protein OS-Homo sapiens GN-HSPA8 PE-1 Sv1+1 [GRP78_HUMAN]	53.75	5	29	36	532	1,000	376	7.883	1354.465	564	72.288
P07323	Protein sapiens GN-PCNA PE-1 Sv1+1 [PCNA_HUMAN]	51.18	15	15	15	118	1,000	15	0.000	1280.091	168	58.011
I3L4N	Actin, cytoplasmic 2 (Fragment) OS-Homo sapiens GN-AC1G PE-1 Sv1+3 [I3L4N_HUMAN]	43.8	45	1	10	478	1,000	1	0.000	1254.509	242	28.917
Q5CAG5	Tumor rejection antigen (CD98) OS-Homo sapiens GN-TRAP PE-1 Sv1+1 [Q5CAG5_HUMAN]	43.52	12	39	40	420	1,000	335	7.375	1414.490	802	82.282
B5G527	Mitochondrial heat shock protein 70 OS-Homo sapiens GN-HSPA70 PE-2 Sv1+1 [B5G527_HUMAN]	55.18	2	24	24	398	1,000	7	0.000	1978.859	476	51.583
P10412	Histone H1.4 OS-Homo sapiens GN-H1H4 PE-1 Sv1+2 [H1A_HUMAN]	53.88	7	18	368	1,000	84	11.091	1067.153	219	21.852	
P14618	Pyruvate kinase PGM OS-Homo sapiens GN-PFKFB3 PE-2 Sv1+1 [PFKFB3_HUMAN]	55.18	43	2	30	398	1,000	52	4.498	1090.090	445	49.790
B4DR73	Pyruvate kinase OS-Homo sapiens PE-2 Sv1+1 [B4DR73_HUMAN]	52.64	42	1	29	391	1,144	3	6.155	1035.127	511	55.891
P07195	L-lactate dehydrogenase B chain OS-Homo sapiens GN-LDHB PE-1 Sv1+2 [LDHB_HUMAN]	56.32	8	14	16	376	1,000	315	4.624	1044.110	334	38.815
P00725	Frustrate-aspartate lyase OS-Homo sapiens GN-ALDOA1 PE-1 Sv1+2 [ALDOA_HUMAN]	50.19	11	19	21	362	1,000	286	10.413	1001.402	364	38.285
ENF989	Heat shock cognate 71 kDa protein (Fragment) OS-Homo sapiens GN-HSPA8 PE-1 Sv1+1 [ENF989_HUMAN]	56.97	2	1	19	358	0.756	2	43.216	983.109	334	34.797
BZ442	cDNA FL15197, highly similar to Stress-70 protein, mitochondrial OS-Homo sapiens PE-2 Sv1+1 [BZ442_HUMAN]	55.18	2	35	37	373	1,000	305	3.005	1967.627	465	72.586
B6104	Elongation factor 1-alpha OS-Homo sapiens GN-EEF1A1 PE-1 Sv1+1 [EF1A1_HUMAN]	39.83	37	4	21	454	0.997	82	13.269	955.071	462	50.104
P13796	Plastin 2 OS-Homo sapiens GN-LCP1 PE-1 Sv1+1 [PLS1_HUMAN]	48.48	12	24	30	401	1,000	267	4.876	947.082	327	72.288
P13693	Histone H1.2 OS-Homo sapiens GN-H1H2 PE-1 Sv1+1 [H2A_HUMAN]	51.17	4	5	15	301	0.962	56	5.813	942.017	213	21.352
P07437	Tubulin beta chain OS-Homo sapiens GN-TUBB PE-1 Sv1+2 [TUBB1_HUMAN]	36.81	32	1	16	353	1,000	3	10.773	928.133	444	48.639
P08371	Tubulin beta chain OS-Homo sapiens GN-TUBB2 PE-1 Sv1+1 [TUBB2_HUMAN]	35.73	31	2	16	352	1,000	62	4.498	909.090	445	49.790
P13639	Elongation factor 2 OS-Homo sapiens GN-EEF2 PE-1 Sv1+4 [EF2_HUMAN]	39.04	13	33	37	353	1,000	313	6.126	900.070	658	95.277
B3Q719	Protein disulfide-isomerase OS-Homo sapiens PE-2 Sv1+1 [B3Q719_HUMAN]	43.96	8	19	26	231	1,000	211	7.657	894.335	480	54.004
P00725	Brain acidic phosphatase OS-Homo sapiens GN-NAPE1 PE-1 Sv1+1 [NAPE1_HUMAN]	43.14	10	43	43	310	0.966	63	11.010	692.822	353	44.808
P18338	Nucleolin OS-Homo sapiens GN-NCL PE-1 Sv1+1 [NCL_HUMAN]	40.07	10	45	47	360	1,000	347	10.583	860.177	710	76.568
P18402	Histone H3 OS-Homo sapiens GN-H3T1 PE-1 Sv1+2 [H3T1_HUMAN]	42.53	8	16	16	604	0.823	63	12.592	122.592	221	23.336
Q7M79	Malate dehydrogenase (Fragment) OS-Homo sapiens GN-MDH2 PE-1 Sv1+1 [Q7M79_HUMAN]	51.87	6	15	15	314	1,000	308	8.888	848.312	316	33.208
P00558	Phosphoglycerate kinase 1 OS-Homo sapiens GN-PGK1 PE-1 Sv1+1 [PGK1_HUMAN]	63.48	6	22	26	296	1,000	218	1.538	808.234	417	44.598
B2003	Moens OS-Homo sapiens GN-MOES PE-1 Sv1+1 [MOES_HUMAN]	45.46	6	24	13	246	1,000	24	1.434	271.277	127	14.443
Q8LC01	mRNA encoding beta-tubulin (from clone D-beta-1) (Fragment) OS-Homo sapiens PE-2 Sv1+1 [Q8LC01_HUMAN]	31.81	10	1	15	322	1.143	2	19.890	750.051	447	48.848
Q8LC01	Protein sapiens GN-TUBB1 PE-1 Sv1+1 [TUBB1_HUMAN]	31.81	10	1	15	322	1.143	2	19.890	750.051	447	48.848
B2RDE1	cDNA FL18668, highly similar to Stress-70 protein (TPM3) mRNA OS-Homo sapiens PE-2 Sv1+1 [B2RDE1_HUMAN]	68.55	15	13	27	270	1,000	122	6.823	744.881	248	29.000
Q9J323	Deoxyribonuclease triphosphate hydrolytase SAMHD1 OS-Homo sapiens GN-SAMHD1 PE-1 Sv1+2 [SAMH1_HUMAN]	46.94	4	30	30	287	1,000	272	8.421	721.561	626	72.155
Q94405	Cyclophilin B OS-Homo sapiens GN-CYPB PE-1 Sv1+1 [CYPB_HUMAN]	54.86	8	14	14	304	1,000	14	0.000	625.232	243	26.812
P34932	Heat shock 70 kDa protein 4 OS-Homo sapiens GN-HSPA70 PE-1 Sv1+4 [HSPA70_HUMAN]	54.84	18	41	43	275	1,000	242	7.733	703.591	840	94.271
ATP15705	ATP synthase subunit 6 OS-Homo sapiens GN-ATP6B PE-1 Sv1+1 [ATP6B_HUMAN]	45.82	2	22	22	659	1,000	62	1.623	659.827	62	65.124
Q0610	Claflavin heavy chain 1 OS-Homo sapiens GN-CLTC PE-1 Sv1+1 [ATPA_HUMAN]	21.25	11	36	36	266	1,000	251	4.766	692.530	1675	191.453
P18401	Histone H1.5 OS-Homo sapiens GN-H1H5 PE-1 Sv1+3 [H15_HUMAN]	40.02	4	13	18	259	1.116	117	16.416	673.664	226	22.568
B18527	RNA-dependent RNA polymerase catalytic subunit OS-Homo sapiens GN-RPO21 PE-1 Sv1+3 [PRKDC_HUMAN]	42.02	4	8	22	242	1,000	26	1.114	1164.220	428	78.768
P08525	AnneXin A4 OS-Homo sapiens GN-ANXA4 PE-1 Sv1+4 [ANXA4_HUMAN]	53.92	9	20	22	242	1,000	217	3.098	646.589	319	35.860
B18525	Ubiquitin-like protein OS-Homo sapiens GN-UBQL1 PE-1 Sv1+1 [UBQL1_HUMAN]	54.3	5	2	10	262	1,000	1	0.000	635.417	466	53.619
P08670	Vimentin OS-Homo sapiens GN-VIM PE-1 Sv1+4 [VIME_HUMAN]	59.23	38	24	31	242	1,000	274	0.000	635.417	466	53.619
Q8CNE7	ATP synthase subunit beta (Fragment) OS-Homo sapiens GN-ATP6B PE-2 Sv1+1 [Q8CNE7_HUMAN]	42.02	4	13	14	220	1,000	169	0.000	635.417	466	53.619
Q8CNE7	Brain acidic phosphatase OS-Homo sapiens GN-NAPE1 PE-1 Sv1+1 [NAPE1_HUMAN]	42.02	4	13	14	220	1,000	169	0.000	635.417	466	53.619
B4D1	cDNA FL15273, highly similar to Elongation factor 1-alpha OS-Homo sapiens PE-2 Sv1+1 [B4D1_HUMAN]	39.24	13	1	16	324	1,000	1	0.000	635.417	466	53.619
P07371	Protein sapiens GN-PCNA PE-1 Sv1+1 [PCNA_HUMAN]	35.73	10	10	16	353	1,000	10	0.000	635.417	466	53.619
P62258	14-3-3 protein epsilon OS-Homo sapiens GN-YWHA4 PE-1 Sv1+1 [1433E_HUMAN]	59.61	11	13	16	224	1,000	140	6.819	603.899	255	29.155
P62258	Cofilin 1 OS-Homo sapiens GN-CFL1 PE-1 Sv1+1 [COF1_HUMAN]	69.28	11	16	22	299	1,000	168	11.415	602.258	198	18.491
B09C38	HAIEP (Fragment) OS-Homo sapiens GN-HAIEP PE-2 Sv1+2 [B09C38_HUMAN]	51.22	2	1	16	224	0.991	3	6.890	263.2	353	37.643
AT836	180 ribonucleic protein OS-Homo sapiens GN-RBP1 PE-2 Sv1+2 [AT836_HUMAN]	52.92	11	5	61	214	1.073	8	15.233	598.980	1540	166.649
B09C38	Tubulin beta chain OS-Homo sapiens GN-TUBB1 PE-1 Sv1+1 [TUBB1_HUMAN]	31.81	10	1	14	342	1,000	3	1.174	1734.174	167	17.443
FKP05	ABU1 (Fragment) OS-Homo sapiens PE-2 Sv1+1 [FKP05_HUMAN]	50.34	14	22	22	238	0.939	229	13.067	588.308	585	66.488
Q9P29	Ribosome-binding protein 1 OS-Homo sapiens GN-RBP1 PE-1 Sv1+4 [RBP1_HUMAN]	46.01	9	1	57	208	1,000	3	0.000	585.763	110	152.381
Q2203	Heterotrimeric G-protein beta-2 OS-Homo sapiens GN-HR23B PE-1 Sv1+2 [ROA2_HUMAN]	45.07	14	3	11	256	1,000	14	1.056	649.232	353	37.643
B4D1	L-lactate dehydrogenase OS-Homo sapiens PE-1 Sv1+1 [B4D1_HUMAN]	55.47	26	16	18	212	1,000	148	9.150	566.858	305	33.572
B4D1	Ubiquitin-ribosomal protein S27a OS-Homo sapiens GN-HS27A PE-1 Sv1+2 [RS27A_HUMAN]	45.13	3	14	9	208	1,000	14	0.000	566.858	305	33.572
Q91981	14-3-3 protein gamma OS-Homo sapiens GN-YWHA4 PE-1 Sv1+2 [1433G_HUMAN]	52.83	4	10	15	224	1,000	73	9.853	565.423	247	28.285
P68139	Elongation factor 1-alpha 2 OS-Homo sapiens GN-EEF1A2 PE-1 Sv1+1 [EF1A2_HUMAN]	21.61	5	3	12	272	1.044	119	12.341	565.988	403	50.438
Q8L12	Heat shock 70 kDa protein 4 (Fragment) (brain) OS-Homo sapiens GN-HSPA70_0312 PE-3 Sv1+1 [Q8L12_LEIUM]	55.09	1	27	17	615	1,000	718	7.815	610.521	704	75.021
P13667	Protein disulfide-isomerase A4 OS-Homo sapiens GN-PA4 PE-1 Sv1+2 [PDIA4_HUMAN]	45.43	7	31	32	276	1,000	229	7.338	561.181	445	72.288
P13667	14-3-3 protein zeta/delta OS-Homo sapiens GN-YWHA2 PE-1 Sv1+3 [1433Z_HUMAN]	51.53	7	13	18	228	1,000	127	10.388	625.232	243	27.728
Q95666	Neuroblast differentiation-associated protein ANNAK OS-Homo sapiens GN-ANNAK PE-1 Sv1+2 [AHNK_HUMAN]	34.87	17	34	37	236	1,000	212	7.455	549.544	5890	628.699
B8L224	14-3-3 protein beta/gamma OS-Homo sapiens GN-YWHA4 PE-1 Sv1+1 [B8L224_HUMAN]	51.22	5	8	14	230	1,000	45	12.311	530.479	246	28.095
B19155	Heterotrimeric G-protein beta-3 OS-Homo sapiens GN-HR23B PE-1 Sv1+3 [B19155_HUMAN]	45.07	19	6	7	272	1,000	204	7.272	514.24	418	41.811
P59290	T-complex protein 1 subunit beta OS-Homo sapiens GN-TC1B PE-1 Sv1+4 [TCPO_HUMAN]	52.74	5	28	28	228	1,000	216	8.261	530.462	548	59.583
B7384	Calnexin OS-Homo sapiens GN-CANX PE-1 Sv1+1 [CANX_HUMAN]	38.47	27	27	27	264	1,000	264	0.000	520.072	662	62.626
P62897	Ubiquitin-60S ribosomal protein OS-Homo sapiens GN-UBA52 PE-1 Sv1+2 [RL40_HUMAN]	42.92	40	1	7	194	0.932	1	0.000	514.394	128	14.794
P11446	Coronin-1A OS-Homo sapiens GN-COR1A1 PE-1 Sv1+4 [COR1A_HUMAN]	36.39	15	22	25	228	1,000	204	8.026	510.637	401	50.199

ESR609	Annein OS-homo sapiens GN-ANNA6 PE1 SV=1	[ESR609_HUMAN]	38.48	4	1	21	115	1,000	6	8,000	270,580	460	51,744
CS2K63	40S ribosomal subunit OS-homo sapiens GN-CS2K63 PE1 SV=3	[CS2K63_HUMAN]	32.58	7	9	64	26	1,000	62	2,000	26,800	268	25,487
B4E0X8	cDNA FL1021, highly similar to F4 upstream element-binding protein 1 OS-homo sapiens PE=2 SV=1	[B4E0X8_HUMAN]	38.63	12	7	24	106	1,000	30	4,143	267,679	629	66,191
BA3221	Nuclear autoantigenic sperm protein OS-homo sapiens GN-NAASP PE1 SV=2	[NAASP_HUMAN]	39.59	15	29	26	106	1,000	94	7,162	263,823	789	85,186
P53969	Activated DNA polymerase II essential coactivator P53 OS-homo sapiens GN-P53969 PE1 SV=1	[P53969_HUMAN]	39.12	10	6	10	112	1,000	9	12,026	267,117	267	17,439
PE2626	GTP-binding nuclear protein Rat OS-homo sapiens GN-RANR1 PE1 SV=1	[RAN_HUMAN]	27.78	8	5	6	87	1,000	85	12,884	262,554	216	24,408
P13423	NADPH-dependent cytosolic mitochondrial OS-homo sapiens GN-H13423 PE1 SV=2	[NADPH_HUMAN]	24	24	6	6	91	1,000	67	14,737	261,833	1,086	113,423
PE2623	60S ribosomal protein S14 OS-homo sapiens GN-RP514 PE1 SV=3	[RS14_HUMAN]	37.75	4	6	6	77	1,000	75	10,000	261,525	151	16,263
P22446	Splicing factor, protein and glutamine-rich OS-homo sapiens GN-SF20 PE1 SV=2	[SF20_HUMAN]	27.02	6	20	21	113	1,000	105	12,702	261,232	707	78,102
CB3035	Ribonucleic protein inhibitor leucine OS-homo sapiens GN-RIC2 PE1 SV=2	[RIC2_HUMAN]	38.2	6	10	10	107	1,000	81	10,079	261,127	312	31,426
AA048W7T11	Polyadenylation-binding protein 1 OS-homo sapiens GN-PABPC1 PE1 SV=1	[AA048W7T11_HUMAN]	37.38	25	15	20	119	1,000	76	10,000	259,588	520	58,499
Q75944	Cytosolic nuclear protein 1 homolog OS-homo sapiens GN-CPN1 PE1 SV=1	[PACT1_HUMAN]	18.11	9	9	9	130	1,000	63	10,000	259,618	476	47,618
P52786	Proteasome subunit alpha type 1 OS-homo sapiens GN-PSMA1 PE1 SV=1	[PSA1_HUMAN]	42.97	6	13	13	138	1,000	79	3,354	257,931	283	29,537
Q2841	Protein ATP-dependent RNA helicase DDX17 OS-homo sapiens GN-DDX17 PE1 SV=2	[DDX17_HUMAN]	34.29	6	21	21	112	1,000	29	12,888	257,252	729	80,222
Q2765	Alpha-2B-glycoprotein OS-homo sapiens GN-ALB2 PE1 SV=1	[ALB2_HUMAN]	19.9	6	6	6	124	1,000	6	10,000	256,517	307	30,716
AR676	cDNA FL7824, highly similar to OS-homo sapiens eukaryotic translation initiation factor 4A, isoform 1 (EIF4A1), mRNA OS-homo sapiens PE=2 SV=1	[AR676_HUMAN]	41.38	31	7	18	114	1,000	40	10,420	256,085	406	46,093
Q62434	60S ribosomal protein L27a OS-homo sapiens GN-RPL27A PE1 SV=1	[RPL27A_HUMAN]	34.02	5	19	19	119	1,000	75	13,502	249,966	652	67,759
P17987	T-complex protein 1 subunit alpha OS-homo sapiens GN-TCP1 PE1 SV=1	[TCP1_HUMAN]	29.68	12	16	16	104	1,000	99	2,600	252,660	556	60,306
PE25930	Tyrosine-protein phosphatase non-receptor type 6 OS-homo sapiens GN-PTNP6 PE1 SV=1	[PTNP6_HUMAN]	31.13	13	23	23	98	1,000	83	5,127	251,880	595	67,519
B3D90	Transaldolase OS-homo sapiens GN-TALDO1 PE1 SV=2	[TALDO_HUMAN]	40.59	11	15	15	105	1,000	78	10,000	250,771	337	37,516
B3K54	Transaldolase OS-homo sapiens PE=2 SV=1	[B3K54_HUMAN]	31.13	13	23	23	98	1,000	83	5,127	249,928	540	59,944
P17937	Transaldolase OS-homo sapiens PE=1 SV=1	[B4D90_HUMAN]	40.59	11	15	15	105	1,000	78	10,000	249,577	337	37,516
ETU044	Eukaryotic translation initiation factor 4 gamma 1 OS-homo sapiens GN-EIF4G1 PE1 SV=1	[ETU044_HUMAN]	38.08	11	18	34	111	1,000	52	11,291	249,217	1,650	171,535
BA3025	Malee dehydrogenase, cytoplasmic OS-homo sapiens GN-HMD1 PE1 SV=4	[HMD1_HUMAN]	18.53	6	14	14	98	1,000	95	12,259	248,346	334	36,403
Q75719	Tropomyosin alpha chain (Fragment) OS-homo sapiens GN-TPM1 PE1 SV=1	[TROP1_HUMAN]	40.19	6	6	6	102	1,000	6	10,000	247,754	79	79,754
Q06874	Poly (ADP-ribose) polymerase 1 OS-homo sapiens GN-PARP1 PE1 SV=4	[PARP1_HUMAN]	32.45	8	33	33	99	1,000	89	17,683	247,754	1,014	113,012
Q68654	Protein LYR3 OS-homo sapiens GN-HYH7H PE1 SV=2	[LYR3_HUMAN]	34.02	5	19	19	119	1,000	75	13,502	246,966	652	67,759
P18124	60S ribosomal protein L7 OS-homo sapiens GN-RPL7 PE1 SV=1	[R7_HUMAN]	39.52	8	7	7	116	1,000	40	8,761	245,711	248	29,207
PA411	Elongation factor 1a, mitochondrial OS-homo sapiens GN-ELF1A PE1 SV=2	[ELF1A_HUMAN]	47.57	2	21	21	103	1,000	84	7,323	245,109	452	49,810
P12235	ADP-ATF1, isoenzyme 3 OS-homo sapiens GN-AC2AF1 PE1 SV=4	[AD13_HUMAN]	21.95	9	15	15	100	1,000	7	1,817	244,841	298	32,845
BA3MFS	Glutamate dehydrogenase OS-homo sapiens PE=2 SV=1	[BA3MFS_HUMAN]	30.15	12	7	18	103	1,000	51	1,436	244,899	509	56,568
Q43707	Alpha-actinin-4 OS-homo sapiens GN-ACTN4 PE1 SV=2	[ACTN4_HUMAN]	32.27	17	27	27	103	1,000	85	12,298	244,899	509	56,568
PA5477	Tyrosine-RNA ligase, cytoplasmic OS-homo sapiens GN-YARS1 PE1 SV=4	[YARS1_HUMAN]	39.39	2	24	24	104	1,000	97	12,288	243,035	528	59,106
PE27070	Tyrosine-RNA ligase 5A, isoform OS-homo sapiens GN-HYAS5A PE1 SV=2	[HYAS5A_HUMAN]	50.57	3	9	9	104	1,000	99	12,940	240,317	203	20,979
Q6AMU8	Islet 1 alpha-2-macroglobin C2 (2010) (I103) OS-homo sapiens GN-IMC2 PE1 SV=1	[I103_HUMAN]	40.39	5	14	14	103	1,000	62	14,625	239,712	317	31,712
PE2873	60S ribosomal protein L13 OS-homo sapiens GN-RPL13 PE1 SV=4	[RL13_HUMAN]	40.76	8	12	12	105	1,000	109	13,873	237,646	211	24,247
Q6A083	Annein OS-homo sapiens GN-ANNA1 PE1 SV=2	[ANNA1_HUMAN]	40.75	14	14	14	90	1,000	63	5,020	236,836	246	26,860
P19147	14-3-3 protein sigma OS-homo sapiens GN-SFN PE1 SV=1	[143SS3_HUMAN]	16.53	1	5	5	103	1,000	1	1	236,286	248	27,277
BA3E38	Glucose-6-phosphate isomerase OS-homo sapiens PE=2 SV=1	[BA3E38_HUMAN]	28.11	15	16	17	101	1,000	98	5,851	233,698	530	61,148
Q6241	Radiol OS-homo sapiens GN-RAD1 PE1 SV=1	[RAD1_HUMAN]	21.96	13	14	15	108	1,000	80	21,028	233,661	1,023	108,661
PE26640	Vinculin-RNA ligase OS-homo sapiens GN-VARS1 PE1 SV=4	[SVIC_HUMAN]	23.11	19	25	28	85	1,000	8,000	2,089	233,246	1,204	140,387
Q6A0Y07	Ribonucleic protein (Fragment) OS-homo sapiens GN-RNP1 PE1 SV=1	[RNP1_HUMAN]	41.91	1	7	7	109	1,000	6	10,000	232,811	248	24,811
Q53709	Pulvinar uncharacterized protein XRC05 (Fragment) OS-homo sapiens GN-XRC05 PE1 SV=1	[Q53709_HUMAN]	30.99	2	18	18	104	1,000	76	15,207	229,813	688	64,203
P18015	Sarcoplasmic/endoplasmic reticulum calcium ATPase 2 OS-homo sapiens GN-ATP2A2 PE1 SV=1	[AT2A2_HUMAN]	26.1	9	22	29	85	1,000	71	9,040	228,199	1,642	114,883
Q62402	NAP1C4 OS-homo sapiens GN-NAP1C4 PE1 SV=1	[NAP1C4_HUMAN]	30.76	7	6	6	23	1,000	23	23,773	227,927	248	24,811
BA3Y08	Heterogeneous nuclear ribonucleoprotein C1/C2 OS-homo sapiens GN-HNRNPCC1 PE1 SV=1	[BA3Y08_HUMAN]	44.1	55	14	14	77	1,000	70	7,617	227,278	288	31,952
Q62750	60S ribosomal protein G16 OS-homo sapiens GN-RPL16 PE1 SV=1	[RPL16_HUMAN]	45.21	11	11	11	111	1,000	61	10,259	226,199	1,686	17,686
PE15149	Ras-related protein Rab-7a OS-homo sapiens GN-RAB7A PE1 SV=1	[RAB7A_HUMAN]	58.45	10	4	12	83	1,000	21	6,566	225,612	207	23,475
PE1706	Voltage-dependent anion-selective channel protein 1 OS-homo sapiens GN-VDAC1 PE1 SV=2	[VDAC1_HUMAN]	44.88	4	10	10	78	1,000	72	6,710	223,612	283	30,754
Q62403	LUBIN OS-homo sapiens GN-LUBIN PE1 SV=2	[LUBIN_HUMAN]	50.03	3	4	4	103	1,000	64	4,818	223,333	189	19,878
Q9P497	Protein D.J.1 OS-homo sapiens GN-P497 PE1 SV=2	[P497_HUMAN]	45.03	4	12	13	101	1,000	84	4,923	222,942	283	30,754
AA024RDF4	Heterogeneous nuclear ribonucleoprotein D (AU-rich element RNA binding protein 1, 370Da), isoform CRA_A OS-homo sapiens GN-HNRNPDE4 PE1 SV=1	[AA024RDF4_HUMAN]	33.35	8	3	12	98	1,000	11	11,819	222,715	306	32,814
Q7A227	EB ubiquitin protein ligase HUB1 OS-homo sapiens GN-HUB1 PE1 SV=1	[HUB1_HUMAN]	8.3	15	37	37	82	1,000	72	3,639	221,995	4374	481,589
Q7A2344	Baiter nucleic acid binding protein 2 OS-homo sapiens GN-NAB2 PE1 SV=3	[NAB2_HUMAN]	46.37	14	13	13	103	1,000	74	10,000	221,995	317	31,712
BA3D02	cDNA FL159379, highly similar to Hematopoietic lineage cell-specific protein OS-homo sapiens PE=2 SV=1	[BA3D02_HUMAN]	41.2	10	2	7	83	1,000	13	15,396	220,948	449	42,586
CNA1_FL3932	cDNA FL3932, highly similar to human tissue inhibitor of metalloproteinases 2 OS-homo sapiens PE=2 SV=1	[CNA1_FL3932_HUMAN]	48.73	11	18	18	109	1,000	28	4,442	220,948	449	42,586
AR6079	cDNA FL75422, highly similar to Homo sapiens capping protein (actin filament) muscle Z line, alpha 1, mRNA OS-homo sapiens PE=1 SV=1	[AR6079_HUMAN]	31.82	2	7	8	85	1,000	75	2,488	220,433	286	32,888
PE26838	Cytosol aminopeptidase OS-homo sapiens GN-LAP3 PE1 SV=3	[APL3_HUMAN]	46.86	5	21	21	82	1,000	79	9,935	219,926	519	55,131
CS74271	CS7 ALP1 OS-homo sapiens PE=2 SV=1	[CS74271_HUMAN]	40.77	2	2	2	107	1,000	6	10,000	219,926	268	26,816
Q02099	Cytosolic intracellular channel protein OS-homo sapiens GN-CLIC1 PE1 SV=4	[CLIC1_HUMAN]	58.77	2	10	10	83	1,000	75	4,934	219,324	241	26,906
Q62664	60S ribosomal protein G16 OS-homo sapiens GN-RPL16 PE1 SV=1	[RPL16_HUMAN]	45.21	16	16	16	104	1,000	61	10,000	219,324	241	26,906
P30050	60S ribosomal protein L12 OS-homo sapiens GN-RPL12 PE1 SV=1	[RL12_HUMAN]	67.27	5	10	10	85	1,000	79	7,323	217,259	165	17,205
Q6A0ZQ24	Cis-divisoin control protein 42 homolog OS-homo sapiens GN-CCDC42 PE1 SV=2	[CCDC42_HUMAN]	26.87	18	4	5	75	1,000	81	6,084	215,533	191	21,486
BA3Z08	Human CR4, isoform 2 OS-homo sapiens GN-CLC4 PE1 SV=1	[AA024RDF4_HUMAN]	46.93	6	6	6	103	1,000	62	15,465	214,712	1,068	113,423
BA3D028	cDNA FL15705, highly similar to Acetate hydrolyase, mitochondrial (EC 4.2.1.3) OS-homo sapiens PE=2 SV=1	[BA3D028_HUMAN]	27.46	9	9	9	117	1,000	37	6,084	215,117	761	83,361
FBW12	Adenomatous polyposis coli OS-homo sapiens GN-APC PE1 SV=1	[FBW12_HUMAN]	49.93	60	9	9	80	1,000	61	9,201	214,712	1,068	113,423
MOY07	Tubulin beta-4A chain (Fragment) OS-homo sapiens GN-TUBB4A PE1 SV=1	[MOY07_HUMAN]	32.3	6	1	4	68	1,000	1	1	210,468	161	17,823
PA4782	EL SLMCO protein ligase RABP2 OS-homo sapiens GN-RABP2 PE1 SV=2	[RBP2_HUMAN]	11.82	19	24	24	96	1,000	40	6,246	211,751	3224	357,974
Q62404	60S ribosomal protein S2 OS-homo sapiens GN-RPS2 PE1 SV=2	[RPS2_HUMAN]	40.2	10	21	21	90	1,000	109	13,089	211,424	408	46,838
BSB085	Autotaxin LA (Fragment) OS-homo sapiens GN-STS2 PE1 SV=1	[BSB085_HUMAN]	40.2	10	21	21	90	1,000	109	13,089	211,424	408	46,838
Q6A0Y11	cDNA FL75521, highly similar to human protein (P254), mRNA (Fragment) OS-homo sapiens PE=2 SV=1	[Q6A0Y11_HUMAN]	43.72	13	15	15	100	1,000	82	10,000	210,887	367	36,716
Q1011	Delta(3,5)-Delta(4,5)-diolyl-CoA isomerase, mitochondrial OS-homo sapiens GN-ECH1 PE1 SV=2	[ECH1_HUMAN]	42.07	7	11	11	103	1,000	80	8,107	210,328	328	35,793
Q20212	Nucleoside diphosphate kinase B OS-homo sapiens GN-NME2 PE1 SV=1	[Q20212_HUMAN]	38.91	7	11	11	104	1,000	82	11,186	209,042	292	32,621
PE26262	Nucleoside diphosphate kinase 1A OS-homo sapiens GN-NME1 PE1 SV=1	[NME1_HUMAN]											

B4DXL9	cDNA FL35877, highly similar to Dextrin-like protein OS-Homo sapiens Pez-2 Sv1-1 [B4DXL9_HUMAN]	31.93	3	1	11	55	1000	5	12.003	151.203	379	42.700
B4DVN3	RBM14 OS-Homo sapiens Pez-4 Sv1-1 [B4DVN3_HUMAN]	14.38	1	14	62	1000	274	1	14.036	364	14.440	364
A0A087WU2	Heterogeneous nuclear ribonucleoprotein D-like OS-Homo sapiens GN-HNRPD1 PE-4 Sv1-1 [A0A087WU2_HUMAN]	19.28	5	7	8	67	1009	24	9.111	150.683	383	40.016
P1105	Nucleon regulatory light chain 12A OS-Homo sapiens GN-NM12A PE-1 Sv2-2 [JML2A_HUMAN]	33.92	6	2	7	81	1000	25	0.000	150.225	171	19.781
A0A087WZ7	Myristoylated substrate OS-Homo sapiens GN-MA087WZ7 PE-4 Sv1-1 [A0A087WZ7_HUMAN]	15.46	6	4	10	45	1000	39	15.067	150.330	131	17.177
Q6P209	Pie-nRNA processing splicing factor 8 OS-Homo sapiens GN-PRP8 PE-1 Sv2-2 [PRP8_HUMAN]	12.29	8	31	31	63	1000	62	9.729	149.897	2335	27.427
Q52073	Translational OS-Homo sapiens GN-TPO1 PE-1 Sv2-2 [TPO1_HUMAN]	13.59	7	11	11	60	1000	40	6.000	149.809	160	10.228
FW115	Myosin light chain 6B OS-Homo sapiens GN-MYL6B PE-1 Sv1-1 [FW115_HUMAN]	20	3	1	3	50	1000	1	1.492	149.725	115	19.024
H38PE1	Microtubule-actin cross-linking factor 1, isoform 1 OS-Homo sapiens GN-HMCF1 PE-1 Sv1-1 [H38PE1_HUMAN]	18.94	2	2	39	58	985	36	33.932	149.008	7555	85.346
Q2635	Thyrosine phosphatase 3.4 OS-Homo sapiens GN-PTP3.4 PE-1 Sv2-2 [PTP3.4_HUMAN]	22.27	9	23	23	57	1000	53	7.461	148.719	1189	13.929
Q9Y281	Coflin-2 OS-Homo sapiens GN-CFL2 PE-1 Sv1-1 [CFL2_HUMAN]	19.28	3	1	4	51	1000	1	1.472	148.766	186	16.275
Q9Y282	Thymidine phosphorylase CRA 4 OS-Homo sapiens GN-TMPO PE-4 Sv1-1 [Q9Y282_HUMAN]	18.76	2	2	4	49	1000	2	1.760	148.714	117	14.442
Q13409	Cytoplasmic dyxins 1 intermediate chain 2 OS-Homo sapiens GN-DYX12C1 PE-1 Sv3-3 [DC12_HUMAN]	20.22	18	13	13	49	1000	48	0.000	147.231	638	71.412
Q13408	Prothelin (Fragment) OS-Homo sapiens GN-PTT1 PE-1 Sv2-2 [Q13408_HUMAN]	34.96	11	9	10	100	1000	48	5.471	146.948	246	20.875
Q13404	CNA FL3784, highly similar to CNA FL3784 OS-Homo sapiens Pez-2 Sv1-1 [B0AZ04_HUMAN]	12.02	3	2	2	6	1000	2	0.000	146.513	130	14.442
Q15459	Salivary factor 3A subunit 1 OS-Homo sapiens GN-SF3A1 PE-1 Sv1-1 [SF3A1_HUMAN]	26.12	4	22	22	64	1000	62	7.369	146.010	793	88.831
Q9Y943	Microtubule cross-linking factor 1, isoform 1 OS-Homo sapiens GN-HMCF1 PE-1 Sv1-1 [Q9Y943_HUMAN]	18.76	2	2	39	58	985	36	33.932	145.909	7588	87.377
HY03P2	Eukaryotic translation initiation factor 4 gamma 2 OS-Homo sapiens GN-EIF4G2 PE-1 Sv1-1 [HY03P2_HUMAN]	18.76	17	17	17	50	987	50	8.000	144.748	895	98.056
EP9P01	Elongation factor 1-delta (Fragment) OS-Homo sapiens GN-E1FD1 PE-1 Sv1-1 [EP9P01_HUMAN]	20.89	27	8	8	85	1000	46	5.551	144.647	201	28.804
EP9P02	Arginine-tryptophan transferase OS-Homo sapiens GN-TRP1 PE-1 Sv2-2 [TRP1_HUMAN]	30.36	5	6	6	85	1000	46	7.849	144.647	201	28.804
PE2917	60S ribosomal protein L8 OS-Homo sapiens GN-RL8 PE-1 Sv2-2 [RL8_HUMAN]	30.35	7	8	9	85	1000	54	6.845	144.642	257	29.007
PE2918	60S ribosomal protein L9 OS-Homo sapiens GN-RL9 PE-1 Sv2-2 [RL9_HUMAN]	30.47	10	17	17	58	1000	50	14.123	144.163	301	33.948
PE8731	60S ribosomal protein L24 OS-Homo sapiens GN-RL24 PE-1 Sv1-1 [RL24_HUMAN]	47.77	3	10	10	82	942	59	14.124	144.123	157	17.768
Q60763	General vesicular transporter p115 OS-Homo sapiens GN-VSP1 PE-1 Sv2-2 [VSP1_HUMAN]	20.69	18	18	18	50	1000	49	8.038	143.517	962	107.828
Q13167	MHC class I alpha OS-Homo sapiens GN-FC1 PE-1 Sv2-2 [FC1_HUMAN]	46.39	13	11	12	69	1000	66	6.522	142.883	194	22.578
Q97955	Serine/arginine-rich splicing factor 4 OS-Homo sapiens GN-SRSF4 PE-1 Sv2-2 [SRSF4_HUMAN]	55.24	8	14	14	67	1000	66	11.628	143.003	249	27.728
PE8714	60S ribosomal protein L12 OS-Homo sapiens GN-RL12 PE-1 Sv1-1 [RL12_HUMAN]	46.39	13	11	12	69	1000	66	6.522	142.883	194	22.578
B58174	ATP-dependent RNA helicase DDX3X OS-Homo sapiens GN-DDX3X PE-2 Sv1-1 [B58174_HUMAN]	29.61	12	6	19	56	927	16	17.773	142.596	682	73.128
Q10898	2,4-dienyl-CoA reductase, mitochondrial OS-Homo sapiens GN-DCR1 PE-1 Sv1-1 [DCR1_HUMAN]	36.72	10	11	11	54	1000	52	9.774	142.183	335	36.045
B24343	Leu proline-rich protein OS-Homo sapiens GN-LP1 PE-1 Sv2-2 [LP1_HUMAN]	23.08	20	19	19	57	1000	51	7.260	142.072	374	45.092
Q10897	Pu.2-like nuclear protein (Fragment) OS-Homo sapiens Pez-2 Sv1-1 [Q10897_HUMAN]	39.57	14	3	3	57	1000	14	11.890	141.880	374	42.726
P13073	Cytosolic c-myc coactivator 1, mitochondrial OS-Homo sapiens GN-COAC1 PE-1 Sv1-1 [C0K41_HUMAN]	39.64	6	8	9	70	1000	6	6.890	141.758	169	18.044
P24534	Elongation factor 1-beta OS-Homo sapiens GN-E1FB2 PE-1 Sv3-3 [E1FB_HUMAN]	41.78	4	3	9	59	1006	14	4.215	141.656	225	24.748
EP9A4	Palmitoyl transferase 1 (Fragment) OS-Homo sapiens GN-PTP1 PE-1 Sv1-1 [EP9A4_HUMAN]	22.44	6	6	6	49	1000	43	7.923	141.388	205	23.008
TEC14	Acceptor complex in the nucleus OS-Homo sapiens GN-ACN1 PE-1 Sv2-2 [TEC14_HUMAN]	41.91	2	2	2	6	1000	47	9.858	141.372	143	15.727
Q04780	Lactoylglutathione lyase OS-Homo sapiens GN-LGL1 PE-1 Sv1-1 [LGL1_HUMAN]	19.13	2	10	10	68	967	67	6.984	140.805	184	20.764
A0A087WZ0	Eukaryotic translation initiation factor 4 gamma 2 OS-Homo sapiens GN-EIF4G2 PE-1 Sv1-1 [A0A087WZ0_HUMAN]	22.06	5	6	6	6	1000	5	15.337	140.589	149	16.445
Q9WMM7	Alixan-2 subunit OS-Homo sapiens GN-ATXN2 PE-1 Sv2-2 [ATXN2_HUMAN]	37.77	17	19	19	61	1000	58	11.864	140.673	1075	113.304
P05592	Intraflagellar body OS-Homo sapiens GN-IFIB1 PE-1 Sv2-2 [IFIB_HUMAN]	19.16	11	16	16	46	1000	46	10.730	140.459	798	87.377
Q14157	Similar to ribosomal protein 2-8 OS-Homo sapiens GN-RL2 PE-1 Sv2-2 [RL2_HUMAN]	17.76	12	15	15	49	1000	49	11.337	140.352	119	13.929
BRDX5	CNA FL36812, highly similar to CNA FL36812 OS-Homo sapiens Pez-2 Sv1-1 [BRDX5_HUMAN]	28.27	16	20	20	59	1000	55	10.773	140.067	711	82.061
Q26966	Colig protein OS-Homo sapiens GN-FC1 PE-1 Sv2-2 [FC1_HUMAN]	17.73	23	23	23	63	1000	63	1.000	139.723	119	13.929
Q98526	Endoplasmic reticulum resident protein 44 OS-Homo sapiens GN-ERP44 PE-1 Sv1-1 [ERP44_HUMAN]	26.6	1	10	11	64	1000	59	4.984	139.286	406	46.941
BZ2204	MHC class I antigen (Fragment) OS-Homo sapiens GN-HLA-A PE-1 Sv1-1 [BZ2204_HUMAN]	37	275	0	8	48	1000	49	0.000	139.000	273	31.553
P14598	Neuronal-specific factor 1 OS-Homo sapiens GN-NSF1 PE-1 Sv1-1 [NSF1_HUMAN]	36.871	1	12	12	53	1000	49	1.000	138.560	369	40.829
P26447	Protein S100 A4 OS-Homo sapiens GN-S100A4 PE-1 Sv1-1 [S100A4_HUMAN]	19.74	1	4	4	58	1000	58	15.221	138.515	101	11.721
AD3025	Adaptin complex subunit 3 OS-Homo sapiens GN-AP3 PE-1 Sv1-1 [AD3025_HUMAN]	21.84	2	7	20	64	1000	64	15.275	138.456	104	11.721
BK3V93	cDNA FL42590.8s, clone BRAC300978, highly similar to Sodium/potassium-transporting ATPase alpha-chain (EC 3.6.3.9) OS-Homo sapiens Pez-2 Sv1-1 [BK3V93_HUMAN]	23.91	8	1	11	47	1025	58	1.000	138.278	920	101.237
B6E00	Topsome-associated factor 1 OS-Homo sapiens GN-TAF1 PE-1 Sv1-1 [B6E00_HUMAN]	26.41	25	20	21	58	1000	53	12.292	138.250	765	90.643
Q9N82	Similar to ribosomal protein L23 OS-Homo sapiens GN-RL23 PE-1 Sv1-1 [Q9N82_HUMAN]	27.22	3	1	6	52	1000	51	11.877	138.174	319	8.752
Q9Y959	Protein 2-5 OS-Homo sapiens GN-FC1 PE-1 Sv2-2 [FC1_HUMAN]	30.35	6	5	6	49	1000	48	6.288	138.156	105	10.177
Q92474	Rho guanine nucleotide exchange factor 2 OS-Homo sapiens GN-ARHGEF2 PE-1 Sv4-4 [ARHG2_HUMAN]	26.55	11	26	26	55	1000	55	10.241	138.787	898	111.473
A0A024R4E5	High density lipoprotein binding protein (Vglinin) subunit CRA OS-Homo sapiens GN-HLBP1 PE-1 Sv1-1 [A0A024R4E5_HUMAN]	19.77	30	30	30	62	1000	60	7.269	138.209	1208	141.352
B2V02	Eukaryotic translation initiation factor 4 gamma 2 OS-Homo sapiens GN-EIF4G2 PE-1 Sv1-1 [B2V02_HUMAN]	21.05	21	18	18	52	1000	51	12.320	138.209	1208	141.352
Q9Y959	RNA-binding protein 8A OS-Homo sapiens GN-RBM8A PE-1 Sv1-1 [RBM8A_HUMAN]	31.61	1	6	6	47	1000	47	0.000	136.461	174	19.877
B2V02	Bifunctional protein PUR1 OS-Homo sapiens GN-TP1 PE-1 Sv1-1 [B2V02_HUMAN]	31.61	1	6	6	47	1000	47	0.000	136.461	174	19.877
PZ718	Microtubule-associated protein 4 OS-Homo sapiens GN-MAP4 PE-1 Sv3-3 [MAP4_HUMAN]	25.35	16	29	29	58	994	57	13.211	134.586	1152	120.930
Q9Y913	ATP-dependent protein L35 OS-Homo sapiens GN-RL35 PE-1 Sv1-1 [RL35_HUMAN]	34.29	5	4	4	56	1000	52	0.000	134.325	105	12.246
Q9Y913	MHCs complex subunit MHC19 OS-Homo sapiens GN-RL19 PE-1 Sv1-1 [RL19_HUMAN]	17.58	14	14	14	50	1000	49	11.864	134.277	227	27.177
Q01838	60S ribosomal E-phosphotransferase, platelet type OS-Homo sapiens GN-PPK1 PE-1 Sv2-2 [PPK1_HUMAN]	22.27	11	14	14	50	1000	49	6.210	134.137	784	85.542
Q62633	Cebulin OS-Homo sapiens GN-CBP1 PE-1 Sv1-1 [CBP1_HUMAN]	30.33	40	40	40	62	1000	62	5.746	133.767	177	19.877
EA5K7	Chaperon HSP90, mitochondrial OS-Leishmania mexicana (strain MHOM/GT/2001/1103) GN-LMXM3_26_2020 PE=3 Sv1-1 [EA5K7_LEIMU]	29.51	2	4	14	50	2556	10	236.330	133.590	566	60.288
Q72426	Myosin-14 OS-Homo sapiens GN-MYH14 PE-1 Sv2-2 [MYH14_HUMAN]	31.91	13	1	10	52	908	51	0.000	133.516	1995	227.732
B4M407	Histone H4, highly similar to Histone H4 OS-Homo sapiens Pez-2 Sv1-1 [B4M407_HUMAN]	17.66	2	10	10	52	1000	18	0.000	133.400	334	33.021
GBL1_C1	Structural maintenance of chromosomes protein 1A OS-Homo sapiens GN-SMC1A PE-1 Sv2-2 [GBL1_C1_HUMAN]	19.08	11	25	25	44	1000	42	7.550	133.111	1211	140.772
P15101	Histone H2B OS-Homo sapiens GN-H2B PE-1 Sv2-2 [H2B_HUMAN]	12.38	6	2	5	49	1000	2	11.371	133.088	117	13.929
Q8T222	Protein-methionine sulfotransferase MICAL1 OS-Homo sapiens GN-MICAL1 PE-1 Sv2-2 [MICAL1_HUMAN]	12.37	5	17	17	51	993	47	13.628	132.742	1067	117.801
EPH2Q	Protein disulphide isomerase OS-Homo sapiens GN-DIP1 PE-1 Sv1-1 [EPH2Q_HUMAN]	17.54	16	24	25	52	1000	51	11.874	132.608	1200	139.914
Q13408	PRO175 OS-Homo sapiens Pez-2 Sv1-1 [Q13408_HUMAN]	17.54	16	24	25	52	1000	51	11.874	132.608	1200	139.914
PA2186	Lamina-associated polypeptide 2, isoform alpha OS-Homo sapiens GN-TMPO PE-1 Sv2-2 [LAP2A_HUMAN]	17	1	4	9	45	714	7	8.772	132.365	894	75.446
A0A087WZ2	Splicing factor 2 OS-Homo sapiens GN-SF2 PE-1 Sv1-1 [A0A087WZ2_HUMAN]	25.83	9	23	23	52	1000	49	14.688	132.022	1488	152.015
Q13428	Triadecan protein OS-Homo sapiens GN-TCDF1 PE-1 Sv1-1 [Q13428_HUMAN]	19.29	10	30	30	55	1000	54	13.651	132.022	1488	152.015
B7Z527	CNA FL35862, highly similar to Vesicle-fusing ATPase (EC 3.6.4.4) OS-Homo sapiens Pez-2 Sv1-1 [B7Z527_HUMAN]	28.89	14	20	21	51	988	45	12.087	131.984	739	82.006
B7Z527	Putative RNA-binding protein 7 OS-Homo sapiens GN-RBP7 PE-1 Sv2-2 [B7Z527_HUMAN]	19.29	10	20	21	51	1000	49	7.468	131.984	739	82.006
PE2805	Histone H4 OS-Homo sapiens GN-H4 PE-1 Sv2-2 [H4_HUMAN]	30.49	3	5	5	57	1000	51	13.227	131.503	110	11.360
PE2807	60S ribosomal protein L34 OS-Homo sapiens GN-RL34 PE-1 Sv1-1 [RL34_HUMAN]	6.88	2	6	6	49	1000	48	6.288			

A02198	HCG19890 OS-Homo sapiens GNC0329793 PE-1 SV1 - [ADM1M_HUMAN]	32	1	1	7	46	0.855	1	109.113	225	24.875
Q58123	Agouti-related protein containing a CARD OS-Homo sapiens GNC057490 PE-1 SV2 - [ASC_HUMAN]	33.85	6	1	7	42	1.000	1	0.991	109.073	225
Q58128	MHC class I antigen (Fragment) OS-Homo sapiens GNC1448 PE-1 SV1 - [Q58128_HUMAN]	21.66	309	0	6	39	1.000	1	109.070	337	38.095
Q14847	LIM and SH3 domain protein 1 OS-Homo sapiens GNC1541 PE-1 SV2 - [LASP1_HUMAN]	46.74	11	14	14	42	1.000	51	8.129	109.016	201
A03611	CNA FL1772, highly similar to Homo sapiens cell cycle-associated and repressible 1 (CCAND1), mRNA OS-Homo sapiens PE-2 SV1 - [A03611_HUMAN]	10.21	13	13	13	42	1.000	51	7.231	109.015	120
Q19782	H1A protein (Fragment) OS-Homo sapiens GNC1448 PE-1 SV1 - [Q19782_HUMAN]	21.43	452	0	6	39	1.000	6	5.832	109.426	336
Q15052	Hectonin protein OS-Homo sapiens GNC1511 PE-1 SV1 - [HTN1_HUMAN]	11.17	11	6	6	42	1.000	21	2.622	109.360	369
Q43684	Midline checkpoint protein BUB3 OS-Homo sapiens GNC1448 PE-1 SV1 - [BUB3_HUMAN]	29.88	4	8	8	42	1.000	21	5.839	107.645	328
Q13046	Lysine-4-methyltransferase 3 OS-Homo sapiens GNC1511 PE-1 SV1 - [SYK_HUMAN]	29.88	4	15	15	43	1.000	43	12.770	107.513	597
Q08107	Terminin family homolog 3 OS-Homo sapiens GNC1511 PE-1 SV1 - [TERF3_HUMAN]	9.47	8	15	15	43	1.000	43	9.258	107.271	597
E1NZA1	ATP synthase subunit 6 OS-Homo sapiens GNC1511 PE-1 SV1 - [ATP6B_HUMAN]	20.94	4	25	25	39	1.000	38	6.038	107.271	2671
Q19479	High molecular weight protein 1 OS-Homo sapiens GNC1511 PE-1 SV1 - [HWP1_HUMAN]	10.21	13	7	7	42	1.000	38	6.038	107.271	161
Q15123	AD-PLC2, highly similar to Transmembrane emp24 domain-containing protein 2 OS-Homo sapiens PE-2 SV1 - [ADP27_HUMAN]	31.89	5	5	5	43	1.000	43	10.000	107.085	180
B04547	Actin-related protein 23 complex subunit 10 OS-Homo sapiens GNC1511 PE-1 SV1 - [ARPC10_HUMAN]	29.85	7	10	10	43	1.000	39	14.230	109.844	372
Q19516	WDR52, actin-binding dependent regulator of chromatin 3 variant (Fragment) OS-Homo sapiens PE-2 SV1 - [Q19516_HUMAN]	15.66	6	12	12	43	1.000	39	10.000	109.844	1156
B1PW03	MHC class I antigen (Fragment) OS-Homo sapiens GNC1448 PE-3 SV1 - [B1PW03_HUMAN]	30.4	255	0	6	38	1.000	6	10.000	109.537	273
M0R326	OS-Homo sapiens GNC1511 PE-1 SV1 - [M0R326_HUMAN]	47.52	7	7	7	42	1.000	39	3.499	109.355	141
P48634	Protein PRRC2A OS-Homo sapiens GNC1511 PE-1 SV1 - [PRRC2A_HUMAN]	11.87	3	17	17	47	1.000	44	10.000	106.112	2157
Q59298	2S1 protein subunit 7 OS-Homo sapiens GNC1511 PE-1 SV1 - [PR57_HUMAN]	29.79	4	11	11	42	1.000	38	6.369	109.108	433
Q53715	Aspartate aminotransferase 2 OS-Homo sapiens GNC1511 PE-1 SV1 - [AS2T_HUMAN]	11.55	10	14	14	42	1.000	42	10.000	109.616	548
Q9UG35	Serine/threonine protein kinase OS-Homo sapiens GNC1511 PE-1 SV1 - [SRPK2_HUMAN]	10.21	12	22	22	46	1.000	42	19.143	106.875	2752
Q59255	Protein PRRC2B OS-Homo sapiens GNC1511 PE-1 SV1 - [PRRC2B_HUMAN]	12.05	11	14	14	46	1.000	42	6.200	109.894	2216
P48444	Coatomer subunit delta OS-Homo sapiens GNC1511 PE-1 SV1 - [COPD_HUMAN]	31.12	5	20	20	49	0.951	48	14.168	106.391	511
P61006	Ras-related protein Rap-3A OS-Homo sapiens GNC1511 PE-1 SV1 - [RAB3A_HUMAN]	41.06	36	3	3	36	1.000	5	4.487	105.229	207
Q9KJ28	Aspartate aminotransferase 2 OS-Homo sapiens GNC1511 PE-1 SV1 - [AS2T_HUMAN]	11.52	4	17	17	42	1.000	31	37.065	101	153.100
B0ZG28	MHC class I antigen (Fragment) OS-Homo sapiens GNC1448 PE-3 SV1 - [B0ZG28_HUMAN]	26.37	444	0	6	37	1.000	42	9.186	104.779	273
Q15511	Actin-related protein 23 complex subunit 5 OS-Homo sapiens GNC1511 PE-1 SV1 - [ARPC5_HUMAN]	17.52	4	10	11	43	1.000	42	10.244	105.171	313.300
F8V12L	Dynamin light chain 1, cytoplasmic OS-Homo sapiens GNC1511 PE-1 SV1 - [F8V12L_HUMAN]	61.7	4	2	2	2	1.000	28	10.000	104.003	47
P13153	S-adenosylmethionine synthase isoform type 2 OS-Homo sapiens GNC1511 PE-1 SV1 - [MET2C_HUMAN]	29.85	7	11	12	43	0.999	42	5.356	103.358	395
M0R291	4S5 (bovine) OS-Homo sapiens GNC1511 PE-1 SV1 - [M0R291_HUMAN]	18.69	6	8	8	42	1.000	37	10.000	102.621	207
B03024	CNA FL146929, clone H174UJ014372, highly similar to DNA replication licensing factor MCM2 OS-Homo sapiens PE-2 SV1 - [B03024_HUMAN]	27.85	6	16	16	24	1.000	38	16.245	103.650	380
CNA FL195615	CNA FL195615, highly similar to Homo sapiens transcriptional coactivator subunit 10 (TBCO10) transcript variant 1, mRNA OS-Homo sapiens PE-2 SV1 - [B0R1]	20.6	20	4	4	4	1.000	38	11.221	103.310	866
Q59398	4S5 ubiquitin-protein ligase RNF213 OS-Homo sapiens GNC1511 PE-1 SV1 - [RNF213_HUMAN]	6.34	7	31	31	40	1.000	37	10.400	103.270	5207
B4E182	CNA FL13591, highly similar to Serotransferrin OS-Homo sapiens PE-2 SV1 - [B4E182_HUMAN]	25.81	13	14	14	41	1.000	37	5.414	103.020	678
B4C402	CNA FL13591, highly similar to Serotransferrin OS-Homo sapiens PE-2 SV1 - [B4C402_HUMAN]	25.81	13	14	14	41	1.000	37	5.414	103.020	678
P59687	Actin leucine-rich nuclear phospholipid 32 family member A OS-Homo sapiens GNC1511 PE-1 SV1 - [AN32A_HUMAN]	26.1	9	6	6	37	1.000	37	11.440	102.776	249
Q58109	CapZ-interacting protein OS-Homo sapiens GNC1511 PE-1 SV1 - [CIPZP_HUMAN]	10.82	39	6	6	37	1.000	37	3.458	102.496	416
B0R659	CNA FL192603, highly similar to Homo sapiens hydroxysteroid (17-beta) dehydrogenase 4 (HSD17B4), mRNA OS-Homo sapiens PE-2 SV1 - [B0R659_HUMAN]	23.51	13	6	6	17	1.000	37	11.788	102.345	730
B4D033	CNA FL152089, highly similar to Microtubule-associated protein RFBP family member 1 OS-Homo sapiens PE-2 SV1 - [B4D033_HUMAN]	40.38	2	11	11	33	0.976	32	10.471	102.179	238
Q914379	CapZ subunit A member 2 OS-Homo sapiens GNC1511 PE-1 SV1 - [CAPZA2_HUMAN]	10.38	2	11	11	33	1.000	32	10.471	102.179	238
Q15181	Inorganic pyrophosphatase OS-Homo sapiens GNC1511 PE-1 SV1 - [PP2C_HUMAN]	37.72	2	8	9	34	1.000	31	10.467	102.041	289
Q15904	Signal recognition particle subunit 5 OS-Homo sapiens GNC1511 PE-1 SV1 - [SRP5_HUMAN]	37.72	2	8	9	34	1.000	31	10.467	102.041	289
AK9K00	CNA FL178309, highly similar to Homo sapiens neurotensin nuclear ribonucleoprotein U-like 1 (HNRNPUL1), transcript variant 1, mRNA OS-Homo sapiens PE-2 SV1 - [AK9K00_HUMAN]	18.22	3	1	1	14	1.000	1	10.161	101.856	95.589
D4L90	MHC class I antigen OS-Homo sapiens GNC1448 PE-3 SV1 - [D4L90_HUMAN]	18.51	552	0	6	38	1.000	42	8.051	101.227	362
Q52626	OS-Homo sapiens GNC1511 PE-1 SV1 - [Q52626_HUMAN]	20.95	12	14	14	42	1.000	42	10.000	101.227	362
Q43399	Tumor protein D54 OS-Homo sapiens GNC1511 PE-1 SV1 - [TPD54_HUMAN]	14.17	3	9	9	36	1.000	34	3.439	100.943	206
Q15167	OS-Homo sapiens GNC1511 PE-1 SV1 - [Q15167_HUMAN]	15.63	7	6	6	31	1.000	36	10.000	100.352	220
P13130	Cytochrome b-c1 complex subunit 1, mitochondrial OS-Homo sapiens GNC1511 PE-1 SV1 - [C13R1_HUMAN]	45.63	3	6	7	50	1.677	43	3.260	100.352	480
Q59831	Apoptosis-inducing factor 1, mitochondrial OS-Homo sapiens GNC1511 PE-1 SV1 - [AIFM1_HUMAN]	18.11	4	11	11	37	1.000	37	4.752	100.314	613
Q13162	Herpesin OS-Homo sapiens GNC1511 PE-1 SV1 - [PROD4_HUMAN]	10.42	4	6	6	39	1.000	41	11.950	100.261	207
H3B027	H3B024799 OS-Homo sapiens GNC1511 PE-1 SV1 - [H3B027_HUMAN]	15.12	4	13	13	37	1.000	31	11.465	100.349	716
A03617	RCC2 protein (Fragment) OS-Homo sapiens GNC1511 PE-1 SV1 - [RCC2_HUMAN]	18.11	4	9	9	39	1.000	41	11.465	100.349	716
A04248E8	Sulfolipase family 2 (Mitochondrial carrier phosphate carrier), member 3, isoform CRA_b OS-Homo sapiens GNC1511 PE-1 SV1 - [A04248E8_HUMAN]	17.73	7	7	7	37	1.000	37	7.657	100.247	457
Q914379	Dihydrodipyrrole-lysine succinyltransferase component of 2-oxoglutarate dehydrogenase complex, mitochondrial OS-Homo sapiens GNC1511 PE-1 SV1 - [DHDH]	23.18	11	8	8	37	1.000	35	6.242	99.967	361
B4D074	DRP1 OS-Homo sapiens GNC1511 PE-1 SV1 - [B4D074_HUMAN]	19.12	2	10	10	38	1.000	35	20.035	99.465	453
M0R210	Calpain-2 OS-Homo sapiens GNC1511 PE-1 SV1 - [M0R210_HUMAN]	62.29	20	8	10	38	0.960	33	6.219	99.319	298
Q59831	Keratin-type I cytoskeleton-associated protein 2 OS-Homo sapiens GNC1511 PE-1 SV1 - [K2P223_HUMAN]	29.33	17	10	10	38	1.000	33	10.481	99.319	65.338
Q59831	4S5 (bovine) protein subunit 5 OS-Homo sapiens GNC1511 PE-1 SV1 - [M0R210_HUMAN]	32.71	11	11	11	50	1.000	50	12.719	99.314	129
Q59831	DNA repair protein RAD50 OS-Homo sapiens GNC1511 PE-1 SV1 - [RAD50_HUMAN]	10.21	8	16	16	36	1.000	36	18.478	98.887	1312
Q59831	ARPC10 OS-Homo sapiens GNC1511 PE-1 SV1 - [ARPC10_HUMAN]	19.11	4	13	13	37	1.000	36	11.917	98.887	1312
A04342	Eukaryotic translation initiation factor 4 gamma 3 OS-Homo sapiens GNC1511 PE-1 SV1 - [IF4G3_HUMAN]	9.29	8	10	10	36	1.000	37	3.131	98.363	1585
Q48404	Serine/threonine protein kinase OS-Homo sapiens GNC1511 PE-1 SV1 - [STK10_HUMAN]	15.91	2	14	14	39	1.000	41	11.809	98.169	808
Q9N122	Human OS-Homo sapiens GNC1511 PE-1 SV1 - [Q9N122_HUMAN]	46.103	46	12	12	46	1.000	46	6.751	98.351	596
Q15716	Cytochrome P-450 2C9 OS-Homo sapiens GNC1511 PE-1 SV1 - [CYP2C9_HUMAN]	12.37	23	17	17	40	1.000	38	5.197	98.318	1253
Q59831	Coatomer subunit beta OS-Homo sapiens GNC1511 PE-1 SV1 - [COPB_HUMAN]	19.16	17	16	16	37	1.000	36	11.917	98.318	1253
Q13200	2S1 protein subunit 2 OS-Homo sapiens GNC1511 PE-1 SV1 - [PR52D2_HUMAN]	20.93	6	17	17	43	1.000	42	11.173	97.959	908
P46080	RNase P large subunit OS-Homo sapiens GNC1511 PE-1 SV1 - [RPLP_HUMAN]	30.83	8	15	16	34	1.000	33	12.571	97.914	637
ESLR59	1-phosphate-associated protein 1 OS-Homo sapiens GNC1511 PE-1 SV1 - [ESLR59_HUMAN]	20.93	6	17	17	40	1.000	38	8.995	97.902	163
AKK015	CNA FL177388, highly similar to Homo sapiens UDP-glucose ceramide glucosyltransferase-like 1, transcript variant 2, mRNA OS-Homo sapiens PE-2 SV1 - [AKK015_HUMAN]	10.58	5	14	14	38	1.000	34	6.627	97.549	1531
Q17653	Splicing factor 3B subunit 1 OS-Homo sapiens GNC1511 PE-1 SV1 - [SF3B1_HUMAN]	19.12	2	10	10	38	1.000	34	12.840	97.549	1531
J3L025	Serine/threonine-rich splicing factor 2 (Fragment) OS-Homo sapiens GNC1511 PE-1 SV1 - [J3L025_HUMAN]	12.32	12	2	2	38	1.000	34	6.627	96.997	130
F1T012	RFL102, highly similar to OS-Homo sapiens GNC1511 PE-1 SV1 - [F1T012_HUMAN]	61.4	2	29	29	38	1.000	36	6.202	96.786	3104
AKK021	Adipose 1 OS-Homo sapiens GNC1511 PE-1 SV1 - [AKK021_HUMAN]	25.34	19	19	19	39	0.964	38	16.997	96.730	734
Q13784	Palmitate fatty acid domain-containing protein 3B OS-Homo sapiens GNC1511 PE-1 SV1 - [ATD3B_HUMAN]	12.5	1	9	9	32	2.180	1	11.133	96.610	648
P49495	Protein TRAP-2, highly similar to OS-Homo sapiens GNC1511 PE-1 SV1 - [P49495_HUMAN]	45.21	5	1	1	3	1.000	21	0.000	105.627	414
P5420	Alpha-soluble NSF attachment protein OS-Homo sapiens GNC1511 PE-1 SV1 - [NSAA_HUMAN]	33.56	12	8	9	37	1.000	29	19.196	96.419	295
A04248E8	DBP1 and CUL4-associated factor 2 OS-Homo sapiens GNC1511 PE-1 SV1 - [A04248E8_HUMAN]	20.95	14	8	8	37	1.000	29	9.812	96.287	424
Q9N122	Sister chromatid cohesion protein PDSS homolog 1 OS-Homo sapiens GNC1511 PE-1 SV1 - [PDSS1_HUMAN]	10.3	12	12	12	34	1.000	22	9.921	96.383	1447
B0R659	CNA FL192610, highly similar to Homo sapiens protein phosphatase 10 (homology 2), magnesium-dependent, gamma isoform (PPM1G), mRNA OS-Homo sapiens PE-2 SV1 - [B0R659_HUMAN]	29.49	6	15	15	37	1.000	35	6.279	96.186	546
Q13148	Protein phosphatase inhibitor 1 OS-Homo sapiens GNC1511 PE-1 SV1 - [PPI1_HUMAN]	33.56	12	8	8	37	1.000	29	9.812	96.186	546
Q9Y848	Signal recognition particle subunit beta OS-Homo sapiens GNC1511 PE-1 SV1 - [SRPB_HUMAN]	35.28	2	8	8						

B5B0U8	U2 small nuclear RNA auxiliary factor 1 isoform A OS-Homo sapiens GN-UZAF1 PE=2 SV=1	[B5B0U8_HUMAN]	24.17	7	6	7	37	1.000	31	0.000	82.836	240	27.855
Q14165	Nucleolar protein 1 OS-Homo sapiens GN-NP1 PE=1 SV=1	[MLEC_HUMAN]	22.28	4	6	6	6	1.000	6	0.000	62.402	26	11.512
E9A2E9	Putative heat shock protein DNA OS-Hesliamnia mexicana (strain MHOM/GT2001/1103) GN-LMMX_27_2400 PE=1 SV=1	[E9A2E9_LEMUI]	21.97	1	9	9	28	1.000	27	0.000	82.394	396	44.539
FA1688	DNAI1 homolog subfamily A member 1 OS-Homo sapiens GN-DNAI1 PE=1 SV=1	[DNAI1_HUMAN]	20.95	1	12	14	34	1.000	27	16.870	82.305	397	43.828
GN14K47	CENPA-like 1 OS-Homo sapiens protein kinase, CNAP-related, repeat 10, alpha (PRKAR2A), mRNA OS-Homo sapiens PE=2 SV=1	[AR6A_HUMAN]	20.84	1	12	13	36	1.000	27	10.364	82.365	414	46.4
Q00410	Importin-5 OS-Homo sapiens GN-IP5 PE=1 SV=1	[IPO5_HUMAN]	17.78	21	18	18	39	1.000	27	9.521	81.994	1097	123.550
IL30L8	ATP-ADP/ATPase OS-Homo sapiens GN-CDCA19A PE=1 SV=1	[IL30L8_HUMAN]	16.25	1	13	3	3	1.000	28	16.473	81.866	647	69.048
P30085	UMP-CMP kinase OS-Homo sapiens GN-CMPK1 PE=1 SV=1	[KCV_HUMAN]	12.96	5	5	5	10	1.000	28	7.207	81.503	196	22.208
H3N898	Uncharacterized protein (Fragment) OS-Homo sapiens PE=4 SV=2	[H3N898_HUMAN]	22.63	13	2	6	37	1.000	8	22.964	81.240	237	27.130
EDL7	Mitochondrial cytochrome b-like 12 OS-Homo sapiens GN-12B PE=3 SV=1	[EDL7_HUMAN]	22.56	6	10	10	36	1.000	9	11.520	81.227	997	115.12
Q5G9Y3	Argininosuccinate lyase-like 2 OS-Homo sapiens GN-ARSL2 PE=1 SV=1	[Q5G9Y3_HUMAN]	22.58	7	4	8	29	1.336	9	44.974	81.122	879	31.846
Q5G9Y4	Argininosuccinate lyase-like 1 OS-Homo sapiens GN-ARSL1 PE=1 SV=1	[Q5G9Y4_HUMAN]	22.58	7	4	8	29	1.336	9	11.243	81.122	879	31.846
B4D203	cDNA FL155445, highly similar to 5'-UTR exoribionclease 2 (EC 3.11.3.1) OS-Homo sapiens PE=2 SV=1	[B4D203_HUMAN]	11.27	4	11	11	12	3.093	31	7.787	80.906	896	102.351
Q1C122	Dolichyl-diphosphoglyceroacetate-protein glycosyltransferase 48 kDa subunit OS-Homo sapiens GN-48T38 PE=1 SV=1	[Q1C122_HUMAN]	11.27	4	6	28	10	1.000	22	0.000	80.866	282	16.814
Q2D411	Decorin OS-Homo sapiens GN-DCR PE=1 SV=1	[DCR_HUMAN]	4.21	13	5	5	6	1.000	22	0.000	80.866	282	16.814
B4E244	cDNA FL15275, highly similar to Homo sapiens spectrin domain with coiled-coil 1 (SPECC1), transcript variant, mRNA OS-Homo sapiens PE=2 SV=1	[B4E244_HUMAN]	21.99	12	17	19	36	1.000	26	3.542	80.831	987	110.226
PA2022	Alpha OS-Homo sapiens GN-ALPHA PE=1 SV=1	[ALPHA_HUMAN]	23.17	16	9	9	32	1.000	31	12.127	80.783	546	61.653
P17658	ATP-dependent 6-phosphogluconate lyase liver type OS-Homo sapiens GN-PFKL PE=1 SV=6	[PFKAL_HUMAN]	16.28	8	13	29	938	1.000	18	16.995	80.762	780	84.964
Q7393	DNAI1 homolog subfamily C member 8 OS-Homo sapiens GN-DNAI3 PE=1 SV=2	[DNAI3_HUMAN]	24.5	2	9	26	943	1.000	27	9.271	80.518	233	28.823
Q73921	DNAI1 homolog subfamily C member 8 OS-Homo sapiens GN-DNAI3 PE=1 SV=2	[DNAI3_HUMAN]	24.5	2	9	26	943	1.000	27	3.961	80.509	320	35.589
Q13838	Silicosponge RNA helicase DDX39B OS-Homo sapiens GN-DDX39B PE=1 SV=1	[DDX39B_HUMAN]	26.7	16	7	13	35	0.990	16	26.778	80.358	428	49.960
B4D407	RNA polymerase II subunit 2 OS-Homo sapiens GN-RPB2 PE=1 SV=1	[B4D407_HUMAN]	22.25	25	19	33	100	1.000	26	19.219	80.349	980	114.778
Q5T123	SH3 domain-binding glutamic acid-rich-like protein 3 OS-Homo sapiens GN-SH3GL3 PE=1 SV=1	[Q5T123_HUMAN]	23.41	5	6	6	43	1.000	34	0.876	80.133	88	9.375
BSN24	SLMO1 activating enzyme subunit 1, isoform CRA_A OS-Homo sapiens GN-SAE1 PE=1 SV=1	[BSN24_HUMAN]	57.02	10	9	9	27	0.943	20	9.528	79.972	299	33.363
GN14K47	CENPA-like 1 OS-Homo sapiens protein kinase, CNAP-related, repeat 10, alpha (PRKAR2A), mRNA OS-Homo sapiens PE=2 SV=1	[AR6A_HUMAN]	20.84	1	12	13	36	1.000	27	11.878	79.956	396	55.275
AR3A8	cDNA FL175085, highly similar to Homo sapiens glutamyl-RNA synthetase (GARS), mRNA OS-Homo sapiens PE=2 SV=1	[AR3A8_HUMAN]	21.81	15	16	17	37	0.992	35	20.172	79.403	775	87.753
B4D407	RNA polymerase II subunit 2 OS-Homo sapiens GN-RPB2 PE=1 SV=1	[B4D407_HUMAN]	22.25	25	19	33	100	1.000	26	14.387	79.294	987	114.778
Q14008	Cytoskeleton-associated protein 5 OS-Homo sapiens GN-CAKAP5 PE=1 SV=3	[CAKAP5_HUMAN]	9.06	5	18	18	35	1.000	35	14.712	79.247	232	25.352
P5580	Succinyl-CoA:ketoadic coenzyme A transferase 1, mitochondrial OS-Homo sapiens GN-CKX11 PE=1 SV=1	[CKO11_HUMAN]	22.12	5	12	12	34	1.000	34	11.704	79.091	520	58.122
Q5R268	Defucosylated alpha-D-glucosyl-L-lysine 1 OS-Homo sapiens GN-DGLY1 PE=1 SV=1	[DGLY1_HUMAN]	22.29	4	10	10	36	1.000	25	19.879	78.717	121	13.881
B3K9V6	Dedicator of cytokinesis protein 2 OS-Homo sapiens GN-DOCK2 PE=1 SV=2	[DOCK2_HUMAN]	11.10	11	11	20	36	1.000	34	13.940	78.709	1830	211.812
B3K9V6	Eukaryotic translation initiation factor 3 subunit E OS-Homo sapiens GN-EIF3B PE=1 SV=1	[EIF3B_HUMAN]	22.29	4	10	10	36	1.000	25	10.868	78.648	396	44.415
Q15164	Polysialyltransferase II (Fragment) OS-Homo sapiens PE=2 SV=1	[Q15164_HUMAN]	25.81	2	1	13	29	0.961	1	8.714	78.114	183	21.973
P13645	Keratin, type I b-like 10 OS-Homo sapiens GN-KRT10 PE=1 SV=1	[KRT10_HUMAN]	59.69	27	11	14	26	0.350	20	76.073	78.587	584	58.732
AR3K71	cDNA FL175444, highly similar to Homo sapiens nucleobindin 1 (NUCB1), mRNA OS-Homo sapiens PE=2 SV=1	[AR3K71_HUMAN]	10.97	10	19	33	100	1.000	16	11.462	78.169	231	27.071
ESL307	Phosphoribosylaminoimidazole carboxamide (Fragment) OS-Homo sapiens GN-PAICS PE=1 SV=1	[ESL307_HUMAN]	21.07	4	8	9	33	1.000	32	6.110	78.253	413	45.622
Q2H153	Nucleolar protein 1 OS-Homo sapiens GN-NP1 PE=1 SV=1	[NP1_HUMAN]	22.28	4	6	6	6	1.000	27	0.000	82.394	396	44.539
IP3821	Component complex 1 O subcomponent protein, mitochondrial (Fragment) OS-Homo sapiens GN-CC1B PE=1 SV=1	[IP3821_HUMAN]	25.42	4	4	4	24	1.000	22	0.000	78.082	177	19.994
AD3004	Gulathione S-transferase P OS-Homo sapiens GN-GSTP1 PE=1 SV=1	[AD3004_HUMAN]	44.83	6	6	6	32	1.000	31	8.238	77.959	174	18.468
AR3K91	Calcium-binding protein 2 (Fragment) OS-Homo sapiens GN-CBP2 PE=1 SV=1	[AR3K91_HUMAN]	10.12	3	3	3	10	1.000	7	15.776	77.754	998	105.110
GN14K47	CENPA-like 1 OS-Homo sapiens protein kinase, CNAP-related, repeat 10, alpha (PRKAR2A), mRNA OS-Homo sapiens PE=2 SV=1	[AR6A_HUMAN]	20.84	1	12	13	36	1.000	27	11.878	79.956	396	55.275
AD3004	Gulathione S-transferase P OS-Homo sapiens GN-GSTP1 PE=1 SV=1	[AD3004_HUMAN]	44.83	6	6	6	32	1.000	31	8.238	77.959	174	18.468
AR3K91	Calcium-binding protein 2 (Fragment) OS-Homo sapiens GN-CBP2 PE=1 SV=1	[AR3K91_HUMAN]	10.12	3	3	3	10	1.000	7	15.776	77.754	998	105.110
AD3004	Gulathione S-transferase P OS-Homo sapiens GN-GSTP1 PE=1 SV=1	[AD3004_HUMAN]	44.83	6	6	6	32	1.000	31	8.238	77.959	174	18.468
AR3K91	Calcium-binding protein 2 (Fragment) OS-Homo sapiens GN-CBP2 PE=1 SV=1	[AR3K91_HUMAN]	10.12	3	3	3	10	1.000	7	15.776	77.754	998	105.110
AD3004	Gulathione S-transferase P OS-Homo sapiens GN-GSTP1 PE=1 SV=1	[AD3004_HUMAN]	44.83	6	6	6	32	1.000	31	8.238	77.959	174	18.468
AR3K91	Calcium-binding protein 2 (Fragment) OS-Homo sapiens GN-CBP2 PE=1 SV=1	[AR3K91_HUMAN]	10.12	3	3	3	10	1.000	7	15.776	77.754	998	105.110
AD3004	Gulathione S-transferase P OS-Homo sapiens GN-GSTP1 PE=1 SV=1	[AD3004_HUMAN]	44.83	6	6	6	32	1.000	31	8.238	77.959	174	18.468
AR3K91	Calcium-binding protein 2 (Fragment) OS-Homo sapiens GN-CBP2 PE=1 SV=1	[AR3K91_HUMAN]	10.12	3	3	3	10	1.000	7	15.776	77.754	998	105.110
AD3004	Gulathione S-transferase P OS-Homo sapiens GN-GSTP1 PE=1 SV=1	[AD3004_HUMAN]	44.83	6	6	6	32	1.000	31	8.238	77.959	174	18.468
AR3K91	Calcium-binding protein 2 (Fragment) OS-Homo sapiens GN-CBP2 PE=1 SV=1	[AR3K91_HUMAN]	10.12	3	3	3	10	1.000	7	15.776	77.754	998	105.110
AD3004	Gulathione S-transferase P OS-Homo sapiens GN-GSTP1 PE=1 SV=1	[AD3004_HUMAN]	44.83	6	6	6	32	1.000	31	8.238	77.959	174	18.468
AR3K91	Calcium-binding protein 2 (Fragment) OS-Homo sapiens GN-CBP2 PE=1 SV=1	[AR3K91_HUMAN]	10.12	3	3	3	10	1.000	7	15.776	77.754	998	105.110
AD3004	Gulathione S-transferase P OS-Homo sapiens GN-GSTP1 PE=1 SV=1	[AD3004_HUMAN]	44.83	6	6	6	32	1.000	31	8.238	77.959	174	18.468
AR3K91	Calcium-binding protein 2 (Fragment) OS-Homo sapiens GN-CBP2 PE=1 SV=1	[AR3K91_HUMAN]	10.12	3	3	3	10	1.000	7	15.776	77.754	998	105.110
AD3004	Gulathione S-transferase P OS-Homo sapiens GN-GSTP1 PE=1 SV=1	[AD3004_HUMAN]	44.83	6	6	6	32	1.000	31	8.238	77.959	174	18.468
AR3K91	Calcium-binding protein 2 (Fragment) OS-Homo sapiens GN-CBP2 PE=1 SV=1	[AR3K91_HUMAN]	10.12	3	3	3	10	1.000	7	15.776	77.754	998	105.110
AD3004	Gulathione S-transferase P OS-Homo sapiens GN-GSTP1 PE=1 SV=1	[AD3004_HUMAN]	44.83	6	6	6	32	1.000	31	8.238	77.959	174	18.468
AR3K91	Calcium-binding protein 2 (Fragment) OS-Homo sapiens GN-CBP2 PE=1 SV=1	[AR3K91_HUMAN]	10.12	3	3	3	10	1.000	7	15.776	77.754	998	105.110
AD3004	Gulathione S-transferase P OS-Homo sapiens GN-GSTP1 PE=1 SV=1	[AD3004_HUMAN]	44.83	6	6	6	32	1.000	31	8.238	77.959	174	18.468
AR3K91	Calcium-binding protein 2 (Fragment) OS-Homo sapiens GN-CBP2 PE=1 SV=1	[AR3K91_HUMAN]	10.12	3	3	3	10	1.000	7	15.776	77.754	998	105.110
AD3004	Gulathione S-transferase P OS-Homo sapiens GN-GSTP1 PE=1 SV=1	[AD3004_HUMAN]	44.83	6	6	6	32	1.000	31	8.238	77.959	174	18.468
AR3K91	Calcium-binding protein 2 (Fragment) OS-Homo sapiens GN-CBP2 PE=1 SV=1	[AR3K91_HUMAN]	10.12	3	3	3	10	1.000	7	15.776	77.754	998	105.110
AD3004	Gulathione S-transferase P OS-Homo sapiens GN-GSTP1 PE=1 SV=1	[AD3004_HUMAN]	44.83	6	6	6	32	1.000	31	8.238	77.959	174	18.468
AR3K91	Calcium-binding protein 2 (Fragment) OS-Homo sapiens GN-CBP2 PE=1 SV=1	[AR3K91_HUMAN]	10.12	3	3	3	10	1.000	7	15.776	77.754	998	105.110
AD3004	Gulathione S-transferase P OS-Homo sapiens GN-GSTP1 PE=1 SV=1	[AD3004_HUMAN]	44.83	6	6	6	32	1.000	31	8.238	77.959	174	18.468
AR3K91	Calcium-binding protein 2 (Fragment) OS-Homo sapiens GN-CBP2 PE=1 SV=1	[AR3K91_HUMAN]	10.12	3	3	3	10	1.000	7	15.776	77.754	998	105.110
AD3004	Gulathione S-transferase P OS-Homo sapiens GN-GSTP1 PE=1 SV=1	[AD3004_HUMAN]	44.83	6	6	6	32	1.000	31	8.238	77.959	174	18.468
AR3K91	Calcium-binding protein 2 (Fragment) OS-Homo sapiens GN-CBP2 PE=1 SV=1	[AR3K91_HUMAN]	10.12	3	3	3	10	1.000	7	15.776	77.754	998	105.110
AD3004	Gulathione S-transferase P OS-Homo sapiens GN-GSTP1 PE=1 SV=1	[AD3004_HUMAN]	44.83	6	6	6	32	1.000	31	8.238	77.959	174	18.468
AR3K91	Calcium-binding protein 2 (Fragment) OS-Homo sapiens GN-CBP2 PE=1 SV=1	[AR3K91_HUMAN]	10.12	3	3	3	10	1.000	7	15.776	77.754	998	105.110
AD3004	Gulathione S-transferase P OS-Homo sapiens GN-GSTP1 PE=1 SV=1	[AD3004_HUMAN]	44.83	6	6	6	32	1.000	31	8.238	77.959	174	18.468
AR3K91	Calcium-binding protein 2 (Fragment) OS-Homo sapiens GN-CBP2 PE=1 SV=1	[AR3K91_HUMAN]	10.12	3	3	3	10	1.000	7	15.776	77.754	998	105.110
AD3004	Gulathione S-transferase P OS-Homo sapiens GN-GSTP1 PE=1 SV=1	[AD3004_HUMAN]	44.83	6	6	6	32	1.000	31	8.238	77.959	174	18.468
AR3K91	Calcium-binding protein 2 (Fragment) OS-Homo sapiens GN-CBP2 PE=1 SV=1	[AR3K91_HUMAN]	10.12	3	3	3	10	1.000	7	15.776	77.754	998	105.110
AD3004	Gulathione S-transferase P OS-Homo sapiens GN-GSTP1 PE=1 SV=1	[AD3004_HUMAN]	44.83	6	6	6	32	1.000	31	8.238	77.959	174	18.468
AR3K91	Calcium-binding protein 2 (Fragment) OS-Homo sapiens GN-CBP2 PE=1 SV=1	[AR3K91_HUMAN]	10.12	3	3	3	10	1.000	7	15.776	77.754	998	105.110
AD3004	Gulathione S-transferase P OS-Homo sapiens GN-GSTP1 PE=1 SV=1	[AD3004_HUMAN]	44.83	6	6	6	32	1.000	31	8.238	77.959	174	18.468
AR3K91	Calcium-binding protein 2 (Fragment) OS-Homo sapiens GN-CBP2 PE=1 SV=1	[AR3K91_HUMAN]	10.12	3	3	3	10	1.000	7	15.776	77.754	998	105.110
AD3004	Gulathione S-transferase P OS-Homo sapiens GN-GSTP1 PE=1 SV=1	[AD3004_HUMAN]	44.83	6	6	6	32	1.000	31	8.238	77.959	174	18.468
AR3K91	Calcium-binding protein 2 (Fragment) OS-Homo sapiens GN-CBP2 PE=1 SV=1	[AR3K91_HUMAN]	10.12	3	3	3	10	1.000	7	15.776	77.754	998	105.110
AD3004	Gulathione S-transferase P OS-Homo sapiens GN-GSTP1 PE=1 SV=1	[AD3004_HUMAN]	44.83	6	6	6	32	1.000	3				

P5584	Small ubiquitin-related modifier 1 OS=Homo sapiens GN-SUMO3 PE=1 SV=2	[SUMO3_HUMAN]	20.39	4	1	2	19	0.882	3	1.360	50.774	103	11.630	
P10944	AMF-dependent regulatory subunit OS=Homo sapiens GN-HFR19 PE=1 SV=1	[KAP1_HUMAN]	21.78	2	1	2	23	0.936	2	10.918	67.765	147	26.956	
H3R35	Eukaryotic peptide chain release factor GTP-binding subunit EP3A (Fragment) OS=Homo sapiens GN-GSPT1 PE=1 SV=1	[H3R35_HUMAN]	22.11	8	12	12	23	1.000	23	12.679	50.651	475	52.909	
PO123	Alpha-2-macroglobulin OS=Homo sapiens GN-A2M1 PE=1 SV=1	[A2M1_HUMAN]	22.77	6	15	15	20	1.000	30	10.975	50.545	1474	163.188	
Q13617	Calcium channel subunit gamma-1L (Ct) OS=Homo sapiens GN-CCAL1 PE=1 SV=1	[CCAL1_HUMAN]	16.97	7	7	7	10	1.000	7	10.364	50.417	765	87.827	
SAR466	40S ribosomal protein S15 (Fragment) OS=Homo sapiens GN-HRPS15 PE=1 SV=1	[SAR466_HUMAN]	29.41	7	3	3	43	1.000	43	21.532	50.393	88	8.021	
P25946	Nucleolar complex subunit Nuclep1 OS=Homo sapiens GN-NCLP1 PE=1 SV=1	[NCLP1_HUMAN]	17.76	2	2	2	14	1.000	14	11.475	49.917	1817	215.629	
OT5400	Pre-mRNA-processing factor 40 homolog OS=Homo sapiens GN-PRPF40A PE=1 SV=2	[PRPF40A_HUMAN]	9.3	6	2	2	17	0.895	4	6.008	49.263	957	107.737	
Q0487	26S proteasome non-ATPase regulatory subunit 14 OS=Homo sapiens GN-PSMD14 PE=1 SV=1	[PSMD14_HUMAN]	16.13	5	7	7	10	1.000	10	18.817	50.172	310	34.555	
Q13263	CNA1 FL19621, highly similar to Nucleolar protein endonuclease (PRE1) mRNA OS=Homo sapiens GN-CNA1 PE=1 SV=1	[CNA1_HUMAN]	10.49	3	8	8	10	1.000	8	6.620	49.170	710	79.852	
BAD717	Ras GTPase-activating protein-binding protein 1 OS=Homo sapiens GN-GABP1 PE=1 SV=1	[GABP1_HUMAN]	26.32	11	8	8	23	1.000	22	18.016	50.107	486	52.132	
Q06717	40S ribosomal protein L16 OS=Homo sapiens GN-L16 PE=1 SV=1	[L16_HUMAN]	17.76	2	2	2	19	1.000	19	21.609	49.931	623	69.119	
Q06717	Deubiquitinating protein VCP135 OS=Homo sapiens GN-VCP135 PE=1 SV=2	[VCP135_HUMAN]	12.85	2	13	13	20	1.000	19	0.000	50.042	1222	134.236	
Q06717	Ribonuclease T2 OS=Homo sapiens GN-RNASET2 PE=1 SV=1	[RNASET2_HUMAN]	23.39	9	5	5	20	1.000	20	8.434	50.040	218	25.203	
Q13263	CNA1 FL19620, highly similar to Transcription protein 1 (TP1) mRNA OS=Homo sapiens GN-CNA1 PE=1 SV=1	[CNA1_HUMAN]	10.39	3	8	8	10	1.000	8	7.721	49.761	710	79.852	
Q14776	Transcription elongation regulator 1 OS=Homo sapiens GN-TCERG1 PE=1 SV=2	[TCERG1_HUMAN]	10.75	4	12	12	13	25	1.000	21	0.000	49.935	1098	123.823
Q13217	DnaI homology C member 3 OS=Homo sapiens GN-DNAI3 PE=1 SV=1	[DNAI3_HUMAN]	11.06	2	2	2	10	1.000	10	26.911	49.744	104	57.544	
KTEM41	60S ribosomal protein L22 (Fragment) OS=Homo sapiens GN-RPL22 PE=1 SV=1	[RPL22_HUMAN]	13.71	8	3	3	19	1.000	18	14.687	49.701	89	10.416	
P19182	Nucleolar ribonucleoprotein H3 OS=Homo sapiens GN-HNRNP3 PE=1 SV=2	[HNRNP3_HUMAN]	21.39	4	6	6	7	22	1.000	11	22.351	49.660	346	38.903
Q02643	CNA1 FL19620, highly similar to Protein family 8 (isolated) mRNA OS=Homo sapiens GN-CNA1 PE=1 SV=1	[CNA1_HUMAN]	10.46	3	7	7	17	1.000	14	2.341	49.650	671	38.875	
OT5489	MAD3 nuclear ubiquitin-protein iron-sulfur cluster 1, mitochondrial OS=Homo sapiens GN-MNDUF3 PE=1 SV=1	[MNDUF3_HUMAN]	32.58	6	9	9	30	0.993	30	3.774	49.440	284	30.223	
P05771	Protein kinase C delta type OS=Homo sapiens GN-PRCKB1 PE=1 SV=4	[PRCKB1_HUMAN]	9.96	13	7	7	20	0.993	10	13.638	49.400	671	78.819	
Q06717	Serine/threonine protein phosphatase (Fragment) OS=Homo sapiens GN-HPPP1 PE=1 SV=1	[HPPP1_HUMAN]	12.21	12	1	1	6	1.000	6	17.865	49.392	294	33.752	
D9HTB9	Plasma membrane citrate carrier OS=Homo sapiens GN-CLC2A1 PE=1 SV=1	[D9HTB9_HUMAN]	22.84	4	8	8	23	1.000	23	5.899	49.357	318	35.030	
EP9F14	Tropomyosin OS=Homo sapiens GN-TPM1 PE=1 SV=1	[TPM1_HUMAN]	10.47	10	10	10	19	1.000	19	41.116	49.317	872	100.267	
BADKY1	cDNA FL19583, highly similar to Cytosolic RNA polymerase II (EC 6.1.16) OS=Homo sapiens PE=2 SV=1	[BADKY1_HUMAN]	17.05	11	13	13	20	0.987	20	12.688	49.232	739	84.225	
ETCQ39	Ribosomal protein L15 (Fragment) OS=Homo sapiens GN-RPL15 PE=1 SV=1	[RPL15_HUMAN]	38.51	9	7	7	25	1.000	24	13.154	49.169	174	20.497	
Q06717	POZ and LIM domain protein 7 OS=Homo sapiens GN-PDLIM7 PE=1 SV=1	[PDLIM7_HUMAN]	23.41	5	10	11	23	0.919	19	12.559	49.151	457	49.813	
F1VR90	Polycystic protein 2 (Fragment) OS=Homo sapiens GN-GNCCP2 PE=1 SV=2	[F1VR90_HUMAN]	11.81	2	0	0	10	1.058	2	8.970	49.020	310	32.015	
EV373	Cytosolic chaperonin 1 protein (Fragment) OS=Homo sapiens GN-CPC1 PE=1 SV=1	[EV373_HUMAN]	11.35	3	12	12	28	0.928	28	12.688	48.975	412	45.717	
BAD732	CNA1 FL19682, highly similar to Solute carrier family 7, facilitated glucose/transporter member 5 OS=Homo sapiens PE=2 SV=1	[BAD732_HUMAN]	12.44	8	8	8	23	1.009	23	14.237	48.936	386	42.262	
Q03884	DnaI homology C member 3 OS=Homo sapiens GN-DNAI3 PE=1 SV=1	[DNAI3_HUMAN]	11.06	2	2	2	14	1.000	14	11.475	48.916	1817	215.629	
P26440	Isovaleryl-CoA dehydrogenase, mitochondrial OS=Homo sapiens GN-HVD PE=1 SV=1	[HVD_HUMAN]	20.8	5	9	9	19	1.000	19	15.006	48.755	423	46.290	
AKS71	cDNA FL17355, highly similar to Homo sapiens SLUG1 (SLUG1) mRNA OS=Homo sapiens PE=2 SV=1	[AKS71_HUMAN]	28.77	4	3	11	21	0.843	7	19.328	48.642	268	41.028	
Q06717	Protein kinase C delta type OS=Homo sapiens GN-PRCKB1 PE=1 SV=4	[PRCKB1_HUMAN]	9.96	13	7	7	20	0.993	10	13.638	48.642	671	78.819	
P17096	High mobility group protein HMGB1HMGB1 OS=Homo sapiens GN-HMGA1 PE=1 SV=3	[HMGA1_HUMAN]	30.32	4	4	23	10	1.009	23	9.670	48.581	107	11.669	
EQ3AMU9	Strigolactone signaling pathway protein 1 (Fragment) OS=Homo sapiens GN-SLMO1 PE=1 SV=2	[EQ3AMU9_HUMAN]	10.38	2	2	2	15	1.000	15	14.823	48.581	404	44.474	
Q13263	ES ubiquitin-protein ligase BRE1A OS=Homo sapiens GN-RNF201 PE=1 SV=2	[BRE1A_HUMAN]	13.03	6	10	13	19	1.000	15	18.307	48.570	675	114.552	
SAR418	Strigolactone signaling pathway protein 2 (Fragment) OS=Homo sapiens GN-SLMO2 PE=1 SV=2	[SAR418_HUMAN]	10.15	9	8	8	20	1.000	17	0.000	48.517	536	58.988	
Q06717	Ribosomal protein L14 OS=Homo sapiens GN-RPL14 PE=1 SV=1	[RPL14_HUMAN]	15.46	3	2	2	12	1.000	12	21.869	48.517	536	58.988	
D6RG30	Bin1, isoform CRA_b OS=Homo sapiens GN-SEPT11 PE=1 SV=2	[D6RG30_HUMAN]	20.29	10	2	2	21	0.944	6	8.582	48.273	425	49.875	
Q06717	Actin-related protein 3 OS=Homo sapiens GN-ARFIP3 PE=1 SV=1	[ARFIP3_HUMAN]	14.42	4	4	4	13	1.000	13	10.328	48.273	425	49.875	
EPFL01	Signal peptidase complex subunit 2 OS=Homo sapiens GN-SPCS2 PE=1 SV=1	[EPFL01_HUMAN]	33.78	7	5	5	20	1.000	18	6.920	48.201	157	17.017	
GNV919	ATP-dependent RNA helicase DX18 OS=Homo sapiens GN-DX18 PE=1 SV=2	[DX18_HUMAN]	19.19	8	8	18	1.000	18	6.527	48.055	670	73.359		
Q13263	CNA1 FL19682, highly similar to Solute carrier family 7, facilitated glucose/transporter member 5 OS=Homo sapiens PE=2 SV=1	[CNA1_HUMAN]	12.44	8	11	11	23	1.000	22	11.654	47.959	438	47.849	
B2R4V4	CNA1 FL19622, highly similar to Homo sapiens barrier to autophagy factor 1 (BANF1) mRNA OS=Homo sapiens PE=2 SV=1	[B2R4V4_HUMAN]	24.72	6	4	4	20	1.000	19	5.659	47.961	89	10.110	
Q10463	Cytosolic oxidase subunit 1 OS=Homo sapiens GN-COX6A1 PE=1 SV=1	[COX6A1_HUMAN]	11.19	10	6	6	14	1.000	14	16.527	47.961	89	10.110	
Q14288	ES ubiquitin-protein ligase BRE1A OS=Homo sapiens GN-RNF201 PE=1 SV=2	[BRE1A_HUMAN]	11.19	10	6	6	7	15	0.980	14	10.979	47.880	630	70.928
P03870	Packinectin OS=Homo sapiens GN-PLK1 PE=1 SV=3	[PLK1_HUMAN]	11.43	2	5	5	15	1.000	13	8.604	47.747	350	40.089	
B0RY44	Lukocyte adhesion relation factor OS=Homo sapiens GN-LECAE1 PE=1 SV=3	[B0RY44_HUMAN]	21.87	2	10	10	11	1.000	10	11.118	47.747	350	40.089	
Q43488	Allatxin B1 aldehyde reductase member 2 OS=Homo sapiens GN-ARKT42 PE=1 SV=3	[ARKT2_HUMAN]	11.17	5	7	7	8	22	1.000	10	16.948	47.724	359	39.564
Q13263	Mitochondrial oxidase subunit 1 OS=Homo sapiens GN-COX6A1 PE=1 SV=1	[COX6A1_HUMAN]	11.19	10	6	6	14	1.000	14	17.705	47.623	359	39.564	
B3KX23	cDNA FL144516, clone UTERU050260, highly similar to Homo sapiens DEAD (Asp-Glu-Ala-Asp) box polypeptide 42 (DDX42), transcript variant 2, mRNA OS=Homo sapiens	[DDX42_HUMAN]	19.29	7	12	13	20	0.975	18	14.029	47.642	674	73.236	
Q02621	Nuclear pore complex protein Nuclep20 OS=Homo sapiens GN-NUP205 PE=1 SV=3	[NUP205_HUMAN]	7.01	6	13	13	13	1.000	13	13.991	47.608	212	227.776	
Q13263	Orotidine aminotransferase, mitochondrial OS=Homo sapiens GN-OAT1 PE=1 SV=1	[OAT1_HUMAN]	17.54	2	2	2	10	1.000	10	11.654	47.599	438	47.849	
Q03878	Ribonuclease P subunit 1 OS=Homo sapiens GN-RNOL1 PE=1 SV=2	[RNOL1_HUMAN]	10.21	1	14	14	18	0.991	17	11.406	47.583	1498	167.252	
Q12742	Hepatocellular growth protein 1 OS=Homo sapiens GN-HGP1 PE=1 SV=1	[HGP1_HUMAN]	10.41	10	10	10	15	1.000	15	15.672	47.583	1498	167.252	
Q06717	Ankyrin repeat and KH domain-containing protein 1 OS=Homo sapiens GN-ANKRD1 PE=1 SV=1	[ANKRD1_HUMAN]	15.67	17	8	8	12	1.000	11	14.545	47.437	2542	269.291	
V91R05	Epididymis secretary protein L16 OS=Homo sapiens GN-HEL-S5 PE=2 SV=1	[V91R05_HUMAN]	26.63	2	4	4	4	1.000	4	6.540	47.279	162	17.020	
Q06717	OT5489, highly similar to Solute carrier family 7, facilitated glucose/transporter member 5 OS=Homo sapiens PE=2 SV=1	[OT5489_HUMAN]	11.39	3	3	3	23	0.993	23	11.769	47.269	357	38.949	
B2RDR4	CNA1 FL19672, highly similar to Homo sapiens testis derived protein 3 (LIM domain), transcript variant 1, mRNA OS=Homo sapiens PE=2 SV=1	[B2RDR4_HUMAN]	28.65	9	10	10	16	1.000	16	14.714	47.244	421	47.934	
P09951	LE1 anterior rhodopsin OS=Homo sapiens GN-RHOA PE=1 SV=1	[RHOA_HUMAN]	19.82	8	6	6	10	1.000	10	16.265	47.244	421	47.934	
G3V256	Zinc finger CCH domain-containing protein 14 OS=Homo sapiens GN-CCZC14 PE=1 SV=1	[G3V256_HUMAN]	15.21	14	9	9	18	1.000	17	10.488	47.133	605	68.307	
GNV919	Nuclear protein localization factor RBM22 OS=Homo sapiens GN-RBM22 PE=1 SV=1	[RBM22_HUMAN]	18.22	3	10	10	10	1.000	10	8.554	47.130	420	46.865	
Q13263	CNA1 FL19682 OS=Homo sapiens GN-CNA1 PE=1 SV=1	[CNA1_HUMAN]	11.48	3	10	10	19	1.000	17	11.711	47.080	397	43.178	
Q12742	Nuclear protein localization factor RBM22 OS=Homo sapiens GN-RBM22 PE=1 SV=1	[RBM22_HUMAN]	15.13	6	9	9	17	0.998	16	10.372	47.096	608	68.079	
Q06717	Hexasome OS=Homo sapiens GN-H6V1 PE=1 SV=1	[H6V1_HUMAN]	9.58	7	6	6	10	1.000	8	6.108	46.989	889	100.949	
P25774	Cathespian 3 OS=Homo sapiens GN-CTSP3 PE=1 SV=1	[CTSP3_HUMAN]	15.71	3	5	5	19	1.046	18	11.242	46.914	331	37.471	
EPSP01	Nuclear RNA-methyltransferase 1 OS=Homo sapiens GN-RNMT1 PE=1 SV=1	[EPSP01_HUMAN]	16.62	12	6	6	17	1.000	14	12.244	46.782	325	37.688	
Q06717	CNA1 FL19682, highly similar to Homo sapiens acyl-CoA oxidase 2 (mitochondrial 3-oxoacyl-Coenzyme A thioester) (ACAD2), nuclear gene encoding 1	[CNA1_HUMAN]	12.22	8	8	8	13	1.000	12	6.777	46.782	325	37.688	
HOV919	60S ribosomal protein L16 OS=Homo sapiens GN-RPL16 PE=1 SV=1	[RPL16_HUMAN]	20.22	4	5	5	23	1.000	21	16.277	46.693	189	21.556	
Q13263	Nucleolar phosphoprotein OS=Homo sapiens GN-NP1 PE=1 SV=1	[NP1_HUMAN]	15.71	3	3	3	19	1.000	17	9.821	46.693	189	21.556	
ABH93	Centrosomal protein 170kDa OS=Homo sapiens GN-CEP170 PE=2 SV=1	[ABH93_HUMAN]	8.49	15	11	11	18	1.000	17	11.457	46.463			

AA02AR2Y2	HCG3020a, isoform CRA_a OS=Homo sapiens GH-HCG_3020a PE=4 Sv1+ [AA02AR2Y2_HUMAN]	4.83	14	10	10	15	1,000	10	8,288	34,542	2298	297,075
B4D703	CDNA1538, isoform CRA_a OS=Homo sapiens ATPase regulatory subunit 7 OS=Homo sapiens Pe2 Sv1+ [B4D703_HUMAN]	17	6	10	10	15	1,000	15	29,696	64,500	1728	247,860
B3LEU6	TNME24 protein (Fragment) OS=Homo sapiens GH-TNME24 PE=2 Sv1+ [B3LEU6_HUMAN]	9.51	10	6	15	1,000	15	10,000	30,000	34,517	673	76,391
GN09W8	Adenosine and glutamate-rich protein 1 OS=Homo sapiens GH-ANGRLU1 PE=1 Sv1+ [GN09W8_HUMAN]	21.88	8	6	15	1,000	15	18,041	34,428	273	33,197	
B4C052	CDNA15560, highly similar to Hev10casein (EC 2.1.1) OS=Homo sapiens Pe4 Sv1+ [B4C052_HUMAN]	10.93	10	6	15	1,000	15	11,830	21,910	115	10,248	
GN09S2	ZS8 ribosomal protein S18a, mitochondrial OS=Homo sapiens GH-MRPS18a PE=1 Sv1+ [RT18A_HUMAN]	29.52	2	7	14	1,000	1,000	12,837	34,370	196	22,170	
QB09H1	Thrombospondin transmembrane protein 1 OS=Homo sapiens GH-TSMP1 PE=1 Sv1+ [QB09H1_HUMAN]	4.29	10	10	10	1,000	1,000	15,528	29,171	16	17,171	
B4D078	CDNA18158, highly similar to ADP-ribosylation factor-like protein B8 OS=Homo sapiens Pe2 Sv1+ [B4D078_HUMAN]	16.82	5	3	13	1,069	13	13,835	34,318	177	20,585	
B4E146	CDNA157889, highly similar to Cytochrome b-240 ligand like OS=Homo sapiens Pe2 Sv1+ [B4E146_HUMAN]	19.28	2	2	23	1,000	23	16,411	34,305	131	14,071	
BRE543	Putative uncharacterized protein (strain MHOM/GT2001/1103) GH-LHMDM_33_266 PE=4 Sv1+ [BRE543_LEIMUJ]	12.00	2	8	12	1,000	12	24,409	34,265	681	74,808	
B4E122	CDNA151530, highly similar to Helyocyte growth factor-regulated tyrosine kinase substrate OS=Homo sapiens Pe2 Sv1+ [B4E122_HUMAN]	12.55	7	8	12	1,000	12	24,409	34,265	681	74,808	
ES996	Putative ATP-dependent RNA polymerase subunit (strain MHOM/GT2001/1103) GH-LHMDM_34_3100 PE=3 Sv1+ [ES996_LEIMUJ]	4.29	10	10	10	1,000	1,000	15,528	29,171	16	17,171	
AA02AR2C5	Chitinase domain containing 1, isoform CRA_a OS=Homo sapiens GH-CHD1 PE=1 Sv1+ [AA02AR2C5_HUMAN]	12.89	10	5	5	12	1,000	12	2,107	34,178	386	44,090
QB09W4	Delta-catenin-like protein 1 OS=Homo sapiens GH-CTNBL1 PE=1 Sv1+ [QB09W4_HUMAN]	9.41	2	6	8	1,020	14	13,266	34,129	563	63,132	
QB09W5	CDNA157890, highly similar to Cytoskeleton-associated protein 1 OS=Homo sapiens Pe2 Sv1+ [QB09W5_HUMAN]	19.28	2	2	23	1,000	23	16,411	34,265	681	74,808	
DGZG78	RHO-associated protein kinase OS=Homo sapiens GH-ROCK1 PE=1 Sv1+ [DGZG78_HUMAN]	6.43	2	9	13	1,000	13	2,086	34,101	1354	156,145	
QB09W6	HCC2255a, isoform CRA_a OS=Homo sapiens GH-HCC2255a PE=1 Sv1+ [QB09W6_HUMAN]	9.36	14	10	14	1,000	14	15,338	33,629	1153	130,078	
B4E090	CDNA154220, highly similar to Long-chain fatty acid-CoA ligase 1 (EC 6.2.1.3) OS=Homo sapiens Pe2 Sv1+ [B4E090_HUMAN]	13.7	12	8	9	1,012	14	11,295	34,079	684	74,206	
GBE0G6	Et ubiquitin-protein ligase TRIP2 OS=Homo sapiens GH-TRIP2 PE=1 Sv1+ [GBE0G6_HUMAN]	12.77	6	1	8	1,000	2	0,000	34,031	430	45,286	
QB09M1	Putative endonuclease-like protein 1 beta subunit OS=Homo sapiens GH-ENL1 PE=1 Sv1+ [QB09M1_HUMAN]	27.36	1	1	10	1,000	10	7,526	33,842	187	20,761	
P25098	Beta-adrenergic receptor kinase 1 OS=Homo sapiens GH-ADRBK1 PE=1 Sv1+ [P25098_HUMAN]	12.77	6	1	8	1,000	15	17,444	33,943	689	79,522	
QB09A0	Uncoupling protein 3/TfO2 OS=Homo sapiens GH-UCP3 PE=1 Sv1+ [QB09A0_HUMAN]	6.04	6	3	3	12	1,000	12	1,842	33,842	187	20,761
QB09M0	Cystine-rich with EGF-like domain protein 2 OS=Homo sapiens GH-CRELD2 PE=1 Sv1+ [QB09M0_HUMAN]	13.88	3	5	5	1,000	12	11,873	33,801	353	38,186	
QB09M7	UCP9 protein OS=Homo sapiens GH-UCP9 PE=1 Sv1+ [QB09M7_HUMAN]	28.24	2	3	14	1,000	12	13,882	33,785	85	9,947	
AA02AR2G3	HCC2178, isoform CRA_a OS=Homo sapiens GH-HCC2178 PE=1 Sv1+ [AA02AR2G3_HUMAN]	5.3	9	10	11	1,000	10	23,177	33,700	209	23,297	
QB09Q1	Mitochondrial intermembrane space import and assembly protein 4 OS=Homo sapiens GH-IMM4 PE=1 Sv1+ [QB09Q1_HUMAN]	28.87	2	4	4	1,000	13	0,000	33,667	142	15,986	
Q14617	AP-3 complex subunit delta 1 OS=Homo sapiens GH-AP3D1 PE=1 Sv1+ [Q14617_HUMAN]	8.5	7	10	10	1,000	14	10,331	33,616	11	11,611	
AA02AR2C7	Calcium transporting ATPase OS=Homo sapiens GH-ATP2B1 PE=3 Sv1+ [AA02AR2C7_HUMAN]	7.95	16	6	11	1,000	7	6,487	33,611	1220	134,600	
B1ZG03	CDNA181688, highly similar to Transmembrane 9 superfamily member protein 1 OS=Homo sapiens Pe2 Sv1+ [B1ZG03_HUMAN]	12.77	11	6	9	1,000	12	5,887	33,576	615	92,427	
Q1K7C2	NADH dehydrogenase subunit 1 beta subunit OS=Homo sapiens GH-ND1B PE=1 Sv1+ [Q1K7C2_HUMAN]	16.2	1	1	12	1,000	12	10,000	33,567	6	7,681	
QY0256	Translation machinery-associated protein 7 OS=Homo sapiens GH-TMAP PE=1 Sv1+ [QY0256_HUMAN]	43.75	14	3	4	2,047	18	11,991	33,511	64	7,062	
Q1ZK26	Transcription elongation factor 37B OS=Homo sapiens GH-TEF37B PE=1 Sv1+ [Q1ZK26_HUMAN]	6.78	11	10	10	1,000	14	14,840	33,500	128	149,949	
QB09L4	Growth stimulation factor 2 subunit 2 variant OS=Homo sapiens GH-GSTF2 PE=1 Sv1+ [QB09L4_HUMAN]	11.53	1	5	6	1,000	12	10,000	33,433	616	64,398	
GBE0G2	Et ubiquitin-protein ligase TRIM5 OS=Homo sapiens GH-TRIM5 PE=1 Sv1+ [GBE0G2_HUMAN]	9.4	2	6	8	1,000	8	0,000	33,432	758	81,437	
QB09L13	Putative uncharacterized protein (strain MHOM/GT2001/1103) GH-LHMDM_36_1640 PE=4 Sv1+ [QB09L13_HUMAN]	18.13	1	13	10	1,000	10	21,829	33,426	11	12,490	
QB09S8	Nucleic domain-containing protein 1 OS=Homo sapiens GH-NUCD1 PE=1 Sv1+ [QB09S8_HUMAN]	7.55	1	5	12	1,000	12	24,441	33,355	883	66,713	
QB09S9	Pleasin 2 OS=Homo sapiens GH-PLS2 PE=1 Sv1+ [QB09S9_HUMAN]	6.04	9	10	10	1,000	10	14,757	33,345	10	10,248	
BKX11	CDNA146571, clone THYMUS041428, highly similar to Proximal ATP-dependent RNA helicase DDX3 (EC 3.6.1.1) OS=Homo sapiens Pe2 Sv1+ [BKX11_HUMAN]	13.7	11	11	11	1,000	12	5,412	33,187	580	93,777	
B4E3A8	CDNA153363, highly similar to Leucocyte adhesion inhibitor OS=Homo sapiens Pe2 Sv1+ [B4E3A8_HUMAN]	11.21	2	8	8	1,024	14	19,888	33,170	341	38,861	
C126A	GCAM 1, isoform CRA_a OS=Homo sapiens GH-GCAM1 PE=1 Sv1+ [C126A_HUMAN]	14.1	5	2	4	1,000	7	14,876	33,167	318	35,859	
P09091	Ribose-phosphate cyclohydrolase 1 OS=Homo sapiens GH-RP1 PE=1 Sv1+ [P09091_HUMAN]	13.1	5	4	10	1,000	10	5,023	33,149	318	34,812	
Q12965	Uncoupling protein 5 OS=Homo sapiens GH-UCP5 PE=1 Sv1+ [Q12965_HUMAN]	6.05	2	6	10	1,000	10	2,528	33,128	68	12,982	
ARK670	CDNA157549, highly similar to Homo sapiens aquaporin homolog (mouse) (AQR), mRNA OS=Homo sapiens Pe2 Sv1+ [ARK670_HUMAN]	4.58	4	7	7	1,000	11	2,914	33,122	1485	171,187	
BKX740	CDNA150510, highly similar to Homo sapiens eye (JTV1), mRNA OS=Homo sapiens Pe2 Sv1+ [BKX740_HUMAN]	21.25	4	7	7	1,000	10	15,218	33,120	320	35,425	
BKX741	GPA stem-loop containing protein 1 OS=Homo sapiens GH-GP1 PE=1 Sv1+ [BKX741_HUMAN]	10.46	9	7	10	1,000	10	7,745	33,099	338	37,607	
F8V1L1	Densin-like protein OS=Homo sapiens GH-DENL1 PE=1 Sv1+ [F8V1L1_HUMAN]	30	4	5	7	1,000	10	10,298	33,078	160	17,759	
MLLSEP19B	Myosin heavy chain 10 OS=Homo sapiens GH-MHC10 PE=1 Sv1+ [MLLSEP19B_HUMAN]	11.63	1	5	10	1,000	10	18,128	33,069	684	59,944	
Q17LY3	Mitochondrial ribonuclease P protein 3 OS=Homo sapiens GH-TRMT10C PE=1 Sv1+ [Q17LY3_HUMAN]	17.87	2	5	12	1,048	12	15,178	33,065	403	47,717	
P17744	Apoptate aminotransferase, cytoplasmic OS=Homo sapiens GH-GOT1 PE=1 Sv1+ [P17744_HUMAN]	19.72	3	7	7	1,000	12	24,272	33,025	413	46,219	
B1ZG15	Resic-like membrane protein OS=Homo sapiens GH-AMR8 PE=1 Sv1+ [B1ZG15_HUMAN]	22.72	9	12	10	1,000	10	12,886	32,977	93	93,885	
B4D0M3	SWIN5F-related, matrix-associated actin-dependent regulator of chromatin subfamily member 1 OS=Homo sapiens GH-SMARCE1 PE=1 Sv1+ [B4D0M3_HUMAN]	11.2	7	3	4	1,000	7	12,876	33,014	393	44,743	
CDNA154538	CDNA154538, highly similar to Transcription factor 12 OS=Homo sapiens GH-TF12 PE=1 Sv1+ [CDNA154538_HUMAN]	7.61	2	6	14	1,000	13	6,300	33,000	389	89,611	
Q1YH87	Aladin-2 (Fragment) OS=Homo sapiens GH-ALX2 PE=1 Sv1+ [Q1YH87_HUMAN]	8.9	13	3	3	1,006	7	29,478	32,996	916	98,055	
Q13129	Zinc finger protein RF OS=Homo sapiens GH-RFP PE=1 Sv1+ [Q13129_HUMAN]	7.8	2	9	9	1,000	10	0,000	32,963	194	217,813	
AA02AR2S8	Cytoskeleton-associated protein 1 OS=Homo sapiens GH-CAP1 PE=1 Sv1+ [AA02AR2S8_HUMAN]	20.12	1	9	9	1,000	10	7,745	32,960	377	42,406	
QB09T7	Histone-lysine N-methyltransferase 3 OS=Homo sapiens GH-SETD3 PE=1 Sv1+ [QB09T7_HUMAN]	11.4	3	5	5	1,000	12	5,776	32,940	594	67,215	
B4D727	CDNA154709, highly similar to Poly(ADP-ribose) polymerase subunit delta 3 OS=Homo sapiens Pe2 Sv1+ [B4D727_HUMAN]	7.73	11	7	7	1,000	7	2,943	32,924	465	51,310	
B4D730	CDNA150318, highly similar to Lymphoid-specific membrane protein OS=Homo sapiens Pe2 Sv1+ [B4D730_HUMAN]	11.43	3	4	11	1,000	10	0,000	32,925	446	49,047	
QB09K4	Rel1 domain-binding protein 1-like protein 1 OS=Homo sapiens GH-RBP1L1 PE=1 Sv1+ [QB09K4_HUMAN]	6.11	3	7	7	1,000	10	0,000	32,899	1523	161,758	
BKX146	Ubiquitin-like protein OS=Homo sapiens GH-UBL1 PE=1 Sv1+ [BKX146_HUMAN]	12.15	2	13	13	1,000	12	10,000	32,899	1523	161,758	
B7Z381	Rel1 domain OS=Homo sapiens Pe2 Sv1+ [B7Z381_HUMAN]	12.15	2	8	8	1,000	8	3,046	32,853	205	22,913	
ESB278	Putative AER-like fibroblast cell surface heparan sulfate proteoglycan OS=Homo sapiens Pe2 Sv1+ [ESB278_LEIMUJ]	22.47	2	2	4	1,000	2	40,885	32,802	178	179,488	
ESM613	Phenylalanine hydroxylase beta subunit OS=Homo sapiens GH-PAH1 PE=1 Sv1+ [ESM613_HUMAN]	13.82	2	5	5	1,000	14	12,854	32,739	1273	145,085	
BKZC27	Ethylmalonic encephalopathy 1, isoform CRA_a OS=Homo sapiens GH-ETHE1 PE=1 Sv1+ [BKZC27_HUMAN]	27.31	4	5	5	1,000	12	7,692	32,726	227	29,490	
Q1G974	CluG19 protein OS=Homo sapiens GH-CLU19 PE=1 Sv1+ [Q1G974_HUMAN]	10.08	1	5	5	1,000	12	6,463	32,719	684	82,480	
Q15427	Noncarboxylate transferase 4 OS=Homo sapiens GH-SLCA3 PE=1 Sv1+ [Q15427_HUMAN]	8.82	5	4	13	1,002	12	5,118	32,715	465	49,427	
QB09G9	Cytoskeleton cytoskeleton 1 OS=Homo sapiens GH-CTC1 PE=1 Sv1+ [QB09G9_HUMAN]	23.71	1	9	9	1,000	12	5,740	32,713	523	58,584	
EPD43	Negative elongation factor 5 (Fragment) OS=Homo sapiens GH-NEFL5 PE=1 Sv1+ [EPD43_HUMAN]	2.5	4	5	11	1,000	10	0,000	32,683	603	260,040	
H7C475	Muscleblind-like protein 1 (Fragment) OS=Homo sapiens GH-MBLN1 PE=1 Sv1+ [H7C475_HUMAN]	16.16	6	6	8	1,000	12	2,442	32,677	329	33,797	
F7S381	Perlecan core protein 14 OS=Homo sapiens GH-PC14 PE=1 Sv1+ [F7S381_HUMAN]	13.26	1	10	10	1,000	12	12,419	32,677	10	10,248	
B4E0D0	CDNA159482, highly similar to Ecton transferase-like protein OS=Homo sapiens Pe2 Sv1+ [B4E0D0_HUMAN]	13.31	5	7	7	1,000	11	17,949	32,647	556	61,346	
QF7W2	GNAS complex subunit OS=Homo sapiens GH-GNAS PE=1 Sv1+ [QF7W2_HUMAN]	15.53	19	2	3	1,000	12	4,691	32,646	389	42,462	
HBR02	Sulfhydryl oxidase (Fragment) OS=Homo sapiens GH-SFO1 PE=1 Sv1+ [HBR02_HUMAN]	26.62	7	2	10	1,000	6	0,000	32,645	109	15,768	
P20262	Parathyroid hormone OS=Homo sapiens GH-PTH PE=1 Sv1+ [P20262_HUMAN]	23.53	4	4	4	1,000	15	6,513	32,606	102	11,523	
QB09W3	Uncoupling protein 5 OS=Homo sapiens GH-UCP5 PE=1 Sv1+ [QB09W3_HUMAN]	6.05	2	7	7	1,000	10	2,528	32,615	68	12,982	
A4J43	Brain type III malate dehydrogenase OS=Homo sapiens GH-MD3 PE=1 Sv1+ [A4J43_HUMAN]	19.05	4	5	6	1,000	12	17,483	32,428	110	24,802	
AA02AR2H2	Serine acetyltransferase OS=Homo sapiens GH-SAT1, isoform CRA_a OS=Homo sapiens GH-SAT1 PE=1 Sv1+ [AA02AR2H2_HUMAN]	6.17	9	6	17	1,000	11	17,881	32,418	102	138,162	
ARK916	CDNA178121, highly similar to Homo sapiens serine finger CCH-type, anti-hepatic (ZC3H4V1), transmembrane variant 1, mRNA OS=Homo sapiens Pe2 Sv1+ [ARK916_HUMAN]	7.6	7	6	12	1,000	12	9,838	32,483	902	92,476	
P12128	V-type proton ATPase subunit C 1 OS=Homo sapiens GH-VATP1C PE=1 Sv1+ [P12128_HUMAN]	14.42	3	7	7	1,000	14	12,930	32,478	382	43,914	
QB09M8	Protein FAM107B OS=Homo sapiens GH-FAM107B PE=1 Sv1+ [QB09M8_HUMAN]	11.03	10	10	10	1,000	10	5,074	32,467	11	15,438	
B4D9Y9	Interleukin enhancer-binding factor 2 OS=Homo sapiens GH-IEBF2 PE=1 Sv1+ [B4D9Y9_HUMAN]	18.27	5	5	13	1,000	13	13,745	32,413	382	38,886	
Q1456	TM64-type zinc finger protein OS=Homo sapiens GH-ZFP1 PE=1 Sv1+ [Q1456_HUMAN]	11	5	6	6	1,000	11	0,000	32,400	69	69,430	
QB09Z6	Apoptosis C1 OS=Homo sapiens GH-APC3 PE=1 Sv1+ [QB09Z6_HUMAN]	16.16	2	7	7	1,000	10	7,482	32,365	99	10,945	
P20265	CDNA154973, clone TRACD301810, highly similar to 51 kDa FK506-binding protein OS=Homo sapiens Pe2 Sv1+ [P20265_HUMAN]	14.04	1	2	7	1,000	3	1,436	32,361	456	59,833	
Q14966	Tec tyrosine kinase OS=Homo sapiens GH-TEC PE=1 Sv1+ [Q14966_HUMAN]	15.27	10	6	10	1,000	10	10,000	32,361	1078	128,480	
P40306	Proteasome subunit beta type 1 OS=Homo sapiens GH-PSM1 PE=1 Sv1+ [P40306_HUMAN]	11.36	3	4	4	1,000	12	9,076	32,328	273	28,918	
QB09D2	CTC1 protein antigen set2 OS=Homo sapiens GH-CTC1 PE=1 Sv1+ [QB09D2_HUMAN]	9.88										

J3KR4	Cytoplasmic dynein 1 light intermediate chain 2 (Fragment) OS=Homo sapiens GN-DYCNL12C PE=1 SV=1 [J3KR4_HUMAN]	33.53	3	5	5	11	0.000	29.288	167	17.767
Q282D5	35S ribosomal protein OS=Homo sapiens GN-35S PE=2 SV=1 [Q282D5_HUMAN]	3.865	1	1	1	10	0.000	33.175	645	645
AA084X187	Chromatin target of PRMT1 protein OS=Homo sapiens GN-CHTTP PE=1 SV=1 [AA084X187_HUMAN]	30.28	2	2	2	10	0.000	29.269	76	8.515
BDRD51	CDNA FLJ38455, highly similar to Hmo sapiens Downy syndrome critical region gene 2 (DSRC2), mRNA OS=Homo sapiens PE=2 SV=1 - [BDRD51_HUMAN]	13.19	3	3	3	8	0.000	20.226	286	32.861
Q8N919	RNA polymerase II subunit OS=Homo sapiens GN-RNAPII PE=1 SV=1 [Q8N919_HUMAN]	1.266	1	1	1	10	0.000	29.269	76	8.515
BZ7W5	Cystathionine beta-lyase OS=Homo sapiens PE=2 SV=1 - [BZ7W5_HUMAN]	10.15	9	5	10	0	0.000	22.819	29.149	463
BZ3K40	DNA topoisomerase II subunit OS=Homo sapiens GN-POLB1 PE=2 SV=1 [BZ3K40_HUMAN]	7.14	2	2	2	10	0.000	15.602	191.3	1107
BZ8R06	CDNA FLJ38391, Hmo sapiens FK506 binding protein 8, 38kDa (FKBP8), mRNA OS=Homo sapiens PE=2 SV=1 - [BZ8R06_HUMAN]	17.98	6	6	6	12	0.000	22.819	29.149	463
B4D48	CDNA FLJ1221, highly similar to Prokaryotic F2C2 OS=Homo sapiens PE=2 SV=1 - [B4D48_HUMAN]	17.08	9	9	9	6	0.000	17.435	20.126	1023
PT770	Deoxyribonuclease OS=Homo sapiens PE=1 SV=1 [PT770_HUMAN]	10.34	1	1	1	10	0.000	29.269	76	8.515
B4E110	Adenosine nucleoside synthetase isozyme 2 OS=Homo sapiens GN-ADSS2 PE=1 SV=1 [B4E110_HUMAN]	10.8	5	5	5	12	0.000	16.405	29.134	435
Q2Y8V1	Colony-stimulating factor 2, mitochondrial OS=Homo sapiens GN-CSF2C2 PE=1 SV=1 - [Q2Y8V1_HUMAN]	15.23	2	2	2	10	0.000	20.514	15.1	15.003
A4LA43	Alpha thalassaemia intermedia syndrome X-linked OS=Homo sapiens GN-ATRX PE=4 SV=1 - [A4LA43_HUMAN]	3.33	6	7	8	13	0.000	13.756	20.91	2492
P4A33	ATP-binding cassette sub-family D member 1 OS=Homo sapiens GN-ABCD1 PE=2 SV=1 - [P4A33_HUMAN]	6.99	5	5	5	13	0.000	26.810	20.042	745
Q2Y8Z5	Thrombospondin 1 ligase subunit OS=Homo sapiens GN-THSD4B PE=1 SV=1 [Q2Y8Z5_HUMAN]	10.27	1	1	1	10	0.000	29.269	76	8.515
Q76003	Gutathione S-transferase OS=Homo sapiens PE=2 SV=1 - [Q76003_HUMAN]	21.79	1	8	8	13	0.000	16.154	29.009	335
B4D158	CDNA FLJ15692, highly similar to Rhesus erythropoietin 5 OS=Homo sapiens PE=2 SV=1 - [B4D158_HUMAN]	7.92	6	4	4	10	0.000	29.269	76	8.515
B4D100	CDNA FLJ15692, highly similar to mRNA angiotensin OS=Homo sapiens PE=2 SV=1 - [B4D100_HUMAN]	7.92	6	4	4	10	0.000	29.269	76	8.515
AA024R81	Retin (Red-Sternberg cell-expressed intermediate filament-associated protein), isoform CRA A OS=Homo sapiens GN-RSN PE=4 SV=1 - [AA024R81_HUMAN]	17.72	16	7	8	12	0.000	13.863	28.942	1427
Q8R179	CD28 domain OS=Homo sapiens GN-CD28C1 PE=1 SV=2 - [Q8R179_HUMAN]	17.52	1	1	1	10	0.000	11.818	314	35.589
Q8R210	PNAS-20 OS=Homo sapiens PE=2 SV=1 - [Q8R210_HUMAN]	25.32	1	2	2	12	0.000	20.904	28.942	1427
Q8R211	Thymocyte cleaved protein 1 OS=Homo sapiens GN-THY1 PE=1 SV=1 - [Q8R211_HUMAN]	17.52	1	1	1	10	0.000	11.818	314	35.589
Q8R212	Casainicidase B protein homolog OS=Homo sapiens GN-CLPB PE=1 SV=1 - [Q8R212_HUMAN]	6.66	9	5	5	12	0.029	11.923	20.977	707
Q8R213	CLIP-associated protein 2 OS=Homo sapiens GN-CLASP2 PE=1 SV=2 - [Q8R213_HUMAN]	8.56	21	9	9	11	0.000	11.923	20.977	707
Q8R214	Formin-like protein OS=Homo sapiens GN-FML1 PE=1 SV=3 - [Q8R214_HUMAN]	8.56	4	3	3	10	0.000	8.406	29.109	1100
J3CL39	Haptoglobin (Fragment) OS=Homo sapiens GN-HP PE=1 SV=1 - [J3CL39_HUMAN]	15.07	16	5	5	11	0.000	20.248	28.728	365
Q2S41	RNA polymerase-associated-protein 1 homolog OS=Homo sapiens GN-PRP1 PE=1 SV=4 - [Q2S41_HUMAN]	11.68	3	10	10	10	0.000	9.270	29.708	710
B4E0K4	CDNA FLJ56569, highly similar to Hmo sapiens pte-8 cell leukemia transcription factor interacting protein 1 (PBXK1), mRNA OS=Homo sapiens PE=2 SV=1 - [B4E0K4_HUMAN]	11.28	5	6	6	12	0.000	2.048	29.576	68.678
Q3148	mRNA cap guanine N7 methyltransferase OS=Homo sapiens GN-NMT7 PE=1 SV=1 - [Q3148_HUMAN]	20.49	5	5	5	10	0.000	17.769	28.885	476
Q8R215	Patent myelin basic protein OS=Homo sapiens GN-PM1 PE=1 SV=1 - [Q8R215_HUMAN]	20.49	5	5	5	10	0.000	28.841	410	450.68
Q8R216	Vesicle-associated membrane protein-associated protein B OS=Homo sapiens GN-VAPB PE=1 SV=3 - [Q8R216_HUMAN]	17.77	3	4	4	11	0.000	22.281	28.623	247
Q8R217	Mitochondrial ribosomal protein L11 isoform a variant (Fragment) OS=Homo sapiens PE=2 SV=1 - [Q8R217_HUMAN]	38.54	4	4	4	10	0.000	26.851	28.622	1262
Q8R218	Gua mutator factor beta OS=Homo sapiens GN-GMBF PE=1 SV=2 - [Q8R218_HUMAN]	25.35	4	2	2	11	0.000	5.267	28.537	142
Q8R219	Serine diacylglycerol kinase OS=Homo sapiens GN-SDK2 PE=1 SV=1 - [Q8R219_HUMAN]	16.11	4	5	5	9	0.000	9.537	28.335	329
Q8R220	Isolectin B4-binding protein OS=Homo sapiens GN-IB4 PE=1 SV=2 - [Q8R220_HUMAN]	17.08	1	1	1	10	0.000	19.704	28.327	329
T1WFC1	Glycyl-associated P2Z and coiled-coil motif containing protein transcript variant 4 OS=Homo sapiens GN-GOPC PE=2 SV=1 - [T1WFC1_HUMAN]	17.34	3	6	6	10	0.000	10.928	28.516	398
Q8N9H1	DnaI topoisomerase I OS=Homo sapiens GN-DNAI1 PE=1 SV=1 - [Q8N9H1_HUMAN]	10.27	1	1	1	10	0.000	15.013	28.021	659
H3BP76	Prefoldin subunit 5 (Fragment) OS=Homo sapiens GN-PFD5 PE=1 SV=1 - [H3BP76_HUMAN]	26.7	4	4	4	11	0.000	17.524	28.456	317
Q8R21	Small nuclear ribonucleoprotein-associated protein OS=Homo sapiens GN-SNRAP PE=2 SV=1 - [Q8R21_HUMAN]	22.08	13	5	5	14	0.000	16.261	28.408	231
Q8R22	RNA polymerase II subunit 4 OS=Homo sapiens GN-RNAPII PE=1 SV=1 - [Q8R22_HUMAN]	11.68	3	10	10	10	0.000	9.270	29.708	710
AA024R82	KIAA2010, isoform CRA a OS=Homo sapiens GN-KIAA2010 PE=4 SV=1 - [AA024R82_HUMAN]	8.41	9	4	4	7	0.000	15.927	28.363	820
H3R845	Reas-sapin OS=Homo sapiens GN-REAS PE=1 SV=1 - [H3R845_HUMAN]	22.08	13	5	5	14	0.000	16.261	28.408	231
Q15843	NEDD8 OS=Homo sapiens GN-NEDD8 PE=1 SV=1 - [Q15843_HUMAN]	39.51	5	3	3	4	0.000	13.862	28.285	81
Q8R23	Leucocyte antigen B (Fragment) OS=Homo sapiens GN-HLAB PE=4 SV=1 - [Q8R23_HUMAN]	27.12	229	0	0	11	0.000	11.113	28.241	89
Q8R24	Gaig ligand membrane protein 4 OS=Homo sapiens GN-GALM4 PE=1 SV=1 - [Q8R24_HUMAN]	17.48	2	2	2	11	0.000	23.875	28.127	688
Q3J38	Transmembrane-associated protein subunit alpha OS=Homo sapiens GN-SSTR1 PE=1 SV=1 - [Q3J38_HUMAN]	17.17	6	2	2	12	0.000	3.052	28.225	285
Q8R25	CDNA FL3871, highly similar to Hmo sapiens alpha 2-macroglobulin (LYN), mRNA OS=Homo sapiens PE=2 SV=1 - [Q8R25_HUMAN]	17.58	6	2	2	11	0.000	1.554	28.152	512
HY020	Undersulfated protein (Fragment) OS=Homo sapiens GN-UPS4 PE=1 SV=1 - [HY020_HUMAN]	13.38	9	7	7	14	0.000	14.712	28.155	523
Q2Y74	WD40 repeat-containing protein SMU1 OS=Homo sapiens GN-SMU1 PE=1 SV=2 - [Q2Y74_HUMAN]	17.58	1	5	5	11	0.000	11.202	28.149	513
Q8R26	ATG-GAP-associated protein ANK repeat domain containing protein 2 OS=Homo sapiens GN-ANAPC2 PE=4 SV=1 - [Q8R26_HUMAN]	9.66	3	5	5	11	0.000	11.335	28.116	505
Q8R27	Protein FAM1142 OS=Homo sapiens GN-FAM1142 PE=1 SV=4 - [Q8R27_HUMAN]	17.23	12	7	7	10	0.000	13.315	28.116	505
AA024R83	Colony-stimulating factor 2 OS=Homo sapiens GN-CSF2 PE=1 SV=1 - [AA024R83_HUMAN]	15.23	2	2	2	10	0.000	16.808	28.068	619
Q8N9K0	Kinesin light chain 4 OS=Homo sapiens GN-KLCA PE=1 SV=3 - [Q8N9K0_HUMAN]	13.04	8	2	2	6	0.000	10.006	28.016	619
Q1397	Nucleoside-diphosphate Delta-isomerase 1 OS=Homo sapiens GN-NID1 PE=2 SV=2 - [Q1397_HUMAN]	10.36	3	5	5	9	0.000	13.573	28.023	227
Q8R28	LYOXC variant protein OS=Homo sapiens GN-LYOXC PE=2 SV=1 - [Q8R28_HUMAN]	15.13	7	8	8	10	0.000	12.228	28.011	229
G5E97	28S ribosomal protein S22, mitochondrial OS=Homo sapiens GN-MRPS22 PE=1 SV=1 - [G5E97_HUMAN]	17.71	8	6	6	10	0.000	12.888	28.038	319
B4E204	CDNA FL3872, highly similar to Hmo sapiens Nucleoside diphosphate kinase 2 OS=Homo sapiens PE=2 SV=1 - [B4E204_HUMAN]	15.87	6	6	6	10	0.000	12.888	28.038	319
Q8T81	Ribonuclease H2 subunit B OS=Homo sapiens GN-RNASEH2B PE=1 SV=1 - [Q8T81_HUMAN]	18.71	8	6	6	14	0.000	9.922	28.156	312
P8880	Homozygous protein cut-like 1 OS=Homo sapiens GN-CUTL1 PE=3 SV=3 - [P8880_HUMAN]	7.44	2	4	4	9	0.000	12.500	28.006	1505
Q8R29	RNA-binding protein 34 OS=Homo sapiens GN-RBP34 PE=1 SV=2 - [Q8R29_HUMAN]	4.52	4	4	4	9	0.000	9.859	28.000	164
Q8T10	Agmatinase-ribonuclease protein PMSR OS=Homo sapiens GN-PMSR PE=2 SV=2 - [Q8T10_HUMAN]	5.22	5	5	5	11	0.000	11.471	27.997	805
Q8R30	CDC9 regulatory protein 3 OS=Homo sapiens GN-C9ORF3 PE=1 SV=2 - [Q8R30_HUMAN]	5.22	3	3	3	10	0.000	13.334	27.997	805
P2828	ATP-binding cassette sub-family D member 3 OS=Homo sapiens GN-ABCD3 PE=1 SV=1 - [P2828_HUMAN]	17.59	3	5	5	12	0.000	9.024	27.955	659
T1782	CAMP-dependent protein kinase catalytic subunit alpha OS=Homo sapiens GN-PRKACA PE=1 SV=2 - [T1782_HUMAN]	10.99	19	7	7	11	0.000	8.194	27.955	351
Q8R31	Oran 1 interacting protein OS=Homo sapiens GN-OIP1 PE=1 SV=1 - [Q8R31_HUMAN]	15.11	9	10	10	10	0.000	4.704	27.955	351
Q8R32	Proteasome subunit beta type OS=Homo sapiens GN-PSMB7 PE=1 SV=1 - [Q8R32_HUMAN]	14.44	5	4	4	12	0.000	10.104	27.946	297
Q8R33	Colin OS=Homo sapiens GN-COL PE=1 SV=1 - [Q8R33_HUMAN]	4.56	4	4	4	10	0.000	7.944	27.946	297
B3KR73	CDNA FL35079.9a, clone FLAC6205283, highly similar to Lysosome-associated membrane glycoprotein 1 OS=Homo sapiens PE=2 SV=1 - [B3KR73_HUMAN]	7.09	3	3	3	10	0.000	20.166	27.938	395
P41223	Protein BUD31 homolog OS=Homo sapiens GN-BUD31 PE=1 SV=1 - [P41223_HUMAN]	31.94	3	6	6	10	0.000	13.429	27.907	144
B4E173	Ubiquitin carboxyl terminal hydrolase 1 OS=Homo sapiens GN-UCHL1 PE=1 SV=1 - [B4E173_HUMAN]	13.38	3	3	3	10	0.000	14.163	27.878	409
Q8R34	POLDP3 (Fragment) OS=Homo sapiens GN-POLDP3 PE=2 SV=2 - [Q8R34_HUMAN]	17.33	12	7	7	11	0.000	15.935	27.898	417
Q8R35	HEX1 (Fragment) OS=Homo sapiens GN-HEX1 PE=2 SV=1 - [Q8R35_HUMAN]	19.34	13	6	6	7	0.000	14.353	27.898	417
Q8R36	Vacuolar protein sorting-associated protein 4A OS=Homo sapiens GN-VPS4A PE=1 SV=1 - [Q8R36_HUMAN]	13.96	7	14	14	9	0.000	6.414	27.859	437
Q8R37	Enhancer of mRNA-decapping protein 4 OS=Homo sapiens GN-EDC4 PE=1 SV=1 - [Q8R37_HUMAN]	5.21	2	7	7	11	0.000	8.097	27.841	1401
Q8R38	Transcriptase represser alpha OS=Homo sapiens GN-TARDBP PE=1 SV=1 - [Q8R38_HUMAN]	7.8	2	7	7	11	0.000	41.472	27.841	1401
Q8R39	Tyrosine protein kinase BAZ2B OS=Homo sapiens GN-BAZ2B PE=1 SV=2 - [Q8R39_HUMAN]	4.45	1	7	7	8	0.000	21.678	27.712	1483
Q8R40	Translating protein 7 OS=Homo sapiens GN-TM7 PE=1 SV=1 - [Q8R40_HUMAN]	3.95	4	8	8	10	0.000	24.468	27.698	1276
Q8R41	Calpain 2, large [catyalytic] subunit variant (Fragment) OS=Homo sapiens PE=2 SV=1 - [Q8R41_HUMAN]	11.25	7	8	8	12	0.000	9.158	27.624	729
Q8R42	Pre-mRNA-splicing factor CWC22 homolog OS=Homo sapiens GN-CWC22 PE=1 SV=3 - [Q8R42_HUMAN]	7.05	2	6	6	12	0.000	10.000	27.617	908
Q8R43	GAP-98B OS=Homo sapiens GN-GAP98B PE=1 SV=1 - [Q8R43_HUMAN]	15.21	1	1	1	10	0.000	11.011	27.617	908
Q14981	TATA-binding protein associated factor 17 OS=Homo sapiens GN-TAF17 PE=1 SV=2 - [Q14981_HUMAN]	2.97	4	5	5	11	0.000	0.000	27.561	1849
Q8R44	Transferrin protein 3 OS=Homo sapiens GN-TFN3 PE=1 SV=1 - [Q8R44_HUMAN]	14.14	2	2	2	10	0.000	16.903	27.561	1849
B4D28	CDNA FLJ54170, highly similar to Cytosolic non-specific dipeptidase OS=Homo sapiens PE=2 SV=1 - [B4D28_HUMAN]	16.41	22	7	7	14	0.000	1.484	27.529	643
AA024R84	HLA-A associated transcript 3, isoform CRA a OS=Homo sapiens GN-AB3T3 PE=4 SV=1 - [AA024R84_HUMAN]	8.17	8	6	6	10	0.000	14.113	27.521	1126
Q8R45	Transferrin protein 2 OS=Homo sapiens GN-TFN2 PE=1 SV=1 - [Q8R45_HUMAN]	13.16	3	3	3	10	0.000	16.473	27.521	1126
P5160	Nucleo-associated protein 1-like OS=Homo sapiens GN-NAP1L1 PE=1 SV=3 - [P5160_HUMAN]	5.94	6	7	7	10	0.000	9.917	27.456</	

O5182	NADH dehydrogenase [ubiquinone] alpha subcomplex subunit 7 OS=Homo sapiens GN=NDUFA7 PE=1 SV=3 [INDUAT_HUMAN]	55.75	5	6	6	9	1,000	9	3,178	22,119	113	12,544
X53771	C-terminal domain of histone H2B OS=Homo sapiens GN=H2B.F1 PE=1 SV=1 [H2B.F1_HUMAN]	11.007	2	2	2	7	0.981	7	0.268	2.08	1	0.234
MOX06	Nucleolar protein glycoprotein p22 OS=Homo sapiens GN=HNPUR2 PE=1 SV=1 [MOX06_HUMAN]	1.717	2	3	4	7	1.183	7	20.286	22,049	446	45,588
B7220	Nucleolar receptor-associated protein 29 OS=Homo sapiens GN=HNCAP29 PE=1 SV=1 [B7220_HUMAN]	21.09	9	4	4	6	0.923	6	7.432	22,016	147	17,363
BRN0C3	CNA FL1422, clone NT2050262, highly similar to Nucleolar complex protein 29 OS=Homo sapiens PE=2 SV=1 [BRN0C3_HUMAN]	21.09	9	4	4	6	0.923	6	7.432	22,016	147	17,363
ESANA1	Putative small GTP-binding protein 1 OS=Leishmania mexicana (strain MHOM/GT2001/U1103) GN=LMXM_10_0910 PE=3 SV=1 [ESANA1_LEIMU]	10.528	27	1	1	2	1,000	1	21.967	20,909	238	23,344
K7E30	Methionine synthase (cytosolic) OS=Homo sapiens GN=MSMC2 PE=1 SV=1 [K7E30_HUMAN]	26.06	11	2	2	6	0.989	6	12.875	21,908	217	24,478
OT6031	ATP-dependent Clp protease ATP-binding subunit cpx-like, mitochondrial OS=Homo sapiens GN=CLXP PE=1 SV=1 [OT6031_HUMAN]	11.06	4	7	7	9	1,010	8	4.001	11,967	633	13,641
Q9N18	Complex assembly factor TIMMDC1, mitochondrial OS=Homo sapiens GN=TIMMDC1 PE=1 SV=2 [TDC1_HUMAN]	13.88	4	3	3	6	0.995	6	13.812	21,902	286	32,158
B4E04	Suppressor 1 Y homolog CNA FL1000, highly similar to Suppressor 1 Y homolog CNA FL1000 OS=Homo sapiens PE=2 SV=1 [B4E04_HUMAN]	13.88	4	3	3	6	0.995	6	13.812	21,902	286	32,158
B4D32	CNA FL16105, highly similar to Ubiquitin conjugating factor E4A (Fragment) OS=Homo sapiens PE=2 SV=1 [B4D32_HUMAN]	13.88	4	3	3	6	1,000	5	5.006	18,892	1405	116,732
Q95912	Mitochondrial homolog OS=Homo sapiens GN=TM2B2 PE=1 SV=1 [TM2B2_HUMAN]	26.06	11	2	2	6	0.989	6	12.875	21,908	217	24,478
B9A18	ULILU5 ltr snRNP-associated protein 2 OS=Homo sapiens GN=USP39 PE=1 SV=1 [B9A18_HUMAN]	8.02	7	5	5	8	1,000	8	10.001	18,866	536	62,005
Q9IC77	Colicoid domain-containing protein 124 OS=Homo sapiens GN=CDC124 PE=1 SV=1 [C124_HUMAN]	24.86	2	6	6	8	0.990	8	5.315	21,852	233	25,820
Q95913	Protein 43 member 1 OS=Homo sapiens GN=SLC43A1 PE=1 SV=1 [P43M1_HUMAN]	14.6	6	4	4	6	1,000	4	11.267	21,842	142	25,132
Q14289	Protein-tyrosine kinase zeta beta OS=Homo sapiens GN=PTK2B PE=1 SV=2 [FK2C_HUMAN]	5.55	5	7	7	9	1,000	9	7.173	21,837	1009	116,800
B4D327	CNA FL16682, highly similar to 2 OS=Homo sapiens PE=2 SV=1 [B4D327_HUMAN]	5.55	5	7	7	9	1,000	9	7.173	21,837	1009	116,800
O15371	Eukaryotic translation initiation factor 3 subunit D OS=Homo sapiens GN=EIF3D PE=1 SV=1 [EIF3D_HUMAN]	8.76	6	5	5	8	0.949	8	5.88	18,817	548	63,932
EP8E5	Lipopolysaccharide-responsive and beige-like anchor protein OS=Homo sapiens GN=LRBA PE=1 SV=1 [EP8E5_HUMAN]	28.8	5	5	5	7	1,000	6	31.732	21,780	2575	280,750
P1780	Phosphatidylesterase OS=Homo sapiens GN=PE1 PE=1 SV=1 [B3KMS5_HUMAN]	18.65	5	5	5	7	1,000	6	11.718	21,688	445	51,328
K0J58	TRK-like gene product isoform 1 OS=Homo sapiens GN=TRFG PE=2 SV=1 [K0J58_HUMAN]	20.36	10	5	5	9	1,000	9	11.945	21,758	280	30,902
B39A5	Protein 124 OS=Homo sapiens GN=124 PE=1 SV=1 [B39A5_HUMAN]	11.24	3	4	4	8	1,000	7	11.24	21,688	136	15,328
HY8B3	Adenosylhomocysteinase (Fragment) OS=Homo sapiens GN=AMCYL2 PE=3 SV=1 [HY8B3_HUMAN]	13.51	4	1	5	9	0.825	1	11.697	21,518	587	58,077
B3K97	Inhibitor of kappa light polypeptide gene enhancer in B-cells, kinase beta, isoform CRA_a OS=Homo sapiens GN=IKBKB PE=2 SV=1 [B3K97_HUMAN]	19.19	4	4	4	9	1,121	8	24.577	21,692	533	60,781
P4358	Caprin-1 OS=Homo sapiens GN=CAPN1 PE=1 SV=1 [P4358_HUMAN]	15.3	3	3	3	6	0.964	3	8.357	21,687	317	34,877
V9H19	DNA mismatch repair protein Msh2 OS=Homo sapiens GN=MSH2 PE=2 SV=1 [V9H19_HUMAN]	9.51	23	7	7	8	0.943	8	29.715	21,683	810	99,798
Q95946	CNA FL16682, highly similar to 2 OS=Homo sapiens PE=2 SV=1 [Q95946_HUMAN]	11.31	2	4	4	9	1,000	5	10.001	21,670	315	35,942
Q9T16	Protein bicaudal D OS=Homo sapiens GN=BCID2 PE=1 SV=1 [BCID2_HUMAN]	6.8	1	6	6	8	1,000	8	20.886	21,666	824	93,476
Q9L30	Protein FAM88 OS=Homo sapiens GN=FAM88 PE=1 SV=1 [FAM88_HUMAN]	12.42	3	4	4	9	0.971	5	4.321	21,644	330	37,167
F5967	Colicoid domain-containing protein 1 OS=Homo sapiens GN=CCDC19 PE=1 SV=1 [F5967_HUMAN]	18.65	5	5	5	6	1,000	5	15.522	21,634	638	72,696
B4D45	CNA FL17346, highly similar to Protein transmembrane domain SEC23B OS=Homo sapiens PE=2 SV=1 [B4D45_HUMAN]	7.95	10	5	5	6	1,000	10	4.981	21,630	742	83,756
UPL87	Upl1 OS=Homo sapiens GN=UPL1 PE=1 SV=1 [UPL1_HUMAN]	17.65	2	2	2	7	0.961	2	10.463	21,618	136	15,328
B4D41	CNA FL155810, highly similar to Golgi reassembly-stacking protein 2 OS=Homo sapiens PE=2 SV=1 [B4D41_HUMAN]	14.19	4	3	3	10	0.910	3	14.029	21,614	310	31,774
K7EP0	Cytosolic c caseinase assembly factor 1, highly similar, mitochondrial OS=Homo sapiens GN=CCAA PE=1 SV=1 [K7EP0_HUMAN]	39.44	2	4	4	8	1,042	8	14.723	21,602	71	7,801
Q95947	CNA FL155810, highly similar to Golgi reassembly-stacking protein 2 OS=Homo sapiens PE=2 SV=1 [Q95947_HUMAN]	39.44	2	4	4	8	1,042	8	14.723	21,602	71	7,801
HY0N3	Signal peptide complex catalytic subunit SEC11A OS=Homo sapiens GN=SEC11A PE=1 SV=1 [HY0N3_HUMAN]	14.63	8	4	4	12	1,000	8	1.469	21,520	183	18,639
CNA FL16959	CNA FL16959 OS=Homo sapiens GN=16959 PE=1 SV=1 [CNA FL16959_HUMAN]	14.38	4	4	4	10	1,000	4	12.352	21,502	368	39,877
B4D16	CNA FL16627, highly similar to Rattus norvegicus ubiquitin-conjugating enzyme E2 (ubiquitin) (Ube2z), mRNA OS=Homo sapiens PE=2 SV=1 [B4D16_HUMAN]	14.63	8	4	4	10	1,000	9	7.641	21,532	287	32,871
B4D18	NAD(P)+-ubiquitin-conjugating enzyme 1 OS=Homo sapiens GN=UBO1 PE=1 SV=1 [B4D18_HUMAN]	14.63	8	4	4	10	1,000	9	15.307	21,515	202	22,779
Q9IC55	Serine protease inhibitor alpha 4 OS=Homo sapiens GN=SERPINA4 PE=1 SV=1 [Q9IC55_HUMAN]	12.1	4	4	4	10	1,000	4	1.469	21,498	973	110,116
Q9P25	Vacuolar protein sorting-associated protein 18 homolog OS=Homo sapiens GN=VPS18 PE=1 SV=2 [VPS18_HUMAN]	4.85	4	4	4	10	1,000	4	15.733	21,483	505	65,800
Q9820	Serine protease inhibitor alpha 10 OS=Homo sapiens GN=SERPINA10 PE=1 SV=1 [PP2BA_HUMAN]	10.88	3	3	3	9	0.988	3	10.701	21,405	307	36,035
Q13287	NMYC-interactor OS=Homo sapiens GN=NMIF PE=1 SV=1 [NMIF_HUMAN]	22.15	6	7	7	10	0.928	10	6.205	21,387	102	12,293
Q9G55	NMYC-ubiquitin oxidoreductase B2 subunit (Fragment) OS=Homo sapiens PE=2 SV=1 [Q9G55_HUMAN]	22.15	6	7	7	10	0.928	10	6.205	21,387	102	12,293
PT580	Nucleolar protein 3 OS=Homo sapiens GN=NP3 PE=1 SV=1 [PT580_HUMAN]	10.81	4	4	4	9	1,000	4	10.81	21,379	349	43,685
Q9D90	CNA FL13478, clone NT26201634, moderately similar to NADH:UBIQUINONE OXIDOREDUCTASE 9 K SUBUNIT (EC 1.6.5.3) OS=Homo sapiens PE=2 SV=1 [Q9D90_HUMAN]	13.82	1	5	5	10	1,000	10	2.837	21,365	456	49,215
B4D47	Nucleolar protein 1 OS=Homo sapiens GN=NP1 PE=1 SV=1 [B4D47_HUMAN]	11.11	2	2	2	9	1,000	9	118.498	21,313	1,038	122,807
B2R87	CNA FL18482, highly similar to 2 OS=Homo sapiens interlaminar consensus sequence binding protein 1 [ICSBP1], mRNA OS=Homo sapiens PE=2 SV=1 [B2R87_HUMAN]	12.44	8	5	5	8	0.945	8	14.598	21,328	428	48,353
ETL09	N-alpha-acetyltransferase 5 OS=Homo sapiens GN=NAAD5 PE=1 SV=1 [ETL09_HUMAN]	31.55	8	5	5	8	1,000	10	8.936	21,289	168	19,289
Q9N13	DNA-binding protein 28 OS=Homo sapiens GN=DNBP28 PE=1 SV=1 [DNBP28_HUMAN]	14.23	3	3	3	6	1,000	3	10.362	21,289	105	12,293
ANR89	Structural maintenance of chromosomes flexible hinge domain-containing protein 1 OS=Homo sapiens GN=SMCHD1 PE=1 SV=2 [SMHD1_HUMAN]	3.14	2	2	2	6	1,000	2	0.300	21,259	205	226,231
B3K4M	CNA FL1774, clone NT26201634, moderately similar to NADH:UBIQUINONE OXIDOREDUCTASE 9 K SUBUNIT (EC 1.6.5.3) OS=Homo sapiens PE=2 SV=1 [B3K4M_HUMAN]	13.82	1	5	5	10	1,000	10	2.837	21,259	205	226,231
HY047	Eukaryotic translation elongation factor 1 epsilon-1 (Fragment) OS=Homo sapiens GN=EEF1E1 PE=3 SV=1 [HY047_HUMAN]	19.85	5	6	6	8	1,000	8	1.534	21,213	136	15,329
Q9D57	Tyrosine-protein phosphatase non-receptor type 23 (Fragment) OS=Homo sapiens GN=PTP23 PE=1 SV=1 [PTN23_HUMAN]	4.03	6	6	6	8	1,000	8	0.000	21,132	1636	178,881
B4D47	Ublap1 OS=Homo sapiens GN=Ublap1 PE=1 SV=1 [B4D47_HUMAN]	19.85	5	6	6	8	1,000	8	1.534	21,213	136	15,329
A1101	Acetylactate synthase-like protein OS=Homo sapiens GN=ALVBL PE=1 SV=2 [ALVBL_HUMAN]	4.95	5	3	3	6	1,000	3	0.000	21,183	632	67,825
B4D46	CNA FL16959, highly similar to 2 OS=Homo sapiens PE=2 SV=1 [B4D46_HUMAN]	14.38	4	4	4	10	1,000	4	12.352	21,166	344	37,922
D3D46	Signal peptide complex subunit 3 homolog (S. cerevisiae), isoform CRA_a OS=Homo sapiens GN=SPCS3 PE=4 SV=1 [D3D46_HUMAN]	11.67	2	2	2	10	1,000	10	0.819	21,146	180	20,300
ESAT14	Uncharacterized protein OS=Leishmania mexicana (strain MHOM/GT2001/U1103) GN=LMXM_36_1010 PE=1 SV=1 [ESAT14_LEIMU]	3.68	1	3	3	7	1,000	6	0.000	21,139	984	105,819
CNA FL16959	CNA FL16959 OS=Homo sapiens GN=16959 PE=1 SV=1 [CNA FL16959_HUMAN]	14.38	4	4	4	10	1,000	4	12.352	21,166	344	37,922
B4D49	CNA FL157179, highly similar to Homo sapiens ATP-binding cassette, subfamily F (ABCN2), member 1 (ABCF3), mRNA OS=Homo sapiens PE=2 SV=1 [B4D49_HUMAN]	3.76	1	3	3	7	1,000	6	19.988	21,123	689	75,527
B4D48	NADH dehydrogenase (ubiquinone) cytochrome b5 complex subunit 1 OS=Homo sapiens GN=ND5B PE=1 SV=1 [ND5B_HUMAN]	10.43	3	3	3	6	1,000	3	10.43	21,123	689	75,527
Q72781	Inverted form of 2 OS=Homo sapiens GN=INFP2 PE=1 SV=2 [INFP2_HUMAN]	3.78	1	4	4	7	1,000	4	26.118	21,064	1249	135,540
Q9D362	PREL protein OS=Homo sapiens GN=PREL PE=1 SV=1 [Q9D362_HUMAN]	1.71	5	5	5	8	0.972	8	2.168	21,028	345	37,808
Q9N129	DNA-binding protein 12 OS=Homo sapiens GN=DNBP12 PE=1 SV=1 [DNBP12_HUMAN]	10.12	7	7	7	10	1,000	7	9.324	21,028	344	37,808
Q9B21	DRBP complex subunit ZNF30 OS=Homo sapiens GN=ZNF30 PE=1 SV=2 [ZNF30_HUMAN]	6.19	1	4	4	8	1,000	7	0.000	21,016	582	65,613
Q95922	DnaJ OS=Homo sapiens GN=DNAJ1 PE=1 SV=1 [DNAJ1_HUMAN]	14.36	2	2	2	6	1,000	2	14.36	21,016	582	65,613
PE318	Guanine nucleotide-binding protein (Gq)(G12)(G13) subunit gamma-5 OS=Homo sapiens GN=GN5G PE=1 SV=3 [GN5G_HUMAN]	33.82	1	3	3	9	0.956	9	6.742	21,008	68	7,314
Q9L11	DNA-directed RNA polymerase I, II, and III subunit RPBAC1 (Fragment) OS=Homo sapiens GN=POLR2H PE=1 SV=3 [Q9L11_HUMAN]	19.46	2	2	2	6	1,000	6	8.283	20,988	149	16,885
PT580	Progesterone receptor OS=Homo sapiens GN=PCRG PE=1 SV=1 [PT580_HUMAN]	10.43	3	3	3	6	1,000	3	10.43	21,008	191	19,191
Q9D57	Lysophosphatidylcholine acyltransferase 1 OS=Homo sapiens GN=PCAT1 PE=1 SV=2 [PCAT1_HUMAN]	3.75	2	2	2	6	1,000	6	0.000	20,910	534	59,113
MRP1	MRP1 (Fragment) OS=Homo sapiens GN=MRP1 PE=1 SV=1 [MRP1_HUMAN]	18.89	9	5	5	6	1,000	5	6.529	20,892	302	34,484
Q9Z74	Zinc finger CCHC domain-containing protein 8 OS=Homo sapiens GN=ZCCHC8 PE=1 SV=2 [ZCCHC8_HUMAN]	7.5	6	5	5	8	1,000	7	6.465	20,885	707	78,529
ESAP9	Putative uncharacterized protein OS=Leishmania mexicana (strain MHOM/GT2001/U1103) GN=LMXM_10_0400 PE=4 SV=1 [ESAP9_LEIMU]	28.93	1	4	4	8	1,000	4	3.021	20,875	121	13,315
B4K63	CNA FL16959, highly similar to 2 OS=Homo sapiens PE=2 SV=1 [B4K63_HUMAN]	14.38	4	4	4	10	1,000	4	12.352	21,166	344	37,922
AA024R394	Cysteine and histidine-rich domain (CHORD) containing 1, isoform CRA_a OS=Homo sapiens GN=CHORDC1 PE=4 SV=1 [AA024R394_HUMAN]	18.07	6	6	6	9	1,000</					

P48840	Cytochrome synthase kinase 3 alpha OSH-homolog sapiens GN-GSK3A PE1 S V1+ [GSK3A_HUMAN]	10,35	6	2	3	5	0,703	4	51,485	19,036	483	50,949
P50468	Protein subunit beta OSH-homolog sapiens GN-SC2V18 PE1 S V2+ [SC2V18_HUMAN]	30,21	3	4	5	1	1,138	6	21,938	15,807	156	9,928
Q00161	Synaptosomal-associated protein 23 OSH-homolog sapiens GN-SNAP23 PE1 S V1+ [SNAP23_HUMAN]	25,54	12	5	6	1	1,000	6	14,907	19,022	211	23,340
Q01303	Minimally-associated OSH-homolog sapiens GN-NDUFAP2 PE1 S V1+ [NDUFAP2_HUMAN]	23,08	3	3	8	1	1,000	6	10,000	19,018	169	18,844
Q01304	EF1F3 protein kinase 1, isoform CRA_a OSH-homolog sapiens GN-SRPK1 PE1 S V1+ [A0A024RUCR_HUMAN]	22,77	1	1	2	1	1,000	3	21,277	19,022	166	15,524
Q024478	COP9 complex phosphatase/homolog subunit TB (Arabidopsis), isoform CRA_a OSH-homolog sapiens GN-COP9B PE1 S V1+ [A0A024R78_HUMAN]	24,84	8	3	3	3	1,000	6	4,974	18,956	157	18,145
Q02720	Zinc finger CCH domain-containing protein 1 OSH-homolog sapiens GN-ZFC1 PE1 S V1+ [ZFC1_HUMAN]	4,2	1	1	1	1	1,000	6	29,662	19,013	169	15,719
Q04091	cDNA FLJ55368, highly similar to Epsin-1 OSH-homolog sapiens PE1 S V2+ [BDU91_HUMAN]	8,4	9	4	4	7	1,000	6	1,030	18,905	536	55,798
EP9136	Transcription factor p65 (Fragement) OSH-homolog sapiens GN-RELA PE1 S V1+ [EP9136_HUMAN]	30,81	19	6	6	8	0,137	8	28,351	18,901	185	20,826
Q01104	cDNA OSH-homolog sapiens GN-COPB1 PE1 S V1+ [COPB1_HUMAN]	19,29	1	1	1	1	1,000	6	19,290	18,877	168	18,501
Q01203	Gephyrin OSH-homolog sapiens GN-GPHN PE1 S V1+ [GPHN_HUMAN]	8,42	1	6	6	7	1,000	6	28,732	18,888	736	76,698
Q01204	cDNA FLJ18177, highly similar to Phosphatidylinositol-3-OH kinase 4-isoform gamma (EC 2.7.1.8), OSH-homolog sapiens PE1 S V1+ [BDVZ29_HUMAN]	12,84	3	3	7	7	1,000	6	0,000	18,840	641	70,142
BD4Y5	Mitogen-activated protein kinase kinase 1 OSH-homolog sapiens GN-MAP2K1 PE1 S V1+ [BD4Y5_HUMAN]	19,76	6	3	6	9	1,000	4	7,523	18,847	371	18,230
Q0961	Endophilin A2 OSH-homolog sapiens GN-SH3GL1 PE1 S V1+ [SH3GL1_HUMAN]	18,76	16	7	7	9	1,000	4	14,022	18,847	389	41,464
Q08209	Ribonuclease P18, mitochondrial OSH-homolog sapiens GN-HMGP22(1U1103) GN-LMXXM_15_0275 PE4 S V1+ [E0A0209_LEIMU]	20,16	2	2	2	2	1,000	6	1,120	18,847	187	18,230
Q14554	Protein disulfide-isomerase A5 OSH-homolog sapiens GN-PDI5A PE1 S V1+ [PDI5A_HUMAN]	4,43	2	3	3	8	1,000	7	10,000	18,831	519	59,556
Q06355	Mediator of RNA polymerase II transcription subunit 8 OSH-homolog sapiens GN-MED14 PE1 S V2+ [MED14_HUMAN]	14,55	6	4	4	4	1,000	6	16,121	18,828	208	20,062
Q00022	Actin nucleation promoting factor (Fragement) OSH-homolog sapiens GN-AP2 PE1 S V1+ [A00022_HUMAN]	14,66	25	4	5	7	0,039	6	13,192	18,801	410	41,576
H3BV22	Serine/threonine protein phosphatase (Fragement) OSH-homolog sapiens GN-PPP4C PE1 S V1+ [H3BV22_HUMAN]	12,27	18	1	3	6	0,864	3	64,183	18,798	203	23,130
Q03633	Poly (ADP-ribose) polymerase 4 OSH-homolog sapiens GN-PARP4 PE1 S V1+ [PARP4_HUMAN]	5,17	3	5	7	1	1,000	7	9,545	18,772	174	15,472
Q08V92	Protein FAM134C OSH-homolog sapiens GN-FAM134C PE1 S V1+ [FAM134C_HUMAN]	15,27	1	2	2	2	1,000	7	10,000	18,772	466	51,364
Q01445	Ubiquitin-protein ligase ARH1 OSH-homolog sapiens GN-ARH1 PE1 S V2+ [ARH1_HUMAN]	6,72	2	4	4	4	0,942	8	26,675	18,771	557	64,070
Q08V74	Protein RNA N6 adenosine methyltransferase OSH-homolog sapiens GN-NSGEP PE1 S V1+ [NSGEP_HUMAN]	10,15	6	3	4	7	1,000	5	1,114	18,768	365	38,403
Q08V74	Transmembrane protein 43 OSH-homolog sapiens GN-TMEM43 PE1 S V1+ [TMEM43_HUMAN]	11,13	5	5	7	7	0,056	7	6,953	18,708	400	44,847
Q08V74	HMGB1 protein (Fragement) OSH-homolog sapiens PE1 S V1+ [Q08V74_HUMAN]	9,71	2	2	2	2	1,000	7	11,965	18,702	175	19,336
F8V8V1	Coatomer subunit zeta-1 (Fragement) OSH-homolog sapiens GN-COZP1 PE1 S V1+ [F8V8V1_HUMAN]	22,83	9	2	2	7	1,000	7	13,576	18,682	92	10,621
Q04342	ER membrane protein complex subunit 8 OSH-homolog sapiens GN-ERIC8 PE1 S V1+ [ERIC8_HUMAN]	6,52	1	3	3	3	0,943	8	11,908	18,666	210	23,748
Q08V65	Conserved domain subunit 1 OSH-homolog sapiens GN-CDSG1 PE1 S V2+ [CDSG1_HUMAN]	1,21	1	3	3	3	1,000	7	17,949	18,663	612	12,094
Q08L63	SRS1 ribosomal protein L53, mitochondrial OSH-homolog sapiens GN-MRPL53 PE1 S V1+ [MRPL53_HUMAN]	40,18	1	3	3	8	1,000	8	67,893	18,653	112	12,094
Q08617	3HT12 transcription associated protein 1 (Fragement), isoform CRA_a OSH-homolog sapiens GN-TAP1 PE1 S V1+ [A0A024R286_HUMAN]	8,87	6	4	4	7	0,850	5	11,058	18,625	523	60,586
A0A024R56	Protein LAP2 OSH-homolog sapiens GN-ERBBP2 PE1 S V2+ [LAP2_HUMAN]	5,37	3	5	5	5	0,979	5	18,254	18,594	547	60,898
V9WHQ4	Protein LAP2 OSH-homolog sapiens GN-ERBBP2 PE1 S V2+ [V9WHQ4_HUMAN]	5,37	3	5	5	5	0,979	5	18,254	18,594	547	60,898
Q08Q08	Vitamin K epoxide reductase complex subunit 1 OSH-homolog sapiens GN-UKORC1 PE1 S V1+ [UKORC1_HUMAN]	12,27	5	2	2	7	1,021	7	3,669	18,568	103	18,223
H8BV9	Nucleolar organizer factor 2 (Fragement) OSH-homolog sapiens GN-NOLF2 PE1 S V1+ [H8BV9_HUMAN]	10,08	1	1	1	1	1,000	6	10,000	18,561	107	12,115
P01859	gamma-2 chain c region OSH-homolog sapiens GN-HMG2 PE1 S V1+ [HMG2_HUMAN]	15,18	3	4	4	8	1,000	5	10,000	18,539	328	37,878
P0859	LIM and senescent cell antigen-like domain protein 1 OSH-homolog sapiens GN-LSM1 PE1 S V1+ [LSM1_HUMAN]	16	12	5	5	5	1,000	6	10,070	18,529	325	37,226
Q08Q08	Charged multivesicular body protein 1a OSH-homolog sapiens GN-CHMP1A PE1 S V1+ [CHMP1A_HUMAN]	19,39	6	3	3	4	1,000	9	8,474	18,518	166	18,589
Q10479	Interleukin-inducible protein with tetrapeptide repeats 3 OSH-homolog sapiens GN-ITP3 PE1 S V1+ [ITP3_HUMAN]	19,18	2	3	3	3	1,000	6	7,142	18,500	490	55,950
Q08Q08	Protein kinase (Fragement) OSH-homolog sapiens GN-CK1 PE1 S V1+ [CK1_HUMAN]	12,86	6	6	6	6	1,000	6	11,850	18,482	143	45,442
EBAL33	Putative GTP-binding protein OSH-Leishmania mexicana (strain MHOM/GT/2001/1103) GN-LMXXM_08_2200 PE3 S V1+ [EBAL33_LEIMU]	3,62	1	2	3	3	1,000	6	10,000	18,471	691	76,850
Q08Q08	BRX domain-containing protein BRX OSH-homolog sapiens GN-BRX PE1 S V1+ [BRX_HUMAN]	11,82	4	2	2	4	1,000	6	11,820	18,461	104	45,442
A0A024R34	Uncharacterized protein GN-HSP148 PE1 S V1+ [A0A024R34_HUMAN]	31,25	3	5	5	7	0,992	7	1,219	18,454	96	10,621
Q15212	Protein subunit 5 OSH-homolog sapiens GN-PFD5 PE1 S V1+ [PFD5_HUMAN]	25,88	3	5	5	8	0,896	8	21,303	18,448	129	14,574
Q08V74	Actin-binding protein 5 OSH-homolog sapiens PE1 S V1+ [Q08V74_HUMAN]	18,53	2	2	2	2	1,000	6	27,103	18,435	151	19,967
Q03VY3	Proteasome-associated protein E2C9 OSH-homolog sapiens GN-E2C9 PE1 S V2+ [E2C9_HUMAN]	4,17	5	7	7	7	1,000	10	10,000	18,415	1845	204,180
P0710	Acyl-CoA-binding protein OSH-homolog sapiens GN-COBI PE1 S V2+ [COBI_HUMAN]	47,13	3	4	4	4	1,000	7	2,538	18,407	112	126,200
Q08Q02	Actin filament and activator of transcription factor 1 OSH-homolog sapiens PE1 S V1+ [Q08Q02_HUMAN]	5,01	13	4	4	7	1,000	6	14,030	18,402	679	70,878
BD4Y29	cDNA FLJ5342, highly similar to transcription intermediary factor 1 alpha OSH-homolog sapiens PE1 S V1+ [BD4Y29_HUMAN]	7,39	5	6	7	7	1,000	6	10,000	18,390	981	107,636
CNA FLR9815	Highly similar to protein kinase C (beta) OSH-homolog sapiens PE1 S V1+ [CNA FLR9815_HUMAN]	11,88	1	1	1	1	1,000	6	11,880	18,376	143	15,826
P42356	Phosphatidylinositol 4-kinase alpha OSH-homolog sapiens GN-P4KA PE1 S V1+ [P4KA_HUMAN]	17,16	13	3	3	3	1,001	3	53,575	18,379	2044	231,170
B7726	cDNA FLJ5509, highly similar to Vacuole ATP synthase subunit D (EC 3.6.3.4) OSH-homolog sapiens PE1 S V1+ [B7726_HUMAN]	10,68	3	3	3	3	1,000	6	10,680	18,370	143	15,826
Q08Q02	Proteoglycan 3, type 1 OSH-homolog sapiens GN-PRG1 PE1 S V1+ [A0A024Q2L1_HUMAN]	24,68	2	4	4	3	0,949	6	22,519	18,351	158	17,613
Q03Q02	Mortality factor 4 like protein 2 OSH-homolog sapiens GN-MORF4L2 PE1 S V1+ [Q03Q02_HUMAN]	18,85	9	3	3	6	1,000	5	10,070	18,350	177	19,819
Q08V74	SRS ribosomal protein L17, mitochondrial OSH-homolog sapiens GN-MRPL17 PE1 S V1+ [MRPL17_HUMAN]	12,42	1	1	1	1	1,000	6	12,420	18,349	143	15,826
ESAK51	Putative ubiquitin-conjugating enzyme E2 OSH-Leishmania mexicana (strain MHOM/GT/2001/1103) GN-LMXXM_04_0880 PE1 S V1+ [ESAK51_LEIMU]	20,95	1	1	1	1	1,000	7	10,000	18,344	148	17,039
MG2288	Gamma-CASP-10 OSH-homolog sapiens GN-CASP10 PE1 S V1+ [MG2288_HUMAN]	29,13	5	3	3	3	1,000	6	6,080	18,321	103	11,571
Q13848	Protein CASP-8 OSH-homolog sapiens GN-CASP8 PE1 S V2+ [CASP8_HUMAN]	29,96	1	7	7	7	0,446	1	6,980	18,291	678	77,428
CB3LV4	Apoptotic protease-activating factor 1 OSH-homolog sapiens GN-PAF1 PE1 S V1+ [CB3LV4_HUMAN]	3,1	4	3	4	4	0,931	3	10,000	18,270	1163	152,379
A0A024R04	Poly (ADP-ribose) polymerase 1 OSH-homolog sapiens GN-PARP1 PE1 S V1+ [A0A024R04_HUMAN]	49,63	4	4	4	4	1,000	3	6,244	18,266	366	39,629
Q08V74	Protein GTPase-activating protein 3 OSH-homolog sapiens GN-GRAP3 PE1 S V3+ [GRAP3_HUMAN]	4,27	4	5	6	8	0,986	6	2,093	18,187	1499	170,407
CA3818	Small nuclear RNA-interacting protein OSH-homolog sapiens GN-SNIRP1 PE1 S V1+ [CA3818_HUMAN]	6,42	1	1	1	1	1,000	6	56,158	18,187	51	6,809
Q08V74	U3 small nuclear ribonucleoprotein OSH-homolog sapiens GN-SMNL3 PE1 S V1+ [SMNL3_HUMAN]	12,23	2	5	6	9	1,000	9	14,789	18,131	338	37,878
Q08Q02	U3 small nuclear ribonucleoprotein OSH-homolog sapiens GN-SMNL3 PE1 S V1+ [Q08Q02_HUMAN]	12,23	2	5	6	9	1,000	9	14,789	18,131	338	37,878
Q08Q02	U3 small nuclear ribonucleoprotein OSH-homolog sapiens GN-SMNL3 PE1 S V1+ [Q08Q02_HUMAN]	12,23	2	5	6	9	1,000	9	14,789	18,131	338	37,878
Q08Q02	U3 small nuclear ribonucleoprotein OSH-homolog sapiens GN-SMNL3 PE1 S V1+ [Q08Q02_HUMAN]	12,23	2	5	6	9	1,000	9	14,789	18,131	338	37,878
Q08Q02	U3 small nuclear ribonucleoprotein OSH-homolog sapiens GN-SMNL3 PE1 S V1+ [Q08Q02_HUMAN]	12,23	2	5	6	9	1,000	9	14,789	18,131	338	37,878
Q08Q02	U3 small nuclear ribonucleoprotein OSH-homolog sapiens GN-SMNL3 PE1 S V1+ [Q08Q02_HUMAN]	12,23	2	5	6	9	1,000	9	14,789	18,131	338	37,878
Q08Q02	U3 small nuclear ribonucleoprotein OSH-homolog sapiens GN-SMNL3 PE1 S V1+ [Q08Q02_HUMAN]	12,23	2	5	6	9	1,000	9	14,789	18,131	338	37,878
Q08Q02	U3 small nuclear ribonucleoprotein OSH-homolog sapiens GN-SMNL3 PE1 S V1+ [Q08Q02_HUMAN]	12,23	2	5	6	9	1,000	9	14,789	18,131	338	37,878
Q08Q02	U3 small nuclear ribonucleoprotein OSH-homolog sapiens GN-SMNL3 PE1 S V1+ [Q08Q02_HUMAN]	12,23	2	5	6	9	1,000	9	14,789	18,131	338	37,878
Q08Q02	U3 small nuclear ribonucleoprotein OSH-homolog sapiens GN-SMNL3 PE1 S V1+ [Q08Q02_HUMAN]	12,23	2	5	6	9	1,000	9	14,789	18,131	338	37,878
Q08Q02	U3 small nuclear ribonucleoprotein OSH-homolog sapiens GN-SMNL3 PE1 S V1+ [Q08Q02_HUMAN]	12,23	2	5	6	9	1,000	9	14,789	18,131	338	37,878
Q08Q02	U3 small nuclear ribonucleoprotein OSH-homolog sapiens GN-SMNL3 PE1 S V1+ [Q08Q02_HUMAN]	12,23	2	5	6	9	1,000	9	14,789	18,131	338	37,878
Q08Q02	U3 small nuclear ribonucleoprotein OSH-homolog sapiens GN-SMNL3 PE1 S V1+ [Q08Q02_HUMAN]	12,23	2	5	6	9	1,000	9	14,789	18,131	338	37,878
Q08Q02	U3 small nuclear ribonucleoprotein OSH-homolog sapiens GN-SMNL3 PE1 S V1+ [Q08Q02_HUMAN]	12,23	2	5	6	9	1,000	9	14,789	18,131	338	37,878
Q08Q02	U3 small nuclear ribonucleoprotein OSH-homolog sapiens GN-SMNL3 PE1 S V1+ [Q08Q02_HUMAN]	12,23	2	5	6	9	1,000	9	14,789	18,131	338	37,878

B7Z2N7	cDNA FL156812, highly similar to Sec1 family domain-containing protein 1 OS=Homo sapiens PE=2 Sv1+ [B7Z2N7_HUMAN]	12,247	6	6	6	10	0.937	10	17,994	16,636	457	51,511
Q8N890	Spennin-2-like domain-containing protein OS=Homo sapiens GN=SPN2L1 PE=1 Sv1+ [SPN2L1_HUMAN]	5,862	3	3	3	7	1.000	5	0.000	0.000	893	59,843
EQS251	ATP-dependent RNA helicase DDX3 OS=Homo sapiens GN=DDX3 PE=1 Sv2+ [DDX3_HUMAN]	4,466	3	3	3	4	1.000	4	0.000	16,322	1008	114,888
Q8A910	Cysteine peptidase A (CBA) OS=Leishmania mexicana (strain MHOM/GT2001/11/103) GN=LMMX_10_440 PE=3 Sv1+ [E8A996_LEIMU]	5,085	11	2	3	4	1.091	2	12,960	16,622	354	38,721
AA024R06	Triplicate motif-containing protein OS=Homo sapiens GN=TRIM33 PE=1 Sv1+ [TRIM33_HUMAN]	1,844	7	3	8	10	1.000	3	31,399	16,620	1127	122,444
B4DS89	Afpap1-1 OS=Homo sapiens GN=ARFP1 PE=1 Sv1+ [B4DS89_HUMAN]	14,451	5	2	3	8	1.000	6	0.000	16,548	159	22,041
Q83R48	Syntaxin 10 OS=Homo sapiens GN=STX10 PE=1 Sv1+ [Q83R48_HUMAN]	20,113	7	2	7	7	1.000	6	7,746	16,648	398	459,369
HY8Y80	Transmembrane protein 33 (Frangini) OS=Homo sapiens GN=TMEM33 PE=1 Sv1+ [HY8Y80_HUMAN]	12,258	4	2	2	6	1.090	6	25,178	16,584	155	17,905
Q93Z52	Heme-binding protein 2 OS=Homo sapiens GN=HEBP2 PE=1 Sv1+ [HEBP2_HUMAN]	18,105	3	3	3	3	0.884	5	11,422	16,528	205	22,861
Q82879	Adenosine 3 OS=Homo sapiens GN=AD3 PE=1 Sv1+ [Q82879_HUMAN]	17,185	4	2	3	3	0.834	2	7,862	16,463	345	84,713
DD3D13	Fibrinogen beta chain, isoform CRA_1 OS=Homo sapiens GN=FGB PE=1 Sv1+ [DD3D13_HUMAN]	17,185	4	5	7	10	1.000	4	8,843	16,490	344	39,711
CNA1	CNA1 OS=Homo sapiens GN=CNA1 PE=1 Sv1+ [CNA1_HUMAN]	17,185	4	2	3	3	1.000	3	0.000	19,110	633	68,686
B4DF08	cDNA FL157186, highly similar to Retinol dehydrogenase 1 (EC 1.1.3.36) OS=Homo sapiens PE=2 Sv1+ [B4DF08_HUMAN]	11,714	14	1	3	8	1.000	2	0.000	16,470	422	45,968
Q7L344	MOB kinase activator 1 OS=Homo sapiens GN=MOBK1 PE=1 Sv1+ [MOBK1_HUMAN]	13,899	5	3	3	3	1.000	6	4,839	16,460	216	23,075
Q81884	Protein tyrosine kinase 1 beta OS=Homo sapiens GN=PTK1B PE=1 Sv1+ [Q81884_HUMAN]	17,185	4	2	2	2	1.000	2	0.000	16,420	212	23,075
EA0N58	Proteasome subunit type 10 OS=Leishmania mexicana (strain MHOM/GT2001/11/103) GN=LMMX_12_030 PE=3 Sv1+ [EA0N58_LEIMU]	7,777	1	2	2	2	1.553	5	72,811	16,452	283	30,462
ABK41	CNA1 OS=Homo sapiens GN=CNA1 PE=1 Sv1+ [ABK41_HUMAN]	17,185	4	2	3	3	1.000	3	12,805	16,410	415	40,410
AA024R08	Bromodomain containing 7, isoform CRA_1 OS=Homo sapiens GN=BRD7 PE=1 Sv1+ [AA024R08_HUMAN]	3,155	3	2	2	2	1.000	2	0.000	16,404	58	57,428
AA024R26	High affinity immunoglobulin Fc gamma receptor 1b (Fragment) OS=Homo sapiens GN=HCFCR1B PE=4 Sv1+ [AA024R26_HUMAN]	8,843	3	3	3	3	1.000	5	9,899	16,403	230	28,947
Q82878	Small nuclear ribonucleoprotein Sm D1 OS=Homo sapiens GN=SNRPD1 PE=1 Sv1+ [Q82878_HUMAN]	13,135	1	2	2	2	1.000	5	34,425	16,392	1163	128,211
J3L018	Small nuclear ribonucleoprotein Sm D1 OS=Homo sapiens GN=SNRPD1 PE=1 Sv1+ [J3L018_HUMAN]	17,133	3	2	2	2	1.000	5	18,221	16,353	75	8,388
B2R90	Zinc finger protein 516 OS=Homo sapiens GN=ZNF516 PE=1 Sv1+ [B2R90_HUMAN]	13,933	2	3	3	3	1.000	2	0.000	16,336	244	27,756
B2R90	cDNA FL153029, highly similar to Hemo sapiens COP9 constitutive photomorphogenic homolog subunit 2 (Arabidopsis) (COP9.2), mRNA OS=Homo sapiens PE=2 Sv1+ [B2R90_HUMAN]	2,244	13	4	5	11	1.000	10	3,843	16,332	443	51,583
GVZ260	V-type proton ATPase subunit D OS=Homo sapiens GN=VATP4D PE=1 Sv1+ [GVZ260_HUMAN]	9,926	4	4	4	4	1.000	6	6,504	16,323	192	21,908
Q91920	Protein tyrosine kinase 1 OS=Homo sapiens GN=PTK1B PE=1 Sv1+ [Q91920_HUMAN]	17,185	4	2	2	2	1.000	1	0.000	16,320	323	37,289
AD2V5	MIR-10 OS=Homo sapiens GN=MIR10 PE=1 Sv1+ [AD2V5_HUMAN]	2,18	2	1	1	1	1.000	5	0.000	16,315	597	64,964
Q91923	Methylenetetrahydrofolate synthase OS=Homo sapiens GN=METTL2 PE=2 Sv1+ [METTL2_HUMAN]	13,933	2	3	3	3	1.000	2	0.000	16,312	244	27,756
P17268	Squalene synthase OS=Homo sapiens GN=SQS1 PE=1 Sv1+ [P17268_HUMAN]	11,999	7	5	5	5	0.983	8	12,846	16,301	417	48,084
Q91924	Hypothetical noncoding region HMJ-RMS-403 (Fragment) OS=Homo sapiens PE=2 Sv1+ [Q91924_HUMAN]	8,74	18	6	6	6	1.000	7	0.000	16,299	735	84,417
Q91925	Serine/threonine kinase PRK2 OS=Homo sapiens GN=PRK2 PE=1 Sv1+ [Q91925_HUMAN]	9,06	3	3	3	3	1.000	4	14,960	16,298	552	63,243
Q60636	Tyrosine methyltransferase 38 OS=Homo sapiens GN=TRIM33 PE=1 Sv1+ [Q60636_HUMAN]	1,733	2	2	2	2	1.000	5	0.000	16,278	465	53,381
Q23212	U6 snRNA-associated Sm-like protein OS=Homo sapiens GN=U6AP1 PE=1 Sv1+ [Q23212_HUMAN]	33,755	1	1	1	1	1.000	3	7,426	16,277	80	91,232
Q9NF91	Nesprin-1 OS=Homo sapiens GN=SYNE1 PE=1 Sv1+ [Q9NF91_HUMAN]	0,58	11	5	6	7	0.938	5	7,777	16,263	8797	101,046
PE1111	Serine beta-lactamase-like protein LACTB, mitochondrial OS=Homo sapiens GN=LACTB PE=1 Sv2+ [LACTB_HUMAN]	6,95	2	5	5	5	0.944	6	13,744	16,247	547	60,655
Q91926	Integrin complex subunit 1 OS=Homo sapiens GN=IT1B PE=1 Sv2+ [Q91926_HUMAN]	11,205	3	3	3	3	1.000	2	0.000	16,242	393	44,143
F8W49	Rab-like protein 3 OS=Homo sapiens GN=RABL3 PE=1 Sv1+ [F8W49_HUMAN]	20,75	6	1	1	1	1.000	1	16,241	16,241	3	5,642
FKCZM4	PKCZeta OS=Homo sapiens GN=PKCZ PE=1 Sv1+ [FKCZM4_HUMAN]	5,37	6	1	1	1	1.000	4	25,763	16,238	1043	119,424
EA0T77	Insulin-like growth factor 1 OS=Leishmania mexicana (strain MHOM/GT2001/11/103) GN=LMMX_36_4630 PE=3 Sv1+ [EA0T77_LEIMU]	3,42	1	1	1	1	1.000	2	6,485	16,234	234	25,097
Q91927	Target of EGR1 protein OS=Homo sapiens GN=TOE1 PE=1 Sv1+ [Q91927_HUMAN]	13,37	3	3	3	3	1.000	3	0.000	16,233	510	59,512
HY8Y82	Relaxin OS=Homo sapiens GN=RELX1 PE=1 Sv1+ [HY8Y82_HUMAN]	9,376	1	1	1	1	1.000	2	0.000	16,232	216	23,075
HY8Y82	Putative deoxyribonuclease TADT1 (Fragment) OS=Homo sapiens GN=TADT1 PE=1 Sv1+ [HY8Y82_HUMAN]	11,337	11	2	3	3	0.904	3	10,190	16,169	202	22,653
B2R915	Larval-specific protein 4 OS=Homo sapiens GN=LSP4 PE=1 Sv1+ [B2R915_HUMAN]	2,21	4	4	4	4	1.000	3	28,199	16,162	718	80,503
AR7A0	cDNA FL15753, highly similar to Homo sapiens primase, polypeptide 2A, 580a (PRIM2A), mRNA OS=Homo sapiens PE=2 Sv1+ [AR7A0_HUMAN]	5,5	5	3	3	3	1.000	2	26,024	16,162	509	58,797
A7E27	CAP-GLY domain-containing linker protein 2 OS=Homo sapiens GN=CLIP2 PE=2 Sv1+ [A7E27_HUMAN]	3,36	7	2	2	2	0.945	2	8,426	16,143	1011	111,655
FS815	Protein tyrosine kinase 1 OS=Homo sapiens GN=PTK1B PE=1 Sv1+ [FS815_HUMAN]	21,109	1	1	1	1	1.000	2	0.000	16,139	256	29,453
F8V58	CNA1 OS=Homo sapiens GN=CNA1 PE=1 Sv1+ [F8V58_HUMAN]	16,67	10	4	4	4	0.935	7	13,778	16,116	276	29,906
Q91928	CTP domain family tyrosine kinase OS=Homo sapiens GN=CTPK1 PE=1 Sv1+ [Q91928_HUMAN]	11,205	3	3	3	3	1.000	4	12,775	16,112	379	39,962
Q91929	Asparagine aminopeptidase, isoform CRA_1 OS=Homo sapiens GN=ONPEP PE=2 Sv1+ [Q91929_HUMAN]	8,61	17	3	3	3	0.884	6	31,301	16,092	287	29,693
EPF63	Rab GTPase-activating protein 1-like (Fragment) OS=Homo sapiens GN=RAAGAP1L PE=1 Sv1+ [EPF63_HUMAN]	23,99	8	4	4	4	1.000	11	10,330	16,070	190	22,449
P46929	Protein tyrosine kinase 1 OS=Homo sapiens GN=PTK1B PE=1 Sv1+ [P46929_HUMAN]	19,58	3	3	3	3	1.000	6	14,677	16,067	717	78,747
Q13636	Ras-related protein Rab-31 OS=Homo sapiens GN=RAB31 PE=1 Sv1+ [Q13636_HUMAN]	3,959	3	3	3	3	0.989	4	7,479	16,034	194	21,555
Q10288	Transferrin subunit 4 OS=Homo sapiens GN=TF4 PE=1 Sv1+ [Q10288_HUMAN]	2,76	3	3	3	3	1.000	3	6,899	16,034	194	21,555
DR9Y1	Polysialyltransferase protein-interacting protein 2 OS=Homo sapiens GN=PIIP2 PE=1 Sv1+ [DR9Y1_HUMAN]	22,39	4	2	2	2	0.7	7	21,738	16,031	67	7,684
SRF90	Nucleic acid-binding protein 2 OS=Homo sapiens GN=NUBP2 PE=1 Sv1+ [SRF90_HUMAN]	5,91	2	2	2	2	0.871	6	5,186	16,028	132	14,734
Q91930	TBC1 domain family member 1 OS=Homo sapiens GN=TBC1D1B PE=1 Sv1+ [Q91930_HUMAN]	11,205	3	3	3	3	1.000	2	0.000	16,028	988	98,8
Q91931	Alcaminase-like OS=Homo sapiens GN=ACYL1 PE=1 Sv1+ [Q91931_HUMAN]	17,16	6	7	7	7	1.033	6	8,121	15,998	408	45,866
Q91932	Cytosolic acyltransferase 1 OS=Homo sapiens GN=ACAT1 PE=1 Sv1+ [Q91932_HUMAN]	9,47	4	4	4	4	0.978	4	4	15,998	408	45,866
B4MD03	cDNA FL158174, highly similar to WW domain-binding protein 11 OS=Homo sapiens PE=2 Sv1+ [B4MD03_HUMAN]	7,3	5	5	5	5	1.000	7	3,965	15,990	589	64,887
Q91933	Retinol dehydrogenase 13 OS=Homo sapiens GN=RDH13 PE=1 Sv2+ [Q91933_HUMAN]	11,205	3	2	2	2	1.000	5	0.000	15,986	331	35,910
Q91934	Helicase domain-containing protein 1 OS=Homo sapiens GN=HDC1 PE=1 Sv1+ [Q91934_HUMAN]	12,65	1	1	1	1	1.000	2	16,014	15,982	107	112,613
Q91935	Putative uncharacterized protein ITSN2 (Fragment) OS=Homo sapiens GN=ITSN2 PE=4 Sv1+ [Q91935_HUMAN]	7,141	1	1	1	1	1.000	2	0.047	15,975	1329	150,921
BE3A4	Transmembrane 18 homolog OS=Homo sapiens GN=TMEM18 PE=1 Sv1+ [BE3A4_HUMAN]	6,05	6	6	6	6	1.000	2	0.000	15,972	256	29,453
Q91936	Nucleic acid-binding protein 2 OS=Homo sapiens GN=NUBP2 PE=2 Sv1+ [Q91936_HUMAN]	10,81	3	2	2	2	0.122	6	15,516	15,944	74	7,680
P1938	HCTC factor 9, isoform B OS=Homo sapiens GN=HCTCF9 PE=1 Sv1+ [P1938_HUMAN]	5,48	4	6	6	6	0.867	6	9,507	15,933	968	105,200
CNA1	CNA1 OS=Homo sapiens GN=CNA1 PE=1 Sv1+ [CNA1_HUMAN]	17,185	4	2	3	3	1.000	3	20,262	15,932	269	30,714
K7E8C	Nectin-2 (Fragment) OS=Homo sapiens GN=NLGN2 PE=4 Sv1+ [K7E8C_HUMAN]	12,38	4	3	3	3	0.976	9	21,522	15,921	210	22,738
AA024R03	Nuclear pore complex protein 1 OS=Homo sapiens GN=NUP1 PE=1 Sv1+ [AA024R03_HUMAN]	7,56	2	2	2	2	1.000	4	0.000	15,917	647	69,289
EP6V79	Cyclic GMP-AMP synthase OS=Homo sapiens GN=CMG2 PE=1 Sv1+ [EP6V79_HUMAN]	12,48	2	5	5	5	0.944	8	11,525	15,916	505	56,645
DRK20	Estradiol 17-beta-dehydrogenase 1 OS=Homo sapiens GN=HSD17B1 PE=1 Sv2+ [DRK20_HUMAN]	11,33	2	2	2	2	1.000	2	0.000	15,882	296	28,084
Q91937	Thrombospondin type 1 domain-containing protein 2 OS=Homo sapiens GN=THSD1B PE=1 Sv1+ [Q91937_HUMAN]	11,205	3	3	3	3	1.000	5	11,876	15,871	272	31,584
K7E35	Signal transducer and activator of transcription OS=Homo sapiens GN=STAT5A PE=1 Sv1+ [K7E35_HUMAN]	6,14	4	5	5	5	1.000	4	1,888	15,843	763	87,308
Q13643	Crebin OS=Homo sapiens GN=CREB1 PE=1 Sv1+ [Q13643_HUMAN]	8,63	7	4	4	4	1.000	4	8,63	15,843	649	69,289
P43897	Elongation factor 1b, mitochondrial OS=Homo sapiens GN=EF1B PE=2 Sv1+ [P43897_HUMAN]	13,54	7	5	5	5	0.947	6	11,251	15,835	325	35,368
Q13426	DNA repair protein XRCC4 OS=Homo sapiens GN=XRCC4 PE=1 Sv2+ [Q13426_HUMAN]	11,81	4	4	4	4	0.910	6	18,847	15,833	336	38,263
TE3M7	E3 ubiquitin-protein ligase UBR5 OS=Homo sapiens GN=UBR5 PE=1 Sv1+ [TE3M7_HUMAN]	2,15	3	3	3	3	1.000	2	15,811	15,826	2792	308,362
ASU01	Rho GTPase-activating protein OS=Homo sapiens GN=RAO1 PE=1 Sv1+ [ASU01_HUMAN]	14,37	2	3	3	3	1.000	6	3,240	15,815	683	74,931
BLT1	BLT1 OS=Homo sapiens GN=BLT1 PE=1 Sv1+ [BLT1_HUMAN]	1,76	2	2	2	2	1.000					

QBW08	Calcium homeostasis endoplasmic reticulum protein OS-Homo sapiens GN-CHERP1 PE1 SV+3 - [CHERP_HUMAN]	4	69	5	4	4	6	0.992	6	27.820	14.743	916	103.637
B14K08	Roslinin OS-Homo sapiens GN-ROSLIN PE1 SV+2 - [B14K08_HUMAN]	3	208	6	4	4	6	14.722	6	12.720	14.638	140	16.868
U14849	Cytochrome b-c1 complex subunit 8 OS-Homo sapiens GN-UOCRC1 PE1 SV+4 - [UOCRC_HUMAN]	4	309	2	4	4	6	1.062	6	11.777	14.688	82	9.900
CSJAB9	Cytochrome c protein NCK1 (Fragment) OS-Homo sapiens GN-NCK1 PE1 SV+1 - [CSJAB9_HUMAN]	18	327	2	3	3	6	1.000	5	0.000	14.687	174	20.056
P41214	Eukaryotic translation initiation factor 2D OS-Homo sapiens GN-EIF2D PE1 SV+3 - [EIF2D_HUMAN]	1	316	1	1	1	6	1.319	6	7.191	14.683	584	66.954
AA0495GDF5	Cytochrome c oxidase subunit 2 OS-Homo sapiens GN-COX2 PE1 SV+1 - [AA0495GDF5_HUMAN]	7	349	1	2	6	6	0.773	3	34.593	14.669	227	25.625
QB49V6	DNA topoisomerase II alpha OS-Homo sapiens GN-TOPII1A PE1 SV+2 - [TOPII1A_HUMAN]	1	373	1	1	1	6	0.954	6	27.054	14.666	360	11.565
BDJ71	CNA FL18318, highly similar to Homo sapiens solute carrier family 20 (phosphate transporter), member 2 (SLC20A2), mRNA OS-Homo sapiens PE1 SV+1 - [BDJ71_HUMAN]	1	373	1	2	2	6	0.955	4	31.893	14.661	454	49.238
BR2R0	CNA FL19431, highly similar to Homo sapiens serine (or cysteine) protease inhibitor, class B (ovastin), member 8 (SERPINB8), mRNA OS-Homo sapiens PE1 SV+2 - [BR2R0_HUMAN]	1	373	1	4	5	6	1.000	6	0.000	14.655	374	42.772
BR2R8	CNA FL19436, highly similar to Homo sapiens serine protease inhibitor, member 8 (SERPINB8), mRNA OS-Homo sapiens PE1 SV+2 - [BR2R8_HUMAN]	1	373	1	4	5	6	1.000	6	0.000	14.654	374	42.772
ARKM4	CNA FL17525, highly similar to Homo sapiens vesicle transport inhibitor with 15NARE4 homologs 18 (vespa1) (VT18), mRNA OS-Homo sapiens PE1 SV+1 - [ARKM4_HUMAN]	1	373	1	4	4	6	0.801	5	21.867	14.643	232	26.672
ESAT12	ESAT12 OS-Homo sapiens GN-ESAT12 PE1 SV+1 - [ESAT12_HUMAN]	1	373	1	1	1	6	0.865	5	27.171	14.643	331	31.616
QB175	Similar to NADH dehydrogenase (Ubiquinone) 1 alpha subcomplex, 9 (ND6) (Fragment) OS-Homo sapiens PE1 SV+1 - [QB175_HUMAN]	1	373	1	2	3	6	1.000	5	13.058	14.630	338	38.417
QB19V1	Vacuolar protein-sorting-associated protein 36 OS-Homo sapiens GN-VP36 PE1 SV+1 - [QB19V1_HUMAN]	1	373	1	4	4	6	1.000	5	7.271	14.571	386	43.789
QB2C2	Protein tyrosine phosphatase SH-PTPase 2 (Fragment) OS-Homo sapiens GN-PTP2 PE1 SV+1 - [QB2C2_HUMAN]	1	373	1	2	2	6	1.000	6	0.000	14.569	387	43.842
Q1L56	Ribonucleoside-diphosphate reductase subunit M2 B OS-Homo sapiens GN-NRMB2 PE1 SV+1 - [R1B2B_HUMAN]	1	373	1	2	1	5	1.000	5	24.094	14.529	351	40.710
ABK41	Mitogen-activated protein kinase 4 (C/CA5) OS-Homo sapiens GN-CA5 PE1 SV+1 - [ABK41_HUMAN]	1	373	1	1	1	6	1.000	5	23.171	14.526	360	40.710
OS168	NADH dehydrogenase (ubiquinone) 1 beta subcomplex subunit 4 OS-Homo sapiens GN-NDUFB4 PE1 SV+3 - [NDUFB4_HUMAN]	1	373	1	2	2	6	1.000	4	0.000	14.503	387	43.789
BQ328	DEAD box polypeptide 27 OS-Homo sapiens GN-DCX27 PE1 SV+1 - [BQ328_HUMAN]	1	373	1	3	4	6	1.000	4	4.265	14.474	765	88.581
BK061	Mitogen-activated protein kinase 17 OS-Homo sapiens GN-MEK17 PE1 SV+1 - [BK061_HUMAN]	1	373	1	1	1	6	1.004	6	0.025	14.465	368	34.338
AA042R22	Fancioni anemia, complementation group D2, isoform CRA A OS-Homo sapiens GN-FANCD2 PE4 SV+1 - [AA042R22_HUMAN]	1	373	1	5	6	6	0.910	6	14.039	14.474	1451	164.025
QB2D8	Mitogen-activated protein kinase 17 OS-Homo sapiens GN-MEK17 PE1 SV+1 - [QB2D8_HUMAN]	1	373	1	1	1	6	1.004	6	0.025	14.465	368	34.338
EBN80	40S ribosomal protein S3a OS-Leishmania mexicana (strain MHOM/GT2001/11/103) GN-LMXXM_34_0400a_1 PE3 SV+1 - [EBN80_HUMAN]	1	373	1	2	2	6	1.000	6	0.000	14.436	264	30.017
B72ZC2	CNA FL18525, highly similar to Peptide N-acetylglucosaminyltransferase 2 (EC 2.4.1.14) OS-Homo sapiens PE1 SV+1 - [B72ZC2_HUMAN]	1	373	1	4	4	6	1.053	6	6.993	14.434	533	60.787
QB27Q	Hydrolytic oxidase (Fragment) OS-Homo sapiens GN-FOXO1 PE1 SV+1 - [QB27Q_HUMAN]	1	373	1	1	1	6	1.07	6	45.978	14.427	545	57.877
EA9V4	Dihydrolytic oxidase-thymidylate synthase OS-Leishmania mexicana (strain MHOM/GT2001/11/103) GN-LMXXM_06_0860 PE1 SV+1 - [EA9V4_HUMAN]	1	373	1	1	1	7	1.083	3	18.359	14.378	520	58.488
ABK72	CNA FL17625, highly similar to Homo sapiens galactose 4-epimerase variant 2, mRNA OS-Homo sapiens PE1 SV+1 - [ABK72_HUMAN]	1	373	1	4	5	6	0.976	6	4.000	14.375	446	52.787
FBWJ6	RNA-binding protein PHO1 OS-Homo sapiens GN-PHO1 PE1 SV+1 - [FBWJ6_HUMAN]	1	373	1	2	2	4	0.969	4	6.353	14.371	316	15.166
ESAT09	Plutative glyco-lysozyme OS-Leishmania mexicana (strain MHOM/GT2001/11/103) GN-LMXXM_36_3840 PE3 SV+1 - [ESAT09_HUMAN]	1	373	1	4	4	6	1.966	6	13.172	14.338	628	70.218
Q2769	MHC class II A, clone T15 (non-T12) associated glycoprotein beta chain (Fragment) OS-Homo sapiens PE1 SV+1 - [Q2769_HUMAN]	1	373	1	4	4	6	1.104	2	14.763	14.330	237	25.865
EBK28	Uncharacterized protein OS-Leishmania mexicana (strain MHOM/GT2001/11/103) GN-LMXXM_31_0840 PE3 SV+1 - [EBK28_HUMAN]	1	373	1	5	5	6	1.225	5	30.750	14.325	519	58.709
HOV26	Glycylglycyl transferase OS-Homo sapiens GN-HGM17 PE1 SV+1 - [HOV26_HUMAN]	1	373	1	1	1	6	1.886	2	11.866	14.320	255	28.267
PF358	Dianthigenin and metalloproteinase domain-containing protein 7 OS-Homo sapiens GN-ADAM17 PE1 SV+1 - [ADAM17_HUMAN]	1	373	1	7	7	8	1.000	7	4.388	14.317	624	92.961
QB27V2C2	General transcription factor IIE, polypeptide 1 (Alpha subunit, 980) variant (Fragment) OS-Homo sapiens PE1 SV+1 - [QB27V2C2_HUMAN]	1	373	1	2	2	6	1.000	6	5.526	14.313	397	40.083
ADAM17V2C2	NADH dehydrogenase (ubiquinone) 1 beta subcomplex subunit 6 OS-Homo sapiens GN-NDUFB6 PE1 SV+1 - [ADAM17V2C2_HUMAN]	1	373	1	2	2	6	1.000	6	16.846	14.299	519	57.123
ESAT4	Cathinone heavy chain OS-Leishmania mexicana (strain MHOM/GT2001/11/103) GN-LMXXM_36_1630 PE3 SV+1 - [ESAT4_HUMAN]	1	373	1	4	4	6	1.000	6	0.000	14.283	1693	191.413
ADLUM4	CNA FL1830, highly similar to Homo sapiens protein phosphatase 2C (PPP1R2C), mRNA OS-Homo sapiens PE1 SV+1 - [ADLUM4_HUMAN]	1	373	1	1	1	6	0.845	3	12.732	14.283	538	58.000
QB27V2C2	Phosphotransferase transfer protein alpha isoform (Fragment) OS-Homo sapiens GN-PITPA PE1 SV+1 - [QB27V2C2_HUMAN]	1	373	1	4	4	6	1.194	6	17.720	14.280	142	16.684
AA047W65	ATP-binding cassette sub-family B member 7, mitochondrial OS-Homo sapiens GN-ABCB7 PE1 SV+1 - [AA047W65_HUMAN]	1	373	1	4	4	6	1.000	6	22.244	14.260	713	73.239
ABK1V1	Suppressor of IKKepsilon 1 (Fragment) OS-Homo sapiens GN-SIK1 PE1 SV+1 - [ABK1V1_HUMAN]	1	373	1	1	1	6	1.000	6	30.521	14.257	520	58.488
BK3S1	Branchial-chitinase amidase transmembrane OS-Homo sapiens GN-BCAT2 PE1 SV+1 - [BK3S1_HUMAN]	1	373	1	2	2	4	0.997	4	0.000	14.249	352	39.890
CNA12202	Highly similar to nucleotide-associated protein kinase 1 OS-Homo sapiens GN-NK1 PE1 SV+1 - [CNA12202_HUMAN]	1	373	1	2	2	4	0.997	4	0.000	14.249	352	39.890
BK3M2	CNA FL11214, clone HEMBA102951, highly similar to Homo sapiens E1H domain binding protein 1 (E1BP1), mRNA OS-Homo sapiens PE1 SV+1 - [BK3M2_HUMAN]	1	373	1	2	2	6	1.000	1	14.228	14.220	232	23.972
OT8709	GaIIane S-transferase M5, isoform CRA A OS-Homo sapiens GN-GSTM5 PE1 SV+1 - [OT8709_HUMAN]	1	373	1	3	3	4	0.916	6	5.035	14.228	202	23.427
ESM3C3	Uncharacterized protein OS-Homo sapiens GN-UCP1 PE1 SV+1 - [ESM3C3_HUMAN]	1	373	1	1	1	6	1.133	6	11.876	14.227	494	55.246
QB685	MYCBP protein OS-Homo sapiens GN-MYCBP PE1 SV+1 - [QB685_HUMAN]	1	373	1	2	2	5	0.971	5	16.873	14.207	103	11.945
QB2913	Decarboxylase (Fragment) OS-Homo sapiens GN-DC1 PE1 SV+1 - [QB2913_HUMAN]	1	373	1	4	4	6	0.969	6	1.969	14.160	1337	151.632
QBKJ8	Methionine synthase reductase OS-Homo sapiens GN-MTRR PE1 SV+3 - [MTRR_HUMAN]	1	373	1	4	5	10	0.000	4	0.000	14.173	725	80.369
P1848	Arylsulfatase B OS-Homo sapiens GN-ARSB PE1 SV+1 - [ARSB_HUMAN]	1	373	1	4	5	6	0.970	5	15.249	14.162	533	59.649
BK3K5	CNA FL1834, clone T15 (non-T12) associated glycoprotein beta chain (Fragment) OS-Homo sapiens PE1 SV+1 - [BK3K5_HUMAN]	1	373	1	4	4	6	1.000	6	0.000	14.157	327	35.849
QB2F2	Coarctator subunit gamma 2 OS-Homo sapiens GN-COCCP2 PE1 SV+1 - [QB2F2_HUMAN]	1	373	1	5	5	6	1.000	6	26.646	14.151	871	97.560
QB2D2	CNA FL1830, highly similar to Homo sapiens mitral valve acid kinase (MLK1), mRNA OS-Homo sapiens PE1 SV+1 - [QB2D2_HUMAN]	1	373	1	4	5	6	0.995	6	12.610	14.150	244	24.842
ESKQF5	Glucocorticoid receptor OS-Homo sapiens GN-NR3C1 PE1 SV+1 - [ESKQF5_HUMAN]	1	373	1	8	8	15	0.5	6	3.682	14.118	742	81.457
QB1R6	Exosome complex component MTR3 OS-Homo sapiens GN-EXO3 PE1 SV+1 - [EXO3_HUMAN]	1	373	1	5	5	6	1.000	6	33.873	14.104	272	28.218
QB1R7	Eukaryotic translation initiation factor 2C OS-Homo sapiens GN-EIF2C PE1 SV+1 - [QB1R7_HUMAN]	1	373	1	1	1	6	1.000	6	14.000	14.103	252	25.842
BK3K1	Adoniamin OS-Homo sapiens PE1 SV+1 - [BK3K1_HUMAN]	1	373	1	3	3	7	1.091	3	12.917	14.097	357	41.943
ESM3C3	Glycylglycyl transferase OS-Leishmania mexicana (strain MHOM/GT2001/11/103) GN-LMXXM_19_0710 PE3 SV+1 - [ESM3C3_LEIUM]	1	373	1	3	3	7	1.091	3	12.917	14.097	357	41.943
QJ0M5	LIM domain-containing protein 2 (Fragment) OS-Homo sapiens GN-LMD2 PE1 SV+1 - [QJ0M5_HUMAN]	1	373	1	2	2	6	1.000	5	0.000	14.089	109	12.006
QZC36	Plutative uncharacterized protein FL4884 OS-Homo sapiens PE1 SV+2 - [YF099_HUMAN]	1	373	1	1	1	6	0.948	6	47.841	14.088	216	22.338
BK3K4	CNA FL1834, highly similar to Homo sapiens acyl-CoA oxidase 2 (acyl-CoA oxidase) Coenzyme A thioesterase, mRNA OS-Homo sapiens PE1 SV+1 - [BK3K4_HUMAN]	1	373	1	1	1	6	0.960	6	14.000	14.088	216	22.338
QYD08	Mitochondrial fission protein 1 OS-Homo sapiens GN-FIS1 PE1 SV+2 - [FIS1_HUMAN]	1	373	1	3	3	6	0.961	5	8.328	14.074	152	16.927
K3E26	Formin 1 (Fragment) OS-Homo sapiens GN-FMN1 PE1 SV+1 - [K3E26_HUMAN]	1	373	1	3	3	6	0.961	5	8.328	14.074	152	16.927
PK232	26S ribosomal protein S6, mitochondrial OS-Homo sapiens GN-MRPS6 PE1 SV+3 - [R106_HUMAN]	1	373	1	3	3	5	1.000	5	0.000	14.014	125	14.218
AD2AC1	Protein phosphatase subunit beta OS-Homo sapiens GN-PPM9 PE1 SV+1 - [AD2AC1_HUMAN]	1	373	1	2	2	6	0.912	5	8.458	14.010	176	20.947
AA042R42	Protein phosphatase 1, regulatory subunit 1C, isoform CRA A OS-Homo sapiens GN-PPP1R12C PE4 SV+1 - [AA042R42_HUMAN]	1	373	1	2	2	6	1.000	5	14.000	14.009	176	20.947
P14384	Cyathoporphyrinase OS-Homo sapiens GN-CYP1 PE1 SV+2 - [CYP1_HUMAN]	1	373	1	4	4	6	1.000	6	13.166	14.000	443	50.841
QB2913	RWD domain-containing protein OS-Homo sapiens GN-RWD1 PE1 SV+1 - [QB2913_HUMAN]	1	373	1	1	1	6	1.000	6	13.953	14.000	243	27.922
QB3J1	GTP-binding protein Rheb OS-Homo sapiens GN-RHEB PE1 SV+1 - [QB3J1_HUMAN]	1	373	1	4	4	6	0.987	6	0.106	13.947	79	8.668
QB1V9	Armadillo repeat-containing protein 1 OS-Homo sapiens GN-NRARC1 PE1 SV+1 - [ARMC1_HUMAN]	1	373	1	3	3	6	1.000	7	14.001	13.939	282	31.261
QB2913	DNA polymerase epsilon subunit 3 OS-Homo sapiens GN-POLE3 PE1 SV+1 - [QB2913_HUMAN]	1	373	1	5	5	6	0.942	6	13.800	13.937	147	16.445
PS235	3-methylcrotonyl sulfoxide transferase OS-Homo sapiens GN-MSTP1 PE1 SV+3 - [MSTP1_HUMAN]	1	373	1	2	2	5	1.022	5	5.428	13.937	297	33.158
CNA1976	CNA FL1976, highly similar to Homo sapiens DNA topoisomerase II alpha OS-Homo sapiens PE1 SV+1 - [CNA1976_HUMAN]	1	373	1	1	1	6	0.865	5	27.171	14.643	331	31.616
U1519	Ubiquitin-conjugating enzyme E2 variant 2 OS-Homo sapiens GN-UBE2V2 PE1 SV+4 - [UBE2V2_HUMAN]	1	373	1	4	4	8	1.069	7	10.351	13.899	145	16.332
ESB303	Uncharacterized protein OS-Leishmania mexicana (strain MHOM/G												

B4DEP8	cDNA FLJ5980, highly similar to Homo sapiens phosphatidylinositol 4-kinase type II (PK4II), mRNA OS-Homo sapiens PE=2 Sv1 - [B4DEP8_HUMAN]	7.8	3	3	3	5	1,000	5	23,447	12,820	449	51,102	
Q0V370	Protein phosphatase 1B isoform alpha OS-Homo sapiens GN=PPP1B1 PE=1 Sv1 - [PPP1B1_HUMAN]	8.81	2	2	2	7	1,000	7	0,668	868	48	2,968	
B4DN7	E3 ubiquitin-protein ligase OS-Homo sapiens PE=2 Sv1 - [B4DN7_HUMAN]	3.3	2	2	2	5	1,000	4	0,000	12,813	757	86,888	
GA087/W990	General transcription factor IIJ repeat domain-containing protein 2B OS-Homo sapiens GN=GTFR2D2 PE=4 Sv1 - [GA087/W990_HUMAN]	3.43	8	1	2	6	1,002	6	4,445	12,799	437	47,779	
Q0BU72	Protein 1 homolog 1 OS-Homo sapiens GN=H1L1 PE=1 Sv1 - [H1L1_HUMAN]	6.88	1	1	2	6	1,002	6	4,445	12,799	437	47,779	
Q0K471	Proteoglycan 2 OS-Homo sapiens GN=PLP2 PE=1 Sv1 - [PLP2_HUMAN]	8.55	1	1	5	1,038	5	22,623	12,776	152	16,880		
Cell AQ02AR66	Cell cycle G1/S transition control, nuclear CR4 D OS-Homo sapiens GN=CCCL5 PE=4 Sv1 - [AQ02AR66_HUMAN]	2.95	1	1	1	1,038	5	2,955	1,041	1,452	15,333		
EA0465	Complete genome, chromosome 4 OS-Leishmania mexicana (strain MHOM/GT2001/10103) GN=LXMM_04_0940 PE=4 Sv1 - [EA0465_HUMAN]	8.29	1	2	1	6	1,000	2	0,000	12,745	493	51,909	
Q0NBQ3	Saccharolipid dehydrogenase-like cytosolic/endothelial OS-Homo sapiens GN=SCDHP PE=1 Sv1 - [SCDHP_HUMAN]	6.53	1	3	3	6	1,000	6	9,098	12,729	429	47,121	
Q1K7C2	CNA FLJ5278, highly similar to C/EBP-beta, highly similar to AT-hook containing protein 1 (Fragment) OS-Homo sapiens PE=2 Sv1 - [B3KTD2_HUMAN]	2.54	1	1	1	1,000	5	4,250	1,000	1,000	1,000		
Q16R10	Extracellular matrix protein 1 OS-Homo sapiens GN=ECM1 PE=1 Sv1 - [ECM1_HUMAN]	11.9	2	2	5	1,037	5	6,489	12,701	540	60,635		
Q1E0D9	CNA FLJ5214, highly similar to Sulfolipase, mitochondrial (EC 1.2.1.24) OS-Homo sapiens PE=2 Sv1 - [B4DGP6_HUMAN]	9.4	1	2	2	5	1,000	5	4,017	12,688	447	52,688	
Q15120	Phosphoenolpyruvate kinase OS-Homo sapiens GN=PFKP PE=3 Sv1 - [PFKP_HUMAN]	21.35	1	4	4	5	1,000	5	14,12	12,687	192	21,981	
Q1TD11	ATP-dependent RNA helicase DDX34 OS-Homo sapiens GN=DDX34 PE=1 Sv1 - [DDX34_HUMAN]	3.75	2	4	4	5	1,000	5	36,377	12,685	891	98,334	
Q1P8Q5	Ribosomal protein L30 OS-Homo sapiens (Fragment) OS-Homo sapiens GN=L30 PE=1 Sv1 - [L30B35_HUMAN]	5.9	1	1	1	1,000	5	2,892	2,701	1,862	271	3,825	
Q0C9C2	Protein twenty homolog 3 OS-Homo sapiens GN=TTTH3 PE=1 Sv1 - [TTTH3_HUMAN]	4.59	2	3	3	4	1,008	4	1,224	12,684	523	57,508	
P19433	Receptor tyrosine phosphatase SHPTP4 PE=1 Sv1 - [SHPTP4_HUMAN]	3.49	2	2	2	1,000	5	14,568	12,572	260	3,825		
I3L0C8	Pulvate subunit-coupled neutral amino acid transporter 10 (Fragment) OS-Homo sapiens GN=SL38A10 PE=4 Sv1 - [I3L0C8_HUMAN]	16.28	1	1	4	6	1,000	5	2,000	12,653	258	27,461	
Q1H419	D1-actin-binding compressor OS-Homo sapiens GN=DRAP1 PE=1 Sv1 - [DRAP1_HUMAN]	14.83	4	4	4	5	1,000	5	23,025	12,641	205	22,338	
Q170J0	Inhibitor of nuclear factor kappa-B kinase-interacting protein OS-Homo sapiens GN=IKIP PE=1 Sv1 - [IKIP_HUMAN]	11.4	2	2	2	7	1,000	7	9,211	12,640	150	38,285	
HM074	Zinc finger protein 592 OS-Homo sapiens GN=ZNF592 PE=1 Sv1 - [HM074_HUMAN]	2.8	2	2	2	6	1,000	5	0,000	12,625	859	91,923	
P20292	Ariston-like 5 cytochrome oxidase protein OS-Homo sapiens GN=ARL5F PE=2 Sv1 - [AL5AF_HUMAN]	11.8	2	3	3	5	1,002	5	2,663	12,615	181	18,145	
P47755	F-actin-capping protein subunit alpha-2 OS-Homo sapiens GN=CAPZ2 PE=1 Sv1 - [CAPZ2_HUMAN]	11.89	5	3	7	7	861	2	22,422	12,598	288	32,929	
EPH92	Protein FAM58A OS-Homo sapiens GN=FAM58A PE=1 Sv1 - [EPH92_HUMAN]	5.45	5	1	2	5	1,000	1	12,589	12,512	312	34,409	
W53170	Ribosomal protein OS-Homo sapiens GN=RP17 PE=1 Sv1 - [W53170_HUMAN]	3.9	2	3	3	4	1,000	3	1,000	12,512	858	99,218	
FR49	MHC class I antigen (Fragment) OS-Homo sapiens GN=HLA-A PE=3 Sv1 - [FR49_HUMAN]	7.12	1	1	5	1,000	5	0,000	12,572	337	38,105		
Q0NF72	Rac-related protein OS-Homo sapiens GN=RRAL1 PE=1 Sv1 - [RRAL1_HUMAN]	13.59	3	3	3	5	1,002	5	14,568	12,572	260	3,825	
Q00653	Nuclear factor NF-kappa-B p100 subunit OS-Homo sapiens GN=NFkB1 PE=1 Sv1 - [NFkB1_HUMAN]	3.67	3	2	1	3	4	955	2	6,788	12,572	800	96,169
I3S254	Peromyscus acyl coenzyme A oxidase 3 OS-Homo sapiens GN=ACOX3 PE=2 Sv1 - [ACOX3_HUMAN]	5.57	2	4	4	6	905	6	28,309	12,569	700	77,880	
Q1788	Splein factor 3B subunit OS-Homo sapiens GN=SF3B1 PE=1 Sv1 - [SF3B1_HUMAN]	30.4	1	2	2	7	1,051	7	7,331	12,564	256	14,778	
QZ7858	Pulvate unanchored protein Dkf2p779F115 (Fragment) OS-Homo sapiens GN=DKF2p779F115 PE=1 Sv1 - [QZ7858_HUMAN]	7.5	2	2	2	5	1,000	5	7,914	12,560	282	27,038	
AQ02AR61	SH3 domain-containing protein OS-Homo sapiens GN=SH3BP1 PE=1 Sv1 - [AQ02AR61_HUMAN]	3.27	2	2	2	5	1,000	5	0,000	12,547	672	73,825	
Q0B773	Centriole-associated protein CEP250 OS-Homo sapiens GN=CEP250 PE=1 Sv1 - [CEP250_HUMAN]	13.2	2	2	3	6	1,000	3	0,000	12,541	2442	206,967	
Q0C085	Pentose-1-phosphatase OS-Homo sapiens GN=ZDHHC5 PE=1 Sv1 - [ZDHHC5_HUMAN]	4.34	7	3	3	6	1,000	6	0,000	12,534	715	77,498	
Q0P100	Colic acid C2 domain-containing protein 1A OS-Homo sapiens GN=CC2A1 PE=1 Sv1 - [CC2A1_HUMAN]	11.78	1	1	1	1,000	5	42,842	12,531	862	103,868		
BR2R85	CNA FLJ52476, highly similar to Homo sapiens LSM3 homolog, U6 small nuclear RNA associated (S. cerevisiae) (LSM3), mRNA OS-Homo sapiens PE=2 Sv1 - [BR2R85_HUMAN]	17.65	3	2	2	4	2	4,449	12,499	102	11,822		
CNA FLJ52414	highly similar to Homo sapiens C/EBP-beta, highly similar to AT-hook containing protein 1 (Fragment) OS-Homo sapiens PE=2 Sv1 - [BR2R85_HUMAN]	9.45	1	1	1	1,000	5	4,250	1,000	1,000	1,000		
Q13564	NEDD8-activating enzyme E1 regulatory subunit OS-Homo sapiens GN=NAE1 PE=1 Sv1 - [JLA1_HUMAN]	7.68	1	4	2	4	6	1,158	6	36,448	12,481	534	60,209
EP9M6	Methionine sulfoxide reductase OS-Homo sapiens GN=MSR1 PE=1 Sv1 - [EP9M6_HUMAN]	22.75	2	2	2	4	1,045	3	6,546	12,455	107	12,488	
EP9M6	Methionine sulfoxide reductase OS-Homo sapiens GN=MSR1 PE=1 Sv1 - [EP9M6_HUMAN]	22.75	2	2	2	4	1,045	3	6,546	12,455	107	12,488	
PA6573	Chromobox protein homolog 5 OS-Homo sapiens GN=CBX5 PE=1 Sv1 - [PA6573_HUMAN]	14.14	3	3	3	3	3	0.879	5	13,919	12,419	191	22,211
EP9B22	Pulvate acyl-CoA dehydrogenase OS-Homo sapiens GN=ACAD10 PE=1 Sv1 - [EP9B22_HUMAN]	3.56	1	1	1	1,000	5	3,903	11,399	917	11,399		
EP9L24	Myoglobin OS-Homo sapiens GN=PDE4IP PE=1 Sv1 - [EP9L24_HUMAN]	4.12	2	2	4	4	4	0.827	2	28,834	12,394	116	128,871
QZ9289	ZEB1 ribonucleoprotein L3, mitochondrial OS-Homo sapiens GN=MRPS7 PE=1 Sv1 - [Z9289_HUMAN]	14.88	5	3	3	3	3	2.638	4	5,678	12,390	242	28,116
IB3T03	AMF2 protein 19 (Fragment) OS-Homo sapiens GN=AMF2 PE=1 Sv1 - [IB3T03_HUMAN]	10.39	1	1	1	1,000	5	0,000	12,375	1,000	1,000		
Q13823	Nucleolin GTP-binding protein OS-Homo sapiens GN=NLN1 PE=1 Sv1 - [Q13823_HUMAN]	5.34	3	4	5	5	975	5	3,751	12,382	731	83,603	
Q0N646	Poly(ADP-ribose) polymerase 9 OS-Homo sapiens GN=PARP9 PE=1 Sv1 - [Q0N646_HUMAN]	18.25	4	4	4	5	1,000	5	23,832	12,174	1,000	12,174	
V5CZ25	Proteasome assembly chaperone 2 (Fragment) OS-Homo sapiens GN=PSMG2 PE=1 Sv1 - [V5CZ25_HUMAN]	8.13	4	2	2	5	0.913	5	9,473	12,300	209	23,491	
Q0R9Y1	FLJ10004 protein (Fragment) OS-Homo sapiens GN=FLJ10004 PE=1 Sv1 - [Q0R9Y1_HUMAN]	3.71	13	4	4	5	1,041	3	0,117	12,277	698	78,828	
Q0R9Y1	NADH dehydrogenase subunit 2 OS-Homo sapiens GN=ND2 PE=1 Sv1 - [Q0R9Y1_HUMAN]	17.17	2	2	2	4	1,000	4	0,000	12,268	84	9,281	
HK0Y33	PCNA-associated factor OS-Homo sapiens GN=AAAF1 PE=1 Sv1 - [HK0Y33_HUMAN]	39.29	4	2	2	4	1,000	4	0,000	12,367	84	9,281	
EP9B22	F-4.5 domain-containing protein OS-Homo sapiens GN=EP9B22 PE=1 Sv1 - [EP9B22_HUMAN]	3.56	1	1	1	1,000	5	3,903	11,399	917	11,399		
JK5W87	Myosin phosphatase Rho-interacting protein (Fragment) OS-Homo sapiens GN=MIRIP PE=1 Sv1 - [JK5W87_HUMAN]	5.09	6	1	3	5	0.996	1	1,332	12,338	844	98,870	
Q0Y8M5	Zinc transporter 1 OS-Homo sapiens GN=SLC30A1 PE=1 Sv1 - [Z0Y8M5_HUMAN]	6.31	3	3	3	6	1,000	5	5,147	12,330	807	95,204	
Q0Y8M5	Zinc transporter 1 OS-Homo sapiens GN=SLC30A1 PE=1 Sv1 - [Z0Y8M5_HUMAN]	6.31	3	3	3	6	1,000	5	5,147	12,330	807	95,204	
Q0Y8M5	Zinc transporter 1 OS-Homo sapiens GN=SLC30A1 PE=1 Sv1 - [Z0Y8M5_HUMAN]	6.31	3	3	3	6	1,000	5	5,147	12,330	807	95,204	
Q0Y8M5	Zinc transporter 1 OS-Homo sapiens GN=SLC30A1 PE=1 Sv1 - [Z0Y8M5_HUMAN]	6.31	3	3	3	6	1,000	5	5,147	12,330	807	95,204	
Q0Y8M5	Zinc transporter 1 OS-Homo sapiens GN=SLC30A1 PE=1 Sv1 - [Z0Y8M5_HUMAN]	6.31	3	3	3	6	1,000	5	5,147	12,330	807	95,204	
Q0Y8M5	Zinc transporter 1 OS-Homo sapiens GN=SLC30A1 PE=1 Sv1 - [Z0Y8M5_HUMAN]	6.31	3	3	3	6	1,000	5	5,147	12,330	807	95,204	
Q0Y8M5	Zinc transporter 1 OS-Homo sapiens GN=SLC30A1 PE=1 Sv1 - [Z0Y8M5_HUMAN]	6.31	3	3	3	6	1,000	5	5,147	12,330	807	95,204	
Q0Y8M5	Zinc transporter 1 OS-Homo sapiens GN=SLC30A1 PE=1 Sv1 - [Z0Y8M5_HUMAN]	6.31	3	3	3	6	1,000	5	5,147	12,330	807	95,204	
Q0Y8M5	Zinc transporter 1 OS-Homo sapiens GN=SLC30A1 PE=1 Sv1 - [Z0Y8M5_HUMAN]	6.31	3	3	3	6	1,000	5	5,147	12,330	807	95,204	
Q0Y8M5	Zinc transporter 1 OS-Homo sapiens GN=SLC30A1 PE=1 Sv1 - [Z0Y8M5_HUMAN]	6.31	3	3	3	6	1,000	5	5,147	12,330	807	95,204	
Q0Y8M5	Zinc transporter 1 OS-Homo sapiens GN=SLC30A1 PE=1 Sv1 - [Z0Y8M5_HUMAN]	6.31	3	3	3	6	1,000	5	5,147	12,330	807	95,204	
Q0Y8M5	Zinc transporter 1 OS-Homo sapiens GN=SLC30A1 PE=1 Sv1 - [Z0Y8M5_HUMAN]	6.31	3	3	3	6	1,000	5	5,147	12,330	807	95,204	
Q0Y8M5	Zinc transporter 1 OS-Homo sapiens GN=SLC30A1 PE=1 Sv1 - [Z0Y8M5_HUMAN]	6.31	3	3	3	6	1,000	5	5,147	12,330	807	95,204	
Q0Y8M5	Zinc transporter 1 OS-Homo sapiens GN=SLC30A1 PE=1 Sv1 - [Z0Y8M5_HUMAN]	6.31	3	3	3	6	1,000	5	5,147	12,330	807	95,204	
Q0Y8M5	Zinc transporter 1 OS-Homo sapiens GN=SLC30A1 PE=1 Sv1 - [Z0Y8M5_HUMAN]	6.31	3	3	3	6	1,000	5	5,147	12,330	807	95,204	
Q0Y8M5	Zinc transporter 1 OS-Homo sapiens GN=SLC30A1 PE=1 Sv1 - [Z0Y8M5_HUMAN]	6.31	3	3	3	6	1,000	5	5,147	12,330	807	95,204	
Q0Y8M5	Zinc transporter 1 OS-Homo sapiens GN=SLC30A1 PE=1 Sv1 - [Z0Y8M5_HUMAN]	6.31	3	3	3	6	1,000	5	5,147	12,330	807	95,204	
Q0Y8M5	Zinc transporter 1 OS-Homo sapiens GN=SLC30A1 PE=1 Sv1 - [Z0Y8M5_HUMAN]	6.31	3	3	3	6	1,000	5	5,147	12,330	807	95,204	
Q0Y8M5	Zinc transporter 1 OS-Homo sapiens GN=SLC30A1 PE=1 Sv1 - [Z0Y8M5_HUMAN]	6.31	3	3	3	6	1,000	5	5,147	12,330	807	95,204	
Q0Y8M5	Zinc transporter 1 OS-Homo sapiens GN=SLC30A1 PE=1 Sv1 - [Z0Y8M5_HUMAN]	6.31	3	3	3	6	1,000	5	5,147	12,330	807	95,204	
Q0Y8M5	Zinc transporter 1 OS-Homo sapiens GN=SLC30A1 PE=1 Sv1 - [Z0Y8M5_HUMAN]	6.31	3	3	3	6	1,000	5	5,147	12,330	807	95,204	
Q0Y8M5	Zinc transporter 1 OS-Homo sapiens GN=SLC30A1 PE=1 Sv1 - [Z0Y8M5_HUMAN]	6.31	3	3	3	6	1,000	5	5,147	12,330	807	95,204	
Q0Y8M5	Zinc transporter 1 OS-Homo sapiens GN=SLC30A1 PE=1 Sv1 - [Z0Y8M5_HUMAN]	6.31	3	3	3	6	1,000	5	5,147	12,330	807	95,204	
Q0Y8M5	Zinc transporter 1 OS-Homo sapiens GN=SLC30A1 PE=1 Sv1 - [Z0Y8M5_HUMAN]	6.31	3	3	3	6	1,000	5	5,147	12,330	807	95,204	
Q0Y8M5	Zinc transporter 1 OS-Homo sapiens GN=SLC30A1 PE=1 Sv1 - [Z0Y8M5_HUMAN]	6.31	3	3	3	6	1,000	5	5,147	12,330	807	95,204	

B3KVJ8	cDNA FL19684.6a, clone TEST403284, highly similar to Chloride channel protein 7 OS-Homo sapiens PE-2 SV1+ [-B3KVJ8_HUMAN]	4.84	13	4	4	6	0.9461	6	16.662	11.238	805	68.640
P15157	Amyloid beta 42 OS-Homo sapiens (ENRNO1_HUMAN)	2.39	4	4	4	6	0.8845	6	48.545	10.227	1007	115.321
ABMYT4	Phosphatidylinositol 3-kinase OS-Homo sapiens GN-PKC3 PE1 SV1+ [-ABMYT4_HUMAN]	2.31	8	2	2	5	1.0000	2	0.000	11.230	824	94.340
P21389	Cytoplasmic acetonide hydrogenase OS-Homo sapiens GN-HCO1 PE1 SV1+ [-P21389_HUMAN]	2.49	4	4	4	6	0.976	6	16.880	11.223	886	103.200
UB1818	Ubrich-associated protein 1 OS-Homo sapiens (ENRNO1_HUMAN) [GL-1480-PE4 SV1+ [-UB1818_LEIMU]]	2.46	1	4	4	4	1.0000	4	11.768	11.217	1000	108.620
ADQA2436	Neutrophil cytosolic factor 2 (Sf90a, chronic granulomatous disease, sarcosin 2), isoform CRA_a OS-Homo sapiens GN-HCF2 PE1 SV1+ [-ADQA2436_HUMAN]	11.6	4	4	4	4	1.0000	4	0.000	11.204	526	59.752
Q2Y75	Ras-GEF domain-containing protein 2 OS-Homo sapiens GN-GRB2 PE1 SV1+ [-Q2Y75_HUMAN]	15.3	4	4	4	4	1.0000	4	13.822	11.203	671	101.615
BRAT70	cDNA FL19479.7a, highly similar to Homo sapiens yvesen-1 Yamaguchi disease viral oncogene homolog 1(YEVS1), mRNA OS-Homo sapiens PE-1 SV1+ [-BRAT70_HUMAN]	4.6	55	1	3	5	1.0999	2	14.094	11.199	643	60.793
QY9D05	Brefeldin A-inhibited guanine nucleotide-exchange protein 2 OS-Homo sapiens GN-ARF2 PE1 SV1+ [-QY9D05_HUMAN]	1.34	19	1	3	5	1.0883	3	12.954	11.195	1785	201.909
FR5420	PER2, a protein with a GYF domain-containing protein 1 OS-Homo sapiens GN-GYF1 PE1 SV1+ [-FR5420_HUMAN]	5.17	2	4	4	4	1.0000	4	11.217	11.192	716	76.759
EA9AR09	Putative poly RNA synthetase, putative bifunctional aminomethyl-RNA synthetase OS-Leishmania mexicana (strain MHOM/GT/2001/1U103) GN-LMMXM_18_1220 PE-3 SV1+ [-EA9AR09_HUMAN]	1.31	2	4	4	4	0.7661	4	8.104	11.184	729	79.844
Q9J886	Neuronal cytoskeleton-associated protein 2 OS-Homo sapiens GN-NCAP2 PE1 SV1+ [-Q9J886_HUMAN]	1.53	4	4	4	4	1.0000	4	11.203	11.184	729	79.844
Q95899	Diphosphoinositide phosphatase phosphorylating 1 OS-Homo sapiens GN-NUDT3 PE1 SV1+ [-Q95899_HUMAN]	22.09	1	2	4	4	0.928	2	11.063	11.140	172	19.459
Q5F320	Aryl hydrocarbon receptor nuclear translocator isoform 2 variant (Fragment) OS-Homo sapiens GN-AHR2 PE1 SV1+ [-Q5F320_HUMAN]	1.29	1	3	3	3	0.857	1	21.373	11.139	315	34.800
EB1822	Hydroxyethyltransferase 4 OS-Homo sapiens GN-HDET4 PE1 SV1+ [-EB1822_HUMAN]	19.19	13	4	4	4	1.0000	3	0.000	11.132	127	15.162
EA9A286	Putative RNA-binding protein OS-Leishmania mexicana (strain MHOM/GT/2001/1U103) GN-LMMXM_27_2100 PE-4 SV1+ [-EA9A286_LEIMU]	5.44	1	4	4	4	1.0000	4	0.000	11.106	423	46.738
E1Z481	cDNA FL19407.1a, highly similar to Homo sapiens PE-2 SV1+ [-E1Z481_HUMAN]	5.94	3	4	4	4	1.0000	4	33.521	11.093	633	68.458
GBLJ2	Superoxide dismutase [Mn] mitochondrial (Fragment) OS-Homo sapiens GN-SOD2 PE1 SV1+ [-GBLJ2_HUMAN]	14.88	15	3	3	4	1.022	4	6.501	11.087	81	6.768
Q2M195	Kinesin-like protein KIF OS-Homo sapiens GN-KIF7 PE1 SV2+ [-Q2M195_HUMAN]	1.86	4	1	4	1	1.0000	1	11.084	11.084	1343	150.458
B3KX03	cDNA FL19757.1a, highly similar to Homo sapiens protein 2 OS-Homo sapiens GN-PE2 SV1+ [-B3KX03_HUMAN]	7.22	1	4	4	4	0.984	4	0.000	10.995	457	62.203
KTER10	WD repeat-containing protein 18 OS-Homo sapiens GN-WDR18 PE1 SV1+ [-KTER10_HUMAN]	1.33	6	3	3	4	1.150	4	37.597	11.064	409	44.809
ESAV98	Histone H2B OS-Leishmania mexicana (strain MHOM/GT/2001/1U103) GN-LMMXM_28_2340 PE-3 SV1+ [-ESAV98_HUMAN]	1.76	1	1	1	4	0.928	1	12.416	11.056	1776	199.887
ADQA2488	Selenin, isoform CRA_b OS-Homo sapiens GN-SETP PE4 SV1+ [-ADQA2488_HUMAN]	3.83	4	5	5	6	0.947	4	8.133	11.052	1871	215.909
Q3V612	Cardiac OS-Homo sapiens GN-CCDC68 PE1 SV2+ [-Q3V612_HUMAN]	2.08	14	3	3	7	0.947	4	0.000	11.052	1871	215.909
EB1814	Putative RNA-binding protein (Fragment) MHOM/GT/2001/1U103) GN-LMMXM_28_2330 PE-3 SV1+ [-EB1814_HUMAN]	14.17	1	1	1	3	1.0000	3	11.052	11.052	1871	215.909
Q9NH91	Alkalin B1 aldehyde reductase member 4 OS-Homo sapiens GN-ARL7 PE2 SV-6+ [-Q9NH91_HUMAN]	5.44	2	1	2	4	1.182	1	21.222	11.047	331	36.941
HTC455	Cytochrome c oxidase copper chaperone (Fragment) OS-Homo sapiens GN-PCP1 PE1 SV1+ [-HTC455_HUMAN]	34.68	3	2	2	4	1.0000	2	31.400	11.020	59	15.468
Q9Z785	Zinc finger protein ub-4 OS-Homo sapiens GN-DFF2 PE1 SV2+ [-Q9Z785_HUMAN]	5.88	3	2	2	5	0.829	4	28.227	11.008	391	44.127
Q9H168	RNA-binding motif protein 5 variant 1 (Fragment) OS-Homo sapiens GN-RBM5 PE1 SV1+ [-Q9H168_HUMAN]	4.75	2	1	3	5	1.157	1	11.008	11.008	505	50.076
P3711	Acetyltransferase 1 OS-Homo sapiens GN-AT2 PE1 SV1+ [-P3711_HUMAN]	2.2	2	2	2	4	0.967	4	4.096	11.003	99	11.294
Q4Q721	Neurogenic locus notch homolog protein 2 OS-Homo sapiens GN-NOTCH2 PE1 SV+3 [-Q4Q721_HUMAN]	1.5	7	4	4	4	1.002	5	20.381	10.978	2471	265.226
IL2L38	Centrosomal protein of 131 kDa OS-Homo sapiens GN-HCPC19 PE1 SV1+ [-IL2L38_HUMAN]	3.63	6	4	4	4	1.0000	4	0.000	10.975	407	17.627
B6VEX5	Abi-interactor 1 variant 72 OS-Homo sapiens PE-2 SV1+ [-B6VEX5_HUMAN]	4.64	14	2	2	4	1.035	4	1.231	10.975	388	42.811
IT0708	Centrosomal protein of 260 kDa OS-Homo sapiens GN-HCPC20 PE1 SV1+ [-IT0708_HUMAN]	1.33	4	4	4	5	2.120	2	156.801	10.965	2479	290.207
KTC020	Hydroxyethyltransferase associated protein 2 OS-Homo sapiens GN-HDET2 PE1 SV1+ [-KTC020_HUMAN]	73.33	3	2	2	4	1.0000	2	7.739	10.925	15	19.11
D3DN04	Poly (ADP-ribose) polymerase family member 14, isoform CRA_b OS-Homo sapiens GN-PARP14 PE4 SV1+ [-D3DN04_HUMAN]	3.58	4	4	4	4	0.914	4	52.677	10.947	1424	160.062
Q9RYV6	Exonuclease complex component 4 OS-Homo sapiens GN-EXOC4 PE1 SV1+ [-Q9RYV6_HUMAN]	1.26	4	4	4	4	1.0000	4	11.276	10.925	423	49.820
Q9RY66	HEAT repeat-containing protein 2 OS-Homo sapiens GN-HEATR2 PE1 SV4+ [-Q9RY66_HUMAN]	4.44	7	4	4	4	1.0000	6	5.842	10.920	855	93.462
D6W522	Karyophilin-like factor 16, isoform CRA_a OS-Homo sapiens GN-KLFP PE-4 SV1+ [-D6W522_HUMAN]	17.54	2	2	2	4	1.0000	2	0.000	10.893	211	25.566
B6H344	Protein L12, highly similar to Homo sapiens protein 12 (Fragment) OS-Homo sapiens PE-2 SV1+ [-B6H344_HUMAN]	1.12	12	1	2	2	1.0000	2	0.000	10.879	376	39.942
B1ALH6	Putative Coq domain-containing protein OS-Homo sapiens GN-PHYH PE1 SV1+ [-B1ALH6_HUMAN]	5.3	5	2	2	4	1.0000	2	0.000	10.879	376	39.942
Q9H130	Elongation of very long chain fatty acids methyltransferase OS-Homo sapiens GN-GLMT1 PE1 SV1+ [-Q9H130_HUMAN]	57.2	2	2	2	4	1.0000	2	0.000	10.861	144	16.414
Q9H330	Transmembrane protein 245 OS-Homo sapiens GN-TMEM245 PE1 SV2+ [-Q9H330_HUMAN]	7.03	2	2	2	3	1.063	4	9.087	10.874	911	100.881
Q9P302	Dual specificity mitogen-activated protein kinase kinase 2 OS-Homo sapiens GN-MA2K2 PE1 SV1+ [-Q9P302_HUMAN]	8	5	1	3	6	0.885	1	17.443	10.869	404	44.386
B4E003	cDNA FL19407.1a, highly similar to Homo sapiens protein 2 OS-Homo sapiens GN-PE2 SV1+ [-B4E003_HUMAN]	3.62	1	1	1	4	1.0000	4	8.062	10.869	453	52.328
EB1E17	Putative G0S acidic ribosomal protein 2 OS-Leishmania mexicana (strain MHOM/GT/2001/1U103) GN-LMMXM_29_2730 PE1 SV1+ [-EB1E17_LEIMU]	19.05	1	2	2	4	1.0000	4	0.000	10.862	105	10.620
Q9T099	Exonuclease complex component 5 OS-Homo sapiens GN-EXOC5 PE1 SV1+ [-Q9T099_HUMAN]	3.01	4	2	2	4	1.0000	4	11.047	10.861	423	49.820
B2R983	cDNA FL195032, highly similar to Homo sapiens zinc finger A20 domain containing 3 (ZAF203), mRNA OS-Homo sapiens PE-2 SV1+ [-B2R983_HUMAN]	16.35	7	2	2	3	0.726	2	50.272	10.854	208	22.527
P57470	Ras association domain-containing protein 2 OS-Homo sapiens GN-RASBP2 PE1 SV1+ [-P57470_HUMAN]	16.26	3	2	2	4	1.0000	2	0.000	10.844	326	37.707
Q9R9V0	Peptide lysozyme 2 OS-Homo sapiens GN-PL2 PE1 SV1+ [-Q9R9V0_HUMAN]	1.3	2	2	2	4	1.0000	4	11.022	10.822	172	18.880
Q9A922	TMED5 protein OS-Homo sapiens GN-TMED5 PE1 SV1+ [-Q9A922_HUMAN]	9.3	5	2	2	4	0.939	4	83.266	10.826	727	79.844
Q9Y323	Ub serine/threonine proteinase 2 OS-Homo sapiens GN-S242 PE1 SV1+ [-Q9Y323_HUMAN]	48.32	3	4	4	4	1.037	4	8.858	10.826	144	16.414
B3KVL0	cDNA FL19691.1a, clone TRACH300092, highly similar to Paxillin OS-Homo sapiens PE-2 SV1+ [-B3KVL0_HUMAN]	4.24	8	2	2	4	1.0000	4	15.997	10.818	828	64.118
GEA206	Cell division cycle 27, isoform CRA_b OS-Homo sapiens GN-CCDC27 PE1 SV1+ [-GEA206_HUMAN]	3.28	8	3	3	2	0.967	4	12.587	10.812	623	91.680
Q9H133	Putative cytoskeleton-binding protein 2 OS-Homo sapiens GN-CYB2 PE1 SV1+ [-Q9H133_HUMAN]	26.78	3	2	2	4	1.0000	2	0.000	10.805	84	8.860
U0X071	Ub serine/threonine proteinase Lsm4 (Fragment) OS-Homo sapiens GN-LSM4 PE1 SV1+ [-U0X071_HUMAN]	16.6	5	2	2	2	1.051	5	7.366	10.804	109	12.447
HTL020	G0S ribosomal protein L54 OS-Homo sapiens GN-L54 PE1 SV1+ [-HTL020_HUMAN]	11.88	1	1	1	4	1.0000	4	0.000	10.844	1000	124.421
Q5T011	Protein SZT2 OS-Homo sapiens GN-SZT2 PE2 SV+3 [-Q5T011_HUMAN]	0.64	1	2	2	6	1.0000	6	0.000	10.795	3432	377.791
DRK911	PILZ and LIM domain protein 7 (Fragment) OS-Homo sapiens GN-POLM7 PE1 SV1+ [-DRK911_HUMAN]	18.89	1	1	2	4	0.981	2	11.101	10.789	390	9.453
DRK974	Cytoskeletal elongation factor 14, isoform CRA_a OS-Homo sapiens GN-ELF14 PE1 SV1+ [-DRK974_HUMAN]	8.00	1	2	2	4	1.0000	2	0.000	10.789	110	16.890
EA9K77	Phenylalanine OS-Leishmania mexicana (strain MHOM/GT/2001/1U103) GN-LMMXM_18_0670 PE3 SV1+ [-EA9K77_LEIMU]	1.41	2	6	6	6	1.078	6	11.221	10.762	454	51.710
Q9H855	Specific PIP2K1A-regulated protein OS-Homo sapiens GN-STUT1 PE1 SV1+ [-Q9H855_HUMAN]	1.35	2	2	2	4	1.0000	4	11.221	10.762	454	51.710
FW0009	Periplanin 1 OS-Homo sapiens GN-PPH1 PE1 SV1+ [-FW0009_HUMAN]	8.31	8	3	4	4	1.0000	3	0.000	10.753	385	44.656
EP073	Protocadherin Fat 3 OS-Homo sapiens GN-FAT3 PE1 SV1+ [-EP073_HUMAN]	3	3	3	3	5	1.002	4	13.583	10.747	4439	488.527
VCY013	Acyl-CoA oxidase 12 OS-Homo sapiens GN-ACO12 PE1 SV1+ [-VCY013_HUMAN]	21.35	3	3	3	3	1.0000	3	20.189	10.746	512	57.13
MOYD15	Vesicle transport protein USE1 (Fragment) OS-Homo sapiens GN-HUSE1 PE1 SV1+ [-MOYD15_HUMAN]	11.8	3	2	2	3	0.879	3	14.909	10.740	161	17.884
cDNA FL19641	cDNA FL19641, highly similar to Homo sapiens protein 2 OS-Leishmania mexicana (strain MHOM/GT/2001/1U103) GN-LMMXM_29_2730 PE1 SV1+ [-cDNA FL19641_HUMAN]	10.93	3	2	2	4	1.0000	4	11.221	10.740	454	51.710
AK936	cDNA FL17824 OS-Homo sapiens PE-2 SV1+ [-AK936_HUMAN]	12.11	6	3	3	3	1.0000	3	0.000	10.731	388	41.688
P11111	Fragile X mental retardation syndrome-related protein 2 OS-Homo sapiens GN-FXR2 PE1 SV2+ [-P11111_HUMAN]	5.94	2	3	3	4	1.0000	3	0.000	10.721	673	74.178
Q9R9V0	cDNA FL19407.1a, highly similar to Homo sapiens protein 2 OS-Homo sapiens GN-PE2 SV1+ [-Q9R9V0_HUMAN]	7.47	1	1	1	4	1.0000	4	11.221	10.721	673	74.178
PE2891	40S ribosomal protein S30 OS-Homo sapiens GN-FU1 PE1 SV1+ [-PE2891_HUMAN]	16.95	2	1	1	5	0.868	5	11.842	10.711	59	6.644
Q9R9V0	Pre-mRNA splicing factor 2 OS-Homo sapiens GN-PSF2 PE1 SV1+ [-Q9R9V0_HUMAN]	7.72	1	1	1	4	1.0000	4	8.000	10.705	265	32.782
Q9JQ05	Atlastin 2 (Fragment) OS-Homo sapiens GN-ATL2 PE1 SV1+ [-Q9JQ05_HUMAN]	12	6	2	2	4	0.977	4	3.463	10.701	175	20.267
IT0581	WD repeat-containing protein 43 OS-Homo sapiens GN-WDR43 PE1 SV1+ [-IT0581_HUMAN]	4.14	3	3	3	3	1.0000	3	0.000	10.693	577	74.843
Q9Y457	Protein tyrosine phosphatase 12 (Fragment) OS-Homo sapiens GN-PTP12 PE4 SV1+ [-Q9Y457_HUMAN]	6.068	3	3	3	4	1.0000	4	32.965	10.693	255	29.358
EA9X03	Putative pyruvate dehydrogenase E1 beta subunit OS-Leishmania mexicana (strain MHOM/GT/2001/1U103) GN-LMMXM_25_1710 PE4 SV1+ [-EA9X03_LEIMU]	8.57	1	2	2	4	1.0000	4	4.022	10.68		

QBRP3	Oxidoreductase HTATP2 OS-Homo sapiens GN-HTATP2 PE1 S v2	[HTA2_HUMAN]	10,774	1	1	3	4	1,079	2	14,287	8,765	242	27,032			
EB361	Proteasome activator subunit 6 (strain MH0MG120011013) GN-LMMX3_31_2820 PE4 S v1	[EB361_LEUJH]	4,441	1	3	2	11,000	0	0	6,000	4,000	408	45,270			
HYK40	Lycopodium-induced tumor necrosis factor- α factor OS-Homo sapiens GN-LITAF PE1 S v1	[HYK40_HUMAN]	8,584	12	3	3	4	8,724	0	6,058	8,775	445	47,732			
QY909	CCDC25 protein (Fragment) OS-Homo sapiens GN-CCDC25 PE2 S v1	[QY909_HUMAN]	2,822	2	3	3	4	973	0	812	875	105	12,289			
QSRP1	Proteinase 3 (Fragment) OS-Homo sapiens GN-PRO3 PE1 S v1	[QSRP1_HUMAN]	2,266	2	3	3	3	1,874	0	18,077	8,775	445	47,732			
ETE52	Claspin OS-Homo sapiens GN-CLSPN PE1 S v1	[ETE52_HUMAN]	1,24	4	2	2	3	1,000	3	79,893	8,768	1286	145,228			
181M4	Fatty acid dehydrogenase (Fragment) OS-Homo sapiens GN-HAD3A PE1 S v1	[181M4_HUMAN]	12,35	4	2	2	3	1,000	3	0	0	0	18,471			
QY217	Miyubunin-related protein 6 OS-Homo sapiens GN-MTR6 PE1 S v1	[QY217_HUMAN]	3,7	3	2	2	3	1,000	3	0	0	8,764	621	71,922		
EU	EU ubiquitin-protein ligase RNF114 OS-Homo sapiens GN-RNF114 PE1 S v1	[RNF114_HUMAN]	14,47	3	5	5	5	8,855	5	13,340	8,746	228	25,877			
FWP15	Proteinase 3 (Fragment) OS-Homo sapiens GN-PRO3 PE1 S v1	[FWP15_HUMAN]	1,821	1	3	3	3	1,000	3	0	0	8,768	89	81,130		
Q3P44	Echordomicro-microtubule-associated protein-like 3 OS-Homo sapiens GN-EMML3 PE1 S v1	[EMML3_HUMAN]	3,447	3	3	3	3	3	51,898	8,762	89	95,138				
Q3P45	Major capsid protein domain-containing protein 1 OS-Homo sapiens GN-MFSD1 PE1 S v1	[MFSD1_HUMAN]	2,866	2	2	2	2	2	25,307	8,762	89	117,745				
BR2C9	cDNA FLJ38204, highly similar to human ostein death-associated protein (DAP), mRNA OS-Homo sapiens PE2 S v1	[BR2C9_HUMAN]	15,69	3	2	2	2	5	9,933	5	20,275	8,727	101,177			
ADA2GR205	2'-O-5'-oligoadenylate synthetase 2, 100kDa, isoform CRA A OS-Homo sapiens GN-OAS3 PE1 S v1	[ADA2GR205_HUMAN]	2,58	3	3	3	3	4	8,971	4	12,507	8,722	108,106			
Q3C10	Cytoplasmic β -caseinase 1 OS-Homo sapiens GN-PCB1 PE1 S v1	[Q3C10_HUMAN]	20,92	2	2	2	2	2	1,000	3	0	0	23,623			
BD30X	cDNA FLJ5747, highly similar to Chgoepin1 (EC 2.4.1.186) OS-Homo sapiens PE2 S v1	[BD30X_HUMAN]	10,37	2	3	3	3	1,104	2	2,321	8,718	193	21,466			
ADA2GR207	HEAT 1 domain-containing protein 1 OS-Homo sapiens GN-HEAT1 PE1 S v1	[ADA2GR207_HUMAN]	1,13	2	2	2	2	2	1,000	3	0	0	2,302			
HBR87	TOX2 variant 5 OS-Homo sapiens GN-TOX2 PE1 S v1	[HBR87_HUMAN]	4,56	7	1	2	2	4	1,004	2	0	0	8,708	350	37,472	
B4E26	cDNA FLJ18109, highly similar to Homo sapiens SMC3 structural maintenance of chromosomes 5-like 1 (SMC5L1), mRNA OS-Homo sapiens PE2 S v1	[B4E26_HUMAN]	3,16	13	2	2	2	3	1,000	2	0	0	7,720	85,451		
AK338	cDNA FLJ18109, highly similar to Homo sapiens SMC3 structural maintenance of chromosomes 5-like 1 (SMC5L1), mRNA OS-Homo sapiens PE2 S v1	[AK338_HUMAN]	3,16	13	2	2	2	3	1,000	2	0	0	7,720	85,451		
EPH95	Sperm-specific antigen 2 OS-Homo sapiens GN-SSFA2 PE1 S v1	[EPH95_HUMAN]	1,86	5	2	2	2	2	3	0	0	8,691	1237	136,054		
OT959	Interferon-inducible double-stranded RNA-dependent protein kinase OS-Homo sapiens GN-PRKRA PE1 S v1	[PRKRA_HUMAN]	4,9	3	3	3	3	3	1,273	4	36,974	8,696	313	34,383		
AK398	2'-deoxyribose 5'-phosphate N-ribosyltransferase OS-Homo sapiens GN-DNPH1 PE1 S v1	[DNPH1_HUMAN]	8,62	2	2	2	2	4	1,000	4	0	0	8,685	174	19,097	
B7Z27	cDNA FLJ5918, highly similar to Echordomicro-microtubule-associated protein-like 2 OS-Homo sapiens PE2 S v1	[B7Z27_HUMAN]	6,24	1	1	2	4	1,078	4	10,463	8,679	807	87,184			
BQ227	DNA topoisomerase II β OS-Homo sapiens GN-PTB1 PE1 S v1	[BQ227_HUMAN]	8,43	3	4	4	4	4	1,000	3	0	0	8,715	498	45,811	
ESAW1	Putative uncharacterized protein OS-Leishmania mexicana (strain MH0MG120011013) GN-LMMX_23_1410 PE4 S v1	[ESAW1_LEUJH]	14,57	1	3	3	3	1,000	3	0	0	8,671	247	27,285		
BR2D9	cDNA FLJ1003, highly similar to human GTP binding protein 1 (GTPBP1), mRNA OS-Homo sapiens PE2 S v1	[BR2D9_HUMAN]	1,55	1	2	2	2	4	9,922	4	3,765	8,669	584	63,438		
Q8UL3	Glycerol-3-phosphate acyltransferase 4 OS-Homo sapiens GN-GPAT4 PE1 S v1	[GPAT4_HUMAN]	6,58	4	3	3	3	4	919	4	18,154	8,668	456	52,037		
BK354	cDNA FLJ36888.6, clone ASTR2015185, highly similar to PCLVYDRIN RGLCFPTP OS-Homo sapiens PE2 S v1	[BK354_HUMAN]	8,78	3	1	1	4	1,000	2	0	0	8,668	962	39,558		
AK338	1 α -carboxylase dehydratase (Fragment) OS-Homo sapiens PE1 S v1	[AK338_HUMAN]	2,93	1	1	1	4	1,915	4	6,756	8,662	27	3,248			
BD424	cDNA FLJ1715, highly similar to 395 ribosomal protein L10, mitochondrial OS-Homo sapiens PE1 S v1	[BD404_HUMAN]	8,76	5	2	2	4	823	4	21,005	8,644	494	22,781			
AK338	Nucleic acid pyrophosphatase 2 OS-Homo sapiens GN-NPP2 PE1 S v1	[NPP2_HUMAN]	1,75	3	2	2	2	2	0	0	0	8,641	459	49,530		
EP817	Oxidoreductase HTATP2 OS-Homo sapiens GN-HTATP2 PE1 S v1	[EP817_HUMAN]	13,78	1	1	3	4	926	2	24,582	8,641	196	21,961			
QNP43	Acyl-coenzyme A thioesterase 13 OS-Homo sapiens GN-ACOT13 PE1 S v1	[ACOT13_HUMAN]	1,74	1	1	1	3	1,129	3	14,298	8,631	140	1,952			
13404	Acyl-coenzyme A thioesterase 13 OS-Homo sapiens GN-ACOT13 PE1 S v1	[13404_HUMAN]	1,74	1	1	1	3	1,129	3	14,298	8,631	140	1,952			
H3V68	UPF0505 protein C16orf82 OS-Homo sapiens GN-C16orf82 PE1 S v1	[H3V68_HUMAN]	17,69	1	2	2	2	2	1,000	3	5,434	8,622	451	50,752		
Q3C10	Protein G1H0A154 PE1 S v1	[Q3C10_HUMAN]	4,31	2	2	2	2	2	1,000	2	0	0	6,628	805	95,138	
Q3D44	PHF2 protein OS-Homo sapiens GN-PHF2 PE2 S v1	[Q3D44_HUMAN]	6,15	3	3	3	3	3	940	3	9,166	8,621	504	57,342		
Q0245	Inaun-like growth factor 2 mRNA-binding protein 3 OS-Homo sapiens GN-IGFBP3 PE1 S v1	[Q0245_HUMAN]	5,53	1	3	3	3	3	945	2	2,721	8,619	579	63,866		
BR2C1	Deacetylase-associated protein 2 OS-Homo sapiens GN-SPD2 PE1 S v1	[BR2C1_HUMAN]	15,34	3	3	3	3	2,86	3	8,942	8,618	206	103,804			
PD289	Topomodulin-1 OS-Homo sapiens GN-TMOD1 PE1 S v1	[TMOD1_HUMAN]	4,18	1	1	1	1	4	970	1	8,611	359	40,544			
BR2D9	Perforin 2 OS-Homo sapiens GN-PCF2 PE1 S v1	[PCF2_HUMAN]	8,91	2	2	2	2	2	2,429	1	8,611	359	40,544			
P3043	Flavin reductase (NADPH) OS-Homo sapiens GN-BLVRB PE1 S v1	[BLVRB_HUMAN]	11,65	3	2	2	2	3	1,165	3	1,496	8,600	206	22,105		
CB352	Sodium/potassium transporting ATPase subunit beta 3 OS-Homo sapiens GN-ATP1B3 PE1 S v1	[ATP1B3_HUMAN]	18,65	4	2	2	2	4	1,113	4	2,458	8,596	89	9,962		
Q3C10	Protein G1H0A154 PE1 S v1	[Q3C10_HUMAN]	4,31	2	2	2	2	2	1,000	2	0	0	8,592	805	95,138	
BR2B4	cDNA FLJ3580, highly similar to human vacuolar protein sorting 41 (yeast) (VPS41), transcript variant 1, mRNA OS-Homo sapiens PE2 S v1	[BR2B4_HUMAN]	2,22	5	2	2	2	4	1,000	4	0	0	8,587	854	98,485	
BR2B4	Putative uncharacterized protein OS-Leishmania mexicana (strain MH0MG120011013) GN-LMMX_29_1960 PE4 S v1	[BR2B4_HUMAN]	5,48	2	2	2	2	4	1,000	4	0	0	8,587	854	98,485	
EAQ74	ABC1 transporter-like protein OS-Leishmania mexicana (strain MH0MG120011013) GN-LMMX_15_0780 PE3 S v1	[EAQ74_HUMAN]	2,56	1	2	2	7	1,000	7	0	0	8,578	2679	201,301		
DD370	F11 receptor, isoform CRA A OS-Homo sapiens GN-F11R PE4 S v1	[DD370_HUMAN]	8,11	4	3	3	3	3	4	1,028	4	26,242	8,571	296	32,203	
BR2C1	Putative water channel 1 OS-Homo sapiens GN-EDEN1 PE1 S v1	[BR2C1_HUMAN]	6,23	1	1	1	4	1,000	4	0	0	8,569	27	3,248		
KTEC7	Zinc finger protein 700 OS-Homo sapiens GN-ZNF700 PE4 S v1	[KTEC7_HUMAN]	14,23	131	1	3	3	3	2,854	1	8,551	724	84,207			
BR2D9	Putative uncharacterized protein OS-Leishmania mexicana (strain MH0MG120011013) GN-LMMX_20_2010 PE4 S v1	[BR2D9_HUMAN]	6,11	4	2	2	2	2	2	1,000	2	0	0	8,551	724	84,207
BR2D0	cDNA FLJ39396, highly similar to Homo sapiens ERO-like beta (c. versine) OS-Homo sapiens PE2 S v1	[BR2D0_HUMAN]	4,71	4	1	2	3	1,025	1	2	0	0	8,542	467	53,485	
ADA2GRW1F1	Protein C16orf82 OS-Homo sapiens GN-C16orf82 PE1 S v1	[ADA2GRW1F1_HUMAN]	10,91	4	2	2	2	3	1,000	2	0	0	8,541	275	29,828	
AK338	ERK5-related lipid transfer protein 2, mitochondrial (Fragment) OS-Homo sapiens GN-STRAD2 PE1 S v1	[AK338_HUMAN]	1,74	1	1	1	1	1	1,000	1	0	0	8,541	275	29,828	
EAQY2	Exon junction inclusion factor 2 alpha subunit, putative OS-Leishmania mexicana (strain MH0MG120011013) GN-LMMX_03_0890 PE4 S v1	[EAQY2_LEUJH]	4,36	5	1	2	4	1,306	1	1,306	8,533	413	46,594			
Q8552	Aluminum-activated oxalate decarboxylase 1 OS-Homo sapiens GN-AOX1 PE1 S v1	[Q8552_HUMAN]	1,49	1	1	1	2	1,000	2	6,103	8,530	186	20,826			
ERJ22	Endoplasmic reticulum lumen 1 OS-Homo sapiens GN-ERLEC1 PE1 S v1	[ERLEC1_HUMAN]	1,222	1	5	5	5	1,044	5	6,108	8,500	483	54,823			
Q85M6	Protein VAC1 OS-Homo sapiens GN-VAC1 PE1 S v1	[VAC1_HUMAN]	4,73	4	4	4	4	4	6	974	4,467	846	782	87,917		
Q6G40	Proteinase 3 (Fragment) OS-Homo sapiens GN-PRO3 PE1 S v1	[Q6G40_HUMAN]	2,822	2	3	3	3	3	1,000	3	0	0	8,500	89	81,130	
Q6G43	Putative peptidyl RNA polymerase PTHRD1 OS-Homo sapiens GN-PTHRD1 PE1 S v1	[PTHRD1_HUMAN]	22,14	1	3	3	3	3	1,084	3	9,472	8,491	140	15,795		
EAQW3	Perforin 2 OS-Homo sapiens GN-PCF2 PE1 S v1	[PCF2_HUMAN]	8,91	2	2	2	2	2	1,000	102,311	2	0	8,492	126	136,054	
QNLN0	Phosphatidyl inositol associated with glycosylphosphatidylinositol-enriched membranes 1 OS-Homo sapiens GN-PAIG1 PE1 S v1	[PAIG1_HUMAN]	6,71	1	2	2	2	3	1,000	3	0	0	8,487	432	46,951	
CL1C9	EU ubiquitin-protein ligase RNF114 OS-Homo sapiens GN-RNF114 PE1 S v1	[CL1C9_HUMAN]	16,55	2	2	2	2	2	0	0	0	8,483	139	16,021		
Q1C637	AP1, complex subunit 2 OS-Homo sapiens GN-AP2 PE1 S v1	[AP2_HUMAN]	6,64	1	1	1	1	1	1,000	3	13,497	8,483	139	16,021		
EB161	Putative 5'-methylthiohydroxyprolyl-glutamate-homocysteine methyltransferase OS-Leishmania mexicana (strain MH0MG120011013) GN-LMMX_30_0010 PE1 S v1	[EB161_HUMAN]	2,86	1	2	2	2	4	21,506	4	5,434	8,472	110	86,403		
UPF0505	UPF0505 protein C16orf82 OS-Homo sapiens GN-C16orf82 PE1 S v1	[UPF0505_HUMAN]	1,99	1	1	1	1	1	1,000	2	0	0	8,472	110	86,403	
Q1323	Mitogen-activated protein kinase kinase 1 OS-Homo sapiens GN-MAKP3 PE1 S v1	[MK1_HUMAN]	3,11	3	3	3	3	3	1,000	3	0	0	8,445	1572	160,366	
PH172	Egghn-B1 OS-Homo sapiens GN-EB1 PE1 S v1	[PH172_HUMAN]	2,02	1	1	1	1	1	1,000	4	10,519	8,444	346	37,802		
BR2D9	Putative uncharacterized protein OS-Leishmania mexicana (strain MH0MG120011013) GN-LMMX_22_1620 PE4 S v1	[BR2D9_HUMAN]	1,4	1	1	1	1	1	1,000	4	0	0	8,445	146	15,795	
Q8X88	Glutathione S-transferase theta 1, mitochondrial OS-Homo sapiens GN-GLRX1 PE1 S v1	[GLRX1_HUMAN]	8,92	1	1	1	1	1	1,000	3	0	0	8,435	157	16,618	
Q7222	Long-chain GTP-binding protein 1 OS-Homo sapiens GN-ETD1 PE1 S v1	[ETD1_HUMAN]	4,2	3	3	3	3	3	1,000	3	22,623	8,434	170	192,816		
QNS01	Cell death regulator Aven OS-Homo sapiens GN-AVEN PE1 S v1	[AVEN_HUMAN]	8,56	1	3	3	3	4	1,000	3	0	0	8,419	362	38,483	
Z2326	Tubulin gamma 1 chain OS-Homo sapiens GN-TUBG1 PE1 S v1	[TUBG1_HUMAN]	2,22	1	1	1	1	1	1,000	4						

BAE100	cDNA FL154839, highly similar to Lactotransferrin (EC 3.2.1.3) OS=Homo sapiens PE=2 Sv1+ [BAE100_HUMAN]	7	7	12	2	2	2	4	1,003	4	7,488	7,743	300	33,004		
BAN145	Proteinase 6 OS=Homo sapiens (strain MHMOMGT2001U1103) GN=MLMXX_34_3200 PE=3 Sv1+ [BAN145_HUMAN]	3	7	11	1	1	1	1	3,000	1	3,000	3,000	640	21,349		
EBB6K2	Putative cystathione gamma lyase OS=Leishmania mexicana (strain MHMOMGT2001U1103) GN=MLMXX_34_3200 PE=3 Sv1+ [EBB6K2_LEIMU]	6	6	11	1	1	1	3	5	1,000	5	1,000	7,732	410	44,418	
ESAM68	Uncharacterized protein OS=Leishmania mexicana (strain MHMOMGT2001U1103) GN=MLMXX_26_2910 PE=4 Sv1+ [ESAM68_LEIMU]	1	1	1	1	1	1	3	1,000	1	1,000	1,000	2,780	324,725		
BCEY13	cDNA FL15228, highly similar to Homo sapiens forkhead box O1 (FOXO1), mRNA OS=Homo sapiens PE=2 Sv1+ [BCEY13_HUMAN]	1	1	1	1	1	1	1	4,199	1	4,199	7,718	2,840	343,728		
BADK03	cDNA FL15228, highly similar to Proboscis-ATP-dependent RNA helicase DDX10 (EC 3.6.1.1) OS=Homo sapiens PE=2 Sv1+ [BADK03_HUMAN]	1	1	1	1	1	1	1	3	1,000	3	0,000	7,709	781	90,260	
QIET71	Protein FAM108B OS=Homo sapiens (strain MHMOMGT2001U1103) GN=MLMXX_26_2910 PE=4 Sv1+ [QIET71_HUMAN]	1	1	1	1	1	1	1	5,446	1	5,446	5,446	669	1,111		
ESR1F0	Mitogen-activated protein kinase OS=Homo sapiens (strain MHMOMGT2001U1103) GN=MLMXX_26_2910 PE=4 Sv1+ [ESR1F0_HUMAN]	5	7	1	1	1	1	1	2	3	1,000	1,000	7,701	316	36,214	
QZV9V9	3S5 ribosomal protein L26, mitochondrial (Fragment) OS=Homo sapiens (strain MHMOMGT2001U1103) GN=MLMXX_26_2910 PE=4 Sv1+ [QZV9V9_HUMAN]	1	1	1	1	1	1	1	3	1,000	3	1,000	2,000	22,827		
ACG178	Acyl-CoA oxidase family member 1, mitochondrial OS=Homo sapiens (strain MHMOMGT2001U1103) GN=MLMXX_26_2910 PE=4 Sv1+ [ACG178_HUMAN]	1	1	1	1	1	1	1	3	1,000	3	1,000	2,000	22,827		
BK3U00	cDNA FL159833, clone SPLN202608, highly similar to Protein CHMP7 OS=Homo sapiens PE=2 Sv1+ [BK3U00_HUMAN]	1	1	1	1	1	1	1	3	1,000	3	1,000	1,000	50,903		
QBA317	Protein FAM108B OS=Homo sapiens (strain MHMOMGT2001U1103) GN=MLMXX_26_2910 PE=4 Sv1+ [QBA317_HUMAN]	1	1	1	1	1	1	1	15,013	1	15,013	15,013	1,664	25,665		
AAQ0W716	Alpha-1,2-mannosyltransferase ALG6 OS=Homo sapiens (strain MHMOMGT2001U1103) GN=MLMXX_26_2910 PE=4 Sv1+ [AAQ0W716_HUMAN]	1	1	1	1	1	1	1	2	1,000	2	1,000	7,665	102	11,352	
QYQ3Q3	Transmembrane beta24 domain-containing protein 3 OS=Homo sapiens (strain MHMOMGT2001U1103) GN=MLMXX_26_2910 PE=4 Sv1+ [QYQ3Q3_HUMAN]	1	1	1	1	1	1	1	2	1,000	2	1,000	7,665	102	11,352	
QICD15	cDNA FL15228, highly similar to Protein SLC12A1 OS=Homo sapiens PE=2 Sv1+ [QICD15_HUMAN]	1	1	1	1	1	1	1	2	1,000	2	1,000	7,665	102	11,352	
OS6566	Mitotic checkpoint serine/threonine protein kinase BUB1, beta OS=Homo sapiens (strain MHMOMGT2001U1103) GN=MLMXX_26_2910 PE=4 Sv1+ [OS6566_HUMAN]	1	1	1	1	1	1	1	3	3	1,000	3	1,000	7,665	102	11,352
Q5SR55	Nucleolar phosphoprotein NUP188 PE=1 Sv1+ [NUP188_HUMAN]	1	1	1	1	1	1	1	3	1,000	3	1,000	7,665	102	11,352	
BK3P46	cDNA FL151953, clone NT2920707610, highly similar to DHH domain containing 2 (DDHD2), mRNA OS=Homo sapiens PE=2 Sv1+ [BK3P46_HUMAN]	1	1	1	1	1	1	1	3	3	1,000	3	1,000	7,665	102	11,352
ESAY87	Proteinase 6 OS=Homo sapiens (strain MHMOMGT2001U1103) GN=MLMXX_26_2910 PE=4 Sv1+ [ESAY87_LEIMU]	1	1	1	1	1	1	1	2	1,758	2	1,758	2,000	134	22,777	
QBNY22	Regulatory subunit of mTOR OS=Homo sapiens (strain MHMOMGT2001U1103) GN=MLMXX_26_2910 PE=4 Sv1+ [QBNY22_HUMAN]	1	1	1	1	1	1	1	1	1,028	1	1,028	2	3,303	30,303	
Q8WVC4	Uncharacterized protein C20487, mitochondrial OS=Homo sapiens (strain MHMOMGT2001U1103) GN=MLMXX_26_2910 PE=4 Sv1+ [Q8WVC4_HUMAN]	1	1	1	1	1	1	1	3	1,024	3	1,024	2,000	134	22,777	
BADQ07	Uncharacterized protein OS=Homo sapiens (strain MHMOMGT2001U1103) GN=MLMXX_26_2910 PE=4 Sv1+ [BADQ07_HUMAN]	1	1	1	1	1	1	1	2	1,000	2	1,000	2,000	134	22,777	
BADQ01	cDNA FL153475, highly similar to Autophagy-related protein 7 OS=Homo sapiens PE=2 Sv1+ [BADQ01_HUMAN]	1	1	1	1	1	1	1	3	1,211	3	1,211	3,000	81	76,548	
HDR85	Strap1 protein 1 (Fragment) OS=Homo sapiens (strain MHMOMGT2001U1103) GN=MLMXX_26_2910 PE=4 Sv1+ [HDR85_HUMAN]	1	1	1	1	1	1	1	3	1,746	3	1,746	2,000	134	22,777	
BS254	Oxidative phosphorylation complex I subunit 1 OS=Homo sapiens (strain MHMOMGT2001U1103) GN=MLMXX_26_2910 PE=4 Sv1+ [BS254_HUMAN]	1	1	1	1	1	1	1	4	1,877	4	1,877	4,000	3,000	30,300	
BAE1C9	cDNA FL152983, highly similar to Synapse-associated protein 1 OS=Homo sapiens PE=2 Sv1+ [BAE1C9_HUMAN]	1	1	1	1	1	1	1	5	5	5	5	5	5	5	5
HTC469	Histone H4 lysine 9 methyltransferase 1 OS=Homo sapiens (strain MHMOMGT2001U1103) GN=MLMXX_26_2910 PE=4 Sv1+ [HTC469_HUMAN]	1	1	1	1	1	1	1	3	1,000	3	1,000	7,619	246	28,652	
P19793	Retinoic acid receptor RXR-alpha OS=Homo sapiens (strain MHMOMGT2001U1103) GN=MLMXX_13_1090 PE=3 Sv1+ [P19793_HUMAN]	1	1	1	1	1	1	1	3	1,000	3	1,000	7,619	246	28,652	
ESAPD3	Putative proteinase regulatory ATPase subunit 2 OS=Leishmania mexicana (strain MHMOMGT2001U1103) GN=MLMXX_13_1090 PE=3 Sv1+ [ESAPD3_LEIMU]	1	1	1	1	1	1	1	2	1,000	2	1,000	7,617	438	49,233	
Q1458	Oxidative phosphorylation complex I subunit 1 OS=Homo sapiens (strain MHMOMGT2001U1103) GN=MLMXX_13_1090 PE=3 Sv1+ [Q1458_HUMAN]	1	1	1	1	1	1	1	2	1,153	2	1,153	7,615	114	12,607	
BDRD65	cDNA FL156655, highly similar to Homo sapiens striatal membrane-associated protein 1 (SMAP1), mRNA OS=Homo sapiens PE=2 Sv1+ [BDRD65_HUMAN]	1	1	1	1	1	1	1	3	3	3	3	3	3	3	3
FSY210	Norgalactosyl deaminase (Fragment) OS=Homo sapiens (strain MHMOMGT2001U1103) GN=MLMXX_13_1090 PE=3 Sv1+ [FSY210_HUMAN]	1	1	1	1	1	1	1	1	3,968	1	3,968	1,000	1,000	10,000	
ESB227	Ubiquitin-conjugating enzyme E2-ubiquitin OS=Leishmania mexicana (strain MHMOMGT2001U1103) GN=MLMXX_30_2880 PE=4 Sv1+ [ESB227_LEIMU]	1	1	1	1	1	1	1	2	6,504	2	6,504	3,869	710	135	14,774
QV087	EPBA1 protein (Fragment) OS=Homo sapiens (strain MHMOMGT2001U1103) GN=MLMXX_30_2880 PE=4 Sv1+ [QV087_HUMAN]	1	1	1	1	1	1	1	3	5,877	3	5,877	7,603	615	68,386	
Q1A0G7W12	GTPase family member 1 OS=Homo sapiens (strain MHMOMGT2001U1103) GN=MLMXX_30_2880 PE=4 Sv1+ [Q1A0G7W12_HUMAN]	1	1	1	1	1	1	1	3	1,850	3	1,850	2,100	519	51,911	
AAQ0W726	Spirogen syndrome nuclear autoantigen 1 OS=Homo sapiens (strain MHMOMGT2001U1103) GN=MLMXX_30_2880 PE=4 Sv1+ [AAQ0W726_HUMAN]	1	1	1	1	1	1	1	3	1,014	3	1,014	2,586	81	9,190	
Q8H9D4	Similar to human OS=Homo sapiens (strain MHMOMGT2001U1103) GN=MLMXX_30_2880 PE=4 Sv1+ [Q8H9D4_HUMAN]	1	1	1	1	1	1	1	2	1,616	2	1,616	2,000	134	30,301	
BK3V05	cDNA FL164300, clone BRACE3009044, highly similar to Centaurin-gamma 1 OS=Homo sapiens PE=2 Sv1+ [BK3V05_HUMAN]	1	1	1	1	1	1	1	2	879	2	879	6,278	561	648	91,344
Q8Q8N8	V type proton ATPase subunit a1 (Fragment) OS=Homo sapiens (strain MHMOMGT2001U1103) GN=MLMXX_30_2880 PE=4 Sv1+ [Q8Q8N8_HUMAN]	1	1	1	1	1	1	1	2	1,244	2	1,244	7,559	125	14,262	
Q8ATK1	Similar to human OS=Homo sapiens (strain MHMOMGT2001U1103) GN=MLMXX_30_2880 PE=4 Sv1+ [Q8ATK1_HUMAN]	1	1	1	1	1	1	1	3	1,539	3	1,539	1,033	551	59,667	
ESAV33	T-complex protein 1 subunit delta OS=Leishmania mexicana (strain MHMOMGT2001U1103) GN=MLMXX_21_1090 PE=3 Sv1+ [ESAV33_LEIMU]	1	1	1	1	1	1	1	3	1,539	3	1,539	1,033	551	59,667	
Q8R9Y7	C2 subunit OS=Homo sapiens (strain MHMOMGT2001U1103) GN=MLMXX_30_2880 PE=4 Sv1+ [Q8R9Y7_HUMAN]	1	1	1	1	1	1	1	3	1,539	3	1,539	1,033	551	59,667	
F0U119	Calcium subunit B type 1 OS=Homo sapiens (strain MHMOMGT2001U1103) GN=MLMXX_30_2880 PE=4 Sv1+ [F0U119_HUMAN]	1	1	1	1	1	1	1	4	1,117	4	1,117	4,166	738	18,196	
AAQ0Z4R72	Laminin, gamma 1 (Formly LAMB2), isoform CRA A OS=Homo sapiens (strain MHMOMGT2001U1103) GN=MLMXX_30_2880 PE=4 Sv1+ [AAQ0Z4R72_HUMAN]	1	1	1	1	1	1	1	2	1,032	2	1,032	2,727	1573	173,900	
ETV19	Uncharacterized protein OS=Homo sapiens (strain MHMOMGT2001U1103) GN=MLMXX_30_2880 PE=4 Sv1+ [ETV19_HUMAN]	1	1	1	1	1	1	1	2	1,328	2	1,328	1,415	1,415	14,150	
CSN1P9	Ubiquitin ligase degradation protein 1 homolog (Fragment) OS=Homo sapiens (strain MHMOMGT2001U1103) GN=MLMXX_30_2880 PE=4 Sv1+ [CSN1P9_HUMAN]	1	1	1	1	1	1	1	2	3,987	2	3,987	22,605	7,513	759	17,542
PH8E22	Isucadecorin OS=Homo sapiens (strain MHMOMGT2001U1103) GN=MLMXX_30_2880 PE=4 Sv1+ [PH8E22_HUMAN]	1	1	1	1	1	1	1	2	3,987	2	3,987	36,158	403	45,827	
HTC330	All-trans-retinol 13,14-reductase (Fragment) OS=Homo sapiens (strain MHMOMGT2001U1103) GN=MLMXX_30_2880 PE=4 Sv1+ [HTC330_HUMAN]	1	1	1	1	1	1	1	2	958	2	958	6,424	750	399	43,789
Q8B7F3	Migration and invasion enhancer 1 OS=Homo sapiens (strain MHMOMGT2001U1103) GN=MLMXX_30_2880 PE=4 Sv1+ [Q8B7F3_HUMAN]	1	1	1	1	1	1	1	3	3	3	3	3	3	3	3
Q8V120	Oxidative phosphorylation complex I subunit 1 OS=Homo sapiens (strain MHMOMGT2001U1103) GN=MLMXX_30_2880 PE=4 Sv1+ [Q8V120_HUMAN]	1	1	1	1	1	1	1	3	3	3	3	3	3	3	3
D8RCL3	Probably dimeric histone H4 lysine 9 methyltransferase OS=Homo sapiens (strain MHMOMGT2001U1103) GN=MLMXX_30_2880 PE=4 Sv1+ [D8RCL3_HUMAN]	1	1	1	1	1	1	1	1	3,811	1	3,811	2,446	7,506	154	17,059
BK3R20	Protein FAM108B OS=Homo sapiens (strain MHMOMGT2001U1103) GN=MLMXX_26_2910 PE=4 Sv1+ [BK3R20_HUMAN]	1	1	1	1	1	1	1	1	1,865	1	1,865	1,865	1,865	1,865	18,650
B2R9R2	cDNA FL194517, highly similar to Homo sapiens baculoviral IAP repeat-containing 4 (BIRC4), mRNA OS=Homo sapiens PE=2 Sv1+ [B2R9R2_HUMAN]	1	1	1	1	1	1	1	2	1,000	2	1,000	7,403	497	56,587	
FZ274	Pyridoxal kinase OS=Homo sapiens (strain MHMOMGT2001U1103) GN=MLMXX_30_2880 PE=4 Sv1+ [FZ274_HUMAN]	1	1	1	1	1	1	1	3	1,077	3	1,077	2,539	748	272	30,819
B2R9R2	Mitochondrial ribosomal L38, isoform CRA J OS=Homo sapiens (strain MHMOMGT2001U1103) GN=MLMXX_30_2880 PE=4 Sv1+ [B2R9R2_HUMAN]	1	1	1	1	1	1	1	3	1,077	3	1,077	2,539	748	272	30,819
ESB221	Uncharacterized protein OS=Leishmania mexicana (strain MHMOMGT2001U1103) GN=MLMXX_30_2880 PE=4 Sv1+ [ESB221_LEIMU]	1	1	1	1	1	1	1	3	4	4	4	4	4	4	4
ESB222	Uncharacterized protein OS=Leishmania mexicana (strain MHMOMGT2001U1103) GN=MLMXX_30_2880 PE=4 Sv1+ [ESB222_LEIMU]	1	1	1	1	1	1	1	3	4	4	4	4	4	4	4
AAQ0W726	Similar to human OS=Homo sapiens (strain MHMOMGT2001U1103) GN=MLMXX_30_2880 PE=4 Sv1+ [AAQ0W726_HUMAN]	1	1	1	1	1	1	1	3	4	4	4	4	4	4	4
BK3V05	cDNA FL164300, clone BRACE3009044, highly similar to Centaurin-gamma 1 OS=Homo sapiens PE=2 Sv1+ [BK3V05_HUMAN]	1	1	1	1	1	1	1	2	958	2	958	6,424	750	399	43,789
Q8Q8N8	V type proton ATPase subunit a1 (Fragment) OS=Homo sapiens (strain MHMOMGT2001U1103) GN=MLMXX_30_2880 PE=4 Sv1+ [Q8Q8N8_HUMAN]	1	1	1	1	1	1	1	2	1,244	2	1,244	7,559	125	14,262	
Q8ATK1	Similar to human OS=Homo sapiens (strain MHMOMGT2001U1103) GN=MLMXX_30_2880 PE=4 Sv1+ [Q8ATK1_HUMAN]	1	1	1	1	1	1	1	3	1,539	3	1,539	1,033	551	59,667	
ESAV33	T-complex protein 1 subunit delta OS=Leishmania mexicana (strain MHMOMGT2001U1103) GN=MLMXX_21_1090 PE=3 Sv1+ [ESAV33_LEIMU]	1	1	1	1	1	1	1	3	1,539	3	1,539	1,033	551	59,667	
Q8R9Y7	C2 subunit OS=Homo sapiens (strain MHMOMGT2001U1103) GN=MLMXX_30_2880 PE=4 Sv1+ [Q8R9Y7_HUMAN]	1	1	1	1	1	1	1	3	1,539	3	1,539	1,033	551	59,667	
F0U119	Calcium subunit B type 1 OS=Homo sapiens (strain MHMOMGT2001U1103) GN=MLMXX_30_2880 PE=4 Sv1+ [F0U119_HUMAN]	1	1	1	1	1	1	1	4	1,117	4	1,117	4,166	738	18,196	
AAQ0Z4R72	Laminin, gamma 1 (Formly LAMB2), isoform CRA A OS=Homo sapiens (strain MHMOMGT2001U1103) GN=MLMXX_30_2880 PE=4 Sv1+ [AAQ0Z4R72_HUMAN]	1	1	1	1	1	1	1	2	1,032	2	1,032	2,727	1573	173,900	
ETV19	Uncharacterized protein OS=Homo sapiens (strain MHMOMGT2001U1103) GN=MLMXX_30_2880 PE=4 Sv1+ [ETV19_HUMAN]	1	1	1	1	1	1	1	2	1,328	2	1,328	1,415	1,415	14,150	
CSN1P9	Ubiquitin ligase degradation protein 1 homolog (Fragment) OS=Homo sapiens (strain MHMOMGT2001U1103) GN=MLMXX_30_2880 PE=4 Sv1+ [CSN1P9_HUMAN]	1	1	1	1	1	1	1	2	3,987	2	3,987	22,605	7,513	759	17,542
PH8E22	Isucadecorin OS=Homo sapiens (strain MHMOMGT2001U1103) GN=MLMXX_30_2880 PE=4 Sv1+ [PH8E22_HUMAN]	1	1	1	1	1	1	1	2	3,987	2	3,987	36,158	403	45,827	
HTC330	All-trans-retinol 13,14-reductase (Fragment) OS=Homo sapiens (strain MHMOMGT2001U1103) GN=MLMXX_30_2880 PE=4 Sv1+ [HTC330_HUMAN]	1	1	1	1	1	1	1	2	958	2	958	6,424	750	399	43,789
Q8B7F3	Migration and invasion enhancer 1 OS=Homo sapiens (strain MHMOMGT2001															

E98709	Plastid uncharacterized protein OS-Leishmania mexicana (strain MHOM/GT2001/11/103) GN-LMXXM_34_4810 PE4 SV1+1	[E98709_LEIMU]	3.66	1	1	1	2	10.000	2	0.000	6.918	382	42.202
E10501	Mitochondrial ribonuclease P protein OS-Homo sapiens GN-RAA0391 PE1 SV2+2	[RNP3P_HUMAN]	4.8	1	3	1	2	11.000	2	0.000	6.811	683	63.722
QNSK7	RNLI protein OS-Homo sapiens GN-RNLS PE1 SV1+1	[RNSK7_HUMAN]	1.32	5	1	1	2	0.845	1	0.000	6.807	908	100.900
ANR24	NCL protein OS-Homo sapiens GN-NCL PE1 SV1+1	[NCL_HUMAN]	1.73	1	1	3	3	1.000	1	0.000	6.800	1099	127.716
QZS27	Vascular cell adhesion molecule-1 OS-Homo sapiens GN-VCAM1 PE1 SV1+1	[VCAM1_HUMAN]	21.78	1	1	1	1	6.312	1	6.312	8.000	1079	127.716
Q6R21	GTP-binding protein Rhes OS-Homo sapiens GN-RASD2 PE1 SV1+1	[RHS_HUMAN]	1.2	1	1	3	3	0.854	3	25.529	6.798	296	30.346
AK945	cDNA AK945, highly similar to Homo sapiens mRNA OS-Homo sapiens PEG2 SV1+1	[AK945_HUMAN]	5.31	3	1	1	1	3.753	1	0.000	6.753	196	19.607
AA087V76	40S ribosomal protein S29 OS-Homo sapiens GN-RPS29 PE4 SV1+1	[AA087V76_HUMAN]	16.09	2	2	3	3	1.000	3	0.000	6.756	53	6.111
Q1D38	Dnk1-like protein 2 OS-Homo sapiens GN-DNKL2 PE1 SV2+1	[DNKL2_HUMAN]	0.32	3	2	2	2	0.927	2	11.252	6.787	3038	339.427
Q1D39	Transcription factor SOX1 OS-Homo sapiens GN-SOX1 PE1 SV1+1	[TFV2D4_HUMAN]	1.91	4	2	2	2	1.000	2	0.000	6.784	176	18.426
BRD8D	cDNA FLJ39587, highly similar to Homo sapiens propionyl Coenzyme A carboxylase, alpha polypeptide(PCCA), mRNA OS-Homo sapiens PEG2 SV1+1	[BRD8D_HUMAN]	3.12	3	2	2	2	1.000	2	0.000	6.764	703	77.365
E590Y	Putative uncharacterized protein OS-Homo sapiens GN-ORF590 PE1 SV1+1	[ORF590_HUMAN]	13.27	1	1	1	1	0.000	1	0.000	6.759	196	19.607
Q9ND9	Putative uncharacterized protein Dkf234.24.12 (Fragment) OS-Homo sapiens GN-DKF234.24.12 PE2 SV1+1	[Q9ND9_HUMAN]	5.91	5	2	3	3	1.000	3	15.187	6.763	614	66.700
ERF4E	Nucleotidyltransferase ESCO2 OS-Homo sapiens GN-ESCO2 PE1 SV1+1	[ERF4E_HUMAN]	3.17	2	1	1	2	1.000	2	0.000	6.744	290	33.177
Q9Y65	Yieldin gene expression factor 2 OS-Homo sapiens PEG2 SV1+1	[YIELDIN_HUMAN]	4.84	2	1	1	1	0.000	1	0.000	6.742	67	6.927
Q9L2Z	Signal-transducing adaptor protein 1 OS-Homo sapiens GN-STAP1 PE1 SV1+1	[STAP1_HUMAN]	3.73	1	1	2	2	1.114	2	16.072	6.738	295	34.270
J3MY1	Guanine nucleotidyltransferase OS-Homo sapiens GN-GNAT4 PE4 SV1+1	[J3MY1_HUMAN]	40.43	3	1	1	1	0.000	1	0.000	6.737	47	5.322
Q9R65	Cytochrome c oxidase assembly factor 7 OS-Homo sapiens GN-COA7 PE1 SV2+2	[COA7_HUMAN]	9.09	1	2	2	2	1.221	2	37.388	6.730	231	25.692
Q1C85	Elongator complex protein 2 OS-Homo sapiens GN-ELP2 PE1 SV2+2	[ELP2_HUMAN]	2.42	1	2	2	2	1.000	2	0.000	6.720	826	92.441
Q9A57V76	Myosin domain-containing protein 4 OS-Homo sapiens GN-MYH4 PE1 SV1+1	[MYH4_HUMAN]	1.95	7	1	1	1	0.000	1	0.000	6.725	240	26.417
HTC1M5	Deacetylase/transferase terminal interacting protein 1 (Fragment) OS-Homo sapiens GN-DNTIP1 PE1 SV1+1	[HTC1M5_HUMAN]	0.607	3	2	2	2	1.884	3	23.454	6.725	280	31.764
Q9R07	Tinindoleidase repeat-containing gene 58 protein OS-Homo sapiens GN-TNRC28 PE1 SV1+1	[TNRC28_HUMAN]	1.53	6	2	3	3	1.000	3	0.000	6.724	1862	210.589
HOV14	Protein DD11 homolog 2 (Fragment) OS-Homo sapiens GN-DD12 PE1 SV1+1	[HOV14_HUMAN]	15.15	3	2	2	2	3.069	2	9.888	6.719	91	11.249
Q9G95	Centrosomal protein of 135 kDa OS-Homo sapiens GN-CCP135 PE1 SV2+2	[CP135_HUMAN]	1.14	7	1	2	2	2.439	1	21.728	6.708	1140	130.408
Q9R78	cDNA FLJ1982 OS-Homo sapiens PEG2 SV1+1	[Q9R78_HUMAN]	0.85	3	1	1	1	0.000	1	0.000	6.698	348	39.260
Q9T80	Protein LSM1A homolog B (Fragment) OS-Homo sapiens GN-LSM14B PE1 SV1+1	[Q9T80_HUMAN]	12.5	9	2	3	3	0.753	1	0.000	6.688	296	32.059
Q9W1Y1	Protein BRD91 OS-Homo sapiens GN-BR91 PE1 SV1+1	[BR91_HUMAN]	1.2	1	1	1	1	0.000	1	0.000	6.685	75	8.729
Q9H4F	Zinc finger FYVE domain-containing protein 1 OS-Homo sapiens GN-ZFYVE1 PE1 SV1+1	[ZFYVE1_HUMAN]	3.09	2	3	3	3	1.000	3	0.000	6.682	777	87.120
AA024Z97	HNA nucleotidyltransferase, CCA-and-1, isoform C, RNA OS-Homo sapiens GN-TRN1 PE1 SV1+1	[AA024Z97_HUMAN]	3.92	2	2	2	2	0.822	2	9.164	6.680	434	50.147
Q9R78	Homocysteine methyltransferase OS-Homo sapiens GN-MTR1 PE1 SV1+1	[MTR1_HUMAN]	11.93	1	1	2	2	0.000	1	0.000	6.660	199	22.265
AD66Z7	Putative 60S ribosomal protein L23 OS-Leishmania mexicana (strain MHOM/GT2001/11/103) GN-LMXXM_34_3930 PE4 SV1+1	[AD66Z7_LEIMU]	7.19	1	1	2	2	4.733	2	10.861	6.660	339	14.912
J3Q09N	Putative uncharacterized protein OS-Homo sapiens GN-ORF1000 PE1 SV1+1	[ORF1000_HUMAN]	1.53	3	2	2	2	0.935	2	0.000	6.658	718	80.271
AK134	cDNA FLJ7545, highly similar to Homo sapiens carboxyl-terminus phosphatase 1, mitochondrial (CPS1), mRNA OS-Homo sapiens PEG2 SV1+1	[AK134_HUMAN]	1.47	8	1	1	1	0.965	1	2.267	6.665	1050	164.764
ETV9	TFIIH basal transcription factor complex heparin binding X-ray domain OS-Homo sapiens GN-HEXCC2 PE1 SV1+1	[ETV9_HUMAN]	1.22	6	1	2	2	1.018	2	2.891	6.662	982	77.873
P55Z7	Serpin OS-Homo sapiens GN-SERP1 PE1 SV1+1	[SERP1_HUMAN]	16.69	1	1	1	1	0.000	1	0.000	6.654	376	42.984
F5CZ7	Gamma-aminobutyric acid receptor-associated polypeptide 1 (Fragment) OS-Homo sapiens GN-GABARAP1 PE1 SV1+1	[F5CZ7_HUMAN]	10	8	1	1	1	0.945	1	0.000	6.654	70	8.572
Q9W1Y4	Transcription factor GNF2 PE1 SV2+2	[TF2_HUMAN]	3.44	1	1	1	1	0.000	1	0.000	6.652	1162	126.668
BDLW6	cDNA FLJ18818, moderately similar to Adrenomedullin 50 kDa protein OS-Homo sapiens PEG2 SV1+1	[BDLW6_HUMAN]	6.3	3	2	2	2	3.000	2	0.000	6.644	270	29.799
EBAL25	Cysteine peptidase C (CPC) OS-Leishmania mexicana (strain MHOM/GT2001/11/103) GN-LMXXM_08_29_3020 PE2 SV1+1	[EBAL25_LEIMU]	8.82	1	2	2	2	1.000	2	0.000	6.637	340	37.154
BAW13	Marine diatom protein (Fragment) OS-Homo sapiens GN-ORF1000 PE1 SV1+1	[BAW13_HUMAN]	11.93	2	2	2	2	0.000	2	0.000	6.637	224	24.658
ESRH4	35S ribosomal protein L15, mitochondrial (Fragment) OS-Homo sapiens GN-MRPL15 PE1 SV1+1	[ESRH4_HUMAN]	0.99	4	2	2	2	0.880	2	23.281	6.632	198	21.930
Q9R78	Coordinated helix-turn-helix protein (Fragment) OS-Homo sapiens GN-CHTH PE1 SV1+1	[Q9R78_HUMAN]	2.67	4	1	1	1	0.000	1	0.000	6.632	105	11.412
AK9L2	cDNA FLJ76729, highly similar to Homo sapiens vaccinia related kinase 2 isoform 6 (VRK2) mRNA OS-Homo sapiens PEG2 SV1+1	[AK9L2_HUMAN]	3.31	4	3	3	3	1.000	3	9.975	6.627	396	44.991
Q3D7D	Myosin IC, isoform C, RNA OS-Homo sapiens GN-MYD1C PE4 SV1+1	[Q3D7D_HUMAN]	6.02	4	3	3	3	1.125	3	32.273	6.624	882	98.872
Q1TAM7	CTT domain-containing protein (Fragment) OS-Homo sapiens GN-CTTNBP2 PE1 SV1+1	[Q1TAM7_HUMAN]	1.92	2	2	2	2	0.872	2	0.000	6.622	217	23.888
ERH5	WSS CABD000000 data contig 43 OS-Leishmania mexicana (strain MHOM/GT2001/11/103) GN-LMXXM_24_1500a_1 PE4 SV1+1	[ERH5_LEIMU]	8.82	2	2	2	2	3.730	2	12.797	6.616	170	19.305
Q9R78	Protein BRD91 OS-Homo sapiens GN-BR91 PE1 SV1+1	[BR91_HUMAN]	1.2	1	1	1	1	0.000	1	0.000	6.616	296	32.059
AA087V76	PHD finger protein 23 OS-Homo sapiens GN-PHF23 PE4 SV1+1	[AA087V76_HUMAN]	8.23	5	1	2	2	1.000	2	0.000	6.610	158	17.801
Q1A2E	Intersectin 1 short form (Fragment) OS-Homo sapiens GN-ITSN1 PE1 SV1+1	[Q1A2E_HUMAN]	1.86	12	2	3	3	1.000	3	0.000	6.609	1710	121.570
Q9R78	Regulator of G-protein signaling 2 (Fragment) OS-Homo sapiens GN-RGS2 PE1 SV1+1	[RGS2_HUMAN]	11.93	1	2	2	2	1.000	2	0.000	6.609	192	21.771
Q1419	Werner syndrome ATP-dependent helicase OS-Homo sapiens GN-WRN PE1 SV2+2	[WRN_HUMAN]	2.37	2	3	3	3	1.000	3	0.000	6.601	1432	162.367
HOV13	cDNA FLJ2044 OS-Homo sapiens PEG2 SV1+1	[HOV13_HUMAN]	1.65	3	1	1	1	0.000	1	0.000	6.598	268	29.689
ESR33	Chromatin type zinc finger protein 1 OS-Homo sapiens GN-ZNF411 PE1 SV1+1	[ESR33_HUMAN]	12.73	11	2	2	2	1.272	2	6.786	6.595	165	18.835
Q3D38	Onion reading frame 123, isoform C, RNA OS-Homo sapiens GN-ORF123 PE4 SV1+1	[Q3D38_HUMAN]	2.03	3	3	3	3	1.000	3	0.000	6.595	130	14.538
Q9R78	CC2D3 protein (Fragment) OS-Homo sapiens GN-CC2D3 PE1 SV1+1	[Q9R78_HUMAN]	10.48	3	1	1	1	0.000	1	0.000	6.594	334	36.140
EAZ75	Protein dylin heavy chain OS-Leishmania mexicana (strain MHOM/GT2001/11/103) GN-LMXXM_27_1750 PE4 SV1+1	[EAZ75_LEIMU]	0.18	1	1	1	1	0.924	1	16.990	6.590	4470	500.458
Q9R78	Zinc finger protein 10 OS-Homo sapiens GN-ZFP10 PE1 SV1+1	[ZFP10_HUMAN]	1.61	1	1	1	1	0.000	1	0.000	6.589	364	39.844
ER800	Putative uncharacterized protein OS-Leishmania mexicana (strain MHOM/GT2001/11/103) GN-LMXXM_28_2290 PE4 SV1+1	[ER800_LEIMU]	0.94	1	1	1	1	0.000	1	0.000	6.584	833	90.233
EA9V9	Putative uncharacterized protein OS-Leishmania mexicana (strain MHOM/GT2001/11/103) GN-LMXXM_28_2640 PE4 SV1+1	[EA9V9_LEIMU]	3.29	1	2	2	2	0.000	2	0.000	6.583	708	70.086
ES24	Exonuclease component 1 OS-Homo sapiens GN-EXO1 PE1 SV1+1	[EXO1_HUMAN]	1.89	1	1	1	1	0.000	1	0.000	6.582	291	31.911
Q9NJM4	Transmembrane protein 106B OS-Homo sapiens GN-TMEM106B PE1 SV2+2	[TM6B_HUMAN]	7.66	4	2	2	2	3.205	3	28.203	6.582	234	25.108
ESR14	Zinc finger protein 729 OS-Homo sapiens GN-ZFP729 PE1 SV1+1	[ZFP729_HUMAN]	14.22	3	1	1	1	0.000	1	0.000	6.582	260	28.622
Q13144	Transition initiation factor eIF-2B subunit epsilon OS-Homo sapiens GN-EIF2B5 PE1 SV1+1	[EIF2B5_HUMAN]	1.58	3	3	3	3	0.988	3	1.775	6.575	721	80.329
Q9R78	Nucleolar protein 1 OS-Homo sapiens GN-NOL1 PE1 SV1+1	[NOL1_HUMAN]	4.39	5	1	1	1	0.000	1	0.000	6.572	719	81.072
EA14H	RNA 5'-terminal cap protein 2 OS-Homo sapiens GN-NTCAP2 PE1 SV1+1	[EA14H_HUMAN]	1.99	72	1	1	1	0.000	1	0.000	6.567	374	40.271
Q9R78	Protein tyrosine phosphatase, receptor type 3, isoform 2 variant (Fragment) OS-Homo sapiens PEG2 SV1+1	[Q9R78_HUMAN]	3.96	4	4	4	4	0.000	4	0.000	6.566	1552	174.769
Q9R78	Protein tyrosine phosphatase, receptor type 3, isoform 1 variant (Fragment) OS-Homo sapiens PEG2 SV1+1	[Q9R78_HUMAN]	3.96	4	4	4	4	0.000	4	0.000	6.565	1552	174.769
EA2H0	Eukaryotic translation initiation factor 3 subunit 2 OS-Leishmania mexicana (strain MHOM/GT2001/11/103) GN-LMXXM_36_3880 PE3 SV1+1	[EA2H0_LEIMU]	2.37	1	1	1	1	0.000	1	0.000	6.566	356	38.577
BR3M6	Protein arginase OS-Homo sapiens PEG2 SV1+1	[BR3M6_HUMAN]	4.48	9	2	2	2	0.000	2	0.000	6.565	782	86.863
HOV14	Protein 1271, moderately similar to DNA single-strand break repair protein 1 OS-Homo sapiens PEG2 SV1+1	[HOV14_HUMAN]	1.99	2	2	2	2	0.000	2	0.000	6.564	293	31.878
EAJAC9	Complete genome, chromosome 1 OS-Leishmania mexicana (strain MHOM/GT2001/11/103) GN-LMXXM_01_0410 PE4 SV1+1	[EAJAC9_LEIMU]	8.82	5	1	2	2	0.000	2	0.000	6.547	200	23.836
Q9H11	Regulator of G-protein signaling 2 (Fragment) OS-Homo sapiens GN-RGS2 PE1 SV1+1	[RGS2_HUMAN]	11.93	1	2	2	2	1.000	2	0.000	6.547	192	21.771
AND21	Putative L-asparaginase OS-Homo sapiens GN-ASP1 PE2 SV2+2	[ASP_HUMAN]	2.83	1	1	1	1	0.000	1	0.000	6.543	283	29.927
ESR19	Ribulose-1-phosphate protein subunit 25 OS-Homo sapiens GN-RP25 PE1 SV1+1	[RP25_HUMAN]	6.53	1	1	1	1	0.000	1	0.000	6.543	199	20.620
HT28D	Putative uncharacterized protein OS-Homo sapiens GN-ORF14 PE1 SV1+1	[ORF14_HUMAN]	1.79	3	1	1	1	0.000	1	0.000	6.542	234	25.108
Q9R78													

QBRY7	Probable guanine nucleotide exchange factor MCF2.2 OS-Homo sapiens GN-MCF2.2P2 S=V1 - [MCF2.2_HUMAN]	1.71	1	2	2	2	4.931	2	829.351	4.223	1114	128.913
DW825	Chromatin factor 1 OS-Homo sapiens GN-CHAF1A S=V1 - [DWR82_HUMAN]	1.78	2	1	2	2	17.477	2	17.477	4.216	868	108.872
QNC96	Adipin ear-binding coil-associated protein 1 OS-Homo sapiens GN-NECAP1 S=V2 - [NECAP1_HUMAN]	8.73	3	2	2	2	33.761	2	33.761	4.218	275	29.719
DL313	EG3-specific cyclin E1 (Fragment) OS-Homo sapiens GN-CNNE1 PE=V1 - [DL313_HUMAN]	7.07	4	1	2	2	0.855	1	0.855	4.218	283	32.352
ESB42	Putative uncharacterized protein OS-Leishmania mexicana (strain MHOM/GT2001/1103) GN-LMXM_33_0240 PE=4 S=V1 - [ESB42_LEIMU]	8.73	3	1	2	2	0.855	1	0.855	4.214	136	14.011
QZ728	Transcription initiation factor TFIID subunit 8 OS-Homo sapiens GN-TAF9 PE=V1 - [TAF9_HUMAN]	9.35	4	2	2	2	0.901	2	15.580	4.209	377	36.241
ESB54	Uncharacterized protein OS-Leishmania mexicana (strain MHOM/GT2001/1103) GN-LMXM_33_0240 PE=4 S=V1 - [ESB54_LEIMU]	9.35	4	2	2	2	0.901	2	15.580	4.209	377	36.241
BADN75	cDNA FL383.16, highly similar to Apolipoprotein L1 OS-Homo sapiens PE=2 S=V1 - [BADN75_HUMAN]	5.05	3	1	2	2	0.811	1	4.208	4.208	210	24.242
ESAD01	Putative uncharacterized protein OS-Leishmania mexicana (strain MHOM/GT2001/1103) GN-LMXM_25_0540 PE=4 S=V1 - [ESAD01_LEIMU]	2.37	1	1	1	1	0.862	2	2.862	4.205	295	32.409
UC265	Mediator complex subunit 27 OS-Homo sapiens GN-MED27 PE=2 S=V1 - [UC265_HUMAN]	1.26	1	1	1	1	0.862	2	2.862	4.205	295	32.409
OT5604	DENN domain-containing protein 4B OS-Homo sapiens GN-DENND4B PE=V1 - [DENND4B_HUMAN]	1.74	3	3	3	3	4.000	2	4.000	4.204	1496	163.743
ESF11	Glutathione S-transferase 2 (Fragment) OS-Homo sapiens GN-GSTM2 PE=V2 - [ESF11_HUMAN]	14.29	9	1	2	2	1.925	2	44.194	4.202	167	17.598
ESAT8	Putative ATP synthase OS-Leishmania mexicana (strain MHOM/GT2001/1103) GN-LMXM_36_3100 PE=4 S=V1 - [ESAT8_LEIMU]	3.7	1	1	2	2	1.483	2	32.207	4.196	216	25.242
ESR19	Putative uncharacterized protein OS-Leishmania mexicana (strain MHOM/GT2001/1103) GN-LMXM_17_0470 PE=4 S=V1 - [ESR19_LEIMU]	2.96	1	1	1	1	1.000	2	1.000	4.195	3547	378.880
UC262	Mediator complex subunit 27 OS-Homo sapiens GN-MED27 PE=2 S=V1 - [UC262_HUMAN]	1.26	1	1	1	1	0.862	2	2.862	4.194	295	32.409
QBLU3	Activator of basal transcription 1 OS-Homo sapiens GN-ABT1 PE=V1 - [ABT1_HUMAN]	5.51	1	2	2	2	1.864	2	116.000	4.190	272	31.060
QSRJ40	Histone H4 methyltransferase 2 OS-Homo sapiens GN-HMT2 PE=V1 - [QSRJ40_HUMAN]	2.48	1	2	2	2	1.166	2	2.166	4.187	362	43.632
BADY07	cDNA FL354.35, highly similar to Gamma-tubulin complex component 3 OS-Homo sapiens PE=2 S=V1 - [BADY07_HUMAN]	1.9	4	2	2	2	0.784	2	37.371	4.188	897	102.508
QBLU2	Cell division cycle protein 23 homolog OS-Homo sapiens GN-CCDC23 PE=V1 - [CCDC23_HUMAN]	2.88	1	2	2	2	1.075	2	10.688	4.183	597	68.790
QSRJ63	Thiosulfate transferase 2 OS-Homo sapiens GN-TST2 PE=V1 - [QSRJ63_HUMAN]	3.27	1	1	1	1	1.166	2	2.166	4.182	362	43.632
ESAW02	T complex protein 1 subunit gamma OS-Leishmania mexicana (strain MHOM/GT2001/1103) GN-LMXM_23_1220 PE=V1 - [ESAW02_LEIMU]	5.44	1	2	2	2	3.000	3	14.962	4.179	551	60.192
Q7W05	Cyclin D2 OS-Homo sapiens GN-CCND2 PE=V1 - [Q7W05_HUMAN]	4.72	2	1	2	2	1.622	2	17.477	4.176	857	70.150
Q9419	Endonuclease domain-containing protein OS-Homo sapiens GN-ENDDO1 PE=V2 - [ENDDO1_HUMAN]	2.8	1	1	1	1	1.206	1	1.206	4.172	500	54.981
QYV14	DNAI1 homolog subfamily C member 13 OS-Homo sapiens GN-DNAI13 PE=V1 S=V2 - [DUC15_HUMAN]	6.87	1	1	2	2	1.000	1	0.000	4.171	150	16.373
QSRK3	Nyxon 13 OS-Homo sapiens GN-NYX13_HUMAN]	1.81	1	1	1	1	0.952	2	4.171	4.171	1938	225.655
ATE21	Mysan-7B OS-Homo sapiens GN-MYH7B PE=V3 - [MYH7B_HUMAN]	1.34	7	3	3	3	1.000	1	1.000	4.171	1941	221.251
ESK82	Putative ATP-dependent RNA helicase OS-Leishmania mexicana (strain MHOM/GT2001/1103) GN-LMXM_05_0360 PE=5 S=V1 - [ESK82_LEIMU]	2.42	1	2	2	2	1.594	2	2.594	4.170	521	60.225
BAD336	cDNA FL35287, highly similar to CD97 antigen OS-Homo sapiens PE=2 S=V1 - [BAD336_HUMAN]	2.29	12	2	2	2	1.119	2	8.396	4.169	655	72.248
Q5H93	Putative uncharacterized protein DPK0277M164 (Fragment) OS-Homo sapiens GN-DPK0277M164 PE=4 S=V1 - [Q5H93_HUMAN]	1.91	5	2	2	2	0.843	2	67.546	4.167	1134	134.483
QSR07	CNA FL362.01, clone PLACE1106.10, highly similar to Gamma-secretase subunit APH4 OS-Homo sapiens PE=2 S=V1 - [QSR07_HUMAN]	0.97	2	1	1	1	0.862	2	1.862	4.157	247	27.571
F2256	General transcription factor 3C polypeptide 4 OS-Homo sapiens GN-GTF3C4 PE=V1 - [F2256_HUMAN]	4.7	3	1	2	2	0.878	2	92.333	4.156	149	16.491
Q5W15	N-acetyltransferase 5 (EC:2.3.1.5) OS-Homo sapiens GN-NAT5 PE=V1 - [Q5W15_HUMAN]	0.95	1	1	1	1	0.862	2	2.862	4.156	295	32.409
B7256	cDNA FL362.56, highly similar to Choline/ethanolamine kinase OS-Homo sapiens PE=2 S=V1 - [B7256_HUMAN]	6.2	2	1	1	1	0.866	1	1.866	4.148	274	32.087
K7L60	Histone arginine methyltransferase CARMI1 (Fragment) OS-Homo sapiens GN-CARMI1 PE=V1 - [K7L60_HUMAN]	4.08	2	2	2	2	2.167	2	2.167	4.147	343	38.393
B4C521	cDNA FL324.4, highly similar to histone demethylase protein 1A OS-Homo sapiens PE=2 S=V1 - [B4C521_HUMAN]	1.53	1	1	1	1	1.111	1	1.111	4.147	193	21.679
Q15463	Cit surface glycoprotein (Fragment) OS-Homo sapiens GN-PS9 PE=V1 - [Q15463_HUMAN]	1.0	1	1	1	1	0.296	1	0.296	4.147	276	30.189
Q3D97	Centriolar protein 550A OS-Homo sapiens GN-CEP550A PE=V1 - [Q3D97_HUMAN]	5.17	2	2	2	2	1.035	2	10.355	4.145	464	53.061
QH504	Dimethyladenosine transferase 2, mitochondrial OS-Homo sapiens GN-TFEM2 PE=V1 - [TFEM2_HUMAN]	3.79	3	2	2	2	0.811	2	35.619	4.145	398	45.320
Q8N97	F-box protein 28 OS-Homo sapiens GN-FBX28 PE=V1 - [Q8N97_HUMAN]	1.1	1	1	1	1	1.043	2	6.238	4.143	398	41.123
Q1019	Noy (Fragment) OS-Homo sapiens GN-NOY PE=V1 - [Q1019_HUMAN]	15.91	11	1	2	2	1.864	2	12.864	4.142	194	19.381
ADN09	Adrenomedullin, mitochondrial OS-Homo sapiens GN-ADM1 PE=V1 - [ADN09_HUMAN]	8.15	1	2	2	2	2.001	2	25.224	4.141	194	19.381
Q1919	3'-nucleotidase 2 (Fragment) OS-Homo sapiens GN-NTDC2 PE=V1 - [Q1919_HUMAN]	4.72	2	1	2	2	1.000	1	0.000	4.140	193	21.679
QKWH8	1-phosphatidylinositol 4,5-bisphosphate phosphatidase alpha 1 OS-Homo sapiens GN-PLCH1 PE=V1 - [PLCH1_HUMAN]	0.47	1	1	1	1	0.900	2	15.740	4.138	1693	189.104
ESAV9	Putative B55 ribosomal protein L1 OS-Leishmania mexicana (strain MHOM/GT2001/1103) GN-LMXM_21_1050 PE=4 S=V1 - [ESAV9_LEIMU]	1.97	1	1	2	2	1.000	1	1.000	4.138	190	21.514
ESAV7	Transcription factor 12 OS-Leishmania mexicana (strain MHOM/GT2001/1103) GN-LMXM_02_2075 PE=3 S=V1 - [ESAV7_LEIMU]	1.53	1	1	1	1	1.000	1	1.000	4.137	194	21.679
ESB659	Putative uncharacterized protein OS-Leishmania mexicana (strain MHOM/GT2001/1103) GN-LMXM_34_0310 PE=4 S=V1 - [ESB659_LEIMU]	2.7	1	2	2	2	0.775	2	39.195	4.131	427	46.491
FLK93	cDNA FL361.6, clone pBAC105.9545 OS-Homo sapiens GN-FLK93 PE=V1 - [FLK93_HUMAN]	4.17	3	1	2	2	1.000	1	1.000	4.130	194	21.679
QK645	Mutant methyl CpG binding protein 2 transcrit variant 1 OS-Homo sapiens GN-MEC2 PE=2 S=V1 - [QK645_HUMAN]	4.94	18	2	3	3	0.000	3	0.000	4.130	486	52.375
Q9H42	Trial-iteracting protein OS-Homo sapiens GN-TLIP PE=V1 - [TLIP_HUMAN]	6.2	6	2	2	2	1.019	2	17.858	4.130	274	30.262
Q1A11	Ga1a1c cardiac heparan sulfate lyase 1 OS-Homo sapiens GN-HSPG1 PE=V1 - [Q1A11_HUMAN]	0.44	3	2	2	2	1.002	2	8.005	4.128	434	46.723
ADQ248R8	Heparan sulfate proteoglycan 2 (Perlecan), isoform CRA_b OS-Homo sapiens GN-HSPG2 PE=4 S=V1 - [ADQ248R8_HUMAN]	0.44	3	2	2	2	1.002	2	8.005	4.128	434	46.723
QSRJ13	Caprin-1 OS-Homo sapiens GN-CAPRN1 PE=V1 - [QSRJ13_HUMAN]	4.9	1	1	1	1	0.900	1	0.900	4.126	344	37.768
BK3H0	cDNA FL3819.8a, clone TEST1027271, highly similar to N6-acetylserine-thioltransferase 7 kDa subunit (EC:2.1.1.62) OS-Homo sapiens PE=2 S=V1 - [BK3H0_HL]	3.53	3	2	2	2	0.949	2	7.637	4.127	425	47.685
QO488	Zinc finger protein 593 OS-Homo sapiens GN-ZFP593 PE=V2 - [ZFP593_HUMAN]	10.45	1	1	1	1	2.120	1	2.120	4.126	134	15.150
IL115	Leucocyte adhesion molecule 1 OS-Homo sapiens GN-LAM1 PE=V1 - [IL115_HUMAN]	2.5	2	1	1	1	0.862	2	6.804	4.125	68	7.827
IL30W4	Diamine acetyltransferase 2 OS-Homo sapiens GN-SAT2 PE=V1 - [IL30W4_HUMAN]	11.76	4	2	2	2	1.852	2	17.885	4.124	136	15.047
ESB13	Cytosolic Fe-S cluster assembly factor 1 OS-Homo sapiens GN-CLCAF1 PE=V1 - [ESB13_HUMAN]	10.71	4	1	2	2	0.959	2	32.459	4.123	183	19.659
ESB713	Putative uncharacterized protein OS-Leishmania mexicana (strain MHOM/GT2001/1103) GN-LMXM_34_4850 PE=3 S=V1 - [ESB713_LEIMU]	4	1	1	2	2	1.000	2	0.000	4.120	250	27.248
Q5R44	Cytochrome b 5 domain 1 (Fragment) OS-Homo sapiens PE=2 S=V1 - [Q5R44_HUMAN]	25.76	2	2	2	2	1.000	2	1.000	4.116	132	14.563
Q8N97	Nucleic acid uncharacterized protein OS-Homo sapiens GN-NUC1 PE=V1 - [Q8N97_HUMAN]	1.03	1	1	1	1	0.900	2	12.852	4.116	194	21.679
Q8U01	Intraflagellar transport 17 homolog OS-Homo sapiens GN-IFT17 PE=V2 - [IFT17_HUMAN]	0.102	3	2	2	2	0.799	1	0.799	4.112	1749	197.453
ADQ424R373	Chromatin 12 protein reader 37 OS-Homo sapiens GN-CHR12 PE=2 S=V1 - [ADQ424R373_HUMAN]	1.02	2	2	2	2	0.702	1	7.022	4.112	194	21.679
Q9K21	Glypichon-C OS-Homo sapiens GN-GHYPC PE=V1 - [Q9K21_HUMAN]	27.34	11	2	2	2	1.020	1	1.020	4.110	128	13.802
QO330	Recombining binding protein suppressor of hairless OS-Homo sapiens GN-RBP1 PE=V1 S=V3 - [QO330_HUMAN]	8.4	19	3	3	3	2.158	1	4.108	4.108	500	55.602
B4R507	Putative uncharacterized protein OS-Leishmania mexicana (strain MHOM/GT2001/1103) GN-LMXM_17_1140 PE=4 S=V1 - [B4R507_LEIMU]	1.53	1	1	1	1	1.000	1	1.000	4.107	193	21.679
B2R42	cDNA FL34734, highly similar to CHMP1.5 protein (CHMP1.5), mRNA OS-Homo sapiens PE=2 S=V1 - [B2R42_HUMAN]	2.2	2	2	2	2	0.921	2	16.910	4.099	196	21.763
DN262	DENN domain-containing protein 4B OS-Homo sapiens GN-DENND4B PE=V1 - [DN262_HUMAN]	1.74	3	3	3	3	4.000	2	4.000	4.098	1496	163.743
HNE709	NADH-ubiquinone oxidoreductase chain 2 OS-Homo sapiens GN-NDU2 PE=V1 - [HNE709_HUMAN]	2.02	7	1	2	2	1.000	2	0.000	4.093	347	38.982
P16276	Uncharacterized protein OS-Homo sapiens GN-UCP1 PE=V2 - [P16276_HUMAN]	3.55	7	2	2	2	1.210	2	22.503	4.092	377	40.027
IT2790	Retinol OS-Homo sapiens GN-RET PE=V2 - [IT2790_HUMAN]	3.07	3	2	2	2	0.804	2	32.014	4.092	462	50.842
ADQ248R70	WD repeat domain 66, isoform CRA_a OS-Homo sapiens GN-WDR66 PE=V1 - [ADQ248R70_HUMAN]	1.65	2	2	2	2	0.738	2	1.738	4.091	1154	130.727
QSRJ40	cDNA FL362.01, clone pBAC105.9545 OS-Homo sapiens GN-FLK93 PE=V1 - [QSRJ40_HUMAN]	4.17	3	1	2	2	1.000	1	1.000	4.088	194	21.679
Q9GK5	Serine/threonine protein kinase greatwall OS-Homo sapiens GN-GWAT1 PE=V1 - [Q9GK5_HUMAN]	3.75	13	3	4	4	1.000	3	36.340	4.081	679	97.257
P2504	Adrenomedullin polypeptide chain OS-Homo sapiens GN-ADM1 PE=V1 S=V2 - [ADM1_HUMAN]	0.81	3	2	2	2	1.000	2	1.000	4.081	2843	311.425
QSR44	cDNA FL364.4, highly similar to histone acetyltransferase 1 OS-Homo sapiens PE=2 S=V1 - [QSR44_HUMAN]	2.57	2	1	1	1	0.997	1	3.997	4.078	452	49.824
Q8R78	1-aminocyclopropane-1-carboxylate synthase-like protein 1 OS-Homo sapiens GN-ACSPE PE=V1 - [Q8R78_HUMAN]	3.79	1	1	3	3	1.000	3	0.000	4.071	501	57.287
QSRJ13	Caprin-1 OS-Homo sapiens GN-CAPRN1 PE=V1 - [QSRJ13_HUMAN]	4.9	1	1	1	1	0.900	1	0			

P06673	Profilin-3 OS=Homo sapiens GN-PFN3 PE=2 SV=1	[PROF3_HUMAN]	6,57	1	1	1	1	0.799	2,613	137	14,587
EP8R_C8	Glycylglycylglycyl transferase (Fragment) OS=Homo sapiens GN-GPAA1 PE=1 SV=1	[ESPLR8_HUMAN]	13,58	1	1	1	1	1.000	2,613	81	8,157
D3D3P8	Collagen, type IX, alpha 2, isoform CRA_A OS=Homo sapiens GN-COL9A2 PE=4 SV=1	[D3D3P8_HUMAN]	1,91	2	1	1	1	1.024	2,610	595	59,325
BZ2ZV9	R3S ribosomal protein L30, mitochondrial OS=Homo sapiens GN-HRPL30 PE=1 SV=1	[BZ2ZV9_HUMAN]	9.5	2	1	1	1	1.029	2,610	101	11,927
AA027057	Leucine-rich repeat protein OS=Homo sapiens GN-LRR14 PE=4 SV=1	[AA027057_HUMAN]	1.73	5	1	1	1	1.000	2,610	521	5,305
OS6251	Histone acetyltransferase KAT7 OS=Homo sapiens GN-KAT7 PE=1 SV=1	[KAT7_HUMAN]	1.8	1	1	2	1	1.000	2,608	611	70,598
ES3AL4	Uncharacterized protein OS=Homo sapiens GN-HMMGT2001U1103 GN-LMM_XM_23_280 PE=4 SV=1	[ES3AL4_LEMUR]	0.43	1	1	1	1	1.000	2,608	202	21,702
EB92U9	Plutonic acetylation repeat subunit OS=Leishmania mexicana (strain MHOM/GT2001U1103) GN-LMM_XM_1_170 PE=4 SV=1	[EB92U9_LEMUR]	2.17	1	1	1	1	1.000	2,607	323	34,969
HYK7E7	Calcium B homologous protein 1 OS=Homo sapiens GN-CHP1 PE=1 SV=1	[HYK7E7_HUMAN]	2.04	1	1	1	1	1.000	2,606	123	14,261
BTVM7L	ATV domain-containing protein 1 (Fragment) OS=Homo sapiens GN-DHTW3 PE=1 SV=1	[BTVM7L_HUMAN]	1.26	1	1	1	1	1.000	2,606	152	17,055
EB9233	Putative S-2 trans- <i>enoyl</i> -CoA isomerase, mitochondrial OS=Leishmania mexicana (strain MHOM/GT2001U1103) GN-LMM_XM_20_230 PE=4 SV=1	[EB9233_LEMUR]	0.98	2	1	1	1	1.000	2,603	339	38,357
EB908E	Putative S-2 trans- <i>enoyl</i> -CoA isomerase, mitochondrial OS=Leishmania mexicana (strain MHOM/GT2001U1103) GN-LMM_XM_23_280 PE=4 SV=1	[EB908E_LEMUR]	1.14	2	1	1	1	1.000	2,603	339	38,357
EP3VW4	ES ubiquitin-protein ligase RNF34 (Fragment) OS=Homo sapiens GN-RNF34 PE=4 SV=1	[EP3VW4_HUMAN]	4.29	3	1	1	1	1.000	2,602	163	18,116
GN1504	Fatty acyl-CoA reductase 1 OS=Homo sapiens GN-FAR1 PE=1 SV=1	[GN1504_HUMAN]	1.29	1	1	1	1	1.000	2,599	336	37,458
EP8R22	Enc. Inguis 471 OS=Homo sapiens GN-ZNF471 PE=2 SV=1	[EP8R22_HUMAN]	10,22	172	0	1	1	1.000	2,599	12	12,611
ESAS46	Uncharacterized protein OS=Leishmania mexicana (strain MHOM/GT2001U1103) GN-LMM_XM_36_1000 PE=4 SV=1	[ESAS46_LEMUR]	1.1	1	1	1	1	1.027	2,596	1003	111,367
AD2D51	HCC207 OS=Homo sapiens GN-PE4 SV=1	[AD2D51_HUMAN]	8.49	1	1	1	1	1.000	2,596	162	16,262
BD4P86	cDNA FL156337, highly similar to Colicid-cold domain-containing protein 22 OS=Homo sapiens PE=2 SV=1	[BD4P86_HUMAN]	4.83	4	3	3	2	0.948	2,596	580	65,116
HTC2N6	Cyclic AMP-dependent transcription factor ATF-2 (Fragment) OS=Homo sapiens GN-ATF2 PE=1 SV=1	[HTC2N6_HUMAN]	3.4	10	1	1	1	1.281	2,594	205	23,320
ES9326	Membrane-associated protein 1 OS=Leishmania mexicana (strain MHOM/GT2001U1103) GN-LMM_XM_37_270 PE=4 SV=1	[ES9326_LEMUR]	1.0	1	1	1	1	1.000	2,592	1465	157,758
QJ3Q9F	Uncharacterized protein (Fragment) OS=Homo sapiens PE=4 SV=1	[QJ3Q9F_HUMAN]	23.93	5	2	2	2	1.028	2,591	117	13,120
ES3AV5	Putative uncharacterized protein OS=Homo sapiens GN-HMGT2001U1103 GN-LMM_XM_22_1230 PE=4 SV=1	[ES3AV5_LEMUR]	1.2	1	1	1	1	1.155	2,591	919	103,737
OS9714	ES ubiquitin-protein ligase HERC2 OS=Homo sapiens GN-HERC2 PE=2 SV=1	[HERC2_HUMAN]	0.43	1	2	2	2	0.990	2,589	4834	528,895
HTC317	N-acetylglucosaminase 2 epimerase (Fragment) OS=Homo sapiens GN-NEBP PE=1 SV=1	[HTC317_HUMAN]	0.48	3	1	1	1	1.010	2,589	125	14,149
BS9E20	DMPK2 OS=Homo sapiens GN-DMPK2 PE=2 SV=1	[BS9E20_HUMAN]	1.86	3	1	1	1	1.000	2,588	534	58,005
HY0E88	RNA binding protein 40 (Fragment) OS=Homo sapiens GN-RNBP34 PE=4 SV=1	[HY0E88_HUMAN]	5.49	2	1	1	1	1.000	2,586	182	21,320
ES3AL5	Uncharacterized protein OS=Homo sapiens GN-ANSND1 PE=4 SV=1	[ES3AL5_LEMUR]	2.33	1	1	1	1	1.000	2,582	202	22,421
LOR819	Alternative protein ANSD1 OS=Homo sapiens GN-ANSND1 PE=4 SV=1	[LOR819_HUMAN]	8.33	2	1	1	1	1.000	2,580	96	11,243
J3CR26	Homozygous protein MOK-1 (Fragment) OS=Homo sapiens GN-MEOK1 PE=4 SV=1	[J3CR26_HUMAN]	7.32	6	2	2	2	1.018	2,580	205	23,380
BD4K05	cDNA FL156814 OS=Homo sapiens PE=2 SV=1	[BD4K05_HUMAN]	1.7	5	1	1	1	1.000	2,579	205	24,197
Q63C34	Nucleoside diphosphate protein 1 OS=Homo sapiens GN-HNKP1 PE=2 SV=1	[Q63C34_HUMAN]	1.67	5	1	1	1	1.000	2,577	718	81,407
Q63H25	Enhancer of polycomb homolog 1 OS=Homo sapiens GN-EPC1 PE=1 SV=1	[Q63H25_HUMAN]	1.25	1	1	1	1	1.000	2,576	830	93,405
BT2Z65	cDNA FL1560, highly similar to Tigt junction protein ZC2 OS=Homo sapiens PE=2 SV=1	[BT2Z65_HUMAN]	0.99	3	1	1	1	1.074	2,575	1108	124,801
OS3015	Dipeptidyl peptidase-like protein 8 variant (Fragment) OS=Homo sapiens GN-PP2R1 PE=1 SV=1	[OS3015_HUMAN]	1.0	1	1	1	1	1.000	2,570	424	47,707
BR2728	cDNA FL156255, highly similar to Homo sapiens solute carrier family 7, cationic amino acid co-transporter, y+ system, member 1 (SLC7A1), mRNA OS=Homo sapiens PE=	[BR2728_HUMAN]	1.92	2	1	1	1	1.000	2,574	629	67,606
OS5836	Phosphatidylinositol-3-OH kinase class I OS=Homo sapiens GN-PI3K PE=2 SV=1	[OS5836_HUMAN]	4.48	2	1	1	1	1.000	2,573	145	16,120
BD4G83	cDNA FL150136, highly similar to Induced myeloid leukemia cell differentiation protein Mpl-1 OS=Homo sapiens PE=2 SV=1	[BD4G83_HUMAN]	2.59	4	1	1	1	1.000	2,571	240	26,404
BD4F08	cDNA FL15447, highly similar to Lpfn-beta (Fragment) OS=Homo sapiens PE=2 SV=1	[BD4F08_HUMAN]	0.15	4	1	1	1	1.011	2,570	74	87,005
KTEU19	Ornithine transcarbamoylase OS=Homo sapiens GN-OTC PE=1 SV=1	[KTEU19_HUMAN]	21.62	1	1	1	1	1.000	2,569	34	34,200
GN5V4	Protein disphospho homolog 3 OS=Homo sapiens GN-DPH3 PE=1 SV=1	[GN5V4_HUMAN]	0.75	1	1	1	1	1.000	2,568	1193	136,839
BD4T90	cDNA FL15641, moderately similar to colicid-cold domain-containing protein 22 OS=Homo sapiens PE=2 SV=1	[BD4T90_HUMAN]	1.73	4	1	1	1	1.000	2,567	142	15,727
F9H4R1	Mitogen-activated protein kinase kinase 4 OS=Homo sapiens GN-MAKP4 PE=1 SV=1	[F9H4R1_HUMAN]	1.8	1	2	2	1	1.000	2,566	1442	162,912
Q6P8C1	Putative membrane-spanning 4-domain subfamily A member 4 OS=Homo sapiens GN-MS4A4 PE=2 SV=1	[Q6P8C1_HUMAN]	12.12	1	1	1	1	1.000	2,566	132	15,159
EP8R13	Uncharacterized protein OS=Homo sapiens GN-CHCR7 PE=1 SV=1	[EP8R13_HUMAN]	0.89	10	1	1	1	1.000	2,566	169	19,072
BAE1R1	cDNA FL152389, highly similar to Alcohol dehydrogenase 1B (EC 1.1.1.1) OS=Homo sapiens PE=2 SV=1	[BAE1R1_HUMAN]	1.06	4	1	1	1	1.000	2,562	166	17,910
Q3N4V1	Membrane-associated protein 1 OS=Homo sapiens GN-ANSND1 PE=4 SV=1	[Q3N4V1_HUMAN]	2.87	1	1	1	1	1.000	2,561	211	24,877
J3KNV5	Integrator complex subunit 8 OS=Homo sapiens GN-INTS8 PE=1 SV=1	[J3KNV5_HUMAN]	1.04	8	1	1	1	1.000	2,561	758	86,674
EB9028	Conserved zinc finger protein OS=Leishmania mexicana (strain MHOM/GT2001U1103) GN-LMM_XM_23_2900 PE=4 SV=1	[EB9028_LEMUR]	1.26	1	1	1	1	1.000	2,560	371	41,488
Q70W9	Maat3 protein OS=Homo sapiens PE=2 SV=1	[Q70W9_HUMAN]	2.19	1	1	1	1	1.001	2,554	203	20,850
EP8R16	Kinase D-related protein 1 OS=Homo sapiens GN-HSR1 PE=3 SV=1	[EP8R16_HUMAN]	0.84	8	1	1	1	1.000	2,553	823	92,086
ESAY9	Putative uncharacterized protein OS=Leishmania mexicana (strain MHOM/GT2001U1103) GN-LMM_XM_26_1110 PE=4 SV=1	[ESAY9_LEMUR]	0.31	1	1	1	1	1.000	2,552	472	445,292
EP8R17	Mitochondrial DNA polymerase 1 (Fragment) OS=Leishmania mexicana (strain MHOM/GT2001U1103) GN-LMM_XM_13_1630 PE=4 SV=1	[EP8R17_LEMUR]	0.51	1	1	1	1	1.000	2,551	1979	177,207
ES3AV7	Crease protein KIF2A (Fragment) OS=Homo sapiens GN-KIF2A PE=1 SV=1	[ES3AV7_HUMAN]	1.2	1	1	1	1	1.000	2,550	81	9,127
OS3J24	Protein lin-9 OS=Homo sapiens GN-LIN9 PE=1 SV=1	[OS3J24_HUMAN]	2.25	5	1	1	1	1.000	2,550	489	55,898
CNA FL2287	cDNA FL2287 OS=Homo sapiens PE=2 SV=1	[CNA FL2287_HUMAN]	0.96	2	1	1	1	1.000	2,550	201	22,122
ESAW44	Putative uncharacterized protein OS=Leishmania mexicana (strain MHOM/GT2001U1103) GN-LMM_XM_23_1280 PE=4 SV=1	[ESAW44_LEMUR]	0.51	1	1	1	1	1.038	2,549	1528	166,198
QDTC01	CMR35-like molecule 1 OS=Homo sapiens GN-CDL3 PE=3 SV=1	[QDTC01_HUMAN]	3.1	3	1	1	1	1.001	2,548	296	32,334
Q63C31	Protein MNA1 OS=Homo sapiens GN-MNA1 PE=1 SV=1	[Q63C31_HUMAN]	14.10	1	1	1	1	1.000	2,548	95	8,451
Q63Q49	Protein SDE2 OS=Homo sapiens GN-SDE2 PE=1 SV=1	[Q63Q49_HUMAN]	2.88	1	2	2	2	1.075	2,548	405	49,711
ESAR70	Uncharacterized protein OS=Homo sapiens GN-HMGT2001U1103 GN-LMM_XM_23_2266 PE=4 SV=1	[ESAR70_HUMAN]	1.2	1	1	1	1	1.000	2,548	96	10,410
HY0EY4	ATP synthase mitochondrial F1 complex assembly factor 1 (Fragment) OS=Homo sapiens GN-FAF1 PE=1 SV=1	[HY0EY4_HUMAN]	6.32	4	1	1	1	1.063	2,541	174	19,898
OS3JF6	UDP-glycose acyl deacetylase 1 (Fragment) OS=Homo sapiens GN-HX51 PE=4 SV=1	[OS3JF6_HUMAN]	9.78	4	1	1	1	1.413	2,540	121	13,537
BT2B72	cDNA FL17435, highly similar to Homo sapiens protein homolog (PRLN), mRNA OS=Homo sapiens PE=2 SV=1	[BT2B72_HUMAN]	0.79	3	1	1	1	1.000	2,540	109	12,120
Y9G0Y1	RAS protein activator-like 3 (Fragment) OS=Homo sapiens GN-RASAL3 PE=4 SV=1	[Y9G0Y1_HUMAN]	1.036	3	1	1	1	1.036	2,538	228	25,762
BD4S12	Putative COP-coated vesicle protein OS=Leishmania mexicana (strain MHOM/GT2001U1103) GN-LMM_XM_23_2900 PE=4 SV=1	[BD4S12_LEMUR]	3.7	1	1	1	1	1.000	2,538	216	24,482
BD4S20	cDNA FL15084, highly similar to Homo sapiens solute carrier family 30 (zinc transporter), member 9 (SLC30A9), mRNA OS=Homo sapiens PE=2 SV=1	[BD4S20_HU]	2.27	4	1	1	1	1.002	2,535	397	44,742
Q6H87R	cDNA FL13228, like, clone CWRK0110180, weakly similar to UBIQUITIN-LIKE PROTEIN D5C OS=Homo sapiens PE=2 SV=1	[Q6H87R_HUMAN]	3.5	4	1	1	1	1.367	2,534	314	33,993
HTC3C3	Uncharacterized protein 3 OS=Homo sapiens GN-CHCP3 PE=1 SV=1	[HTC3C3_HUMAN]	0.76	4	1	1	1	1.000	2,533	169	18,220
HY0GX8	Conserved oligomeric Golgi complex subunit 8 (Fragment) OS=Homo sapiens GN-COG8 PE=4 SV=1	[HY0GX8_HUMAN]	0.72	4	1	1	1	1.039	2,531	134	15,287
CNA FL5432	cDNA FL5432, highly similar to Homo sapiens PE=2 SV=1	[CNA FL5432_HUMAN]	1.2	1	1	1	1	1.000	2,531	868	98,008
ESAP25	Putative uncharacterized protein OS=Leishmania mexicana (strain MHOM/GT2001U1103) GN-LMM_XM_14_1470 PE=4 SV=1	[ESAP25_LEMUR]	2.27	1	1	1	1	1.012	2,531	484	58,329
ADNP16	Argininosuccinate lyase OS=Homo sapiens GN-ALM1 PE=1 SV=1	[ADNP16_HUMAN]	4.86	6	2	2	2	1.125	2,531	597	68,330
ESAV16	Putative uncharacterized protein OS=Leishmania mexicana (strain MHOM/GT2001U1103) GN-LMM_XM_26_2000 PE=4 SV=1	[ESAV16_LEMUR]	1.2	1	1	1	1	1.000	2,530	348	39,484
HY0EY7	Autophagy-related protein 13 (Fragment) OS=Homo sapiens GN-ATG13 PE=4 SV=1	[HY0EY7_HUMAN]	11.52	6	1	1	1	1.000	2,529	193	20,571
Q63W61	Serpin Z1 (Fragment) OS=Homo sapiens GN-SERP1 PE=1 SV=1	[Q63W61_HUMAN]	1.28	2	1	1	1	1.000	2,529	181	20,421
Q6Y819	CDMT1 duplicated region transcript 15 protein OS=Homo sapiens GN-CDRT15 PE=2 SV=1	[Q6Y819_HUMAN]	7.42	2	1	1	1	1.000	2,529	188	20,638
G3VYF3	Loss of heterozygosity 12 chromosomal region 1 protein OS=Homo sapiens GN-LOH12CR1 PE=1 SV=1	[G3VYF3_HUMAN]	1.36	2	1	1	1	1.442	2,527	147	16,235
OS3J30	Putative uncharacterized protein OS=Leishmania mexicana (strain MHOM/GT2001U1103) GN-LMM_XM_23_2266 PE=4 SV=1	[OS3J30_HUMAN]	0.56	2	1	1	1	1.000	2,527	172	20,607
OS3J30	Putative uncharacterized protein OS=Leishmania mexicana (strain MHOM/GT2001U1103) GN-LMM_XM_23_2266 PE=4 SV=1	[OS3J30_HUMAN]	1.15	8	1	1	1	1.000	2,527	172	20,607
CL12E219	CD12E219 (Fragment) OS=Homo sapiens GN-CD12E219 PE=1 SV=1	[CL12E219_HUMAN]	0.52	1	1	1	1	1.000	2,525	133	15,049
B3K1P8	cDNA FL13094, like, clone FBRA2007622, highly similar to RAD50-interacting protein 1 OS=Homo sapiens PE=2 SV=1	[B3K1P8_HUMAN]	1.52	2	1	1	1	1.000	2,525	792	90,540
AD6A7WU02	Dehydrogenase-like domain-containing protein 2 (Fragment) OS=Homo sapiens GN-DHS12 PE=4 SV=1	[AD6A7WU02_HUMAN]	9	2	1	1	1	1.136	2,525	100	10,779

B4E108	cDNA FL1597, highly similar to C4b-binding protein alpha chain OS-Homo sapiens PE-2 Sv1+ [B4E108_HUMAN]	1.49	3	1	1	1	1	1,755	1	2,309	636	60,366	
ESASV9	Uncharacterized protein OS-Leishmania mexicana (strain MHOM/GT2001/1103) GN-HLMMX_36_2129 PE4 Sv1+ [ESASV9_LEIMU]	0.46	1	1	1	1	1	2,307	1	1,527	1526	18,894	
BREGRS	MGA protein OS-Homo sapiens GN-HMGA PE-2 Sv1+ [BREGRS_HUMAN]	0.32	2	1	1	1	1	2,889	1	2,307	2856	31,940	
HYK49	Tetraspanin-3 OS-Homo sapiens GN-TSPAN PE-2 Sv1+ [HYK49_HUMAN]	4.27	1	1	1	1	1	1,000	1	2,305	160	13,337	
GENGLAD	Seven transmembrane helix receptor OS-Homo sapiens GN-7S PE-2 Sv1+ [GENGLAD_HUMAN]	0.28	1	1	1	1	1	1,000	1	2,305	301	33,507	
ESAT52	Uncharacterized protein OS-Leishmania mexicana (strain MHOM/GT2001/1103) GN-HLMMX_36_4890 PE4 Sv1+ [ESAT52_LEIMU]	3.19	1	1	1	1	1	1,000	1	2,304	313	34,463	
PC387	Putative uncharacterized protein OS-Homo sapiens GN-PC387 PE-2 Sv1+ [PC387_HUMAN]	1.83	1	1	1	1	1	1,000	1	2,303	120	13,378	
HYC06	PWWP domain-containing protein D4 (Fragment) OS-Homo sapiens GN-PWWP2 PE4 Sv1+ [HYC06_HUMAN]	15.94	2	1	1	1	1	1,000	1	2,303	68	7,948	
BZ792	cDNA FL7896, highly similar to Ras guanyl releasing protein 1 (catom and DAG-regulated) (RASGRP1), mRNA OS-Homo sapiens PE-2 Sv1+ [BZ792_HUMAN]	1.1	1	1	1	1	1	1,070	1	2,302	749	85,105	
B4E04	GN1A4, highly similar to DNAP1 protein complementing PF-C cell OS-Homo sapiens GN-1A4 PE-2 Sv1+ [B4E04_HUMAN]	9.37	1	1	1	1	1	1,000	1	2,302	201	22,429	
D3D74	Glutamate-oxaloacetate transaminase 2 OS-Homo sapiens GN-GLOM PE4 Sv1+ [D3D74_HUMAN]	0.27	2	2	2	2	2	859.39	2	2,302	224	25,898	
B4D912	C-proximal receptor like OS-Homo sapiens GN-B4D912 PE-2 Sv1+ [B4D912_HUMAN]	1.24	1	1	1	1	1	32,661	1	2,302	320	36,109	
QHN96	cDNA FL22037 fl, clone HEF0868 (Fragment) OS-Homo sapiens GN-MFH16 PE-2 Sv1+ [QHN96_HUMAN]	1.14	1	1	1	1	1	1,140	1	2,300	746	86,940	
ESAD3	Putative serine/threonine protein phosphatase 2B catalytic subunit AC OS-Leishmania mexicana (strain MHOM/GT2001/1103) GN-HLMMX_36_1980 PE4 Sv1+ [ESAD3_LEIMU]	1.72	1	1	1	1	1	1,000	1	2,299	407	45,080	
ESAM3	Uncharacterized protein OS-Leishmania mexicana (strain MHOM/GT2001/1103) GN-HLMMX_36_2000 PE4 Sv1+ [ESAM3_LEIMU]	0.43	1	1	1	1	1	1,000	1	2,299	133	15,043	
ESB225	Uncharacterized protein OS-Leishmania mexicana (strain MHOM/GT2001/1103) GN-HLMMX_31_2150 PE4 Sv1+ [ESB225_LEIMU]	1.66	1	1	1	1	1	1,000	1	2,299	1082	117,446	
Q8Y02	Similar to uncharacterized protein OS-Homo sapiens GN-Q8Y02 PE-2 Sv1+ [Q8Y02_HUMAN]	3.38	1	1	1	1	1	1,000	1	2,298	251	28,229	
JK0V4	Transcription elongation factor A protein-like 4 (Fragment) OS-Homo sapiens GN-TCEA4 PE1 Sv1+ [JK0V4_HUMAN]	2.2	7	1	1	1	1	1,000	1	2,297	50	5,815	
ESM43	Putative uncharacterized protein OS-Leishmania mexicana (strain MHOM/GT2001/1103) GN-HLMMX_16_0640 PE4 Sv1+ [ESM43_LEIMU]	1.09	1	1	1	1	1	1,115	1	2,297	640	68,223	
ESM45	Modern OS-Homo sapiens GN-ESM45 PE-2 Sv1+ [ESM45_HUMAN]	4.12	1	1	1	1	1	1,367	1	2,297	364	39,247	
ESAP19	Putative uncharacterized protein OS-Leishmania mexicana (strain MHOM/GT2001/1103) GN-HLMMX_13_1550 PE4 Sv1+ [ESAP19_LEIMU]	2.37	2	1	2	2	2	1,000	1	2,296	1182	124,440	
ESAP10	Uncharacterized protein OS-Leishmania mexicana (strain MHOM/GT2001/1103) GN-HLMMX_22_025 PE4 Sv1+ [ESAP10_LEIMU]	1.1	1	1	1	1	1	1,000	1	2,294	1024	115,085	
CSJW7	SISF protein kinase 2 (Fragment) OS-Homo sapiens GN-SPK2 PE-1 Sv1+ [CSJW7_HUMAN]	4.33	1	1	1	1	1	1,000	1	2,295	231	25,848	
ESW12	Uncharacterized protein OS-Leishmania mexicana (strain MHOM/GT2001/1103) GN-HLMMX_21_1555 PE4 Sv1+ [ESW12_LEIMU]	2.28	1	1	1	1	1	2,000	2,000	2,294	395	48,545	
Q8Y42	NLS family GTP domain containing protein OS-Homo sapiens GN-Q8Y42 PE-1 Sv1+ [Q8Y42_HUMAN]	0.88	1	1	1	1	1	1,000	1	2,294	1024	115,085	
Q7Z402	HEAT repeat-containing protein 3 OS-Homo sapiens GN-HEATR3 PE1 Sv1+ [Q7Z402_HUMAN]	1.32	1	1	1	1	1	1,000	1	2,293	804	74,525	
Q8Y30	NG2-like methyltransferase dimethylaminylcholine 1 OS-Homo sapiens GN-Q8Y30 PE1 Sv1+ [Q8Y30_HUMAN]	4.46	2	1	2	2	2	4,055	2	2,293	285	31,102	
BZM2	ARAP1 protein OS-Homo sapiens GN-ARAP1 PE-2 Sv1+ [BZM2_HUMAN]	3.69	4	3	3	3	3	1,000	3	2,292	1194	134,621	
Q8Y96	Cargulin-like protein 1 OS-Homo sapiens GN-CGLN1 PE1 Sv1+ [Q8Y96_HUMAN]	0.84	1	1	1	1	1	1,000	1	2,291	302	148,889	
ESK63	Uncharacterized protein OS-Leishmania mexicana (strain MHOM/GT2001/1103) GN-HLMMX_02_0460 PE4 Sv1+ [ESK63_LEIMU]	2.95	1	1	1	1	1	2,859	1	2,291	291	31,884	
Q8Y80	Polyprenyl reductase OS-Homo sapiens GN-PPR PE1 Sv1+ [Q8Y80_HUMAN]	2.28	2	2	2	2	2	1,228	2	2,623	2,290	138	36,497
ADQAR563	ID motif containing E, isoform CRA_3 OS-Homo sapiens GN-ADQAR563 PE-4 Sv1+ [ADQAR563_HUMAN]	1.43	1	1	1	1	1	1,000	1	2,290	545	71,168	
Q8Y88	Sodium/hydrogen exchanger (Fragment) OS-Homo sapiens GN-SHEX PE-2 Sv1+ [Q8Y88_HUMAN]	2.67	2	1	1	1	1	1,000	1	2,289	374	41,437	
ADQAR1X1P1	Protein LOC1272453 OS-Homo sapiens GN-LOC1272453 PE4 Sv1+ [ADQAR1X1P1_HUMAN]	3.24	2	1	1	1	1	1,000	1	2,289	585	58,519	
Q1357	Lysine-specific protein 5 OS-Homo sapiens GN-LSP5 PE1 Sv1+ [Q1357_HUMAN]	0.44	1	1	1	1	1	1,000	1	2,287	262	29,117	
Q8R65	Lymphokine-activated killer cell-originated protein kinase OS-Homo sapiens GN-PAK PE1 Sv1+ [Q8R65_HUMAN]	2.17	1	1	1	1	1	1,000	1	2,287	322	36,062	
HD4053	HD4053, a novel OS-Homo sapiens GN-HD4053 PE-4 Sv1+ [HD4053_HUMAN]	0.13	3	1	1	1	1	1,000	1	2,287	99	99,299	
BZRT05	LRRRC16-like protein OS-Homo sapiens GN-LRRRC16 PE-2 Sv1+ [BZRT05_HUMAN]	0.88	2	1	1	1	1	1,000	1	2,287	1365	150,821	
ESB04	Putative uncharacterized protein OS-Leishmania mexicana (strain MHOM/GT2001/1103) GN-HLMMX_33_3620 PE4 Sv1+ [ESB04_LEIMU]	1.25	1	1	1	1	1	1,715	1	2,286	289	31,575	
ESK12	GN112, clone E2010 (Fragment) OS-Homo sapiens GN-ESK12 PE-1 Sv1+ [ESK12_HUMAN]	0.95	1	1	1	1	1	1,000	1	2,286	289	31,575	
BRAT1	cDNA FL35992, highly similar to Homo sapiens TRAD3 protein (TRAD3), mRNA OS-Homo sapiens GN-TRAD3 PE1 Sv1+ [BRAT1_HUMAN]	2.42	5	1	1	1	1	1,000	1	2,285	488	56,688	
ESK14	Ester hydrolase C11orf45 (RHC-11orf45) OS-Homo sapiens GN-ESK14 PE-3 Sv1+ [ESK14_HUMAN]	1.29	2	1	1	1	1	1,000	1	2,285	289	31,575	
BK304	cDNA FL4497 fl, clone BRAW0310726, highly similar to Membrane-associated phosphatidylinositol transfer protein 1 OS-Homo sapiens GN-PE2 Sv1+ [BK304_HU]	4.37	3	1	1	1	1	1,000	1	2,285	528	57,717	
ESPR04	NADH dehydrogenase [ubiquinone] 1 subunit C2, isoform 2 OS-Homo sapiens GN-NHDC2 CT-CTD14 PE1 Sv1+ [ESPR04_HUMAN]	33.33	7	1	2	2	2	1,000	1	2,283	66	7,481	
ESPR11	Putative uncharacterized protein OS-Leishmania mexicana (strain MHOM/GT2001/1103) GN-HLMMX_17_0420 PE4 Sv1+ [ESPR11_LEIMU]	0.92	1	1	1	1	1	1,000	1	2,283	289	31,575	
Q8E57	SAGA-associated factor 29 homolog OS-Homo sapiens GN-CACD101 PE1 Sv1+ [Q8E57_HUMAN]	4.44	1	1	1	1	1	1,066	1	2,282	293	33,217	
Q8Y53	TPA-190 transmembrane protein OS-Homo sapiens GN-Q8Y53 PE-1 Sv1+ [Q8Y53_HUMAN]	2.81	1	1	1	1	1	1,000	1	2,282	289	31,575	
Q8Y42	ERG membrane protein complex subunit 10 OS-Homo sapiens GN-EMC10 PE1 Sv1+ [EMC10_HUMAN]	3.05	2	1	2	2	2	1,656	2	12,992	282	27,330	
B4D50	cDNA FL35904, highly similar to Homo sapiens luciferin rib repeat and coiled-coil domain containing 1 (LRCC1), mRNA (Fragment) OS-Homo sapiens PE-2 Sv1+ [B4D50_HUMAN]	1.6	2	1	1	1	1	1,000	1	2,278	717	87,352	
ESW4	Putative uncharacterized protein OS-Leishmania mexicana (strain MHOM/GT2001/1103) GN-HLMMX_02_0240 PE4 Sv1+ [ESW4_LEIMU]	0.84	1	1	1	1	1	1,000	1	2,278	103	12,683	
ESK19	Putative uncharacterized protein OS-Leishmania mexicana (strain MHOM/GT2001/1103) GN-HLMMX_06_0810 PE4 Sv1+ [ESK19_LEIMU]	0.21	1	1	1	1	1	1,014	1	2,277	329	34,803	
Q8Y21	IRF6 (Fragment) OS-Homo sapiens GN-Q8Y21 PE-1 Sv1+ [Q8Y21_HUMAN]	1.4	1	1	1	1	1	1,000	1	2,276	13	2,296	
Q7Z73	Cytosolic RNA 2-hydrolation protein 1 OS-Homo sapiens GN-CTU1 PE1 Sv1+ [Q7Z73_HUMAN]	4.31	1	1	1	1	1	1,686	1	2,276	348	36,427	
ESK14	Putative uncharacterized protein OS-Leishmania mexicana (strain MHOM/GT2001/1103) GN-HLMMX_34_0710 PE4 Sv1+ [ESK14_LEIMU]	2.84	1	1	1	1	1	1,000	1	2,276	531	59,823	
ADQAR437	TBC1 domain family member 4, isoform CRA_3 OS-Homo sapiens GN-TBC1 PE-1 Sv1+ [ADQAR437_HUMAN]	0.36	2	1	1	1	1	1,000	1	2,276	1,998	145,457	
Q6774	Cytosolic phospholipase A2 gamma OS-Homo sapiens GN-PLA2G7 PE-2 Sv1+ [Q6774_HUMAN]	38.78	1	1	1	1	1	1,180	1	2,275	49	5,063	
ESK19	TBC1 domain family member 4, isoform CRA_2 OS-Homo sapiens GN-TBC1 PE-1 Sv1+ [ESK19_HUMAN]	2.55	1	1	1	1	1	1,000	1	2,275	432	50,021	
ESAP7	Kinesin-like protein OS-Leishmania mexicana (strain MHOM/GT2001/1103) GN-HLMMX_14_1110 PE3 Sv1+ [ESAP7_LEIMU]	1.73	1	1	1	1	1	1,000	1	2,274	2307	254,231	
B4D17	BCL2Ladenovirus E1B 19 kDa protein-interacting protein 3 OS-Homo sapiens GN-HPN3 PE1 Sv1+ [B4D17_HUMAN]	5	5	1	1	1	1	1,000	1	2,274	180	19,931	
ESK19	Uncharacterized protein OS-Leishmania mexicana (strain MHOM/GT2001/1103) GN-HLMMX_36_2010 PE4 Sv1+ [ESK19_LEIMU]	0.21	1	1	1	1	1	1,000	1	2,274	104	11,583	
ESPL2	Epilysin-like protein 1 like OS-Homo sapiens GN-EPFL1 PE-1 Sv1+ [ESPL2_HUMAN]	3.59	4	1	1	1	1	1,099	1	2,273	195	21,178	
HTC114	Protein S1 (Fragment) OS-Homo sapiens GN-S1 PE-4 Sv1+ [HTC114_HUMAN]	4.58	2	1	1	1	1	1,143	1	2,273	25	2,848	
BZM2	3-phosphoindolepyruvate reductase (Fragment) OS-Homo sapiens GN-PIR3 PE-1 Sv1+ [BZM2_HUMAN]	3.94	2	1	1	1	1	1,889	1	2,271	203	22,606	
K7C81	Ketohydrolase phosphatase C OS-Homo sapiens GN-KPCE1 PE-1 Sv1+ [K7C81_HUMAN]	0.7	2	1	1	1	1	1,000	1	2,271	228	25,941	
BZM2	GN12902, highly similar to Homo sapiens interferon regulatory factor 8 (IRF8), mRNA OS-Homo sapiens GN-IRF8 PE1 Sv1+ [BZM2_HUMAN]	1.93	2	1	1	1	1	1,000	1	2,270	49	5,117	
Q8Y59	PX domain-containing protein kinase like protein (Fragment) OS-Homo sapiens GN-PAK PE1 Sv1+ [Q8Y59_HUMAN]	24	11	1	1	1	1	1,000	1	2,269	50	5,167	
BZM2	Coiled-coil domain containing protein OS-Homo sapiens GN-CCDC43 PE-2 Sv1+ [BZM2_HUMAN]	1.48	2	1	1	1	1	1,000	1	2,269	28	24,488	
Q8Y52	Probable E3 ubiquitin protein ligase TRIM1, 1 OS-Homo sapiens GN-TRIM1, 1 PE1 Sv1+ [TRIM1_HUMAN]	2.14	1	1	1	1	1	1,000	1	2,268	468	52,968	
BZM2	Zinc finger protein 346 OS-Homo sapiens GN-ZNF346 PE1 Sv1+ [BZM2_HUMAN]	2.99	1	1	1	1	1	2,098	1	2,268	33	17,046	
Q8Y52	Cric trichostatin A receptor OS-Homo sapiens GN-CTR1 PE-1 Sv1+ [Q8Y52_HUMAN]	1.34	1	1	1	1	1	1,000	1	2,268	1840	207,892	
Q8D93	Ubiquitin ligase E3 UBR2 OS-Homo sapiens GN-UBR2 PE1 Sv1+ [Q8D93_HUMAN]	5.83	1	1	1	1	1	4,000	2,000	2,264	234	28,192	
ESK19	Cystine secretase beta-lyase OS-Homo sapiens GN-ESK19 PE-2 Sv1+ [ESK19_LEIMU]	0.17	1	1	1	1	1	1,000	1	2,264	414	46,994	
B4E28	cDNA FL1540 OS-Homo sapiens GN-B4E28 PE-2 Sv1+ [B4E28_HUMAN]	1.31	3	1	1	1	1	1,000	1	2,263	477	53,479	
Q8Y50	Carbamoyl transferase BAP1 OS-Homo sapiens GN-BAP1 PE1 Sv1+ [BAP1_HUMAN]	2.92	1	1	1	1	1	1,000	1	2,262	729	80,312	
ESK19	Serine/threonine protein kinase like protein OS-Leishmania mexicana (strain MHOM/GT2001/1103) GN-HLMMX_04_0440 PE4 Sv1+ [ESK19_LEIMU]	1.07	1	1	1	1	1	1,000	1	2,262	1,874	179,683	
ESB08	Putative uncharacterized protein OS-Leishmania mexicana (strain MHOM/GT2001/1103) GN-HLMMX_28_2860 PE4 Sv1+ [ESB08_LEIMU]	6.16	1	1	1	1	1	1,000	1	2,261	146	16,559	
HLA17D38	HLA class II protein (Fragment) OS-Homo sapiens GN-HLA17D38 PE-2 Sv1+ [HLA17D38_HUMAN]	0.86	7	1	1	1	1	1,000	1	2,261	66	7,481	
BK327	cDNA FL4597 fl, clone FLAC1079479, highly similar to 182 kDa lankylase 1 binding protein OS-Homo sapiens GN-PE2 Sv1+ [BK327_HUMAN]	1.02	2	1	1	1	1	1,705	1	2,259	1075	113,270	
ESK19													

EA9QJ5	Putative uncharacterized protein OS-Leishmania mexicana (strain MHOM/GT2001/11/103) GN-LMMX_16_1340 PE4 S-V1	[EA9QJ5_LEIUM]	0.26	1	1	1	1	0.842	1	2.187	3749	399.570	
EA9QJ6	CDNA FL3223, model of human protein OS-Homo sapiens (strain HG-9) mRNA OS-Homo sapiens PE-2 S-V1	[EA9QJ6_HUMAN]	0.159	1	1	1	1	1.000	1	2.187	629	658.652	
AK856	CDNA FL77231, highly similar to OS-Homo sapiens homogen (HEMAG), transcript variant 1, mRNA OS-Homo sapiens PE-2 S-V1	[AK856_HUMAN]	0.227	2	1	1	1	1.000	1	2.187	484	525.773	
VL14D3	ADP-4 complex subunit beta-1 (Fragment) OS-Homo sapiens GN-HAF6B PE4 S-V1	[VL14D3_HUMAN]	0.229	1	1	1	1	1.000	1	2.185	175	20.168	
EBK672	CDNA FL1465, clone cDNA102, highly similar to OS-Homo sapiens centrosome protein 70 kDa (CEP170), transcript variant alpha, mRNA OS-Homo sapiens P1	[EBK672_HUMAN]	0.42	1	1	1	1	1.000	1	2.182	203	21.851	
QB749	Protein phosphatase 1 regulatory inhibitor subunit 1B OS-Homo sapiens GN-PPR1B PE1 S-V1	[PP1B_HUMAN]	2.82	1	1	4	1	0.1064	4	0.688	2.183	67.511	
ES9A9B	ES2 OS-Homo sapiens GN-HO2C2.11 PE4 S-V1	[ES9A9B_HUMAN]	15.28	1	1	1	1	1.000	1	2.183	72	7.389	
QOZK7	Uncharacterized protein OS-Homo sapiens GN-C17A97 PE2 S-V2	[QOZK7_HUMAN]	22.08	1	1	1	1	0.686	1	2.184	457	49.626	
BZ756	CDNA FL1723 OS-Homo sapiens PE-2 S-V1	[BZ756_HUMAN]	0.53	1	1	1	1	1.000	1	2.182	1323	145.428	
EA9QJ7	CDNA FL4025, clone TEST10203, highly similar to Actin like protein OS-Homo sapiens PE-2 S-V1	[B3KUPR_HUMAN]	0.53	1	1	1	1	1.000	1	2.182	200	30.175	
EA9QJ8	CDNA FL1540, clone cDNA102, highly similar to OS-Homo sapiens centrosome protein 70 kDa (CEP170), transcript variant alpha, mRNA OS-Homo sapiens P1	[EA9QJ8_HUMAN]	0.53	1	1	1	1	1.000	1	2.182	200	30.175	
Q3R29	FCI uncharacterized protein OS-Leishmania mexicana (strain MHOM/GT2001/11/103) GN-LMMX_14_290 PE4 S-V1	[EA9QJ8_LEIUM]	1.23	1	1	1	1	1.000	1	2.182	111	11.111	
EA9QJ9	CDNA FL1465, clone cDNA102, highly similar to OS-Homo sapiens centrosome protein 70 kDa (CEP170), transcript variant alpha, mRNA OS-Homo sapiens P1	[EA9QJ9_HUMAN]	1.23	1	1	1	1	1.000	1	2.182	111	11.111	
EA9QJ0	Putative uncharacterized protein OS-Leishmania mexicana (strain MHOM/GT2001/11/103) GN-LMMX_05_1110 PE4 S-V1	[EA9QJ0_LEIUM]	1.16	1	1	1	1	1.000	1	2.181	1245	136.960	
BK9P3	CDNA FL2006, clone FIEB4200521, highly similar to Junctophilin 1 OS-Homo sapiens PE-2 S-V1	[BK9P3_HUMAN]	0.26	1	1	1	1	1.000	1	2.181	423	45.652	
EBK673	CDNA FL1465, clone cDNA102, highly similar to OS-Homo sapiens centrosome protein 70 kDa (CEP170), transcript variant alpha, mRNA OS-Homo sapiens P1	[EBK673_HUMAN]	0.26	1	1	1	1	1.000	1	2.181	423	45.652	
EA9QJ1	Putative ATP-dependent DEAD/1 RNA helicase OS-Leishmania mexicana (strain MHOM/GT2001/11/103) GN-LMMX_07_0340 PE4 S-V1	[EA9QJ1_LEIUM]	1.93	1	1	1	1	2.973	1	2.179	415	45.901	
QZC761	CDNA FL1465, clone cDNA102, highly similar to OS-Homo sapiens centrosome protein 70 kDa (CEP170), transcript variant alpha, mRNA OS-Homo sapiens P1	[QZC761_HUMAN]	3.85	1	1	1	1	1.000	1	2.179	180	19.459	
EA9QJ2	Uncharacterized protein OS-Leishmania mexicana (strain MHOM/GT2001/11/103) GN-LMMX_19_0240 PE4 S-V1	[EA9QJ2_LEIUM]	1.19	1	1	1	1	0.966	1	2.178	671	72.815	
Q5T62	Serine/threonine protein kinase Nedd1 (Fragment) OS-Homo sapiens GN-NEK6 PE1 S-V1	[Q5T62_HUMAN]	2.06	1	1	1	1	0.627	1	2.178	171	19.668	
Q5T63	Cytochrome oxidase subunit I (Fragment) OS-Homo sapiens GN-CO1I1 PE1 S-V1	[Q5T63_HUMAN]	1.9	1	1	1	1	1.000	1	2.178	415	45.901	
QYK77	Burkholderia symbiont 2 member A1 OS-Homo sapiens GN-BTN2A1 PE1 S-V3	[BT2A1_HUMAN]	5.29	1	1	1	1	0.039	1	2.177	527	59.594	
ESAK11	2,4-dienyl-coenzyme A reductase-like protein OS-Leishmania mexicana (strain MHOM/GT2001/11/103) GN-LMMX_06_0930 PE4 S-V1	[ESAK11_LEIUM]	1.54	1	1	1	1	0.653	1	2.178	730	80.588	
BZ739	Phosphatase and actin regulator OS-Homo sapiens PE-2 S-V1	[BZ739_HUMAN]	1.74	3	1	1	1	1.000	1	2.176	518	58.500	
AD0758H5	Protein TRBV202R and regulator OS-Homo sapiens GN-TRBV202R PE4 S-V1	[AD0758H5_HUMAN]	0.15	1	1	1	1	1.187	1	2.176	130	14.272	
AD0758H6	Transmembrane protein 222 OS-Homo sapiens GN-TRN222 PE1 S-V1	[AD0758H6_HUMAN]	0.55	1	1	1	1	0.621	1	2.179	926	20.856	
Q8U40	Zinc finger protein 346 OS-Homo sapiens GN-ZNF346 PE1 S-V1	[ZNF346_HUMAN]	2.38	2	1	1	1	0.766	1	2.175	294	32.912	
Q9P218	Zinc finger protein 624 OS-Homo sapiens GN-ZNF624 PE1 S-V1	[ZNF624_HUMAN]	1.55	1	1	1	1	0.989	0	2.174	865	99.864	
POC33	Putative zinc finger protein 735 OS-Homo sapiens GN-ZNF735 PE5 S-V1	[ZNF735_HUMAN]	13.11	171	1	3	5	1.000	2	0.000	2.174	412	47.534
ICDM8	Zinc finger protein 628 protein 1 (Fragment) OS-Homo sapiens GN-ZNF628 PE4 S-V1	[ICDM8_HUMAN]	2.8	175	1	3	4	0.762	1	2.174	218	25.148	
ICDM9	Zinc finger protein 628 protein 2 (Fragment) OS-Homo sapiens GN-ZNF628 PE4 S-V1	[ICDM9_HUMAN]	1.75	173	1	3	4	0.762	1	2.174	218	25.148	
AK8C04	CDNA FL15719, highly similar to OS-Homo sapiens PE-2 S-V1	[AK8C04_HUMAN]	1.49	12	2	2	2	0.758	1	2.174	520	57.583	
C3A369	Proteasome activator complex subunit 1 OS-Homo sapiens GN-PAC1 PE1 S-V1	[C3A369_HUMAN]	1.21	1	1	1	1	1.000	1	2.174	904	93.371	
EBE3H1	Uncharacterized protein OS-Leishmania mexicana (strain MHOM/GT2001/11/103) GN-LMMX_31_3930 PE4 S-V1	[EBE3H1_LEIUM]	0.17	1	1	1	1	0.830	1	2.173	4087	453.583	
Q3K988	Rho GTPase-activating protein 1B OS-Homo sapiens GN-ARHGAP1B PE1 S-V1	[Q3K988_HUMAN]	3.37	3	1	1	1	1.580	1	2.172	207	23.322	
EBK674	Neurokinin receptor 4 OS-Homo sapiens GN-ENK4R PE2 S-V1	[EBK674_HUMAN]	1.45	1	1	1	1	1.000	1	2.172	186	20.858	
EA9QJ4	Putative uncharacterized protein OS-Leishmania mexicana (strain MHOM/GT2001/11/103) GN-LMMX_17_0350 PE4 S-V1	[EA9QJ4_LEIUM]	1.36	1	1	1	1	1.790	1	2.170	680	73.642	
Q15645	Pachyostictus protein OS-Homo sapiens GN-PTSP1 PE1 S-V2	[PCH_HUMAN]	4.63	2	1	1	1	1.000	1	2.172	432	43.200	
AAV06	HPI protein (Fragment) OS-Homo sapiens GN-HPI PE2 S-V1	[AAV06_HUMAN]	1.55	5	1	1	1	1.340	1	2.168	517	57.658	
BK9N7	CDNA FL1386, clone THY1021170, highly similar to 99 kDa Z-D-oligoadenylate synthetase-like protein OS-Homo sapiens PE-2 S-V1	[BK9N7_HUMAN]	1.56	2	1	1	1	1.000	2	0.000	2.168	514	59.219
AD0758M7	Adiponectin OS-Homo sapiens GN-ADPN PE1 S-V1	[AD0758M7_HUMAN]	2.35	1	1	1	1	1.000	1	2.167	104	11.257	
BD4583	CDNA FL15719, highly similar to Nuclear pore 10 OS-Homo sapiens PE-2 S-V1	[BD4583_HUMAN]	1.1	2	1	1	1	1.000	1	2.167	638	74.366	
EBK675	Breast cancer protein 1 (Fragment) OS-Homo sapiens GN-BCP1 PE1 S-V1	[EBK675_HUMAN]	0.22	1	1	1	1	1.000	1	2.167	1147	125.977	
EBP33	Smoothelin-like protein 1 OS-Homo sapiens GN-SMTL1 PE4 S-V1	[EBP33_HUMAN]	1.42	1	1	1	1	0.921	1	2.166	484	52.954	
HOYV7	Calcium transporting ATPase type 2C member 1 (Fragment) OS-Homo sapiens GN-ATP2C1 PE1 S-V1	[HOYV7_HUMAN]	1.77	2	2	2	2	1.023	2	4.789	2.166	903	98.985
EBK676	Putative uncharacterized protein OS-Leishmania mexicana (strain MHOM/GT2001/11/103) GN-LMMX_26_0490 PE4 S-V1	[EA9QJ3_LEIUM]	0.55	1	1	1	1	1.000	1	2.166	106	10.820	
Q8H45	Transmembrane protein 141 OS-Homo sapiens GN-TMEM141 PE1 S-V1	[TM141_HUMAN]	7.41	1	1	1	1	0.877	1	2.163	108	11.867	
EBK677	Transmembrane protein 141 OS-Homo sapiens GN-TMEM141 PE1 S-V1	[EBK677_HUMAN]	1.68	1	1	1	1	1.000	1	2.163	476	52.000	
EA9QJ5	Putative NADH-cytochrome b5 reductase OS-Leishmania mexicana (strain MHOM/GT2001/11/103) GN-LMMX_22_2810 PE4 S-V1	[EA9QJ5_LEIUM]	5.54	1	2	2	2	0.918	2	12.703	2.161	289	31.848
L7R28	TRIM3 (Fragment) OS-Homo sapiens GN-TRIM3 PE4 S-V1	[L7R28_HUMAN]	14.25	13	1	1	1	0.314	1	2.161	62	6.875	
EBK678	Uncharacterized protein OS-Leishmania mexicana (strain MHOM/GT2001/11/103) GN-LMMX_32_1620 PE4 S-V1	[EBK678_LEIUM]	0.32	1	1	1	1	1.000	1	2.161	62	6.875	
Q3K9V0	HES1 protein OS-Homo sapiens GN-HES1 PE2 S-V1	[Q3K9V0_HUMAN]	1.49	2	1	1	1	1.000	1	2.160	277	29.253	
TC119	Rai1 OS-Homo sapiens (Fragment) OS-Homo sapiens GN-RALGAP2 PE1 S-V1	[TC119_HUMAN]	1.61	2	1	1	1	0.286	1	2.160	1740	191.913	
BD4P5	CDNA FL15087, highly similar to Huntingtin-interacting protein 1 OS-Homo sapiens PE-2 S-V1	[BD4P5_HUMAN]	1.37	4	1	1	1	1.381	1	2.159	437	49.959	
Q9Y245	Little elongation complex subunit 1 OS-Homo sapiens GN-LEC1 PE1 S-V5	[Q9Y245_HUMAN]	0.31	1	1	1	1	1.000	1	2.159	226	24.737	
EA9QJ6	Putative uncharacterized protein OS-Leishmania mexicana (strain MHOM/GT2001/11/103) GN-LMMX_24_1070 PE4 S-V1	[EA9QJ6_LEIUM]	1.39	1	1	1	1	1.000	1	0.000	2.159	226	24.737
EBE6E5	Putative uncharacterized protein OS-Leishmania mexicana (strain MHOM/GT2001/11/103) GN-LMMX_24_2860 PE4 S-V1	[EBE6E5_LEIUM]	9.33	1	1	1	1	1.000	1	2.158	107	11.807	
PEV4250	Peptide YY2 OS-Homo sapiens GN-PYY2 PE1 S-V2	[PEV4250_HUMAN]	0.42	1	1	1	1	1.000	1	2.158	1994	219.589	
EA9QJ7	Putative uncharacterized protein OS-Leishmania mexicana (strain MHOM/GT2001/11/103) GN-LMMX_25_1830 PE4 S-V1	[EA9QJ7_LEIUM]	2.79	1	1	1	1	1.000	1	2.157	1002	103.872	
Q3K989	CDNA FL15018, highly similar to Perlecanin biosynthesis factor 1 OS-Homo sapiens PE-2 S-V1	[Q3K989_HUMAN]	1.04	4	1	1	1	1.000	1	2.156	991	105.889	
EA9QJ8	Putative uncharacterized protein OS-Leishmania mexicana (strain MHOM/GT2001/11/103) GN-LMMX_25_1830 PE4 S-V1	[EA9QJ8_LEIUM]	1.04	4	1	1	1	1.000	1	2.156	991	105.889	
Q8D18	Putative uncharacterized protein OS-Leishmania mexicana (strain MHOM/GT2001/11/103) GN-LMMX_25_1830 PE4 S-V1	[Q8D18_HUMAN]	8.7	4	1	1	1	1.000	1	2.152	92	10.472	
EA9QJ9	Kinase-related protein OS-Leishmania mexicana (strain MHOM/GT2001/11/103) GN-LMMX_25_1830 PE4 S-V1	[EA9QJ9_HUMAN]	0.65	1	1	1	1	0.846	1	2.152	1034	113.037	
EA9QJ0	Uncharacterized protein OS-Leishmania mexicana (strain MHOM/GT2001/11/103) GN-LMMX_19_1130 PE4 S-V1	[EA9QJ0_LEIUM]	0.24	1	1	1	1	1.168	1	2.153	5789	614.253	
EA9QJ1	Putative uncharacterized protein OS-Leishmania mexicana (strain MHOM/GT2001/11/103) GN-LMMX_17_1260 PE4 S-V1	[EA9QJ1_LEIUM]	0.26	1	1	1	1	1.000	1	2.153	449	47.462	
BK9N7	CDNA FL1465, clone THY1021170, highly similar to 99 kDa Z-D-oligoadenylate synthetase-like protein OS-Homo sapiens PE-2 S-V1	[BK9N7_HUMAN]	1.56	2	1	1	1	1.000	2	0.000	2.153	449	47.462
EBK679	Uncharacterized protein OS-Leishmania mexicana (strain MHOM/GT2001/11/103) GN-LMMX_31_3290 PE4 S-V1	[EBK679_LEIUM]	7.49	1	1	1	1	1.000	1	2.151	187	20.261	
CDNA FL2002	CDNA FL2002, highly similar to OS-Homo sapiens PE-2 S-V1	[CDNA FL2002_HUMAN]	1.89	1	1	1	1	1.000	1	2.150	633	67.037	
EA9QJ2	Uncharacterized protein OS-Leishmania mexicana (strain MHOM/GT2001/11/103) GN-LMMX_09_0680 PE4 S-V1	[EA9QJ2_LEIUM]	1.89	1	1	1	1	0.998	1	2.150	370	40.432	
EPJ20	Erythroid differentiation-related factor 1 OS-Homo sapiens GN-EDRF1 PE4 S-V1	[EPJ20_HUMAN]	4.08	2	1	1	1	1.000	1	2.150	343	37.371	
AD0758M8	Adiponectin OS-Homo sapiens GN-ADPN PE1 S-V1	[AD0758M8_HUMAN]	1.4	1	1	1	1	1.000	1	2.149	100	10.710	
HTC2L3	Cystine-rich ligand with EGF-like domain protein 1 (Fragment) OS-Homo sapiens GN-CRELD1 PE4 S-V1	[HTC2L3_HUMAN]	12	3	1	1	1	1.000	1	2.149	140	15.170	
Q3K9V1	18kDa histone H2B OS-Homo sapiens GN-H2B PE1 S-V1	[Q3K9V1_HUMAN]	2.45	1	1	1	1	0.773	1	2.149	117	12.542	
Q9NOV1	Protein integral membrane protein SC1B OS-Homo sapiens GN-SC1B PE1 S-V1	[SC1B_HUMAN]	1.53	6	1	2	2	1.000	1	2.149	1179	128.615	
ES9QF1	Small integral membrane protein 12 OS-Homo sapiens GN-SMIM12 PE4 S-V1	[ES9QF1_HUMAN]	14.86	2	1	1	1	0.550	1	2.149	74	8.073	
EBK670	Collin OS-Homo sapiens GN-COL154 PE1 S-V1	[EBK670_HUMAN]	1.72	2	1	1	1	1.000	1	2.149	522	57.412	
G3V58	Serine/threonine protein phosphatase 2A regulatory subunit B' subunit gamma OS-Homo sapiens GN-PPR2C3 PE4 S-V1	[G3V58_HUMAN]	6.6	5	1	1	1	1.006	1	2.148	106	12.916	
EA9QJ0	Putative uncharacterized protein OS-Leishmania mexicana (strain MHOM/GT2001/11/103)												

A1EC81	NK2 transcription factor related box 5 (Fragment) OS-Homo sapiens GN-NK02.5 PE=4 SV=1	[A1EC81_HUMAN]	8	7	1	1	1	1,036	1	1,942	101	11,536
ESP344	Polyoma-5 (Fragment) OS-Homo sapiens GN-C1.P1 PE=1 SV=1	[ESP344_HUMAN]	1	1	1	1	1	1,000	1	1,942	101	11,536
CS1X13	Activated CCKA kinase 1 OS-Homo sapiens GN-TNK2 PE=1 SV=1	[CS1X13_HUMAN]	1	1	1	1	1	1,012	1	1,942	100	11,478
DD3S51	Kinase (PKC) and/or protein 6, isoform CRA_d OS-Homo sapiens GN-HKAPR PE=4 SV=1	[DD3S51_HUMAN]	1.25	0.4	3	1	1	1,899	1	1,942	207	22,327
ESB0V2	Actin-interacting protein-like protein (strain MHOMGT2001U1103) GN-HLMXM_26_110 PE=4 SV=1	[ESB0V2_HUMAN]	0.81	0.1	1	1	1	1,733	1	1,942	166	18,201
Q8N9V6	Trimethyllysine dioxygenase, mitochondrial OS-Homo sapiens GN-TMLHE PE=1 SV=1	[TMTHL_HUMAN]	1.9	1	1	1	1	1,000	1	1,937	421	49,486
AK8044	cDNA FL3544, highly similar to OS-Homo sapiens GN-ADAMTSL1 mRNA OS-Homo sapiens PE=2 SV=1	[AK8044_HUMAN]	0.72	2	1	1	1	1,000	1	1,937	104	837
BADW09	cDNA FL3542, highly similar to Probable ATP-dependent RNA helicase XD058 (EC 3.6.1.1) OS-Homo sapiens PE=1 SV=1	[BADW09_HUMAN]	1.49	0.4	1	1	1	1,269	1	1,932	536	60,663
CG3C35	Zinc finger protein 668 (Fragment) OS-Homo sapiens GN-ZNF668 PE=1 SV=2	[CG3C35_HUMAN]	8.7	6	1	1	2	4,440	1	1,931	82	8,738
GNAM07	Inchworm-like protein (strain MHOMGT2001U1103) GN-HLMXM_29_070 PE=4 SV=1	[GNAM07_HUMAN]	0.24	0.1	1	1	1	1,000	1	1,929	561	56,193
FR5X38	Yield (ADP)-dependent polymerase 8 OS-Homo sapiens GN-PAPR8 PE=4 SV=1	[FR5X38_HUMAN]	1.62	7	1	1	1	1,000	1	1,927	494	55,113
Q55D21	Arginase (Fragment) OS-Homo sapiens GN-ATE1 PE=1 SV=1	[Q55D21_HUMAN]	1.47	1	1	1	1	1,000	1	1,925	222	22,927
EB1W9	Uncharacterized protein OS-Leishmania mexicana (strain MHOMGT2001U1103) GN-HLMXM_30_160 PE=4 SV=1	[EB1W9_LEIUM]	0.931	1	1	1	1	1,000	1	1,921	140	151,406
CLD1V1	Vesicular, overexpressed in cancer, prosurvival protein 1 OS-Homo sapiens GN-VOP1 PE=4 SV=1	[CLD1V1_HUMAN]	5.29	2	1	1	1	1,000	1	1,921	170	11,113
Q8R69	Large nuclear ribonucleoprotein complex OS-Homo sapiens GN-XZ2 PE=1 SV=1	[Q8R69_HUMAN]	1.96	1	1	1	1	1,000	1	1,920	179	20,292
PE2304	Small nuclear ribonucleoprotein E OS-Homo sapiens GN-SNRP E PE=1 SV=1	[RUXE_HUMAN]	11.96	1	1	1	1	1,072	1	1,919	92	10,797
EB2L2	GOS domain-containing protein 1 (Fragment) OS-Homo sapiens GN-GRM1 PE=4 SV=1	[EB2L2_HUMAN]	4.47	1	1	1	1	1,000	1	1,917	179	20,292
EB9639	Uncharacterized protein OS-Leishmania mexicana (strain MHOMGT2001U1103) GN-HLMXM_31_3090 PE=4 SV=1	[EB9639_LEIUM]	0.59	1	1	1	1	1,000	1	1,917	1515	159,654
Q8R17	ADC-adenosin on channel 4 OS-Homo sapiens GN-ASIC4 PE=1 SV=2	[ASIC4_HUMAN]	1.86	3	1	1	1	1,000	1	1,917	647	70,080
PO1276	Glucagon OS-Homo sapiens GN-HGCG PE=1 SV=3	[IGLH3_HUMAN]	11.31	2	1	1	2	1,000	1	1,917	180	19,294
Q57370	Aresalin domain-containing protein 1 (Fragment) OS-Homo sapiens GN-ARRDC1 PE=4 SV=1	[Q57370_HUMAN]	4.06	3	1	1	1	1,141	1	1,917	271	29,236
BAE114	cDNA FL35365, highly similar to Secreted fibronectin type 4 OS-Homo sapiens PE=2 SV=1	[BAE114_HUMAN]	6.41	2	1	1	1	1,444	1	1,917	343	33,150
BAD290	Cystatin B (Fragment) OS-Homo sapiens GN-CSTB PE=4 SV=1	[A2A20_HUMAN]	5.22	2	1	1	1	1,000	1	1,914	134	15,330
BAD294	cDNA FL35466, highly similar to OS-Homo sapiens soluble carrier family 22 (organic anion transporter), member 8 (SLC22A2), mRNA OS-Homo sapiens PE=2 SV=1	[BAD294_HUMAN]	1.33	4	1	1	1	1,612	1	1,914	528	58,300
F2232	26S proteasome non-ATP regulatory subunit 5 OS-Homo sapiens GN-PSMD5 PE=1 SV=1	[F2232_HUMAN]	12.5	3	1	1	1	1,000	1	1,913	72	8,216
BAE114	cDNA FL35365, highly similar to Secreted fibronectin type 4 OS-Homo sapiens PE=2 SV=1	[BAE114_HUMAN]	6.41	2	1	1	1	1,444	1	1,912	343	33,150
BADV00	cDNA FL80251, highly similar to Contactin 6 OS-Homo sapiens PE=2 SV=1	[BADV00_HUMAN]	11.5	2	1	1	1	1,000	1	1,911	956	106,772
Q2V2A0	Rad-like GTP-binding protein B (Fragment) OS-Homo sapiens GN-HRACB PE=4 SV=1	[Q2V2A0_HUMAN]	4.84	3	1	1	1	1,000	1	1,910	194	22,905
ED2002	Uncharacterized protein OS-Leishmania mexicana (strain MHOMGT2001U1103) GN-HLMXM_27_110 PE=4 SV=1	[ED2002_LEIUM]	1.877	1	1	1	1	1,000	1	1,910	505	52,937
DEW5X5	Susac carrier family 12 (Potassium-uniporter transporters), member 9, isoform CRA_c OS-Homo sapiens GN-SLC12A9 PE=4 SV=1	[DEW5X5_HUMAN]	2.02	8	1	1	1	1,000	1	1,910	446	47,425
Q2V9V0	Protein pizote OS-Homo sapiens GN-PZO1 PE=1 SV=4	[PZO1_HUMAN]	0.896	2	2	3	1	1,000	1	1,910	505	52,937
FBVW97	25-hydroxylase D-1 alpha hydroxylase, mitochondrial (Fragment) OS-Homo sapiens GN-HV2P1 PE=3 SV=1	[FBVW97_HUMAN]	6.37	2	1	1	1	1,000	1	1,909	157	17,444
ESAU78	Uncharacterized protein OS-Leishmania mexicana (strain MHOMGT2001U1103) GN-HLMXM_36_6420 PE=4 SV=1	[ESAU78_LEIUM]	4.37	1	1	1	1	1,000	1	1,909	206	22,854
Q2V2V1	ATCC domain-containing protein OS-Homo sapiens GN-RC21 PE=1 SV=1	[Q2V2V1_HUMAN]	2.94	1	1	1	1	1,000	1	1,908	374	38,652
ESAW99	Uncharacterized protein OS-Leishmania mexicana (strain MHOMGT2001U1103) GN-HLMXM_23_1665 PE=4 SV=1	[ESAW99_LEIUM]	2.94	1	1	1	1	1,000	1	1,908	238	25,551
Q8R69	Mitochondrial ornithine transferase OS-Homo sapiens GN-CSD2 PE=1 SV=3	[Q8R69_HUMAN]	1.09	1	1	1	1	1,000	1	1,907	301	30,959
POC7P0	CGDSH non-sulfur domain-containing protein 3, mitochondrial OS-Homo sapiens GN-CSD3 PE=1 SV=1	[CSD3_HUMAN]	5.51	1	1	1	1	1,274	1	1,905	127	14,206
ESAJ39	Uncharacterized protein OS-Leishmania mexicana (strain MHOMGT2001U1103) GN-HLMXM_03_0950 PE=4 SV=1	[ESAJ39_LEIUM]	2.88	1	1	1	1	1,000	1	1,905	556	62,071
ESAS32	Retenonin-3 (Fragment) OS-Homo sapiens GN-SEM3 PE=4 SV=1	[ESAS32_HUMAN]	3.74	1	1	1	1	1,000	1	1,905	185	20,428
ESAS29	Putative ABC transporter OS-Leishmania mexicana (strain MHOMGT2001U1103) GN-HLMXM_19_3800 PE=3 SV=1	[ESAS29_LEIUM]	1.47	1	1	1	1	1,000	2	1,903	612	68,538
Q2T017	Neocytin OS-Homo sapiens GN-NEC1 PE=4 SV=1	[Q2T017_HUMAN]	1.44	1	1	1	1	1,000	1	1,903	612	68,538
KTEL8	Stromal cell-derived factor 2 (Fragment) OS-Homo sapiens GN-SDF2 PE=1 SV=1	[KTEL8_HUMAN]	7.69	2	1	1	1	1,000	1	1,901	109	11,283
KTER3	Metalloproteinase family 1 (Fragment) OS-Homo sapiens GN-MPPE1 PE=4 SV=3	[KTER3_HUMAN]	15.94	9	1	1	1	1,000	1	1,899	69	7,922
FL8K42	cDNA FL7824, highly similar to OS-Homo sapiens nucleolar sorting 34 (NOL34), mRNA OS-Homo sapiens PE=1 SV=1	[ARXAK2_HUMAN]	1.24	3	1	1	1	1,000	1	1,899	188	19,584
EB68L8	Putative uncharacterized protein OS-Leishmania mexicana (strain MHOMGT2001U1103) GN-HLMXM_34_4180 PE=4 SV=1	[EB68L8_LEIUM]	1.01	1	1	1	1	1,000	1	1,897	592	64,388
ESM927	Transmembrane protein TEAD4 PE=4 SV=1	[ESM927_HUMAN]	3.94	1	1	1	1	1,000	1	1,897	592	64,388
EB6203	Uncharacterized protein OS-Leishmania mexicana (strain MHOMGT2001U1103) GN-HLMXM_30_2040 PE=4 SV=1	[EB6203_LEIUM]	1.2	1	1	1	1	1,000	1	1,894	500	53,350
ABK7C2	cDNA FL75762, highly similar to Homo sapiens, serine, 28 (PRSS25), nuclear gene encoding/mitchondrial protein, transcript variant 1, mRNA OS-Homo sapiens PE=2 SV=1	[ABK7C2_HUMAN]	2.4	2	1	1	1	1,000	1	1,893	458	48,780
EUAYC7	Uncharacterized protein OS-Leishmania mexicana (strain MHOMGT2001U1103) GN-HLMXM_26_110 PE=4 SV=1	[EUAYC7_LEIUM]	0.76	2	1	1	1	1,000	1	1,893	217	23,688
HOY77	Zinc fingers and homeobox protein 3 OS-Homo sapiens GN-ZHX3 PE=4 SV=2	[HOY77_HUMAN]	2.54	1	1	1	1	1,000	1	1,893	318	33,959
Q2P962	14-3-3 protein zeta OS-Homo sapiens GN-PPP4C PE=1 SV=1	[Q2P962_HUMAN]	1.2	1	1	1	1	1,000	1	1,892	719	78,188
EB6263	Uncharacterized protein OS-Leishmania mexicana (strain MHOMGT2001U1103) GN-HLMXM_31_0220 PE=4 SV=1	[EB6263_LEIUM]	0.78	1	1	1	1	1,000	1	1,892	102	114,694
ESAN33	Putative cyclin D5 OS-Leishmania mexicana (strain MHOMGT2001U1103) GN-HLMXM_11_3580 PE=3 SV=1	[ESAN33_LEIUM]	5.83	1	2	2	1	1,369	1	1,892	142	15,851
Q2V2V1	Pumilio domain-containing protein OS-Homo sapiens GN-RAK200 PE=1 SV=3	[Q2V2V1_HUMAN]	1.23	1	1	1	1	1,000	1	1,892	153	16,527
HOY412	Protein PRR20B (Fragment) OS-Homo sapiens GN-PRRC2B PE=1 SV=1	[HOY412_HUMAN]	1.7	2	1	1	1	1,000	1	1,888	685	63,270
CNA FL8D94	cDNA FL8D94, highly similar to OS-Homo sapiens, 3 (EC 2.1.1) OS-Homo sapiens PE=2 SV=1	[CNA FL8D94_HUMAN]	1.32	1	1	1	1	1,000	1	1,888	557	55,007
ENH54	WSS PARC20000 data, contig 97 (Fragment) OS-Leishmania mexicana (strain MHOMGT2001U1103) GN-HLMXM_15_0400 PE=4 SV=1	[ENH54_LEIUM]	3.04	3	1	2	2	1,000	1	1,888	657	73,324
PO1229	Transcription factor HIVEP2 OS-Homo sapiens GN-HIVEP2 PE=1 SV=2	[ZEP2_HUMAN]	0.33	2	1	1	1	1,000	1	1,888	246	26,885
BZ4246	Transmembrane protein 418 OS-Homo sapiens GN-TM418 PE=1 SV=1	[BZ4246_HUMAN]	1.97	1	1	1	1	1,000	1	1,888	166	17,166
Q2V2Z2	Oxytocin b OS-Homo sapiens GN-OXTB PE=1 SV=1	[BZ244E_HUMAN]	7.94	254	2	2	2	1,457	1	1,878	376	42,384
Q2V2Z2	cDNA FL52671, highly similar to Calcium-binding mitochondrial protein Aa2a OS-Homo sapiens PE=2 SV=1	[BZ244E_HUMAN]	1.41	1	1	1	1	1,000	1	1,878	376	42,384
O15014	Zinc finger protein 609 OS-Homo sapiens GN-ZNF609 PE=1 SV=2	[ZNF609_HUMAN]	0.64	1	1	1	1	1,690	1	1,877	1411	151,098
PS8936	Cytin-dependent kinase inhibitor 1 OS-Homo sapiens GN-CDNK1 PE=1 SV=3	[CDNK1_HUMAN]	10.98	4	1	1	2	1,000	1	1,876	144	16,108
ESAW	ESAW tyrosinase (Putative glutamine aminotransferase) OS-Leishmania mexicana (strain MHOMGT2001U1103) GN-HLMXM_22_0110 PE=4 SV=1	[ESAW_ULI_HUMAN]	2.44	2	1	1	1	1,000	1	1,876	174	18,512
ESAW69	Platelet-activating factor acetylhydrolase B subunit gamma (Fragment) OS-Homo sapiens GN-PAFAH1B3 PE=1 SV=3	[BMR38_HUMAN]	4.24	3	1	1	1	1,027	1	1,875	165	18,402
ESAW27	Uncharacterized protein OS-Homo sapiens GN-HMOMGT2001U1103) GN-HLMXM_26_110 PE=4 SV=1	[ESAW27_HUMAN]	1.17	1	1	1	1	1,000	1	1,875	101	11,187
ESAW36	Uncharacterized protein OS-Leishmania mexicana (strain MHOMGT2001U1103) GN-HLMXM_21_1220 PE=4 SV=1	[ESAW36_HUMAN]	0.58	1	1	1	1	1,000	1	1,875	1371	146,697
Q8R69	Lamin OS-Homo sapiens GN-LAMP1 PE=1 SV=1	[LAMP1_HUMAN]	1.54	1	1	1	1	1,000	1	1,872	1308	147,832
Q2V2D8	Chol1 (P40) homolog, subunit C, isoform B, isoform CRA_d OS-Homo sapiens GN-DNAC1B PE=2 SV=1	[Q2V2D8_HUMAN]	1.21	1	1	1	1	1,000	1	1,871	103	11,187
Q9H8M8	cDNA FL7849, highly similar to 1-acyl-sn-glycerol-3-phosphate acyltransferase alpha (EC 2.3.1.51) OS-Homo sapiens PE=2 SV=1	[Q9H8M8_HUMAN]	0.29	5	1	1	1	1,288	1	1,869	171	18,744
LE7449	Altenex protein MS413 OS-Homo sapiens GN-ALN3 PE=1 SV=1	[LE7449_HUMAN]	11.11	6	1	1	1	1,000	1	1,868	63	7,628
G3V276	Uncharacterized protein (Fragment) OS-Homo sapiens PE=4 SV=2	[G3V276_HUMAN]	5.18	2	1	1	1	1,102	1	1,867	183	22,649
SKWR98	Toll-like receptor OS-Homo sapiens PE=2 SV=1	[SKWR98_HUMAN]	1.02	2	1	1	1	1,000	1	1,867	784	89,768
BNVCF2	Transmembrane and coiled-coil domain-containing protein 3 (Fragment) OS-Homo sapiens GN-TMCC3 PE=4 SV=1	[BNVCF2_HUMAN]	0.53	3	1	1	1	1,000	1	1,867	132	13,669
Q9H1V4	Methylmalonic acyl-CoA synthetase OS-Homo sapiens GN-MMAA PE=1 SV=1	[MMAA_HUMAN]	5.48	2	2	2	1,000	1	1,865	418	46,550	
Q9H1V4	IBC-like transfer protein OS-Homo sapiens GN-IBCT PE=1 SV=1	[Q9H1V4_HUMAN]	0.37	1	1	1	1	1,000	1	1,865	105	11,528
EB81X5	Nucleosome assembly protein-like protein OS-Leishmania mexicana (strain MHOMGT2001U1103) GN-HLMXM_30_1750 PE=3 SV=1	[EB81X5_LEIUM]	5.21	2	2	2	2,933	2	1,863	407	45,129	
Q2V2A0	Vesicle assembly-associated transmembrane protein 1 (Fragment) OS-Homo sapiens GN-VAMP1 PE=4 SV=3	[Q2V2A0_HUMAN]	10.26	8	1	1	1	1,000	1	1,862	117	12,674
Q13267	Mitotic spindle assembly checkpoint protein OS-Homo sapiens GN-MAD2L1 PE=1 SV=1	[MAD2L1_HUMAN]	3.34	1	1	1	1	1,000	1	1,860	205	23,495
Q8R69	Q8R69 (1-16) tumor necrosis factor receptor OS-Homo sapiens GN-TNFR1 PE=1											

Q8NWS8	Required for meiotic nuclear division protein 1 homolog OS-Homo sapiens (GN-RNND1) PE=1 SV=2 (RNND1_HUMAN)	4.23	3	2	2	3	1,016	3	37,293	0.000	469	51,571
E3UBN177	E3 ubiquitin ligase GN-HN146 PE=1 SV=1 (HN146_HUMAN)	3.9	1	1	1	1	1,000	1	1	0.000	359	2,368
O15235	26S ribosomal protein S12, mitochondrial OS-Homo sapiens (GN-MRPS12) PE=1 SV=1 (R12_L2_HUMAN)	12.32	1	3	3	3	1,032	3	24,914	0.000	138	16,163
Q8W300	Retain receptor 2 OS-Homo sapiens (GN-RHFP2) PE=1 SV=1 (RHFP2_HUMAN)	1.23	1	1	1	1	1,000	1	1	0.000	754	86,398
Q8R13	Multidrug and toxin extrusion protein 2 OS-Homo sapiens (GN-AT2) PE=1 SV=1 (S7AT2_HUMAN)	1.99	1	1	1	1	1,000	1	1	0.000	62	602
Q8925	Semaphorin 3D OS-Homo sapiens (GN-SEMA3D) PE=2 SV=2 (SEMA3D_HUMAN)	4.63	1	1	1	1	1,000	1	0.000	777	89,554	
Q13756	Protein S13756 OS-Homo sapiens (GN-HNR02) PE=1 SV=1 (S13756_HUMAN)	1.18	1	1	1	1	905	1	1	0.000	17	130
Q7Z380	Small integral membrane protein 15 OS-Homo sapiens (GN-SM15) PE=2 SV=1 (SM15_HUMAN)	1.4	1	1	1	1	1,028	1	1	0.000	74	8,620
Q8C03	Sperm flagellar protein 2 OS-Homo sapiens (GN-SPEF2) PE=1 SV=1 (SPEF2_HUMAN)	2.03	4	2	2	2	1,167	2	2,005	0.000	1822	203,640
Q8C04	Sperm OS-Homo sapiens (GN-SPEF1) PE=1 SV=1 (SPEF1_HUMAN)	1.35	1	1	1	1	1,000	1	1	0.000	807	91,444
Q8Z62	Helicase SRCAP OS-Homo sapiens (GN-SRCAP) PE=1 SV=3 (SRCAP_HUMAN)	0.43	1	1	1	1	1,000	1	1	0.000	3230	343,343
A3VFC9	SCD5L OS-Homo sapiens (GN-HSPO) PE=1 SV=1 (HSPO_HUMAN)	2.25	1	1	1	1	1,000	1	1	0.000	547	51,343
Q8K10	Starch-binding domain-containing protein 1 OS-Homo sapiens (GN-STBD1) PE=1 SV=1 (STBD1_HUMAN)	4.47	1	1	1	1	1,000	1	1	0.000	358	38,983
Q8N82	Transcriptional adaptor 1 OS-Homo sapiens (GN-TAD1) PE=1 SV=1 (TAD1_HUMAN)	3.58	1	1	1	1	1,079	1	1	0.000	336	37,358
Q16514	Transition nucleation factor 12 OS-Homo sapiens (GN-TAF12) PE=1 SV=1 (TAF12_HUMAN)	4.37	1	1	1	1	1,000	1	1	0.000	18	17,913
Q8P244	TBC1 domain family member 14 OS-Homo sapiens (GN-TBC14) PE=1 SV=3 (TBC14_HUMAN)	2.31	1	1	1	1	1,000	1	1	0.000	693	78,088
Q15443	OS-Homo sapiens alpha-1 (GN-TCTA) PE=1 SV=1 (TCTA_HUMAN)	1.62	1	1	1	1	1,000	1	1	0.000	215	23,020
Q8W86	Inactive serine/threonine-protein kinase TEX14 OS-Homo sapiens (GN-TEX14) PE=1 SV=2 (TEX14_HUMAN)	0.53	1	1	1	1	1,193	1	1	0.000	1497	167,798
Q8N82	Tesartoin homolog 2 OS-Homo sapiens (GN-TSH2) PE=1 SV=3 (TSH2_HUMAN)	3.19	1	1	1	1	1,000	1	1	0.000	1034	114,523
Q18664	V-type ATPase subunit F OS-Homo sapiens (GN-TSIF) PE=1 SV=2 (TSIF_HUMAN)	5.72	1	1	1	1	1,074	1	1	0.000	119	13,352
Q7Z514	Vomeronasal type 1 receptor 5 OS-Homo sapiens (GN-VN1R5) PE=2 SV=2 (VN1R5_HUMAN)	10.92	1	1	1	1	1,000	1	1	0.000	337	40,752
Q8Y218	WD repeat-containing protein 82 OS-Homo sapiens (GN-WDR82) PE=1 SV=1 (WDR82_HUMAN)	1.82	1	1	1	1	1,000	1	1	0.000	494	54,532
Q8U99	WD repeat-containing protein 82 OS-Homo sapiens (GN-WDR82) PE=1 SV=1 (WDR82_HUMAN)	2.24	1	1	1	1	1,000	1	1	0.000	313	35,056
O75132	Zinc finger BED domain-containing protein 4 OS-Homo sapiens (GN-ZBED4) PE=1 SV=2 (ZBED4_HUMAN)	1.11	1	1	1	1	1,000	1	1	0.000	1171	130,239
Q15104	Zinc finger protein 1100 OS-Homo sapiens (GN-ZFP110) PE=2 SV=1 (ZFP110_HUMAN)	0.54	1	1	1	1	1,000	1	1	0.000	2466	259,384
Q8H95	Zinc finger protein 1100 OS-Homo sapiens (GN-ZFP110) PE=2 SV=1 (ZFP110_HUMAN)	3.45	1	1	1	1	1,000	1	1	0.000	638	74,708
Q8S60	Zinc finger protein 407 OS-Homo sapiens (GN-ZNF407) PE=1 SV=2 (ZNF407_HUMAN)	0.49	1	1	1	1	1,000	1	1	0.000	248	24,211
Q8UE34	Zinc finger protein 629 OS-Homo sapiens (GN-ZNF629) PE=1 SV=2 (ZNF629_HUMAN)	2.78	71	2	2	3	1,139	1	0.000	869	96,559	
Q8R62	Zinc finger protein 645 OS-Homo sapiens (GN-ZNF645) PE=2 SV=3 (ZNF645_HUMAN)	18.65	79	2	2	5	1,000	1	0.000	970	113,000	
P1040	Zinc finger protein 645 OS-Homo sapiens (GN-ZNF645) PE=2 SV=3 (ZNF645_HUMAN)	9.01	108	1	1	1	1,000	1	1	0.000	1043	117,467
FZ225	ZNF98-like protein 1 OS-Homo sapiens (GN-ZNF98) PE=4 SV=1 (ZNF98_HUMAN)	14.26	1	1	1	1	1,000	1	1	0.000	123	13,516
Q8P11	Zinc finger protein-like 1 OS-Homo sapiens (GN-ZFP1L1) PE=1 SV=1 (ZFP1L1_HUMAN)	21.54	1	1	1	1	1,000	1	1	0.000	65	712
Q8S86	ATP synthase protein 8 OS-Homo sapiens (GN-ATP8) PE=1 SV=1 (ATP8_HUMAN)	52.94	127	2	2	2	1,000	1	0.000	68	7,958	
Q8Y98	Plutative uncharacterized protein DKF2064C07.6 (Fragment) OS-Homo sapiens (GN-DKF2064C07.6) PE=2 SV=1 (Q8Y98_HUMAN)	1.4	1	1	1	1	1,084	1	1	0.000	245	27,621
Q8E83	Chromatin A (Fragment) OS-Homo sapiens (GN-CHGA) PE=1 SV=1 (CHGA_HUMAN)	0.21	1	1	1	1	1,000	1	1	0.000	36	2,428
DNK24	Immunoglobulin-like domain-containing protein 1 OS-Homo sapiens (GN-IGLIM1) PE=4 SV=1 (IGLIM1_HUMAN)	17.24	2	1	1	1	1,000	1	1	0.000	116	12,967
HCC1624	Immunoglobulin-like domain-containing protein 1 OS-Homo sapiens (GN-IGLIM1) PE=4 SV=1 (IGLIM1_HUMAN)	15.14	1	1	1	1	1,000	1	1	0.000	486	67,865
B3UK17	Phosphatidylinositol glycan, class A (Paroxysmal nocturnal hemoglobinuria), isoform CRA_B OS-Homo sapiens (GN-PIGA) PE=2 SV=1 (B3UK17_HUMAN)	7.1	3	1	1	1	1,000	1	1	0.000	189	18,782
BZC27	SMT3 suppressor of mit 2 homolog 1 (Yeast), isoform CRA_A OS-Homo sapiens (GN-SUMO1) PE=1 SV=1 (BZC27_HUMAN)	12.9	3	1	1	1	1,000	1	1	0.000	62	717
SC257	SMN2 OS-Homo sapiens (GN-SCN2) PE=1 SV=1 (SCN2_HUMAN)	14.6	1	1	1	1	1,000	1	1	0.000	374	47,861
Q8P49	RSA13 suppressor of mit 2 homolog 1 (Yeast), isoform CRA_A OS-Homo sapiens (GN-SUMO1) PE=1 SV=1 (BZC27_HUMAN)	8.2	2	1	1	1	1,000	1	1	0.000	70	7,171
Q8E086	KIAA1088 isoform CRA_A OS-Homo sapiens (GN-KIAA1088) PE=1 SV=1 (KIE086_HUMAN)	14.6	1	1	1	1	1,000	1	1	0.000	202	24,748
Q8YV4	Anoctamin 2 OS-Homo sapiens (GN-DKFP243P102) PE=2 SV=1 (Q8YV4_HUMAN)	29.07	3	1	1	1	1,000	1	1	0.000	86	9,443
Q8D37	HCG184279, isoform CRA_A OS-Homo sapiens (GN-HCG184279) PE=3 SV=1 (Q8D37_HUMAN)	18.17	4	1	1	1	1,000	1	1	0.000	191	21,632
Q8Y98	Cyclophilin B (Fragment) OS-Homo sapiens (GN-CYCB) PE=4 SV=1 (Q8Y98_HUMAN)	3.04	1	1	1	1	2,010	1	1	0.000	107	14,433
Q8YV5	Phosphatidase D1 OS-Homo sapiens (GN-PP1349) PE=2 SV=1 (Q8YV5_HUMAN)	12.5	1	1	1	1	1,000	1	1	0.000	152	16,494
Q8Z321	MAGI5 subfamily member 1 OS-Homo sapiens (GN-MAGI5) PE=1 SV=1 (BZC21_HUMAN)	2.34	1	1	1	1	1,000	1	1	0.000	428	47,277
BZC29	Coiled-coil domain-containing protein 115 OS-Homo sapiens (GN-COCC115) PE=4 SV=1 (BZC29_HUMAN)	6.86	3	1	1	1	1,000	1	1	0.000	175	19,044
Q8E08	Poly (ADP-ribose) polymerase family member 12, isoform CRA_A OS-Homo sapiens (GN-PARP12) PE=1 SV=1 (Q8E08_HUMAN)	2.14	1	1	1	1	1,000	1	1	0.000	420	47,544
B4C08	Ring finger protein 185, isoform CRA_A OS-Homo sapiens (GN-RNF185) PE=2 SV=1 (B4C08_HUMAN)	1.54	1	1	1	1	1,000	1	1	0.000	10	1,402
AA024R8.5	Nuclein activated protein kinase binding protein 1, isoform CRA_A OS-Homo sapiens (GN-NAKBP1) PE=4 SV=1 (AA024R8.5_HUMAN)	2.66	1	1	1	1	1,000	1	1	0.000	1015	109,087
Q8Y34	CN143637, isoform CRA_A OS-Homo sapiens (GN-CN143637) PE=1 SV=1 (Q8Y34_HUMAN)	1.2	1	1	1	1	1,000	1	1	0.000	64	6,603
Q8Y34	CN143637, isoform CRA_B OS-Homo sapiens (GN-CN143637) PE=1 SV=1 (Q8Y34_HUMAN)	1.65	1	1	1	1	1,000	1	1	0.000	107	12,407
AA024R8.2	HCG23722, isoform CRA_A OS-Homo sapiens (GN-HCG23722) PE=4 SV=1 (AA024R8.2_HUMAN)	8.54	1	1	1	1	1,000	1	1	0.000	528	58,823
Q8Y34	Coiled-coil domain-containing protein 115, isoform CRA_B OS-Homo sapiens (GN-COCC115) PE=4 SV=1 (Q8Y34_HUMAN)	2.65	1	1	1	1	1,000	1	1	0.000	319	37,811
AA024R8.3	Family with sequence similarity 73, member 8, isoform CRA_A OS-Homo sapiens (GN-FAM73B) PE=4 SV=1 (AA024R8.3_HUMAN)	9.29	3	1	1	1	1,000	1	1	0.000	323	34,561
Q8Y34	CN143637, isoform CRA_B OS-Homo sapiens (GN-CN143637) PE=1 SV=1 (Q8Y34_HUMAN)	2.33	1	1	1	1	1,000	1	1	0.000	64	6,603
Q8P07	NR114 protein (Fragment) OS-Homo sapiens (GN-NR114) PE=1 SV=1 (Q8P07_HUMAN)	5.28	1	1	1	1	1,000	1	1	0.000	475	54,069
DRK97	Ectonucleoside diphosphate/phosphate/serine/threonine phosphatase family member 1 subunit form (Fragment) OS-Homo sapiens (GN-ENPP4) PE=4 SV=1 (DRK97_HUMAN)	10.31	3	1	1	1	1,000	1	1	0.000	194	22,333
Q8R84	ATP synthase protein 8 OS-Homo sapiens (GN-ATP8) PE=1 SV=1 (ATP8_HUMAN)	52.94	127	2	2	2	1,000	1	1	0.000	68	7,958
Q8R84	Mitochondrial pyruvate carrier 2 (Fragment) OS-Homo sapiens (GN-PC2) PE=1 SV=1 (Q8R84_HUMAN)	11.43	1	1	1	1	1,091	1	1	0.000	105	11,673
F4W54	Coiled-coil domain-containing protein 115 OS-Homo sapiens (GN-COCC115) PE=4 SV=1 (F4W54_HUMAN)	6.86	3	1	1	1	1,000	1	1	0.000	41	4,181
H0Y152	Aromatase (Fragment) OS-Homo sapiens (GN-CYP19A1) PE=4 SV=3 (H0Y152_HUMAN)	13.33	14	1	1	1	1,000	1	1	0.000	165	18,456
R4N24	Protein COMMD3-BM1 (Fragment) OS-Homo sapiens (GN-COMMD3-BM1) PE=4 SV=2 (R4N24_HUMAN)	13.64	1	1	1	1	1,000	1	1	0.000	110	12,320
X8R13	G3 ubiquitin ligase (Fragment) OS-Homo sapiens (GN-HUR2) PE=4 SV=2 (X8R13_HUMAN)	2.71	2	1	1	1	1,000	1	1	0.000	245	26,943
B4D03	CN14 FL18110, highly similar to Homo sapiens glycine N-acetyltransferase-like 1 (GLYT1L), mRNA OS-Homo sapiens (PE=2 SV=1) (B4D03_HUMAN)	2.15	3	1	1	1	1,000	1	1	0.000	279	32,254
Q8Y34	CN143637, isoform CRA_A OS-Homo sapiens (GN-CN143637) PE=1 SV=1 (Q8Y34_HUMAN)	1.2	1	1	1	1	1,000	1	1	0.000	13	1,509
CJXD1	Cyclophilin N-acetylglucosaminase 3-beta-galactosyltransferase 1 (Fragment) OS-Homo sapiens (GN-C1GALT1) PE=4 SV=1 (CJXD1_HUMAN)	15	3	1	1	1	996	1	1	0.000	100	11,286
Q8N77	Zinc finger MYM-type protein 3 OS-Homo sapiens (GN-ZNF73) PE=1 SV=1 (Q8N77_HUMAN)	2.3	1	1	1	1	1,188	1	1	0.000	1280	141,897
Q8Y34	CN143637, isoform CRA_B OS-Homo sapiens (GN-CN143637) PE=1 SV=1 (Q8Y34_HUMAN)	2.15	3	1	1	1	1,000	1	1	0.000	13	1,509
Q8T08	MORC repeat-containing protein 1 (Fragment) OS-Homo sapiens (GN-MORF1) PE=4 SV=1 (Q8T08_HUMAN)	8.65	1	1	1	1	1,000	1	1	0.000	185	19,888
F4W54	Palladin OS-Homo sapiens (GN-PALL1) PE=1 SV=1 (F4W54_HUMAN)	4.88	3	1	1	1	1,000	1	1	0.000	164	18,452
AA024R7Y.1	Glutamine synthetase OS-Homo sapiens (GN-GLUL) PE=4 SV=1 (AA024R7Y.1_HUMAN)	16.74	1	1	1	1	1,000	1	1	0.000	233	26,396
AA024R7Y.4	DNA polymerase alpha catalytic subunit OS-Homo sapiens (GN-PCNA) PE=1 SV=1 (AA024R7Y.4_HUMAN)	1.3	1	1	1	1	1,000	1	1	0.000	1481	165,663
Q8Y34	Nuclein activated protein kinase binding protein 1, isoform CRA_B OS-Homo sapiens (GN-NAKBP1) PE=4 SV=1 (AA024R8.5_HUMAN)	33.72	1	1	1	1	1,000	1	1	0.000	580	65,889
HKV83	Oligosaccharyl transferase OS-Homo sapiens (GN-OTOF) PE=4 SV=1 (HKV83_HUMAN)	13.3	2	1	1	1	1,000	1	1	0.000	2852	306,742
Q8Y34	Zinc phosphatidase ELAC (Fragment) OS-Homo sapiens (GN-ELAC1) PE=4 SV=1 (Q8Y34_HUMAN)	4.93	1	1	1	1	1,000	1	1	0.000	223	25,866
Q4VBL9	TAC3 protein (Fragment) OS-Homo sapiens (GN-TAC3) PE=2 SV=1 (Q4VBL9_HUMAN)	1.29	3	1	1	1	1,000	1	1	0.000	464	52,132
MOQ228	Protein LOC88210 OS-Homo sapiens (GN-LOC88210) PE=4 SV=2 (MOQ228_HUMAN)	0.98	1	1	1	1	1,000	1	1	0.000	3231	354,000
Q8Y34	Heat shock receptor 1B (Fragment) OS-Homo sapiens (GN-HSR1B) PE=4 SV=1 (Q8Y34_HUMAN)	1.09	1	1	1	1	1,					

Appendix IV – Published and Presented work

Hide and Spread for intracellular *Leishmania* parasites – from infection to apoptosis

Rajeev Rai and Giulia Getti

School of Science, University of Greenwich, Kent, ME4 4TB

Leishmania is a protozoan parasite responsible for human disease called leishmaniasis. The parasite life cycle alternates between two stages. The promastigotes stage develops inside the sandfly vector and once injected into a mammalian host, enters macrophages and establish itself as intracellular replicating amastigotes. The dissemination of amastigotes to uninfected macrophages is crucial for the development of the disease. However, the molecular mechanism of spreading is largely unknown.

Natural infection studies in mice have shown that early phase of infection occurs silently without accompanying immunopathological changes. A process resembling cell death via apoptosis, which involves the removal of damaged cells by macrophages without eliciting an inflammatory response, speculated us that *Leishmania* parasites could leave the host cell within apoptotic bodies, evading the host immune defense system.

Our study investigates the infection with four GFP expressing species of *Leishmania* on apoptosis of the host cells. Terminally differentiated THP-1 monocyte was employed to model the *in vitro* *Leishmania* infection. Through flow cytometry, infection and early apoptotic features were detected simultaneously for four days both on apoptosis induced and non-induced infected cells. Our results revealed higher level of early apoptosis upon parasite infection compared to uninfected cells. Remarkably apoptotic induction caused a 4 fold increase in percentage of infection when compared with non-induced infected cell. Moreover an increase in the level of apoptosis was also detected, further demonstrating a link between infection and apoptosis. Overall, the results support the hypothesis that apoptosis induction could participate in parasites spreading between human host cells.

Presented at British Society for Parasitology (BSP) Annual Spring meeting, Poster presentation, University of Cambridge, 2014

Hide and spread for intracellular *Leishmania* parasite – from infection to apoptosis

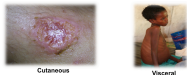


Rajeev Rai and Giulia Getti
School of Life Science, University of Greenwich, Kent, UK

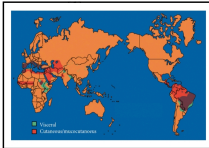


INTRODUCTION

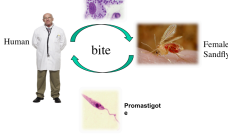
> *Leishmania* is a protozoan parasite responsible for human diseases called leishmaniasis



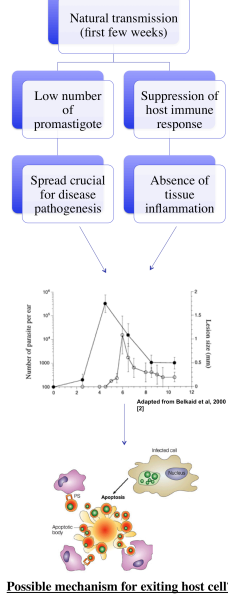
> Leishmaniasis is endemic in tropical and sub-tropical regions of the world with two million cases



> Dual life cycle: amastigote



RESEARCH BACKGROUND



AIMS OF THE STUDY

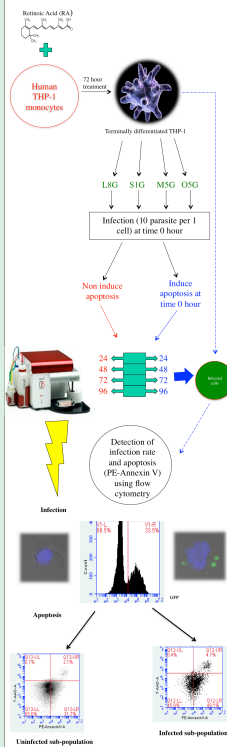
Study the link between apoptosis of terminally differentiated THP-1 monocytes (human monocyte cell line) and infection for four species of GFP expressing *Leishmania* parasites

- *L. aethiopica* (L&G)
- *L. major* (S1G)
- *L. mexicana* (MSG)
- *L. tropica* (O5G)

This will involve:

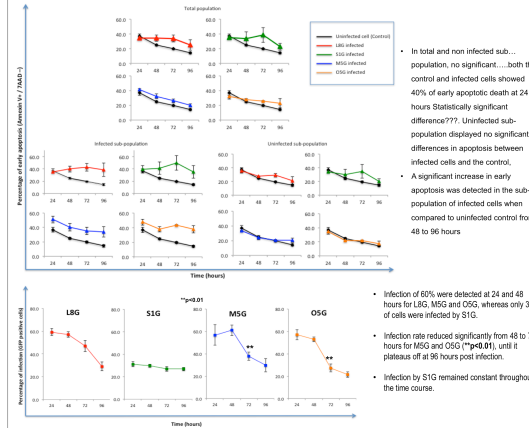
1. Investigating the effect of infection on host cells' apoptosis (24 to 96 hours).
2. Investigating the effect of apoptotic induction on infection (24 to 96 hours).
3. Developing an in vitro model to study late infection (72 to 120).

EXPERIMENTAL MODELS

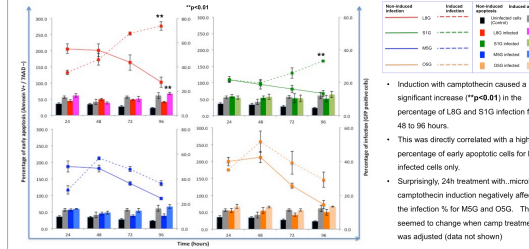


RESULTS and DISCUSSION

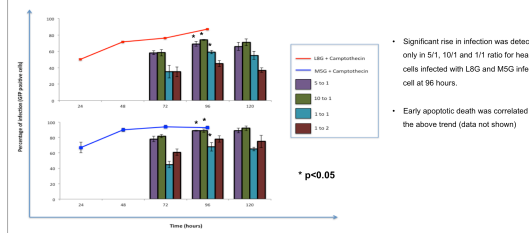
1. Effect of *Leishmania* promastigote infection on the apoptosis of differentiated THP-1



2. Effect of Camptothecin induced apoptosis on infection and host cell viability



3. Infection of autologous cells with an infected cells



CONCLUSIONS

- > The apoptosis of THP-1 cell remains higher during *Leishmania* infection
- > Induction of apoptosis could possibly transform the ability of amastigote to spread between cell.
- > Preliminary studies of cell associated infection suggest a strong link between infection and apoptosis.

REFERENCE

1. World Health Organisation website (www.who.int/leishmaniasis/)
2. Balkaid, Y., Mendez, S., Liu, R., Kadambi, N., Milton, G and Sacks, D. (2006). A natural model of *Leishmania* major infection reveals a prolonged silent phase of parasite amplification in the skin before the onset of lesion formation and immunity. 165: 969-977

THANK YOU

- Giulia Getti
- University of Greenwich
- Lawrence Harbige
- BSP Travel awards 2014

The *in vitro* development of *Leishmania* parasite dissemination during late stage of macrophage infection

Rajeev Rai and Giulia Getti

School of Science, University of Greenwich, Kent, ME4 4TB

The ability of replicating *Leishmania* parasite inside macrophage to spread their progeny towards naïve macrophages is of a paramount importance to initiate the pathogenesis of leishmaniasis. However, the mechanism of parasite spread has not been characterized yet. Research in this area has been largely hindered by the lack of infection models for this stage of the parasitic life cycle. We have developed an *in vitro* model to enhance our understanding on the dissemination of *Leishmania* that occurs during late stage of macrophage infection.

Terminally differentiated THP-1 monocytes were infected with two GFP expressing species, *Leishmania mexicana* (M5G) and *Leishmania aethiopica* (L8G) and treated with an apoptotic inducer. Following 72 hours from infection, both infected cells were used to infect a newly differentiated population of THP-1 cells at different infection ratios. Flow cytometric analysis was carried out to detect the percentage of GFP positive parasite residing in the cell.

We found that 80% of cells were infected by M5G and L8G at 72 hours, under apoptotic induction. Re-infection of the healthy cells at 72 hours with both infected cells at a ratio of 10/1, 5/1 and 1/1 resulted in a significant increase ($p < 0.05$) in the percentage of infection post 24 hours. This infection remained constant from 48 to 72 hours, eventually lowering at 96 hours. Importantly, there was no significant reduction in the total number of viable cell before and after re-infection. This indicated that the infection rise observed was related to the possible spread of the parasites and not caused by death of uninfected THP-1 monocytes.

Our development of an *in vitro* model of *Leishmania* infection of macrophage revealed a potential time frame for parasite dissemination during late infective stage. This would allow further investigation into whether apoptosis could be involved in “hiding” and “spreading” this lethal parasite during leishmaniasis.

Presented at 13th International Congress for Parasitology (ICOPA), Oral presentation, Mexico City, 2014

***Leishmania* modulates host apoptotic signaling pathway in order to disseminate from cell-to-cell during human macrophage infection**

Rajeev Rai and Giulia Getti

School of Science, University of Greenwich, Kent, ME4 4TB

The initiation for the pathogenesis of human leishmaniasis is dependent on the ability of *Leishmania* amastigotes to disseminate from infected to uninfected macrophages. However, the molecular and cellular mechanism behind this unique form of cell-to-cell spreading is one of the least explored topics in the field of *Leishmania* biology. This slow advancement has been largely due to the lack of effective model system to represent the late stage of host-parasite interaction *in vitro*. In this work, we have reported the development of a human cell-based *in vitro* model representative of *Leishmania aethiophica* dissemination in human cells.

The model is based on infecting a healthy population of terminally differentiated THP-1 macrophage with previously (72 hours) infected THP-1 macrophage. Such model showed an increase in *L. aethiophica* (GFP expressing) infection from 35% to 50% after 24 hours of co-culture. This was confirmed using real time lapse microscopy which revealed inter-cellular extrusion and subsequent transfer of amastigotes from infected to a healthy THP-1 macrophage. Interestingly, this form of cell-to-cell spreading appeared to be correlated with apoptotic induction, as there was a significant increase in the percentage of Annexin V and active caspase-3 expression as compared to uninfected control.

Western blot analysis further demonstrated that the above effect within this time period was associated with de-phosphorylation and reduced expression of anti-apoptotic protein AKT, and increased expression of cytochrome C protein. In conclusion, this could indicate that *L. aethiophica* promotes the host cell apoptosis by interfering with AKT pathways resulting in the release of cytochrome C and subsequent caspase-3 activation. This could represent one of the critical and novel mechanisms behind the dissemination of *Leishmania* species during human macrophage infection.

Presented at British Society for Parasitology (BSP) Annual Autumn meeting, Poster presentation, Royal Veterinary College, 2015

Leishmania modulates host apoptotic signaling pathway in order to disseminate from cell-to-cell during human macrophage infection



Rajeev Rai and Giulia Getti
School of Life Science, University of Greenwich, Kent, UK



INTRODUCTION

Leishmania is a protozoan parasite responsible for human diseases called leishmaniasis (Figure 1)

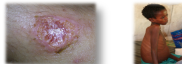
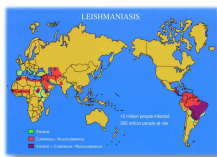
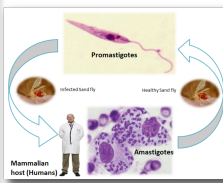


Fig 1A:

Cutaneous leishmaniasis. The disease remains endemic in tropical and sub-tropical regions of the world (Figure 2) with two million cases per year [1].



Dimorphic flagellates world map



RESEARCH BACKGROUND

The dissemination of *Leishmania* amastigotes from infected to uninfected macrophage represents a critical step in the establishment of human leishmaniasis

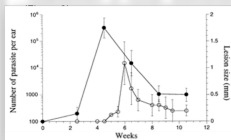


Fig 3: Pathogenic development of Leishmaniasis

- Activation of host cell apoptotic death have been suggested as a potential mode of escape route for intracellular amastigotes [2].
- However, the exact cellular and molecular mechanism behind this form of cell-to-cell spreading is one of the least explored topics in the field of *Leishmania* biology.
- This investigation has been largely due to the lack of effective model system to represent the late stage of host-parasite interaction in vitro.

RESEARCH AIMS

- Validate our newly developed in vitro model (Figure 4) of *L. aethiopsica* dissemination during human macrophage infection via real time lapse microscopy.

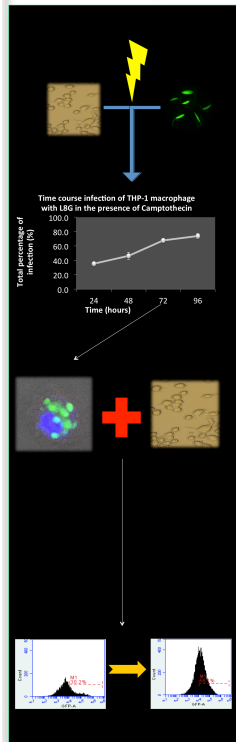
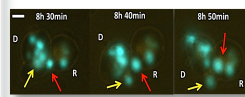


Fig 4: In vitro dissemination model for *L. aethiopsica* during human macrophage infection

- Utilize the above model in order to examine two critical aspects responsible for driving *Leishmania* infection spreading:
 - Investigate the potential role of parasite mediated host cell apoptosis via Annexin V and Caspase-3 assay.
 - Analyze the molecular expression of host intracellular proteins associated with apoptosis regulation, including AKT and cytochrome C.

RESULTS

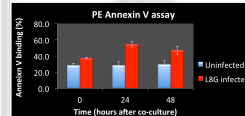
1. Real time-lapse microscopy of amastigote transmission



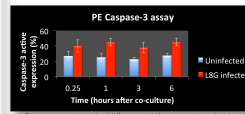
The recipient (R) THP-1 macrophage was pre-stained with Cell mask orange dye for 5 minutes and intensively washed with the PBS. This fresh population was then co-cultured with 72h LBG infected donor cells (D) and live imaged for a period of 12 hours every 10 minutes under TIRF laser (Scale: 25 μm).

At 30 min, the red arrowed amastigote begin to migrate from the peripheral membrane of D. After 40-50 minutes, the amastigote is completely extruded and transfers into R. In addition, the yellow arrowed amastigote is possibly observed to be packaged within apoptotic bodies of D.

2. Link between infection spreading and host cell apoptosis

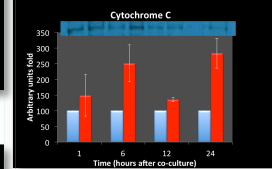
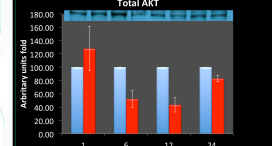
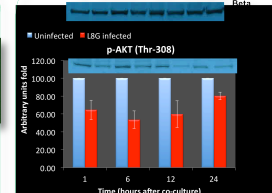


In comparison to the uninfected controls, a significant increase ($p < 0.05$) in Annexin V binding, was detected from 0 to 24 hours of co-culture in LBG infected cells.



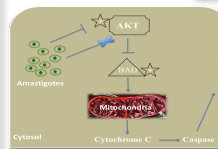
There was no significant difference in the expression of active caspase-3 initially. Interestingly, after 1 hour of co-culture, the expression of active caspase-3 within the infected cells increased by two fold in relative to uninfected controls.

3. Western blot analysis



Within 1 hour after co-culture, there was a marked decrease in the phosphorylation of AKT (Thr-308) within the infected cells as compared to uninfected controls. However, no significant differences in the expression of total AKT and cytochrome C were observed. This level of reduced AKT inactivation was detected at 24 hours. Surprisingly, from 6 hours onwards, the expression of total AKT in infected cells remained significantly lower than the control, as cytochrome C expression was instead found to be higher. Overall, these results potentially suggest parasite mediated apoptotic protein modulation during the cell-to-cell dissemination of *Leishmania* infection.

DISCUSSION



This schematic diagram illustrates the probable apoptotic pathways induced by *Leishmania* amastigotes during cell-to-cell spreading. The parasite could interfere with AKT signalling by either inactivation or degradation of AKT. This could stimulate the release of cytochrome C from mitochondria via BAD activation. This in turn could promote the activation of caspase-3 resulting in the exposure of phosphatidylserine (PS) and subsequent induction of apoptosis.

CONCLUSIONS

- Validation of our in vitro dissemination model was achieved following the visual evidence of *L. aethiopsica* amastigotes transfer from cell-to-cell through real time lapse microscopy.
- Induction of host cell apoptosis by amastigotes appeared to play an instrumental role behind this cell-to-cell dissemination.
- Western blot analysis further demonstrated that the above effect was associated with de-phosphorylation and reduced expression of anti-apoptotic protein AKT, and increased expression of cytochrome C protein.

REFERENCES

- Handman, E. (2001) Leishmaniasis: current status of vaccine development. *Clinical Microbiology Reviews*, 14, 229-243.
- Rai, F. (2014). Cell-to-cell transfer of *L. amazonensis* amastigotes is mediated by immunomodulatory LAMP rich parasitophorous extrusions. *Cellular Microbiology* 16, 1549-1564.